A CONVERTER COMPENSATOR FOR POWER FACTOR CONTROL IN 3-PHASE INDUCTION MACHINES

CHRISTOPHER MULENGA CHILESHE

Doctor of Philosophy

THE UNIVERSITY OF ASTON IN BIRMINGHAM

April 1996

The University of Aston in Birmingham

A Converter Compensator For Power Factor Control in 3-Phase Induction Machines

Christopher Mulenga Chileshe

Doctor of Philosophy

1996

SUMMARY

The advent of the harmonic neutralised shunt Converter Compensator as a practical means of reactive power compensation in power transmission systems has cleared ground for wider application of this type of equipment.

An experimental 24-pulse voltage sourced converter has been successfully applied in controlling the terminal power factor of a 1.5kW, 240V three phase cage rotor induction motor, whose winding has been used in place of the usual phase shifting transformers. To achieve this, modifications have been made to the conventional stator winding of the induction machine. These include an unconventional phase spread and facilitation of compensator connections to selected tapping points between stator coils to give a three phase winding with a twelve phase connection to the twenty four pulse converter.

Theoretical and experimental assessments of the impact of these modifications and attachment of the compensator have shown that there is a slight reduction in the torque developed at a given slip and in the combined system efficiency. There is also an increase in the noise level, also a consequence of the harmonics. The stator leakage inductance gave inadequate coupling reactance between the the converter and the effective voltage source, necessitating the use of external inductors in each of the twelve phases. The terminal power factor is fully controllable when the induction machine is used either as a motor or as a generator.

Key Words: POWER FACTOR CORRECTION, INDUCTION MOTOR, POWER ELECTRONICS, STATCON, STATOR WINDING.

This thesis is dedicated to my parents, Felix. S. Chileshe and Elizabeth N. Chileshe.

ACKNOWLEDGEMENTS

To my supervisor, Professor W.T. Norris, for his invaluable contributions, his many references quoted herein, and the unwavering support.

To Dr. N. R. Fahmi for useful tips on induction motor testing, and to Dr. Jason E. Hill for useful discussions and for his work on the theory of reactive power compensators, upon which has been based a lot of the application described herein.

To Mr. B. Harrison, chief laboratory technician, Mr. M.P. Westrick, Mr. S.M. Boardman and Mr. M. Higlett, research assistants, for their help in building the equipment.

To Mr. R. Baker, Mr. David James, Mr. Stephen Jay, members of the Electric Power Research group, for useful discussions and to Mr. L. Radford, Mr J. Thomas, power engineering laboratory staff at Aston, for their assistance.

To Mr. David Taylor and Mr. David Whitehouse of Electrodrives Limited for the material support and help with the machine winding design and information.

To Mr. A. Wilton and Mr. P.J. Miller for simulator software support.

To my sponsors, the BEIT Trust, for awarding me this unique opportunity to further my education and to the department of Mechanical and Electrical Engineering at the University of Aston for the support.

Finally, to Dr. M. Browne, family and friends for the encouragement and support during the course of this research, and to all persons who have knowingly or not, contributed to this work in whatever capacity.

CONTENTS

001 - LIST OF SYMBOLS AND ABBREVIATIONS

SYMBOL	DESCRIPTION	PAGE
α	phase control parameter in model	37
α	firing angle	40
α_{max}	maximum permissible delay angle for linear operation	148
α_{min}	minimum permissible delay angle for linear operation	148
β	a damping factor given by $\beta = R/2X_L$	40
χ	a pulse number dependent constant for stepped waveform algebra	54
ε	angle given by $\tan^{-1}(R/X_L)$	40
ε	control error defined as setpoint - measurement	148
μ_o	permeability of air $\approx 4\pi \times 10^{-7}$ Hm^{-1}	86
λ_p	span of full pitch coil in electrical degrees or slots	84
λ	(as in λ/λ_p). The span of chorded coil in electrical degrees or slots	84
λ	a constant depending on pulse number in STATCON algebra	40
λ_G	a λ modifying factor for application to stator winding	114
ϕ	phase angle between supply voltage and current	24
ϕ	magnetic flux	87
θ_{exc}	Angle between excitation current and induced emf	79
κ	constant between 0.1 and 0.11 accounting for Carter effect	87
ω	supply voltage angular frequency given by $\omega=2\pi f$	23
τ	angle between centres of adjacent stator slots	94
ϕ_n	flux in phase n of multi-core transformer system	67
A	first phase of three phase supply	68
a	span of chorded coil, in numbers of slots, in a clockwise direction	85
a	number of parallel paths in a winding	107
a'n'	n^{th} of multiple-phase system derived from phase A	57
A_a	area of chorded coil on clockwise span (a)	86
A_b	area of chorded machine coil on anticlockwise span	86
A_O	amplitude of compensator current in model, given by	38
ASVC	Advanced Static VAr Compensator	2
B	magnetic flux density	85
B_a	Flux density due to chorded coil on clockwise span (a)	86
B_b	Flux density due to chorded coil on anticlockwise span (b)	86
B	second phase of three phase supply	68
b	span of chorded coil, in slots, in the anticlockwise direction	85
b'n'	n^{th} of multiple-phase system derived from phase B	57
BJT	Bipolar Junction Transistor	41
C	capacitance	40
C	third phase of three phase supply	68
c	number of magnetic cores in multi-core transformer system	68
c	closed contour line of flux in machine algebra	85
c'n'	n^{th} of multiple-phase system derived from phase C	57

E	induced emf	67
e'n'	emf in phase n of multi-phase system	84
EPROM	Erasable Programmable Read Only Memory	140
f	supply voltage fundamental frequency in Hertz (Hz)	23
FACTS	Flexible A.C. Transmission Systems	31
FFT	Fast Fourier Transform	32
GTO	Gate Turn-off Thyristor	41
g_m	mechanical width of air-gap	87
g	*effective* air gap width	85
H	magnetic field intensity	86
H_a	magnetic field intensity of chorded coil on clockwise span (a)	86
H_b	magnetic field intensity of chorded coil on anti-clockwise span (b)	86
i(t)	instantaneous value of supply current	23
I_1	supply current	37
I_1'	supply current producing mutual flux in equivalent circuit	79
I_2	current sourced by compensator in model	37
I_2	rotor current in equivalent circuit	103
i_a	supply current in single phase model	35
i_a	phase A supply current	191
i_b	supply current in presence of compensator in model	35
I_c	core loss current	79
I_{exc}	Excitation current	79
IGBT	Insulated Gate Bipolar Transistor	41
i_L	current through inductor	34
I_{LC}	current through coupling inductance	42
I_M	magnetising current	79
I_o	peak value of supply current	23
I_{RC}	current through coupling resistance	42
I_s	rms value of supply current	23
j	complex number operator = $\sqrt{-1}$	35
k	STATCON sizing parameter given by $k = \sqrt{\lambda(X_C / X_L) - \beta^2}$	40
k	coupling coefficient in expressions for mutual inductance	193
k_1	complex factor accounting for phase shift in 3-phase supply	67
k_2	as k_1	67
k_C	chording factor of winding, given by $k_c = \sin(\pi\lambda / 2\lambda_p)$	84
k_D	Winding distribution factor given by $k_D = \sin(q\tau / 2) / q\sin(\tau / 2)$	100
k_W	Winding factor given by $k_W = k_D \times k_C$	101
k_i	constant accounting for saturation of iron in inductance calculations	87
k_{IM}	modified resonance ratio for use with stator winding coupling	114
k_n	coupling dependent factor in STATCON reactive power expressions	113
k_S	machine winding skew factor	194
l	axial length of air gap in machine	85
L	inductance	34
L_o	stator inductance constant, used to simplify expressions	91

L_2	coupling inductance in model	37
L_c	coupling reactor in STATCON	41
L_c	Stator coil self inductance	86
L_e	combined stator and rotor per phase leakage inductance	107
L_{ec}	Coil leakage inductance in expressions for coupling reactance	204
L_{ph}	phase self inductance	113
LSB	Least Significant Bit	144
M_{12}	Mutual inductance between 1 and 2	193
M_β	Mutual inductance between stator coils	88
M	STATCON sizing parameter given by $M = k^{-1}$	40
m	number of phases	68
m_r	number of phases on rotor	90
MCT	MOS controlled Thyristor	41
MOSFET	Metal Oxide Semiconductor Field Effect Transistor	41
M_{ph}	Phase mutual inductance	89
N_{eprom}	Number of active pages in switching pattern (EPROMs)	148
N	Number of turns on a winding	85
N_1	Number of turns on primary side of equivalent circuit	79
N_2	Number of turns on secondary side of equivalent circuit	79
N_{ph}	Total series turns per phase	89
N_r	Equivalent number of turns of rotor	90
n	speed of rotor in rpm	195
n_p	number of poles	89
n_s	synchronous speed in rpm	195
P	active power	25
P	counter preset value in control algorithm	148
P_t	counter preset at arbitrary time t	149
P_{t-1}	counter preset at time t-1 used in control algorithm	149
P_o	initial value of preset in control algorithm	148
ΔP	change in preset in control algorithm	149
p	pulse number of multiple pulse system	54
p(t)	instantaneous power	24
PF	Power factor	32
P_m	maximum active power in compensator	44
PWM	Pulse Width Modulation	53
Q	reactive power	26
Q	number of stator slots	85
Q_{IM}	Total machine reactive power	113
Q_r	number of bars in squirrel cage rotor	90
Q_m	maximum reactive power in compensator	44
q_1	normalised value of reactive current at delay $\alpha = 0$	113
q_2	a constant related to the active power in the STATCON	113
R_M	resistance of magnetising branch of equivalent circuit	103
r	power supply source resistance	34

r_r	mechanical radius of rotor	85
r	radius of air gap given by r_r + ½g	85
r_2	coupling reactor resistance in model	38
Rc	coupling inductor series resistance in STATCON	42
S	apparent power	26
S_{CA}	cosine series type A for a stepped waveform	55
S_{CB}	cosine series type B for a stepped waveform	55
S_{SA}	sine series type A for a stepped waveform	55
S_{SB}	sine series type B for a stepped waveform	55
s	slot displacement measured between centres of adjacent stator slots	86
T	fundamental cycle period = 1/f	25
TCR	Thyristor Controlled Reactor	30
THD	Total Harmonic Distortion	63
TSR	Thyristor Switched Capacitor	30
v(t)	instantaneous value of supply voltage	23
V_1	supply voltage rms value	34
V_1'	modified supply voltage in approximate equivalent circuit	201
v_1	as v(t)	34
V_2	rotor (secondary) voltage in equivalent circuit	103
V_2	compensator rms output voltage in model	37
v_2	compensator output voltage in model	37
VA	Volt-Amperes - unit of apparent power S	26
V_A	Phase A to neutral voltage	67
V_B	Phase B to neutral voltage	67
V_C	Phase C to neutral voltage	67
V_{DS}	MOSFET drain to source voltage	72
V_{gs}	MOSFET gate to source voltage	134
V_i	peak inverter output voltage	41
V_{inv}	Inverter output voltage	72
V_o	peak value of supply voltage	23
V_s	rms value of supply voltage	23
V_x	voltage across single phase load terminals	34
x_1	stator leakage reactance in equivalent circuit	103
x_2	rotor leakage reactance in equivalent circuit	103
x_m	reactance of magnetisation branch in equivalent circuit	103
x_e	combined stator and rotor per phase end leakage flux	107
X_C	reactance of reservoir capacitor at fundamental frequency	40
X_L	reactance of coupling reactor at fundamental frequency	40
Y_C	susceptance of reservoir capacitor at fundamental frequency	40
Z_L	impedance of inductance L given by $Z_L=R_L+j\omega L$	210

002 - LIST OF FIGURES AND TABLES

THESIS FORMAT

This thesis can be broadly sub-divided into two halves:

The first five chapters discuss the background to the concepts that have been employed and described in the later chapters. They therefore serve to define the general framework of the work in hand by the use of generic views and performance parameters related to the multiple-pulse STATCON with zigzag transformer connections. The arrangement is discussed in some detail to establish non-ideal behaviour such as the presence of low order harmonics. The system is further used for comparisons when the stator winding is used as the coupling.

This approach was adopted so that discussions directly concerned with the induction machine in this application are not obscured by lengthy derivations and descriptions of associated theory which may require some treatment.

CHAPTER 1

INTRODUCTION

This chapter presents the elementary theory of the power factor and introduces the concept of reactive power compensation. A distinction between *reactive power compensation* and *power factor correction* is made to keep the discussions relevant to the problem in hand.

1.1 - DEFINITION OF POWER FACTOR

When an alternating voltage is applied across the terminals of a linear reactive element such as a capacitor or an inductor, the device sets up an electrical or magnetic field which may be regarded as opposing the voltage or current giving rise to it (Lenz's Law).
A capacitor sets up an electrical field which impedes the rate of accumulation of charge - hence build up of voltage - while an inductor sets up a magnetic field which opposes the rate of change of the current through it. The effect is a shift in the phase relationship between the voltage and the current at the terminals of the device.

Fig 1.1 depicts a linear reactive element connected to a sinusoidal voltage source.

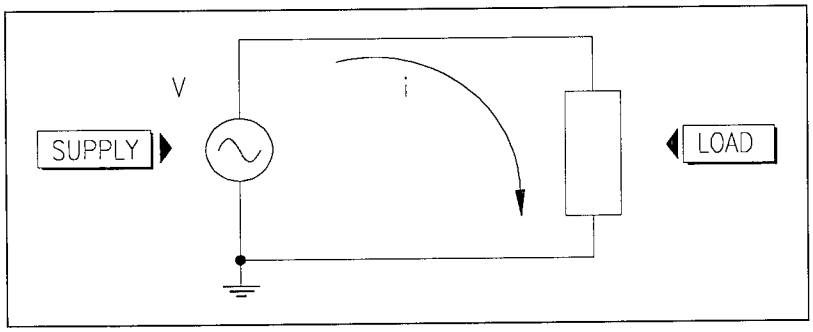

Fig 1.1 - Sinusoidal voltage source feeding a linear reactive element

Let the following be defined thus:

v(t)	the instantaneous value of the supply voltage
i(t)	the instantaneous value of the supply current
V_s	the rms value of the supply voltage
V_o	the peak value of the supply voltage
I_s	the rms value of the supply current
I_o	the peak value of the supply current
f	the supply voltage frequency
ω	the angular supply frequency given by $\omega = 2\pi f$

The terminal voltage and current at the load of **Fig 1.1** are shown graphically in **Fig 1.2a** and **Fig 1.2b** for a purely capacitive and purely inductive load respectively. The voltage is shown as the broken line and the relative magnitudes are arbitrary.

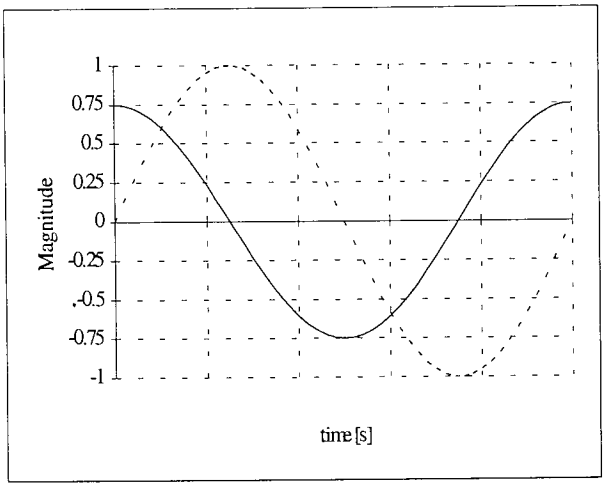

Fig 1.2a - Leading current

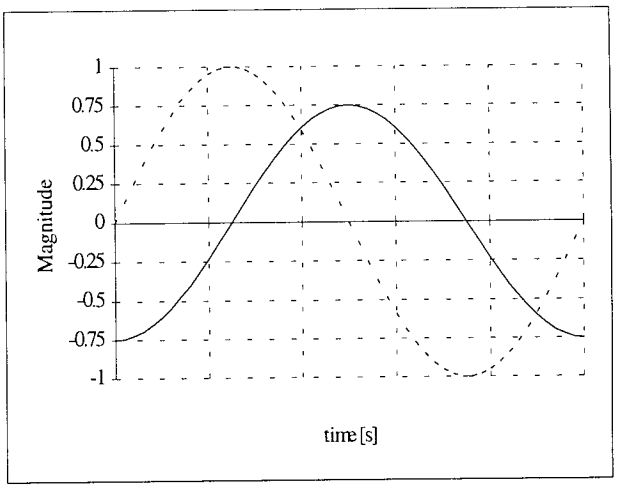

Fig 1.2b - Lagging current

For an a.c. system such as that described, the amount by which the current leads or lags the voltage is the *phase shift* and is normally quoted in degrees or radians. The convention adopted in this text is to use positive and negative values of phase shift for lagging and leading currents respectively. Purely linear reactive elements cause the current to lead or lag the voltage by 90° as shown in **Fig 1.2**. In practice, resistance, which does not give rise to any phase shift itself, gives rise to a component of current in phase with the voltage and so causes the net phase shift to be less than 90°. In general, a linear electric circuit will comprise reactive and non-reactive elements and the overall phase shift is the resultant due to the effects of the individual elements. Throughout this text, the supply voltage will be taken as the reference.

Let the supply voltage v(t) be a sinusoid given by

$$v(t) = V_o.\sin(\omega t) \qquad (1.1)$$

The current i(t) is also a sinusoidal quantity for a linear load, phase shifted by some amount ϕ:

$$i(t) = I_o.\sin(\omega t - \phi) \qquad (1.2)$$

Thus:

$$i(t) = I_o.(\cos\phi.\sin\omega t - \sin\phi.\cos\omega t) \qquad (1.3)$$

The instantaneous power p(t) supplied to the load is, by definition, the product of the supply volts and the current.

Thus:

$$p(t) = v(t) \,.\, i(t) = V_o.I_o.\sin(\omega t).\sin(\omega t - \phi)$$

whence:

$$p(t) = \frac{V_o I_o}{2}.(\cos\phi - \cos(2\omega t - \phi)) \qquad (1.4)$$

This suggests that the instantaneous power comprises two components.

(i) $\frac{V_o I_o}{2}.\cos\phi$

This quantity is a constant for a constant phase angle (ϕ). It is independent of the supply frequency and depends only on the magnitudes of the supply voltage and current, and on the size of the phase angle.

(ii) $-\frac{V_o.I_o}{2}.\cos(2\omega t - \phi)$

This quantity, of zero average value, describes the oscillatory exchange of power between the supply system and the load in an energy conservative process at twice the supply frequency

The **active power, P**, supplied to the load, is the average of the instantaneous power p(t) over a cycle and is measured in **Watts, W**. Thus, if T is the cycle period, then

$$P = \frac{1}{T}\int_0^T p(t)dt \qquad (1.5)$$

and since T = 1/f and $\omega = 2\pi f$, it follows that $T = 2\pi/\omega$, whence:

$$P = \frac{\omega}{2\pi}\int_0^{2\pi/\omega} p(t)dt = \frac{1}{2\pi}\int_0^{2\pi} p(\omega t)d\omega t \qquad (1.6)$$

Performing the integration over the stated limits gives:

$$P = \frac{V_o I_o}{2}.\cos\phi \qquad (1.7)$$

But $V_s = \frac{V_o}{\sqrt{2}}$ and $I_s = \frac{I_o}{\sqrt{2}}$

therefore:

$$P = V_s I_s \cos\phi \qquad (1.8)$$

Cosϕ is the factor by which the product of the supply rms voltage and current must be multiplied in order to determine the active power. It is called the **power factor** and is a dimensionless quantity often quoted as the decimal or as a percentage.

The apparent power S, is the product of the rms voltage and current, and equals the active power when the power factor cosϕ = 1 i.e. ϕ = 0. It is measured in **Volt-Amperes, VA**

Thus:

$$S = V_s I_s \qquad (1.9)$$

These quantities are shown in **Fig 1.3c**.

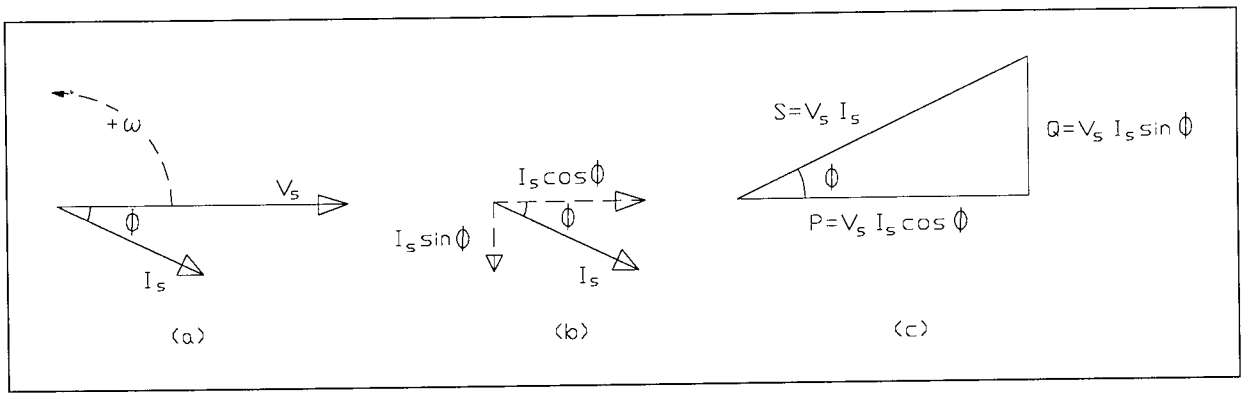

Fig 1.3 - Vector diagrams showing
a) The phasors V and I
b) The current resolved into its phase and quadrature components
c) Power as the product of current and voltage

Fig 1.3c, shows a component of the apparent power, in quadrature with the active power. This is the power exchanged in the energy conservative process described earlier. It is termed the **Reactive Power, Q,** and is measured in **Volt-Amperes reactive, VAr**.

Thus:

$$Q = S.\sin\phi = V_S I_S.\sin\phi \qquad (1.10)$$

Note that it is the product of the rms voltage and the *negative* of the current component $I_S\sin\phi$ in **Fig 1.3b**. The sign is used to conform to convention so that when ϕ is positive (lagging current), sinϕ is positive and hence the reactive power Q. The situation described is therefore one in which the load is absorbing reactive power. The apparent power S and active power P lead to the useful and perhaps more fundamental definition of the power factor as

Power Factor = Active Power / Apparent Power (1.11)

The power factor is therefore a measure of the *utilisation* of electrical energy by a given load.

1.2 - THE PROBLEM OF SUB-UNITY POWER FACTORS

A large percentage of all a.c. machinery operates at sub-unity power factor and does so at lagging rather than leading power factor. Examples include:

- Transformers
- Arc Furnaces
- Welding installations
- Neon signs
- Fluorescent lighting
- Semiconductor converters

The range of motor driven equipment is wide and diverse. An important feature of this group though, is that the majority is induction motor driven and indeed about 80% of all motors used in domestic and industrial appliances are a.c. induction motors, single phase and 3-phase [Matsch, 1977, Chalmers, 1984].

The 3-phase induction motor is very popular on account of its various amicable properties listed in chapter 5. However, it operates at rather poor lagging power factors, typically in the range 0.7 to 0.95 thus giving rise to the presence of reactive power on the transmission system, which has the following implications:

a) The generation and transmission system carries the extra current, leading to higher network losses (I^2R) and so imposes limitations on the system thermal capacity.

b) The extra current produces additional losses in the generator and transformer windings leading to undesirable heating.

c) Transmission of reactive power requires that the generator end of the transmission system is at a higher potential than the load end. The higher voltage has implications on the insulation requirements.

d) To generate the higher voltage in c) above, the generators require extra excitation, and this leads to increased voltage drop per ampere turn.

The work described in this text seeks to apply a relatively new technology to the problem of poor power factor in induction machines. Applied successfully, such control could further reinforce the machine's popularity and in terms of reactive power, improve the quality of power on the transmission system as a whole.

1.3 - THE PRINCIPLE OF COMPENSATION

Consider again the vector diagram of **Fig 1.3b**.
If a current $-I_S \sin\phi$ were introduced at some suitable point in the circuit it should effectively neutralise the reactive component, hence Q. Such an arrangement would cause the active power P to equal the apparent power S, and the situation corresponds to a case where the supply current is not only *in phase* with the supply voltage but is the *minimum* required for useful energy conversion.

A capacitive effect is required of the compensator for lagging power factor load, and an inductive effect for a leading power factor load. In either case, the compensator's role is to produce as much capacitive or inductive effect as is required to completely neutralise the reactive component of the supply current. **Fig 1.4** illustrates a typical compensation scheme and depicts a three phase voltage source delivering power to a sub-unity power factor load.

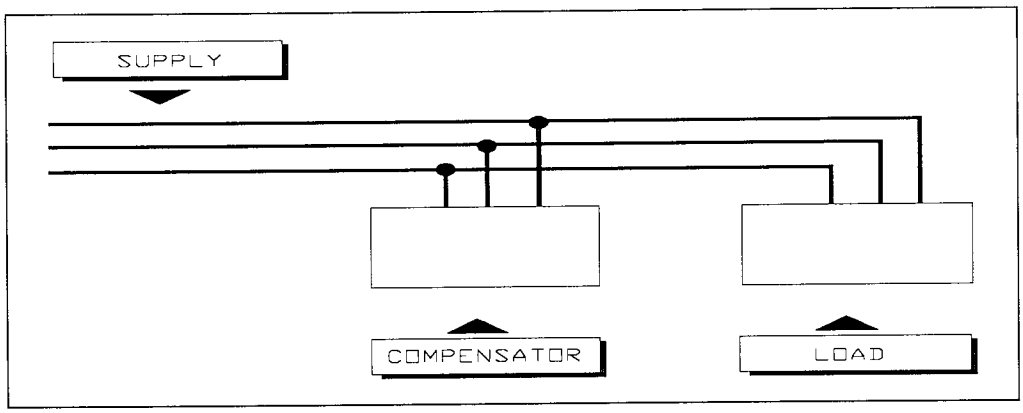

Fig 1.4 - Illustration of the compensator in circuit

The compensator is said to be *generating* reactive power if it is producing a capacitive effect, and *absorbing* reactive power if inductive.
In either case, the power supply system upto the compensator is ideally void of any reactive power and supplies only as much current as is required for the useful energy conversion within the load.

Since there is no alteration to the basic load characteristics, or the voltage across its terminals, the load continues to draw the same lagging current. The impact of the compensator is therefore on the current sourced by the supply and this description highlights the need for appropriate siting of the compensator.

In this thesis, the term *sub-unity* will refer to *lagging* power factor unless otherwise stated. Also, *reactive power compensation* and *power factor correction*, will be distinguished based solely on the location of the compensator thus:

> ***Reactive power compensation*** will be taken to refer to a situation where the compensator is located at some suitable point and intended to compensate for reactive power on the supply and transmission system rather than a particular load.
>
> ***Power factor correction*** will apply to a situation where the compensating equipment is located at the load where the effect is required. In practice, this is usually a section of plant or a particular installation such as an electric arc furnace, transformer or induction motor.

Equipment siting remains a debatable issue in compensation technology but is less complicated for power factor correction i.e. as near the load as possible.

1.4 - TYPES OF COMPENSATOR

There are a number of different types of equipment that can be used to achieve reactive power compensation, but not all make sensible choices for power factor correction, especially when the load is a single installation rather than a section of plant. Examples of general compensators include:

1.4.1 - Capacitors

A capacitor can compensate for a lagging power factor load and is the most widely used scheme in use today. Sizing of the capacitors is important, especially when effecting power factor correction for a single machine rather than a section of plant [Longlund et al., 1992]. This is because under-sizing implies inadequate compensation while over-sizing sometimes leads to destructive self-excitation of the machine when the machine and compensator are isolated as a unit.

Advantages include reliability, robustness and low maintenance requirements.
However, the capacitors are usually bulky and installation is demanding, often requiring good electrical isolation. Also, the amount of compensation is fixed by capacitor size, and the capacitor can only compensate for lagging power factor loads. Depending on size, these devices can also be expensive.

1.4.2 - Synchronous generators

Controlled excitation of the field winding of a synchronous machine leads to controlled reactive power generation or absorption in the armature winding, hence supply.
Advantages include the variable amount of compensation, controlled by the excitation, ability to compensate for leading and/or lagging power factors.

The main disadvantages include high capital cost, high maintenance and installation requirements and excitation losses. The machine is bulky and runs continuously, often housed in a central location and not used for much else.

1.4.3 - Thyristor Switched Capacitors (TSC)

This scheme employs power semiconductors (usually thyristors) to switch as many capacitors into the compensation as are required to meet the reactive power demand present at any time. **Fig 1.5** shows a TSC in circuit.

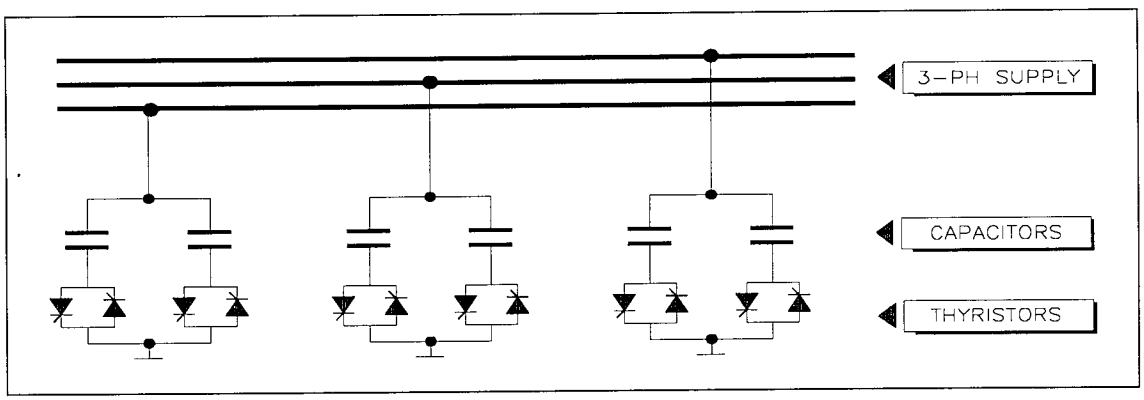

Fig 1.5 - Elementary 3-phase thyristor switched capacitor compenstor

1.4.4 - Thyristor Controlled Reactors (TCR)

This scheme uses inductors as the reactive element, and control is by way of varying the instant at which a fixed inductance is switched into the circuit.

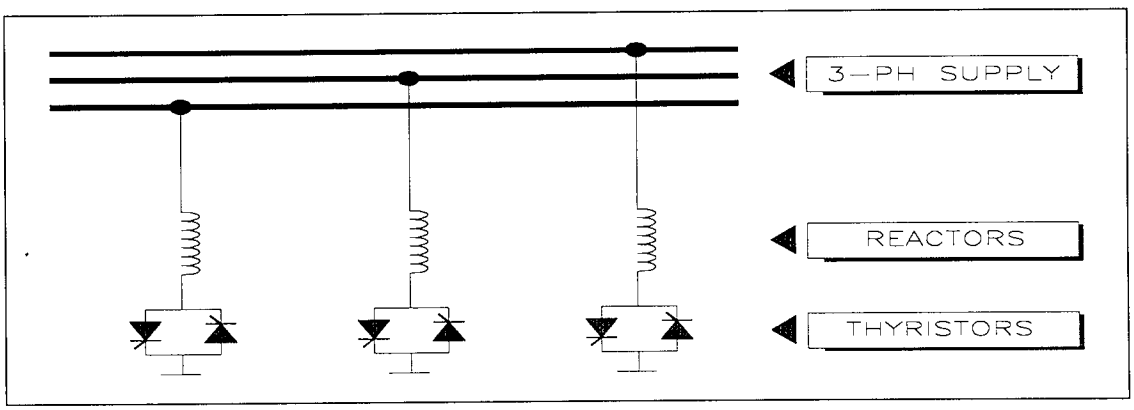

Fig 1.6 - Elementary 3-phase thyristor controlled reactor compensator

The TSR and TCR compensators sometimes require the use of step-down star-delta transformers or a low voltage tertiary winding on a high voltage transformer between the supply and the compensator when the supply voltage is very high, but these can significantly affect the performance of the compensator and are avoided if possible [Miller, 1982, chapt 4]. A practical version of the TCR often incorporates switched shunt capacitors in parallel and sometimes requires tuned filters.

1.4.5 - The Converter Compensator

Sometimes called the Static Converter (STATCON), Static Compensator (STATCOM), Static VAr Generator (SVG), Advanced Static VAr Generator (ASVG) and Advanced Static VAr Compensator (ASVC), this compensator is one of the solid state power converters belonging to the general family of what are termed Flexible A.C. Transmission Systems, or FACTS for short [Gyugyi et al, 1993]. This thesis adopts the term STATCON.

The STATCON comprises a power electronic bridge inverter with integrated rectifier and is capable of generating and/or absorbing reactive power using a single control parameter.
There are essentially two types of such compensators depending on the nature of the energy store which also affects their bridge topology. They are either:

> ***Voltage sourced*** - in which a capacitor is used as an energy reservoir or
> ***Current sourced*** - in which an inductor is the energy store.

Of the types of compensator discussed above, only the fixed capacitor has been extensively used for power factor correction of individual motors. As this technology is long established, the considerations made in installing the equipment are discussed, with a view to outlining how the intended application of the STATCON compares.

In principle, the TSC and TCR compensators can be used, especially where the motor terminal voltage is low enough to permit the direct coupling of the reactive elements without step-down star-delta transformers. However, a common feature of the latter schemes is that of generated harmonics, these being a general characteristic of power semiconductor switching. The switching transients can be severe and are an important consideration in designing these systems.

1.5 - GENERAL AIMS

The work described in this text aims at studying the feasibility of applying the multiple phase STATCON to reactive power compensation in cage rotor induction machines. The underlying concept hinges on the fact that the stator winding of the induction motor can be a source of polyphase voltages. The work is largely qualitative and seeks to assess the ***practicability*** of the proposed scheme, to establish the ***limitations*** of the scheme, the ***implications*** on the machine design and finally to assess the ***suitability*** of the scheme in general by assessing the performance of the compensated machine.

1.6 - NOMENCLATURE

Power factor is referred to extensively throughout the text and has been at times abbreviated to **PF**.

'**STATCON**' has been used to describe the converter compensator, complete with control circuit and power semiconductor bridge. Where reference to the power converter stage only is desired, the term '**bridge**' applies.

'**Coupling**' and '**Magnetic coupling**' have been used to describe the inductance connecting the STATCON to the power supply. It usually adopts the form of a transformer system and has sometimes been referred to as '**magnetic interface**' by others.

'**Compensator**' will be taken to refer to equipment installed specifically for the purpose of reactive power compensation or power factor correction.

1.7 - SUMMARY

This chapter presents a definition of the power factor and explains the concept of reactive power.

The problems associated with reactive power flow in electrical energy transmission are listed, from both a technical and economical view point. The induction motor is also identified as a major contributor to the problem.

A distinction is made between reactive power compensation and power factor correction, for although the principle is the same, there are aspects of reactive power compensation that are not entirely relevant to power factor correction.

The chapter lists some methods of achieving reactive power compensation, and cites the static capacitor as one extensively used both in reactive power compensation and power factor correction applications.

A summary of the general aims of this thesis is given and some key terms are introduced.

CHAPTER 2

THE VOLTAGE SOURCED STATCON

This chapter introduces the STATCON and the terminology used in the remainder of the text. It presents an elementary model of a generic compensator which is then developed into the actual STATCON. The work done on STATCONs was by way of simulation, design and construction of an experimental 24-pulse model. The analyses leading to the formulation of a control philosophy based on firing angle were done by other members of the research group pioneering investigations into related concepts. Relevant aspects of some of their conclusions are included in this thesis to help make the discussions complete.
The discussion includes the single phase STATCON and 3-phase 6-pulse STATCON, but only in brief, presenting simulation results and explanatory notes as supportive background to the 24-pulse STATCON and as a way of introducing performance parameters and highlighting the problem of harmonics. The 24-pulse STATCON is described in greater detail in chapter 3.

2.1 - PRINCIPLE OF OPERATION

Consider the elementary circuit of **Fig 2.1** and let v_1 be a sinusoidal voltage source of peak value V_0 and angular frequency ω. Also, let r be some finite non-zero value of source resistance (small) and suppose R and L to represent some lagging power factor load across which appears some voltage V_x. A practical transmission system has some associated source inductance and capacitance but these are ignored for the purpose of this discussion.

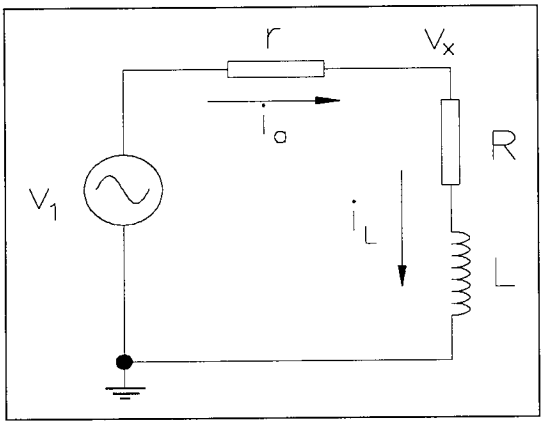

Fig 2.1 - Sinusoidal voltage source feeding lagging power factor load

If the voltage v_1 is described by $v = V_0 \sin\omega t$, then the current i_L through the load will lag the voltage by some angle ϕ, so that if I_0 is the peak value of this current, then:

$$i_L = I_0.\sin(\omega t - \phi) \qquad (2.1)$$

For the case shown, the supply current i_a is the same as the load current i_L and the phasor diagrams are consistent with those of **Fig 1.3**. **Fig 2.3a** shows the current resolved into its phase and quadrature components as before.

In **Fig 2.2**, an independent current source I_S of the same frequency as v_1 is connected as shown. Suppose it is a requirement that the load terminal voltage v_x is not affected by the presence of the current source so that the same current i_L flows.

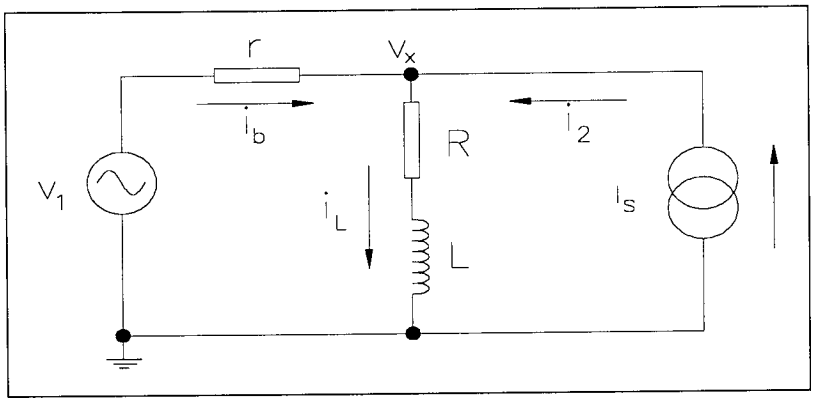

Fig 2.2 - Load supplied by voltage source and additional independent current source

Since v_x is the same, the current i_L for both **Fig 2.1** and **Fig 2.2** is such that:

$$i_L = \frac{v_x}{R + j\omega L} \qquad (2.2)$$

If i_2 (of magnitude I_2) is supplied in phase with i_L, then both sources contribute towards the active and reactive power demands of the load. **Fig 2.3b** illustrates this. The net result is a reduction in the *total* current sourced by v_1, at constant phase angle. Thus, the source v_1 still supplies reactive current. A second consequence of such an arrangement is that the current source needs to supply real power.

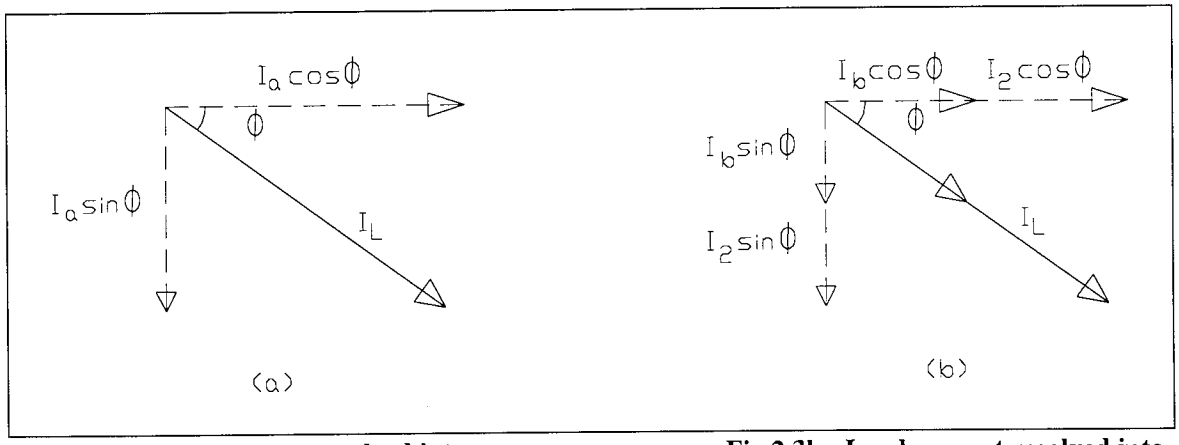

Fig 2.3a - Load current resolved into phase and quadrature components when supplied by v_1 alone

Fig 2.3b - Load current resolved into phase and quadrature components when supplied by v_1 and I_2

If the *phase* of i_2 is adjusted so that it is in phase with the reactive component of i_L, then it has no component in phase with the terminal voltage v_x, and therefore does not contribute towards the active power demands of the load. If i_2 is set so that $i_2 = |\, i_L \,|\sin\phi$, then v_1 need only supply the current required to meet the active power demands. Such a case corresponds to unity power factor viewed from the voltage source. At unity power factor,

$$i_a = |\, i_L \,|.\cos\phi \qquad (2.3)$$

The phasor for such an arrangement would be the same as that of **Fig 2.3a** with $i_a\cos\phi$ replaced by i_a and $i_a\sin\phi$ replaced by i_2.

Any surplus or deficit in the reactive current has to be balanced by v_1. Thus, i_2 is the fundamental control parameter for the supply current i_a in this description.

The magnitude of the supply current i_a can therefore be altered by changing either the phase or the magnitude of i_2.

2.1.1 - Control by Phase

As described previously, a change in phase angle of the current source from phase to lagging causes the total current sourced by v_1 to decrease and approach that required to meet the active power demands only.

2.1.2 - Control by Magnitude

Varying the magnitude of the current supplied by the current source while the phase is maintained at 90° (lagging) also sees a change in the magnitude and phase of the current sourced by v_1.

It is generally possible to emulate a current source with a voltage source and some intermediate circuitry. **Fig 2.4** shows such an arrangement.

For constant v_x and for i_2 to be in quadrature with the reference source v_1 requires that the coupling impedance has the appropriate transfer function i.e. an inductor, ideally of low series resistance to minimise active power dissipation in the coupling i.e. losses.

In **Fig 2.4**, the current source of **Fig 2.2** is been replaced by a voltage source of controllable output magnitude and phase, and an inductor L_2, shown with some *small* value of resistance

r_2 which models the winding resistance of the physical inductor and whatever resistance may exist in the path of the current i_2.

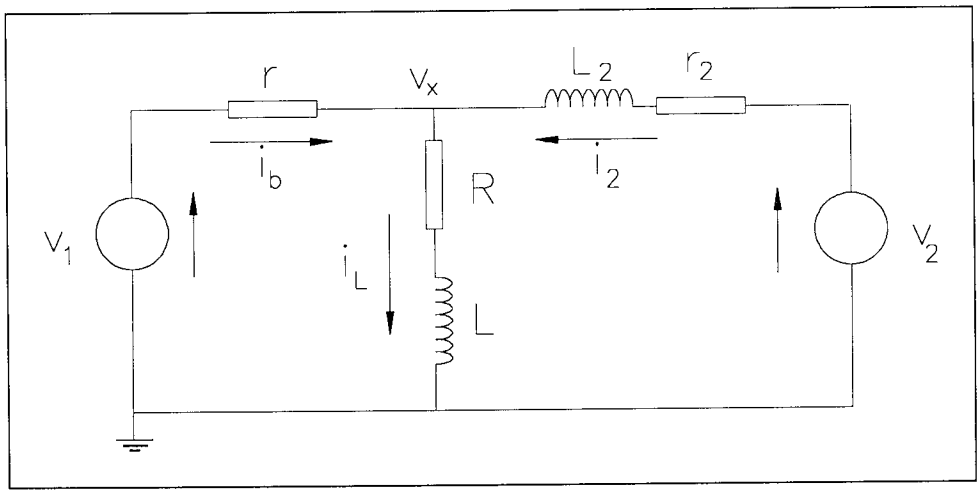

Fig 2.4 Load supplied by direct and inductively coupled voltage sources

Assume $$v_2 = V_2\sin(\omega t + \alpha) \qquad (2.4)$$

Altering V_2 and/or angle α causes the current i_2 , hence i_b to change as required.
Control by phase variation entails an element of active power generation requirement by the current source. Control by magnitude is ideally the preferred option whence

$$v_2 = V_2\sin\omega t \qquad (2.5)$$

Working on the premise that the voltage v_x should not be unaltered by the additional circuitry, the current i_2 through the coupling reactor L_2 is a function of the potential difference across it. This is the voltage v_2 - v_x. Thus:

$$i_2 = \frac{v_2 - v_x}{r_2 + j\omega L_2} \qquad (2.6)$$

For the purpose of qualitative analysis, the assumption $\omega L_2 >> r_2$ may be made, so that i_2 is a current leading or lagging v_2 - v_x by 90°.

For such a case,

$$i_2 = \frac{v_2 - v_x}{j\omega L_2} = -j.\frac{v_2 - v_x}{\omega L_2} \qquad (2.7)$$

Since $v_2 = V_2\sin(\omega t)$ and $v_x \approx V_1\sin(\omega t)$, it follows v_2 - $v_x = (V_2\text{-}V_1)\sin(\omega t)$

Thus, $$i_2 = -j.\left(\frac{v_2 - v_1}{\omega L_2}\right).\sin \omega t \qquad (2.8)$$

Substituting $A_0 = \frac{v_2 - v_1}{\omega L_2}$ leads to the more concise expression:

$$i_2 = -j.A_0.\sin\omega t \qquad (2.9)$$

When $v_2 > v_1$, $i_2 = -jA_0\sin\omega t = A_0\sin(\omega t - \pi/2)$ i.e. lagging v_1 by 90°
When $v_2 < v_1$, $i_2 = --jA_0\sin\omega t = A_0\sin(\omega t + \pi/2)$ i.e. leading v_1 by 90°

The presence of r_2 causes the current i_2 to have an amplitude of less than A_0 and a phase shift of less than 90° as shown in the next section.

The load current comprises active and reactive components and lags the terminal voltage. For constant R and L, the magnitude of this current is determined only by the voltage v_x.

When $v_2 > v_x$, the compensator behaves as the load's source of reactive power. Excess current is sunk by the supply v_1, with the result that the supply current i_b is *leading*.

When $v_x > v_2$, all the load's reactive power requirements have to be met by the supply v_1. In addition, since there is reactive current flow in the direction $v_x \rightarrow v_2$, this current has to be sourced by the supply as well. The result is that i_b is a *lagging* current whose magnitude depends on how much i_2 is less than $|I_L|.\sin\phi$.

This is the principle of compensation of the voltage sourced STATCON. The system effectively generates a voltage of controllable magnitude in phase with the supply, and sources or sinks current in quadrature i.e. reactive.

Inserting an inductor in series with the source resistance r alters the overall phase angle between supply current and voltage, but with sufficient voltage v_2, the compensator can still produce leading and lagging effects in the supply, and so may be regarded as being capable of injecting reactive current between the inductors. This of relevance to the case of a stator winding. The STATCON goes further and makes use of the fact that *reactive power is conserved* in that it uses a passive reactive element to act as an energy reservoir, and so replaces the voltage source v_2 of **Fig 2.5** with a capacitor and an inductively coupled inverter with integrated rectifier.

Fig 2.5 shows the block diagram of a generic STATCON connected to a supply.

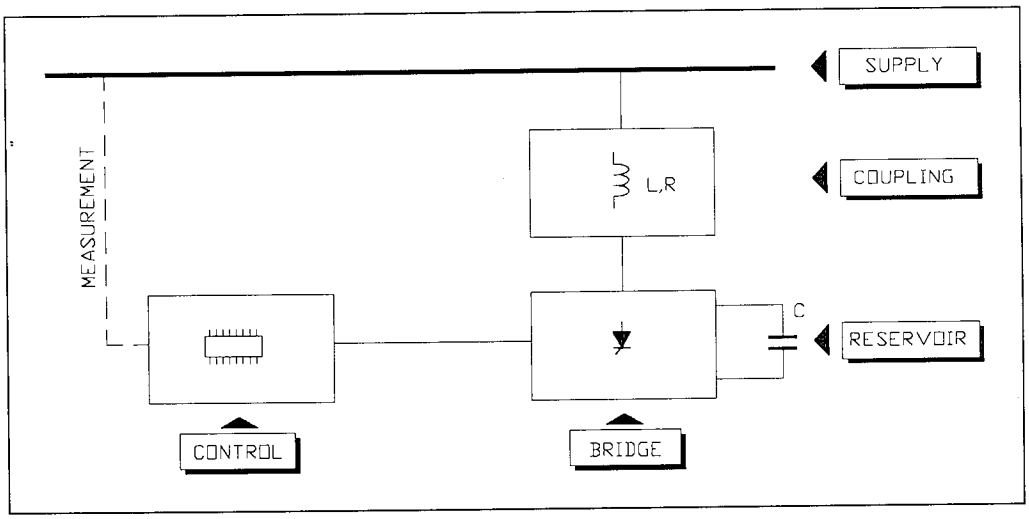

Fig 2.5 - Block diagram of generic STATCON with capacitor store

The capacitor charges through a full wave rectifier. An inverter generates the a.c. voltage v_2. Both rectifier and inverter are connected to the supply via the coupling reactance shown. The capacitor voltage features superimposed ripple which has implications on the output waveform and the type of capacitor.

The coupling assumes different topologies depending on the desired pulse number which in turn affects the number of devices in the bridge.

An important characteristic feature of the STATCON utilising a power semiconductor bridge to generate the in-phase a.c. voltage is that its output voltage is *non-sinusoidal*, and this gives rise to harmonics, apparent in the supply current i_a and potentially, the load voltage v_x.

2.2 - STATCON PERFORMANCE PARAMETERS

Simulations of the single phase and three phase six-pulse STATCONs are included here to present the problem of inverter harmonics and to introduce relevant performance parameters.

In order to function as intended, the compensator needs energy storage components to source and sink the reactive power as required. These are almost invariably inductors and capacitors whose sizes depend on the desired rating and performance. There is a threshold value of the combined energy storage capacity below which the compensator fails to provide the required reactive power and where the capacitor fails to charge to some positive average voltage, the switching of the inverter in effect short circuits the connected phases. Thus, fundamental to the performance of the STATCON are the following parameters:

C - size of the reservoir capacitor
L - size of the coupling inductance
f - supply fundamental frequency from whence $\omega = 2\pi f$ as before
R - *effective* series resistance in the path of the compensator current.
α - delay or firing angle

Analysis of the steady state performance of the voltage sourced STATCON [Hill, 1995] leads to definition of a parameter k and its reciprocal M which are based on the values of the energy storage components. In general, once the pulse number and coupling circuit topology are known, M (which is usually less than unity) is chosen large enough to give good control and few harmonics. Thus:

$$k = \sqrt{\lambda \frac{X_c}{X_L} - \beta^2} \qquad (2.10)$$

and:

$$M = k^{-1} \approx \sqrt{X_L . Y_C} \qquad (2.11)$$

where:

λ is a constant accounting for pulse number and coupling circuit topology
X_C is the reactance of C at fundamental frequency and Y_C its susceptance.
X_L is the reactance of L at fundamental frequency
β is a damping factor given by: $\beta = \frac{R}{2X_L}$ (2.12)

- ε - angle by which inverter current deviates from 90° due to resistance

$$\varepsilon = \tan^{-1}(R / X_L) \qquad (2.13)$$

In design, M is the more fundamental parameter, usually selected from graphs such as that of **Fig B-5** shown in appendix B. The graphs exhibit minima at characteristic integer values of k which Hill [1995, pp 172] states is of significance and that in general, circuits resonant at their pulse number give poor performance.

In the circuit diagrams that follow, the generic symbol for a thyristor has been used to denote any three terminal power semiconductor with forced commutation capability.

2.3 - THE SINGLE PHASE VOLTAGE SOURCED STATCON

Fig 2.6 shows the practical arrangement of a single phase voltage sourced STATCON. The bridge is connected across a capacitor C and coupled to the supply by the inductor L_c assumed of some small finite non zero winding resistance R_c. The bridge will be seen to comprise an inverter with an integrated full-wave rectifier.

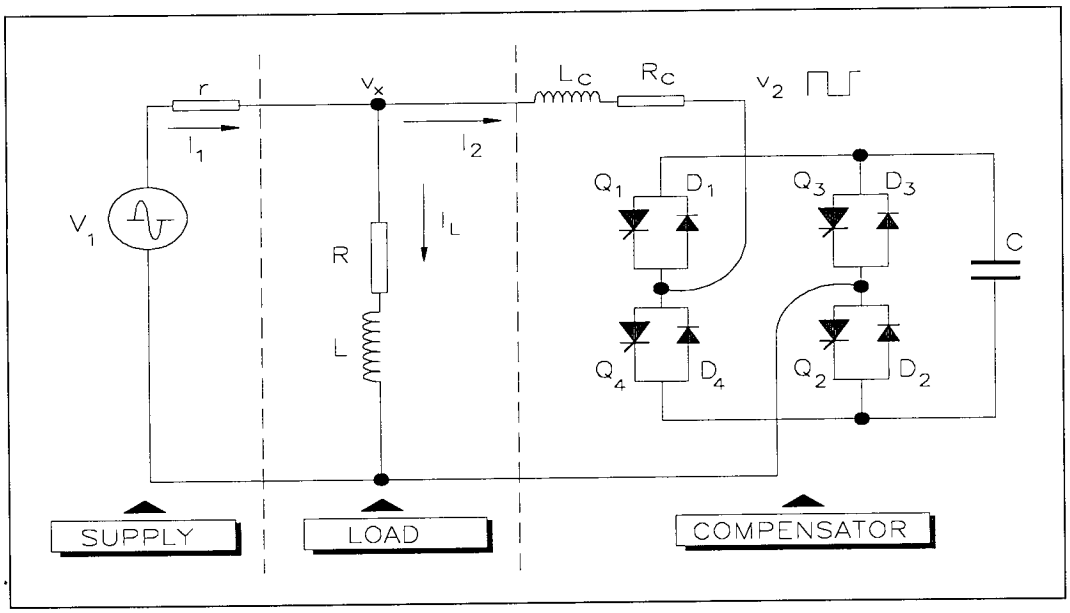

Fig 2.6 The basic single phase voltage sourced STATCON in circuit

2.3.1- OPERATION

The devices are switched in the sequence they are numbered, with diagonal pairs conducting simultaneously for a complete half cycle of the supply fundamental.

If it is assumed that the capacitor voltage stays constant over the complete cycle for a fixed control parameter, then the inverter output voltage is a square wave controlled to the same fundamental frequency as the supply. It has a fundamental component whose peak voltage V_i is, from a fourier series expansion, given by $\mathbf{V_i = 4V_2/\pi}$. V_2 is the average d.c. value of the capacitor voltage. The fundamental component of the voltage across the coupling impedance, earlier given as $v_2 - v_x$ in the model, becomes

$$V_i - V_o$$

where V_o is the peak voltage of the supply fundamental.

If V_s and V_2 are the rms values of the supply and inverter output fundamentals, then the conditions $V_2 > V_s$ for a leading current and $V_2 < V_s$ for a lagging current are given the phasor diagram of **Fig 2.7**, primarily to show the currents.

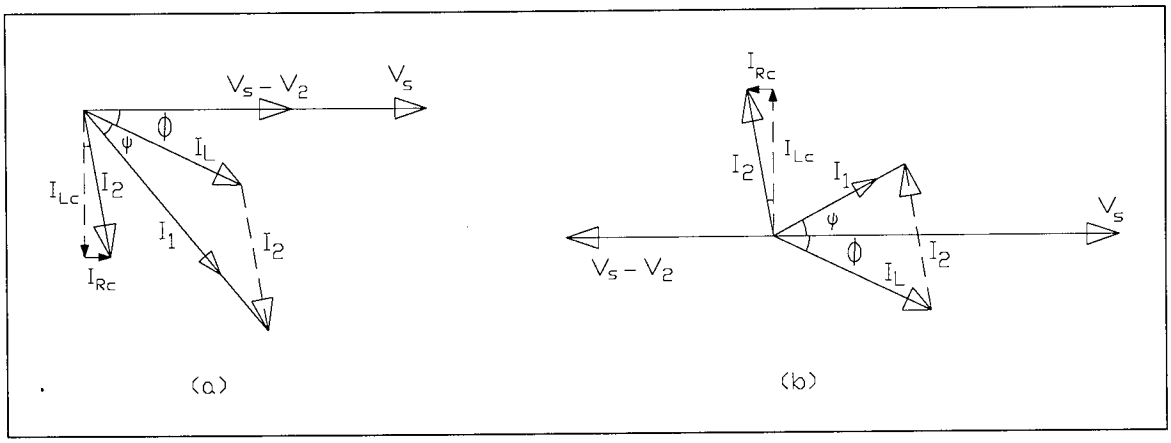

Fig 2.7 Phasor diagrams to show the currents for a) $V_s > V_2$ and b) $V_s < V_2$

2.3.2 - Notes

• The phasors are applicable to any pulse number STATCON as long as V_i is taken to be the *fundamental* component of the generated output.

• The load current I_L lags the supply voltage V_s by the angle ϕ for both cases.

• The current I_2 lags the voltage V_s-V_2 across the coupling impedance by slightly less than 90° because of the finite series resistance R_c of the reactor (c.f. Eqn . **2.13**)

• The current I_2 comprises an active component I_{Rc} in phase with V_s - V_2 as a result of the coupling resistance R_c, and a much larger (by design) reactive component I_{Lc} due to the coupling inductance L_c.

• Depending on the potential difference V_s - V_2 across the coupling impedance, the supply current I_1 may lag the supply voltage (**Fig 2.7a**), lead (**Fig 2.7b**) or be in phase.

To control the magnitude of the capacitor voltage, the square wave output of the inverter is generated slightly out of phase with the supply, within a narrow range of angles roughly centred about zero. This technique provides a controllable voltage across the capacitor which can be greater than, equal to or less than the supply. Inverter output control itself is achieved by firing the power devices at the desired instant before or after supply zero cross i.e. adjusting the *delay angle* α. Thus, some active power is absorbed by the system, evident as delay angle dependent losses. This text uses positive and negative values of α for post and pre zero cross delays respectively.

Fig 2.8 below shows a timing diagram for some arbitrary positive delay angle α.

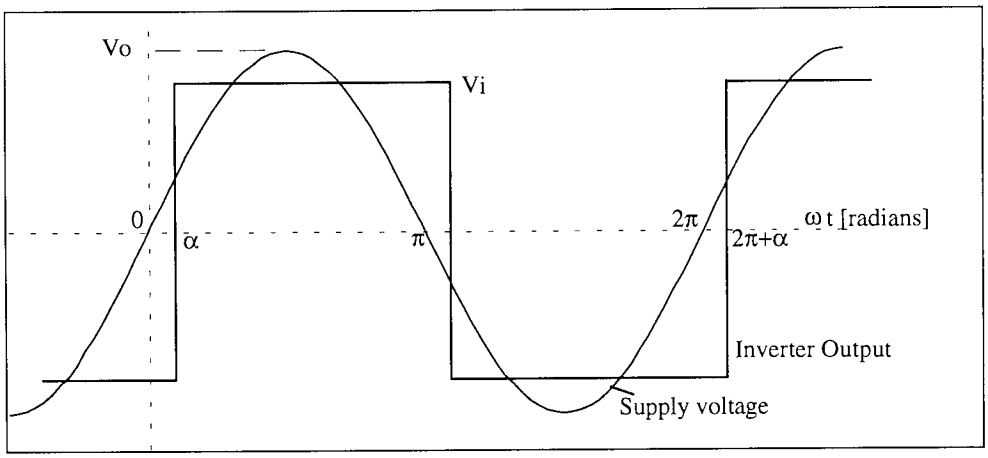

Fig 2.8 Timing diagram for a positive delay angle (magnitudes not to scale).

2.3.3 - Simulations of the Single Phase STATCON

Consider a single phase voltage sourced STATCON with the following parameters:

Supply voltage to neutral = 140V rms = 1 p.u.
Rated power = 1 kVA = 1 p.u.

$f = 50$ $\omega = 100\pi$

$X_L = 0.64$ p.u. $R = 0.05$ p.u.

$\beta = R/2X_L = 0.04$

Choose $M = 0.707$ to give $k \approx \sqrt{2}$.
$\lambda = 1$ for such an arrangement [Hill, 1995], hence

$$X_C = \frac{X_L}{\lambda}(k^2 + \beta^2) = 1.28 \text{ p.u.}$$

Further, from the analyses referred to in describing the parameters M and k, Hill [1995, pp 74] shows that the maximum active power P_m, depicting the losses in the equipment, and the maximum reactive power Q_m that the STATCON is capable of generating occur when the firing angle is 90° and are given by the approximate expressions:

$$Q_m \approx -\frac{V_o^2}{8\beta X_L} \tag{2.14}$$

$$P_m \approx \frac{V_o^2}{8\beta X_L} = -Q_m \tag{2.15}$$

Normally, these lossy conditions are avoided by restricting the firing angle to a few degress about zero.

The results of the simulation are shown for leading, lagging and unity power factor operation in **Fig 2.9** and **Fig 2.10**. In all cases, the supply voltage is used as the reference and shown as the dotted line.

The fundamental of the supply current and that of the inverter voltage is the component at 50Hz on their respective harmonic spectra.

Performance of such inverters has been documented by others [Hill, 1995; Moltgen, 1984].

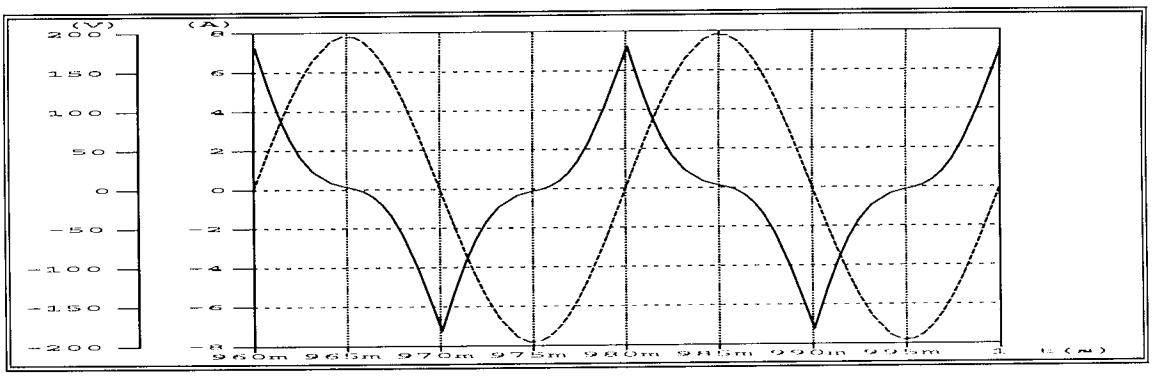

Fig 2.9a Supply Voltage (dotted line) and Current for a single phase STATCON - Leading

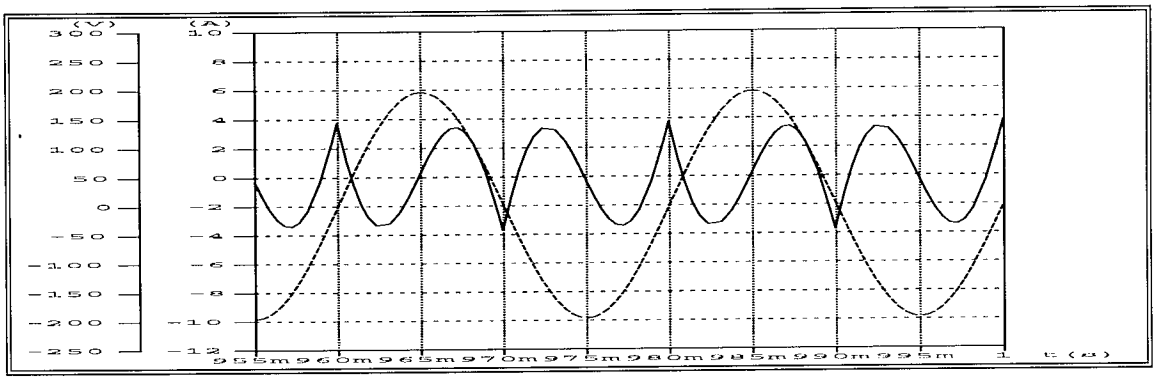

Fig 2.9b Supply Voltage (dotted line) and Current for a single phase STATCON - Unity PF

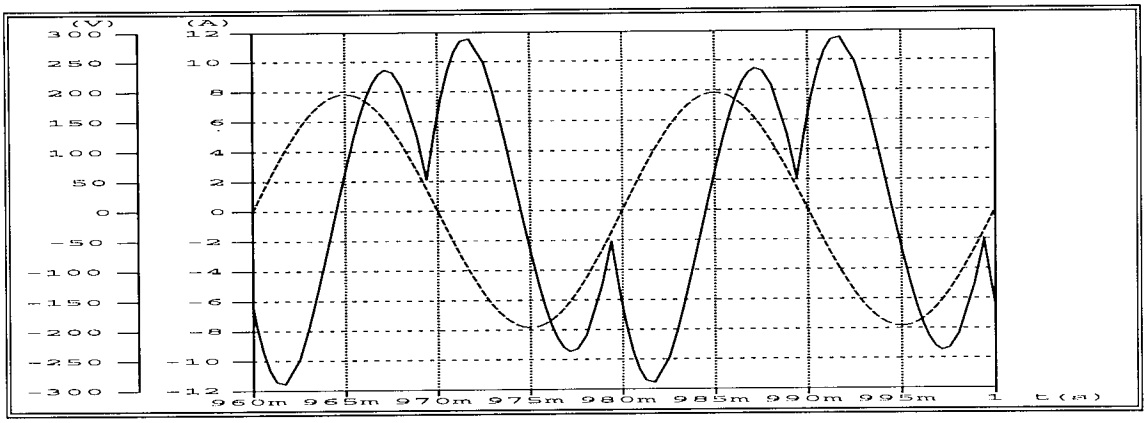

Fig 2.9c Supply Voltage (dotted line) and Current for a single phase STATCON - Lagging

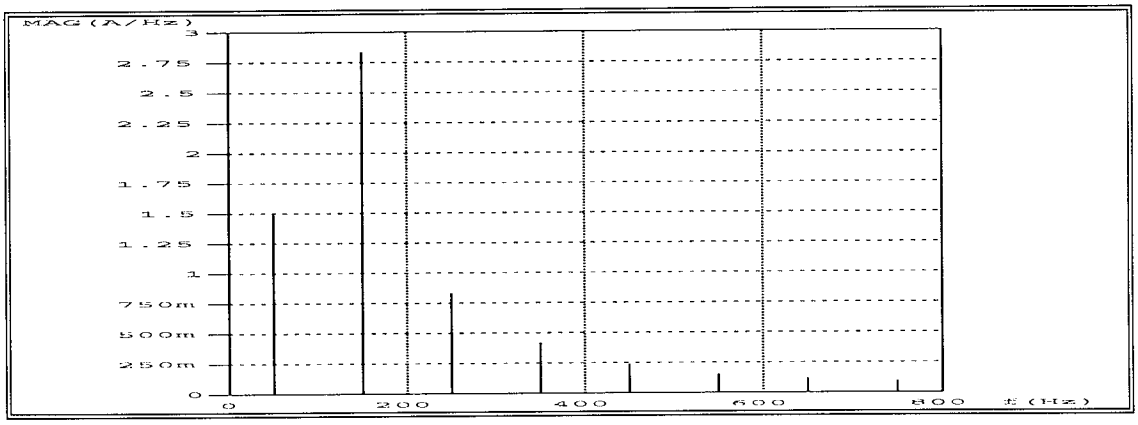

Fig 2.9d - Supply current harmonics for a single phase STATCON - Unity PF

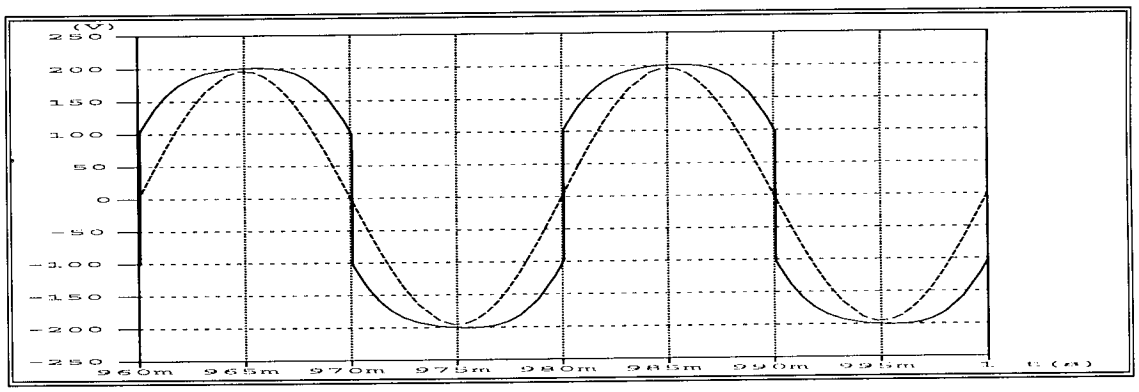

Fig 2.10a - Inverter output (solid line) for single phase STATCON - Leading

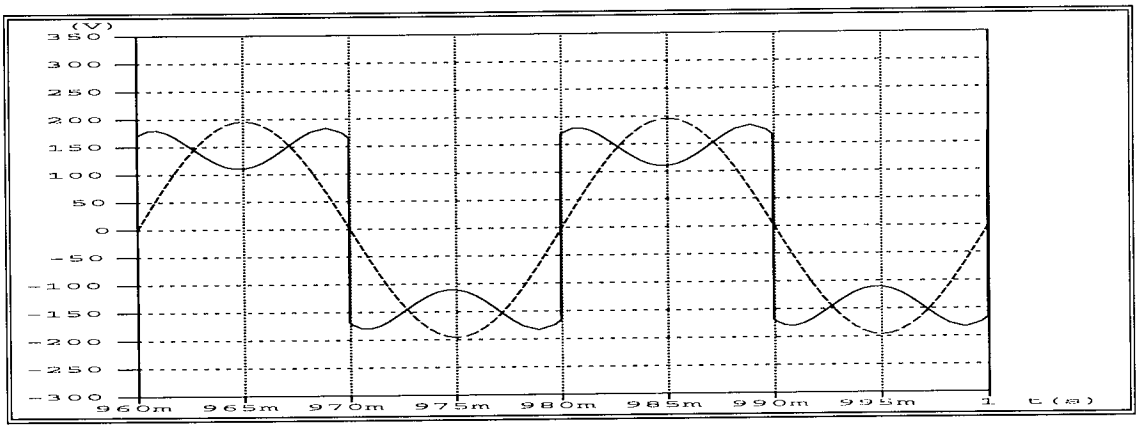

Fig 2.10b - Inverter output (solid line) for single phase STATCON - Unity PF

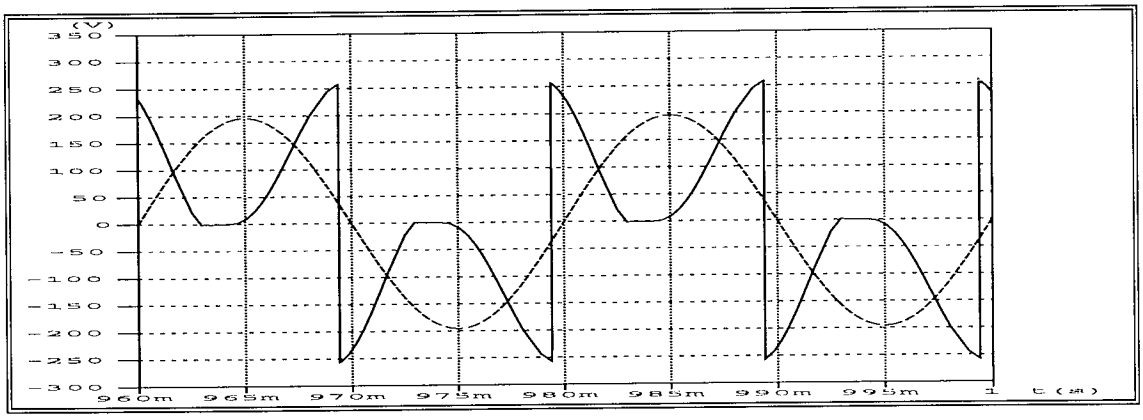

Fig 2.10c - Inverter output (solid line) for single phase STATCON - Lagging

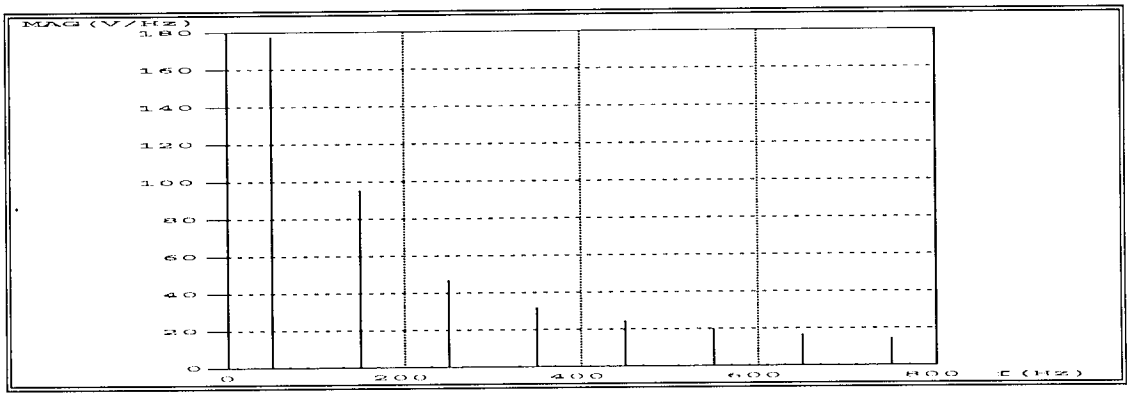

Fig 2.10d - Inverter output harmonics for a single phase STATCON - Unity PF

2.4 - THE BASIC SIX-PULSE VOLTAGE SOURCED STATCON

It is sensible to refer to a STATCON by pulse number rather than phase number for although the distinction between a single phase and three phase STATCON is meaningful, one can have different pulse numbers with three phase STATCONs.

Fig 2.11 shows a 3-phase 6-pulse STATCON in circuit.

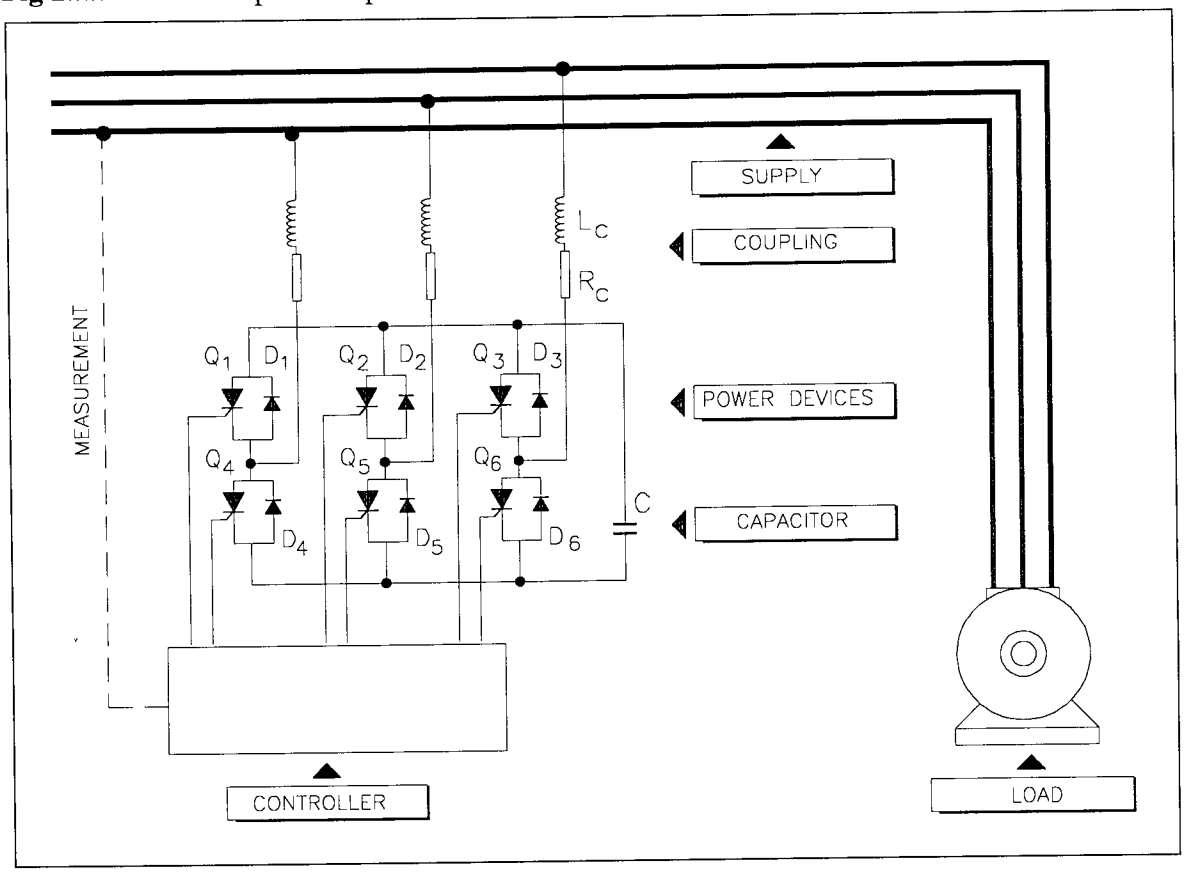

Fig 2.11 - A three phase six-pulse voltage sourced STATCON in circuit

2.4.1 - Operation

The devices are fired in the sequence shown, determined by the zero crossing of the connected phases. Thus, when the first phase connected between devices Q1 and Q4 crosses zero from a negative half cycle, device Q4 is switched off and device Q1 is switched on. The general state of the devices at any time can be determined from the state of the supply phases. Control is achieved by triggering the devices some instant just before or just after zero crossing. Triggering at precisely zero crossing should, in principle, have no effect on the load terminal voltage and current, but in reality, the harmonics generated by the STATCON at any firing angle do affect the waveforms.

2.4.2. - Simulations of the 6-pulse STATCON

Simulation was conducted for a leading, lagging and unity power factor current for a 6-pulse STATCON with the following parameters:

Phase to neutral voltage (= 140V rms) = 1 p.u.
Rated power (= 1000VA) = 1 p.u.

$X_L = 0.64$ p.u. $\quad X_C = 8$ p.u. i.e $Y_C = 0.125$ p.u. $\quad R_c = 0.05$ p.u.
$f = 50Hz \quad \omega = 2\pi f = 100\pi$

$\beta = R_C/2X_L = 0.05/(2 \times 0.64) = 0.04$

$\lambda = 2/3$ for this arrangement [Hill, 1995] whence:

$$k = \sqrt{\frac{2X_c}{3X_L} - \beta^2} = \sqrt{\frac{2 \times 8}{3 \times 0.64} - 0.04^2} \approx 3 \qquad (2.16)$$

Thus, $m = 1/k = 0.33$

Fig 2.12 gives the results of simulation of the above circuit in the absence of the load
In **Fig 2.12**, the 'phase voltage' refers to the supply *phase to neutral* voltage. In all cases, the voltage is sinusoidal and is shown as the dotted line.

The performance of the six pulse voltage sourced inverter has been detailed by others [Hill, 1995; Hill, Norris, 1994; Moltgen, 1984].

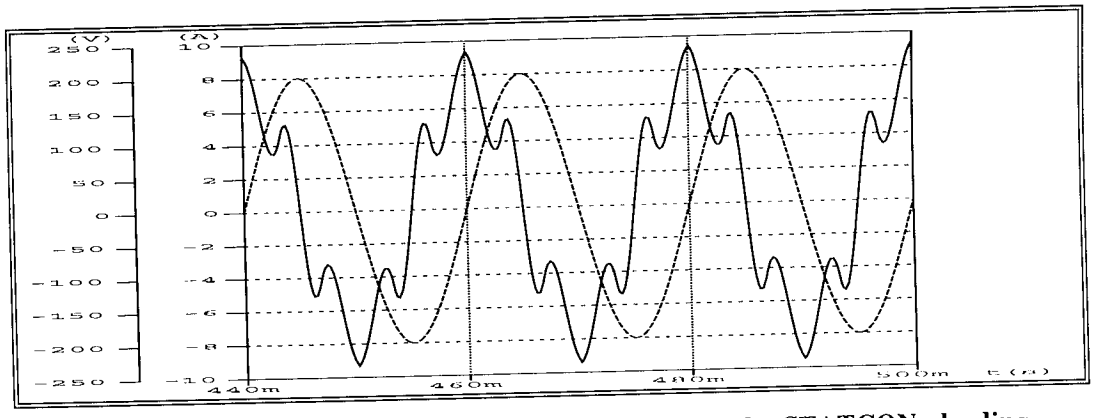

Fig 2.12a - Phase voltage (dotted line) & current for a 6-pulse STATCON - leading

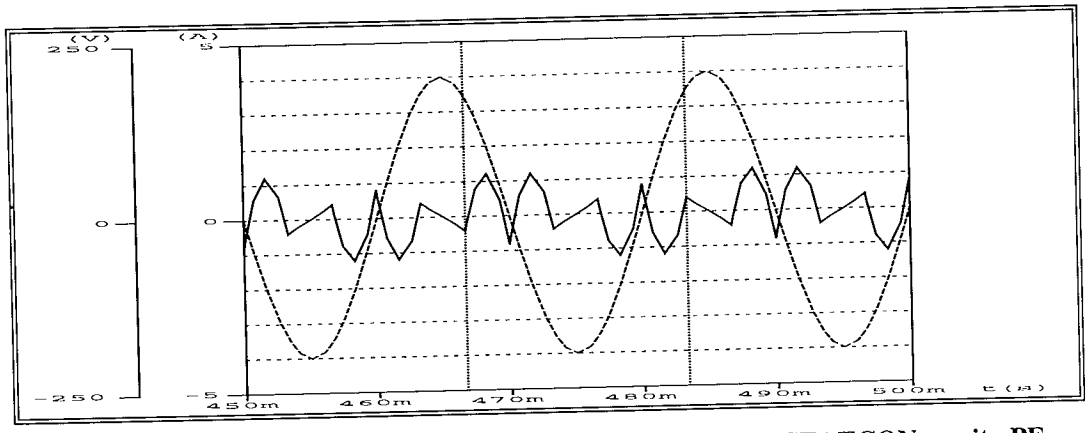

Fig 2.12b - Phase voltage (dotted line) & current for a 6-pulse STATCON - unity PF

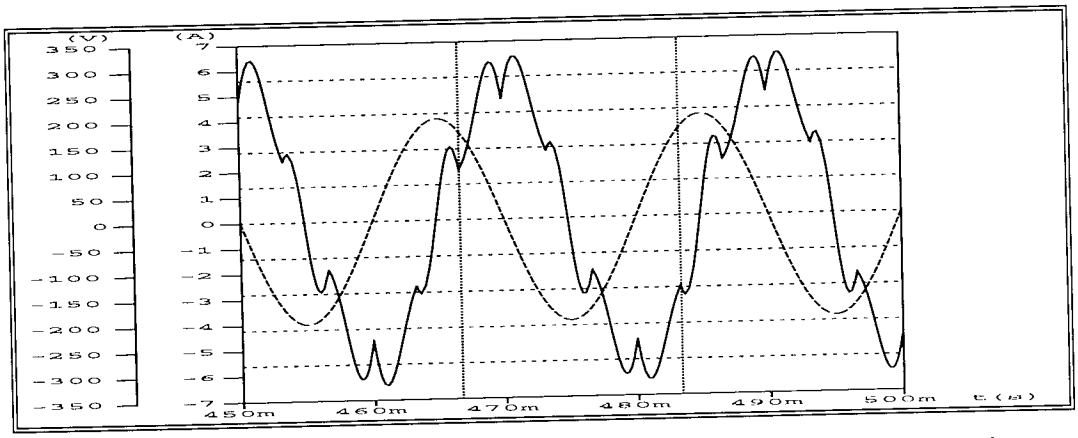

Fig 2.12c - Phase voltage (dotted line) & current for a 6-pulse STATCON - lagging

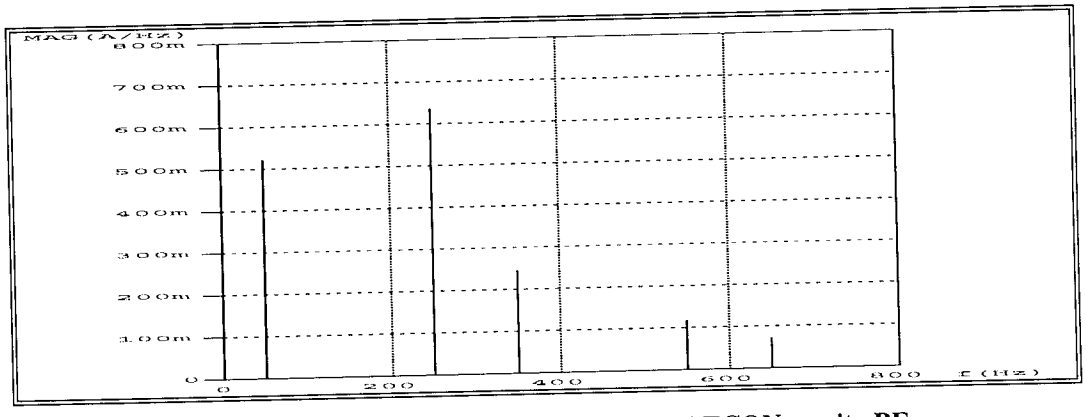

Fig 2.12d - Phase current harmonics for a 6-pulse STATCON - unity PF.

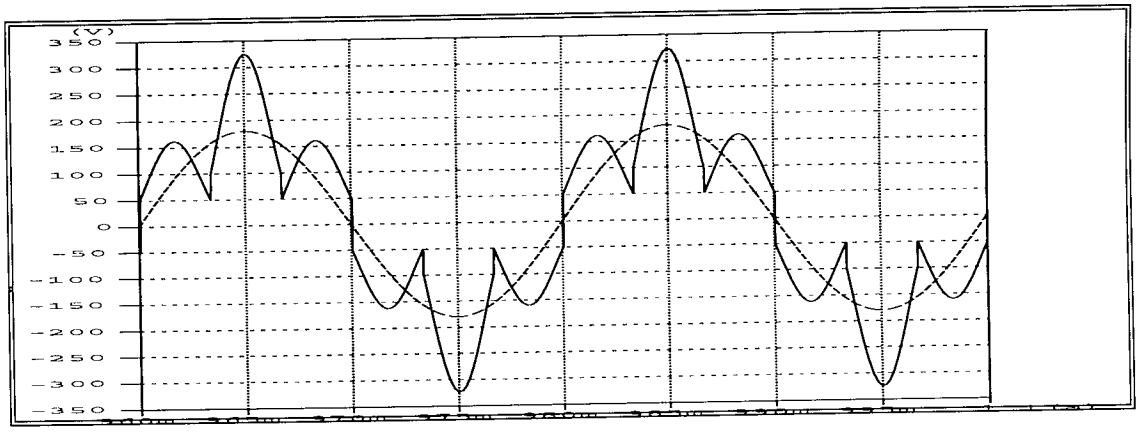

Fig 2.13a Inverter output (solid line) and phase voltage: 6-pulse STATCON - leading

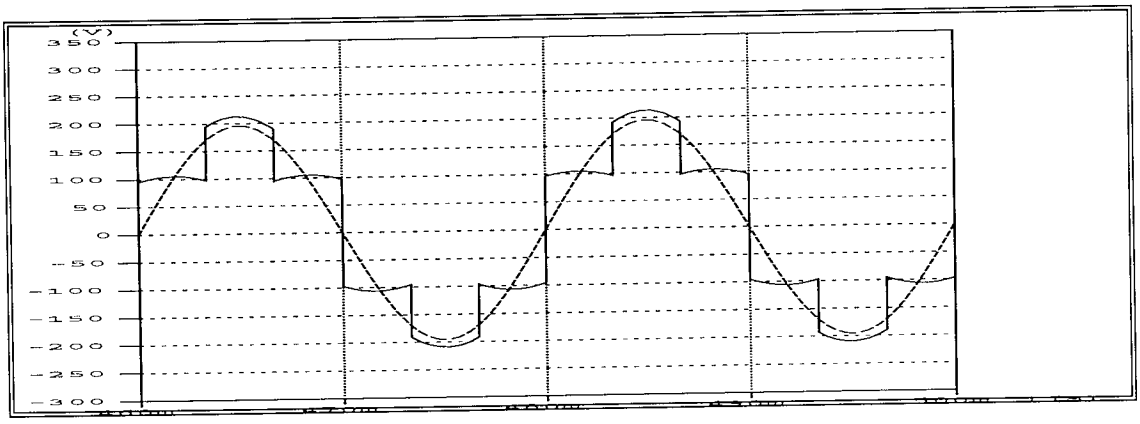

Fig 2.13b - Inverter output (solid line) and phase voltage: 6-pulse STATCON - unity PF

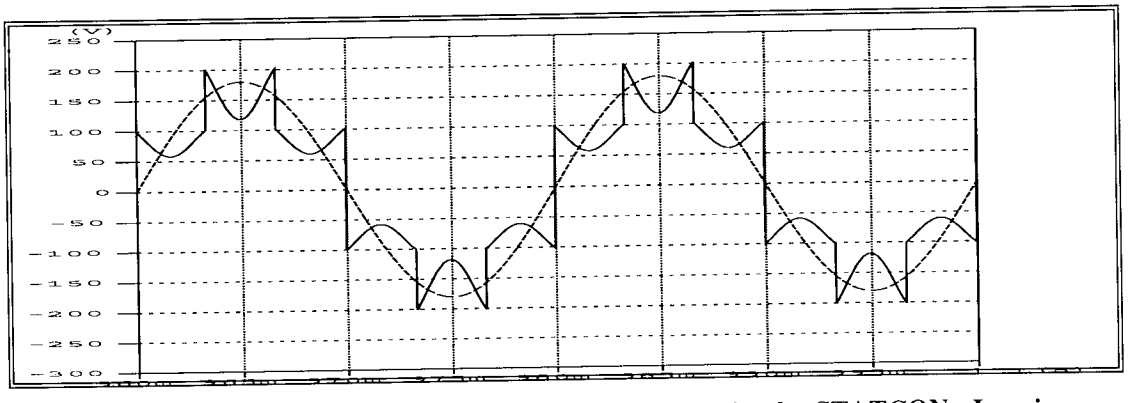

Fig 2.13c - Inverter output (solid line) and phase voltage: 6-pulse STATCON - Lagging

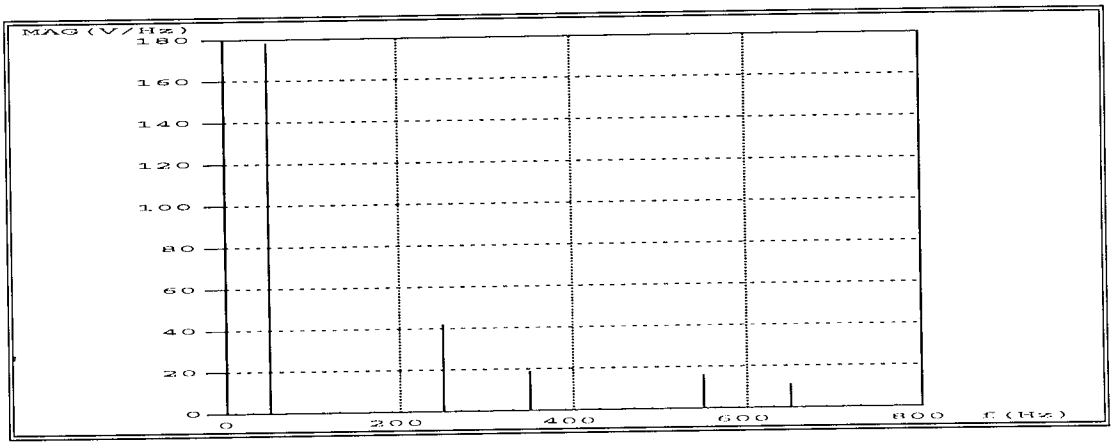

Fig 2.13b - Inverter output harmonic spectrum: 6-pulse STATCON - unity power factor

2.4.3 - Notes on simulation results:

• The range of firing angles was only ±6° about zero reference to achieve maximum reactive power generation and absorption, highlighting the sensitivity of the STATCON to firing angle.

• Unity power factor does not occur at zero firing angle but at some small positive value required to neutralise the already present lagging component of the uncompensated system.

• Leading, lagging or unity power factor operation is determined by the relative magnitudes of the inverter and supply *fundamentals* [Moltgen, 1984].

• The supply current harmonics are affected less by the change in firing angle than the fundamental component. The harmonics are related to firing angle and the choice of M [Hill, 1995].

Further aspects of the six-pulse STATCON which are not obvious from the above discussion include the following:

• If the firing angle is too large, the capacitor may experience net discharge, rendering the compensator ineffective.

• A narrow range of the firing angle exists over which the capacitor voltage varies linearly.

• The reactive power generated varies linearly with firing angle whereas the losses vary as the square. This is further motivation for operating with a reduced firing angle.

• Operation at reduced system voltage requires that the range of firing angles is extended. This has implications on the choice of M and control must take into account any potential non-linearities that may arise as a consequence of operation outside the range for which the '*reduced firing angle*' is defined [Hill, 1995].

The results of the 6-pulse STATCON simulations were verified experimentally in the laboratory using a 1kVA system with N-channel MOSFETS [Hill, Ashbrook, 1993]. The correlation between the simulation and experimental results was very good.

2.5 - HARMONIC REDUCTION IN VOLTAGE SOURCE STATCONS

The preceding section highlights the problem of the basic voltage sourced STATCON in that it generates a non sinusoidal output voltage whose form for six-pulse leading, unity and lagging power factor has been shown in **Fig 2.13**. Methods of reducing the generated harmonics in the *current* include the following:

2.5.1 - Filter Capacitors

A direct approach to the problem would be to introduce passive filters in the form of static capacitors or LC networks, but these can be rather bulky depending on the frequencies they are required to eliminate. The lower the frequency, the bulkier the units. While probably a sensible choice for high power reactive power compensation schemes, there are a number of points to note in regard to the intended application.

- A key point of merit of the STATCON is its small physical size and significantly reduced energy storage components, implying low cost.

- In power factor correction, the Static capacitor is a competitor, and to include it in the proposed scheme anywhere in the power circuit other than the energy storage point across the bridge somewhat defeats the purpose.

The use of static capacitors as filters has its advantages though.

- The devices are passive and require no control circuitry

- The capacitors will reduce harmonics within the passband of the resulting system, whatever their source.

An alternative approach to the problem is to improve the inverter output so that it approaches the sinusoidal ideal and hence contain fewer harmonics.

There are a number of algorithms by which a better output can be achieved with three phase inverters. The waveforms themselves are invariably stepped and may be classified into four general categories [Norris, 1995], discussed in a later section of this chapter.

The most notable schemes for harmonic reduction in use today include the following:

2.5.2 - Pulse Width Modulation (PWM)

This method involves relatively high frequency switching of the inverter devices to synthesise a sinusoidal output by applying pulses of variable width from what is essentially a fixed d.c. level, to the output at predetermined intervals within a cycle of the fundamental. The envelope function is a waveform that better approximates a sinusoid. PWM is a well established and documented technology [Lander, 1987; Ramshaw, 1993] which has found numerous applications in microelectronics, low and medium power applications.

However, although PWM suppresses the lower order harmonics, it tends to give rise to higher order ones and entails increased switching losses in the power devices. Of course, the higher order harmonics can be filtered out using much smaller - hence cheaper - static capacitors.

Moran, Ziogas and Geza Joos [1989] discuss a power factor compensation scheme that uses solid state semiconductor switches in an implementation of PWM.

2.5.3 - Multiple Level Converters

At the time of writing, research into multiple level inverters for STATCONs is becoming increasingly popular [Hill, 1995; Barry et al, 1995]. The basic topology involves a stack of series connected capacitors acting as an energy reservoir with tapping points of graded potential. The power semiconductors connect to these taps and are appropriately switched to apply the desired voltage from the stack at the desired instant. The resultant output waveform is a better sinusoid and for a single phase 2 level STATCON is similar to the three phase output of **Fig 2.13**.

The method achieves better harmonic reduction than the single level equivalent, but at increased component count, circuit complexity and an increased number of energy storage units. Also, the power semiconductors are not necessarily of similar ratings.

2.5.4 - Multiple Phase Converters

Also called the Multiple Pulse Converter, this type normally comprises an integral number of six-pulse bridges connected in parallel and to the same energy reservoir i.e. capacitor. Harmonic cancellation is by way of combining the outputs from the constituent six-pulse converters through phase shifting transformers which derive the desired number of phases from a standard three phase supply.

Unlike PWM, this method does not give rise to higher order harmonics, and has lower switching losses for a given total power output since it entails fewer switching actions per cycle. Also, each semiconductor carries only a fraction of the total inverter current at any time.

Normally, for fixed circuit parameters, the higher the pulse number, the smaller the required energy store. The 24-pulse STATCON is discussed in further detail in the next chapter. It has been used in the experimental aspects of this investigation.

A short note on stepped waveforms is included here to complete the discussion on inverter outputs for reduced harmonic content, and to serve as a reference for later discussions on similar waveforms.

2.6 - STEPPED INVERTER VOLTAGE WAVEFORMS

Norris [1995], describes stepped inverter waveforms from three phase ρ-pulse inverters as containing a limited number of harmonics, and where they feature equal steps of equal duration, contain harmonics at $\rho n \pm 1$ (c.f. **Fig 2.13**), where n is a positive natural number.

The waveforms can be expressed as a fourier series, and can be reduced to a general cosine or sine function. The subscripts c and s in the expressions that follow suggest that the summation reduces to a general *c*osine or *s*ine function. Also, the symbol $\lfloor x \rfloor$ denotes the *floor* of x, defined as the largest integer less than or equal to x, and χ is a ρ-dependent coefficient given by:

$$\chi = \frac{1}{(\rho / \pi).\sin(\pi / \rho)} \qquad (2.17)$$

This broad classification of waveforms as cosine and sine functions gives rise to two main types:

2.6.1 - Type A Stepped Waveform

These can be described by the general expressions:

$$S_{SA} = \sin\theta + \sum_{k=1}^{\infty}\left(\frac{\sin(k\rho+1)\theta}{k\rho+1} + \frac{\sin(k\rho-1)\theta}{k\rho-1}\right) = \chi.\sin\left[(1+2\left\lfloor\frac{\rho\theta}{2\pi}\right\rfloor)\frac{\pi}{\rho}\right] \quad (2.18)$$

and:

$$S_{CA} = \cos\theta + \sum_{k=1}^{\infty}\left(\frac{\cos(k\rho+1)\theta}{k\rho+1} - \frac{\cos(k\rho-1)\theta}{k\rho-1}\right) = \chi.\cos\left[(1+2\left\lfloor\frac{\rho\theta}{2\pi}\right\rfloor)\frac{\pi}{\rho}\right] \quad (2.19)$$

2.6.2 - Type B Stepped Waveform

These can be described by the general expressions:

$$S_{SB} = \sin\theta + \sum_{k=1}^{\infty}(-1)^{-k}\left(\frac{\cos(k\rho+1)\theta}{k\rho+1} + \frac{\sin(k\rho-1)\theta}{k\rho-1}\right) = \chi.\sin\left[2\left\lfloor\frac{1+\rho\theta/\pi}{2}\right\rfloor\frac{\pi}{\rho}\right] \quad (2.20)$$

and:

$$S_{CB} = \cos\theta + \sum_{k=1}^{\infty}(-1)^{-k}\left(\frac{\cos(k\rho+1)\theta}{k\rho+1} - \frac{\cos(k\rho-1)\theta}{k\rho-1}\right) = \chi.\cos\left[2\left\lfloor\frac{1+\rho\theta/\pi}{2}\right\rfloor\frac{\pi}{\rho}\right] \quad (2.21)$$

The characteristics of these waveforms depend on the nature of ρ. For example, type A features a crest and trough of double step width if ρ contains an even power of 2, an if ρ contains an odd power of 2, they have a crest and trough of single step width.

It becomes evident in the next chapter that the inverter output waveforms from a 24-pulse STATCON generally conform to type B and are, by choice, described by Eqn 2.21. An example 24-step waveform (set ρ = 24 in Eqns 2.21 and 2.17) is given in **Fig 2.18**

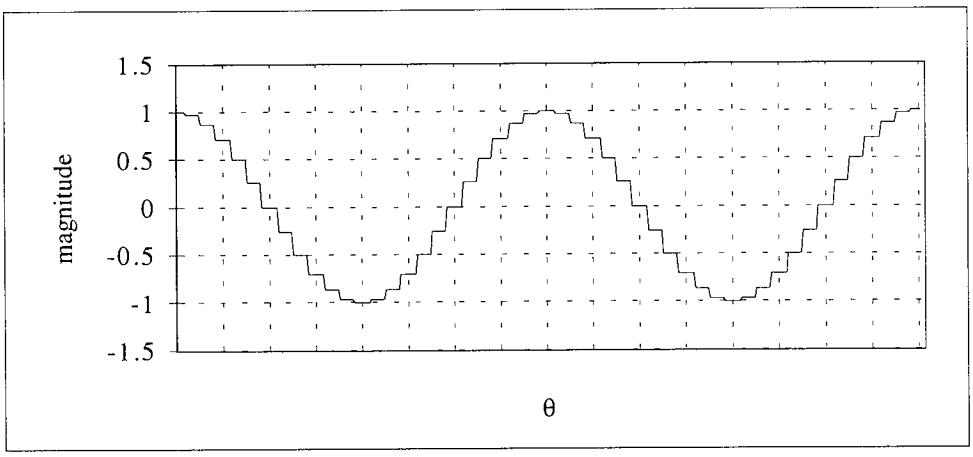

Fig 2.14 - 24 step waveform derived from Equation 2.21 with p = 24

2.7 - SUMMARY

In this chapter, an idealised model of a voltage sourced STATCON behaving as a current source has been presented with a view to highlighting the requirements of the practical device. The STATCON's property of supplying or drawing reactive current at constant load terminal voltage has been discussed.

The single phase and three phase 6-pulse voltage sourced STATCONs have been cited as examples of a practical implementation. Their non-sinusoidal output and its implications on the system harmonics have been highlighted with a view to presenting the 24-pulse STATCON as a suitable alternative that approaches the ideal more closely.

Performance parameters have been introduced and example values used in simulations. It is also mentioned that the results of the 6-pulse STATCON simulations were verified experimentally.

The 3rd harmonic is practically non-existent in the 6-pulse system although a rather significant 5th harmonic component is evident. This is consistent with the theory that the prominent harmonics for a ρ-pulse inverter will occur at $\rho n \pm 1$, where n is a positive natural number. Thus, for a six-pulse system, the first prominent harmonics (n=1) will be the 5th and the 7th.

The stepped nature of the inverter output has been pointed out and expressions introduced for later reference.

CHAPTER 3

THE 24-PULSE VOLTAGE SOURCED STATCON

3.1 INTRODUCTION

The 24-pulse voltage sourced STATCON is an arrangement comprising what may be regarded as four 6-pulse bridges in parallel and connected to the same capacitor. The arrangement appears as shown in **Fig 3.1** in which the generic symbol for the SCR has been used to represent any three terminal power semiconductor device with gate turn on and turn off control. Also shown is an anti-parallel power diode connected across each switching device. In devices like the power MOSFET, the diode is usually integrated into the silicon structure, and is a desirable configuration in that the device characteristics tend to be well matched.

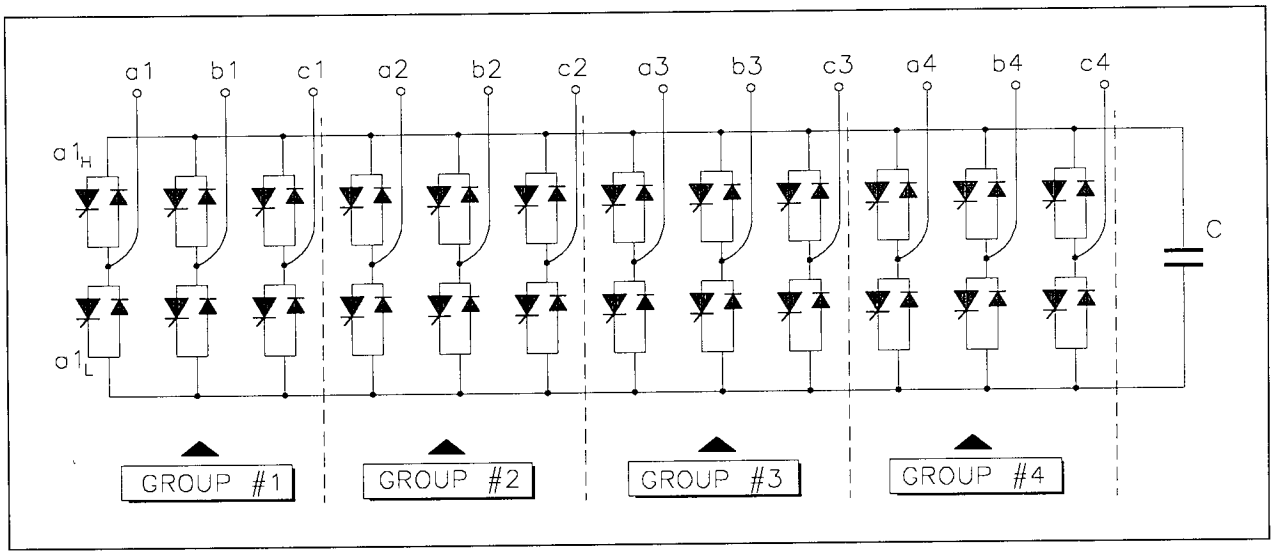

Fig 3.1 - Elementary 24-pulse Voltage Sourced STATCON

The terminals labelled $a1$, $a2$ e.t.c. are the connections to the 12-phase supply.

3.1.1 - Device naming

Convention is to number devices in the sequence they are switched (c.f. **Fig 2.6** and **Fig 2.11**). It has not been adopted here because it loses some of its advantages when the number of devices is large. Thus for this purpose, the devices will be referred to per limb with a subscript 'H' for the high side device connected to the positive terminal of the capacitor and a subscript 'L' for its complementary low side device connected to the negative terminal. Thus for instance, $a1_H$ will refer to the high side device connected to the phase or terminal labelled $a1$ and $a1_L$ will be its complementary device. The device $a1_H$ is therefore that shown at the top left corner of the bridge in **Fig 3.1**. The use of the terms 'High side' and 'Low side' is fairly widespread in power electronics.

Each of the four groups labelled Group #1 through #4 will be seen to be a six-pulse bridge similar to that of **Fig 2.11** and features terminal connections for three voltages phase shifted by 120°.

3.1.2 - Operation

As in the single phase and three phase cases, the capacitor charges up through the anti parallel diodes while the power inverter devices switch in sequence to apply the capacitor voltage to the output.

The switching is normally synchronised to some fixed reference such as the primary red phase zero crossing. All the devices then switch in sequence for a half cycle at the reference signal frequency and at the appropriate instant in relation to the same. Delay angle control is achieved by shifting the switching signals in relation to the reference. It is also important that no two devices in a limb conduct simultaneously, as this constitutes a short circuit across the capacitor.

3.1.3 - Switching Control

If closed loop, a means of measuring the power factor, reactive power or voltage is usually required and the processing can be implemented in an electronic circuit that can be analog, digital, programmable or hybrid. Chapter 7 of this thesis discusses one such control system. An important consideration in the processing of the signals mentioned above is that of noise in the form of transients in the supply, for any reason, and electromagnetic interference from the inverter itself.

3.1.4 - Phase Connections

As there are twelve connections to be made and only three supply phases available, a means of deriving the required 12 phases from the standard three is necessary.
This normally assumes the form of phase shifting transformers whose outputs are such that the resulting phases are correctly spaced. The required angle is 15° for a 24-pulse system. Referring to **Fig 3.1**, each of the four groups is connected to three phases 120° apart. The groups are themselves phase shifted by 15° so that $a1$, $a2$ and $a3$ for instance, are 15° apart while $a1$, b1and c1 are 120° apart.

The polyphase system of voltages required is illustrated in **Fig 3.2a** and the angles between example phases are shown in **Fig 3.2b** and **Fig 3.2c**. The voltages are such that:

- there are 12-phases appropriately phase shifted by 15° in three bands of four, so that each band has four phases 15° apart, and each of these has counterparts at 120° and 240° in the other 2 bands.

- all phase to neutral voltages have similar magnitudes i.e. the phases are equipotential.

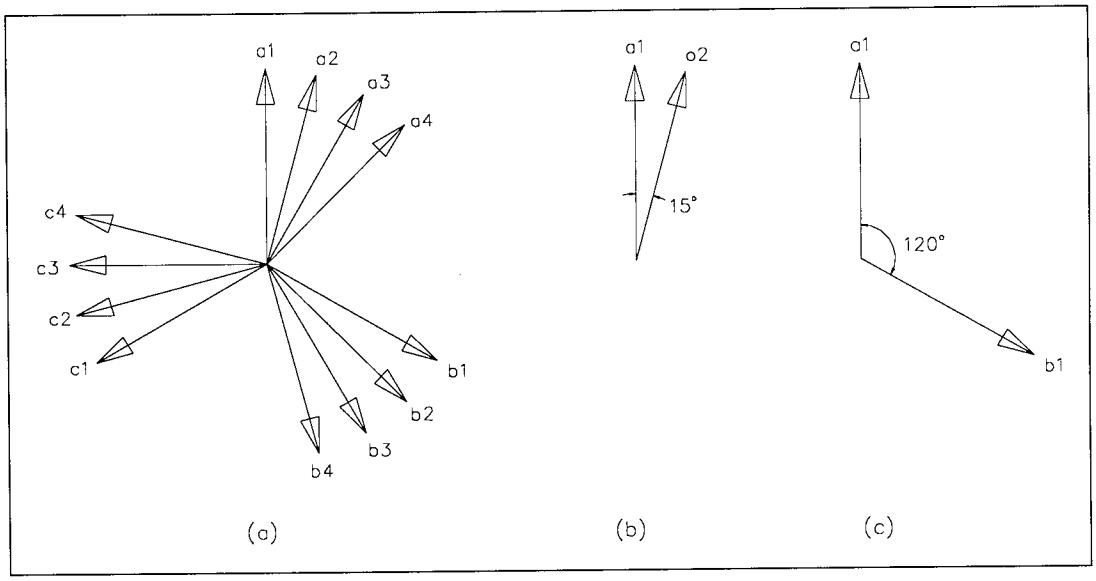

Fig 3.2 - Required 12 phase system showing angles between phasors.

The need for the appropriate phase shift is so the inverter section of the STATCON can achieve the desired harmonic cancellation, while the equipotential voltages enable the rectifier section of the bridge to function as a true multi-pulse system.

3.1.5 - Practical Interfacing

There are a number of methods by which a polyphase system of voltages can be derived from the standard three and a few are mentioned in the next chapter. Almost invariably, this assumes the form of phase shifting transformers whose leakage inductance provides the required coupling reactance.

Quite important to this discussion is that the coupling between the STATCON and the supply appears as a *series* inductance, preferably of low resistance for minimum losses. Such an inductance also has the important property of presenting different values of impedance to different harmonics, and tends to suppress the higher order harmonics more on account of their higher frequencies.

The phases themselves must be such that connection of the STATCON does not cause the voltage to drop outside acceptable limits (loading) as this would reduce the effectiveness of the integrated bridge rectifier in that some diodes would be connected to phase voltages so low that they are permanently reverse biased.

3.2 - 24-PULSE HARMONIC NEUTRALISATION

The voltage waveform across each device is a rectangular wave of peak to peak voltage equal to the capacitor voltage. The wave features superimposed ripple as a result of the ripple on the capacitor. The resultant of each composite 6-pulse unit in a 24-pulse bridge is a 6-pulse waveform, and four such waveforms phase shifted by 15° gives a 24-step waveform which has reduced harmonics [Hill et al, 1994; Chen et al, 1995].

The harmonic spectrum of a 24-step waveform reveals that the lowest harmonics occur at the 23rd and 25th and is consistent with the theory on stepped waveforms presented in chapter 2. Such a waveform and its spectrum are shown in **Fig 3.3**. The spectrum as shown has the magnitude of the fundamental component at 50Hz reduced in order to show the harmonics to a better scale. The 23rd and 25th were actually 4% and 4.5% of the fundamental respectively.

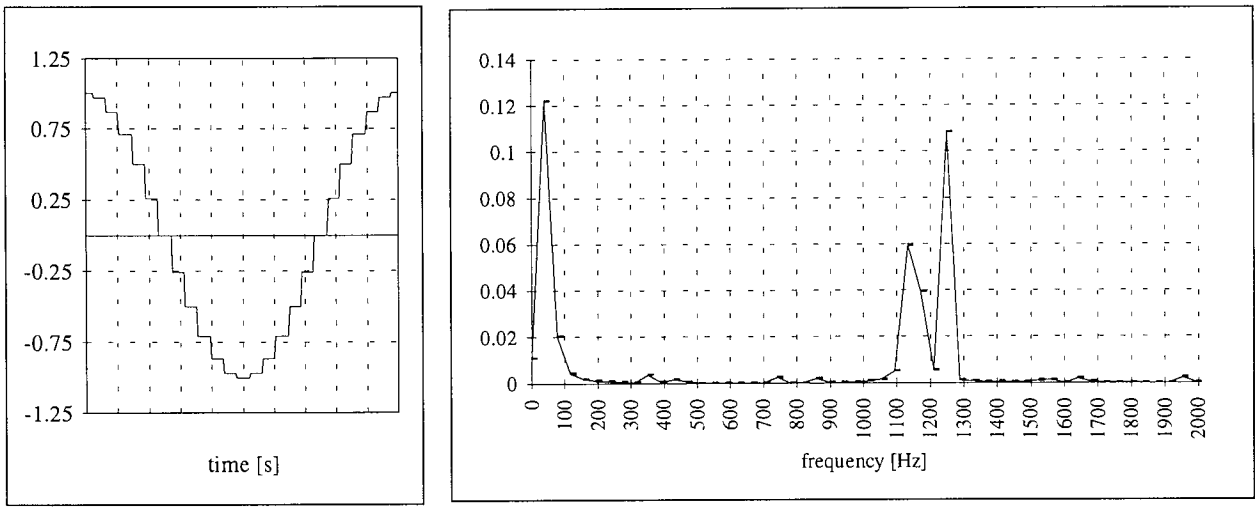

Fig 3.3 - 24-step waveform and harmonics from setting p=24 in equation 2.21

The STATCON in practice produces similar harmonic cancellation as long as the derived multiple phases are of identical voltage levels and phase shifts.

In general, the resulting current features similar harmonics as the resultant inverter output, but greatly attenuated on account of the different impedances presented by the coupling reactance to different harmonics as stated earlier.
For better harmonic reduction therefore, a high value of L may be chosen in satisfying some choice of M, but of course, the associated winding resistance may increase and hence give rise to higher losses in the equipment.

3.3 - PERFORMANCE OF THE 24-PULSE STATCON

A general methodology for analysing STATCONs typified by those discussed in this thesis has been described by others [Norris & Hill, 1994; Hill, 1995]. The authors have presented alternative methods and similar expressions and conclusions have been drawn.
Expressions for the capacitor voltage and current, and the reactive power generated or absorbed have been developed. The general performance parameters described for the single phase and the six-pulse STATCON are applicable. The general results have been applied in selecting design parameters.

Consider therefore, a 24-pulse STATCON with the following parameters:

Supply rms phase to phase voltage (= 240V) = 1 p.u.
Rated power (= 4kVA) = 1 p.u.
X_L = 0.6 p.u. R = 0.07 p.u. X_C= 22 p.u. i.e Y_C = 0.045 p.u.
f = 50Hz $\omega = 100\pi$

Such a device has the following associated parameters:

$\beta = R/2X_L = 0.06$
λ = 8/3 for this arrangement [Hill, 1995], whence $k \approx 10$ and $M \approx 0.1$

Despite the order in which the parameters have been listed, M is the more fundamental design parameter, chosen as explained in chapter 2. Other parameters are then deduced accordingly.

The example values above were chosen so that the experimental model was a scaled version of a high power system. By design, L = 27.5mH and C = 10μF.

N-channel MOSFETs with appropriately connected snubber circuits were used for the bridge. The detail of each switch in the bridge is shown in a later chapter (**Fig 7.8**) when the general experimental arrangement and control is discussed in depth.

The results shown in **Fig 3.4** are experimental. The waveforms were captured with an 8-bit analog to digital converter with a 1μs conversion time and ½LSB error. The data was processed using an off-line computer spreadsheet. Note that the magnitude scale is arbitrary. The rms current in **Fig 3.4a** and **Fig 3.4c** was 10A (0.6 p.u.). The capacitor voltage is generally about twice the supply peak value for leading power factor operation (see **Fig 6.16**).

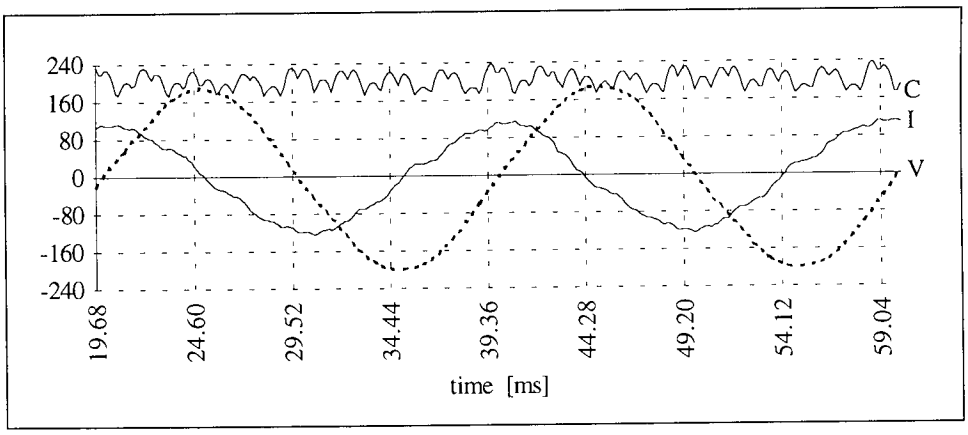

Fig 3.4a - Capacitor volts, supply volts and current - 24-pulse leading.

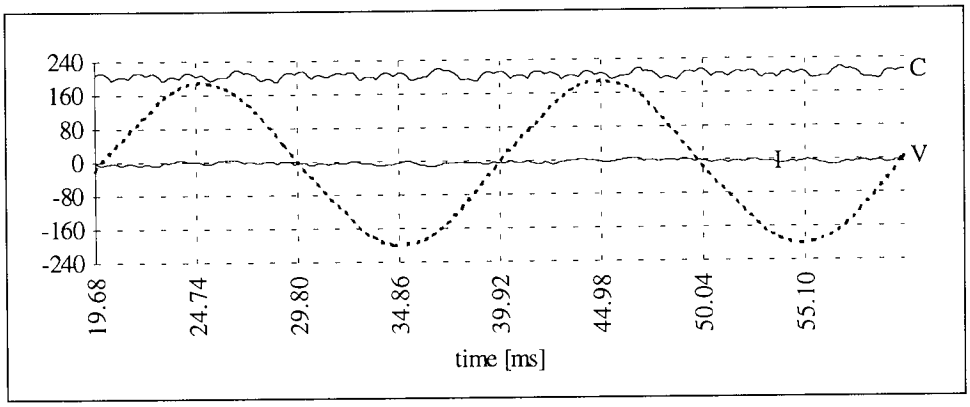

Fig 3.4b - Capacitor volts, supply volts and current - 24-pulse at unity PF.

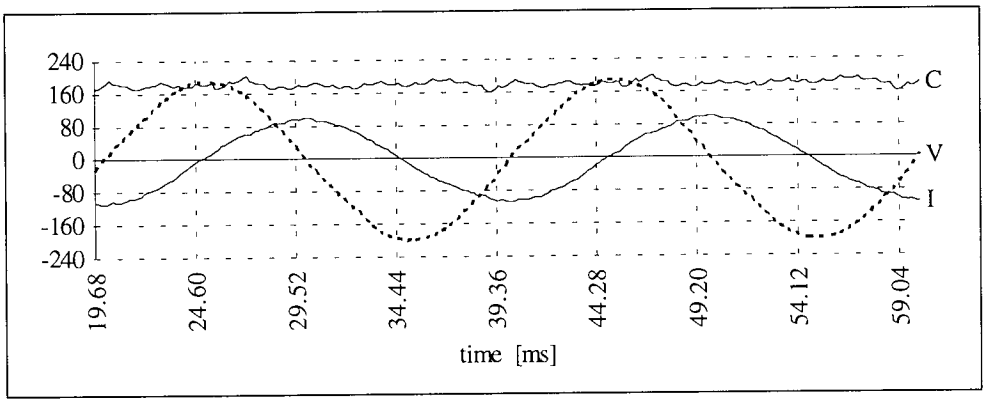

Fig 3.4c - Capacitor volts, supply volts and current - 24-pulse lagging.

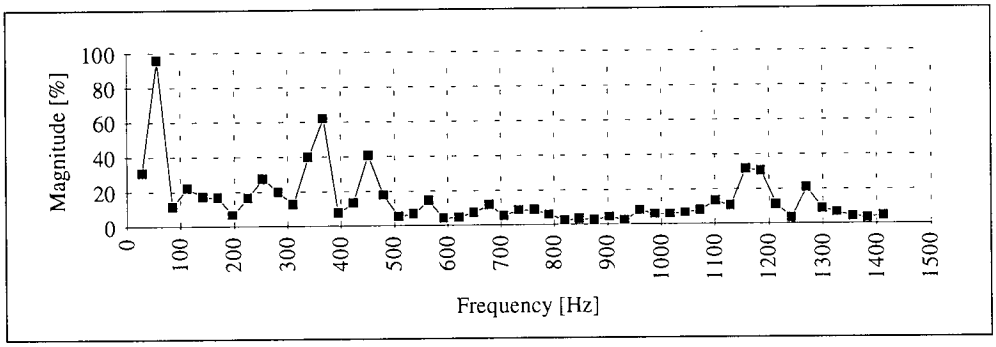

Fig 3.4d - Supply current harmonic spectrum for unity power factor operation

The experimental results of **Fig 3.4** reveal the presence of low order harmonics of the fifth, seventh and ninth order. The seventh is predominant.

While a number of possible causes of these low order harmonics can be suggested, a first step towards conclusive analysis requires that the harmonics already present in the uncompensated system (if any) are established. This was done experimentally by sampling the current waveform with the compensator unconnected. The results are shown in **Fig 3.5**.

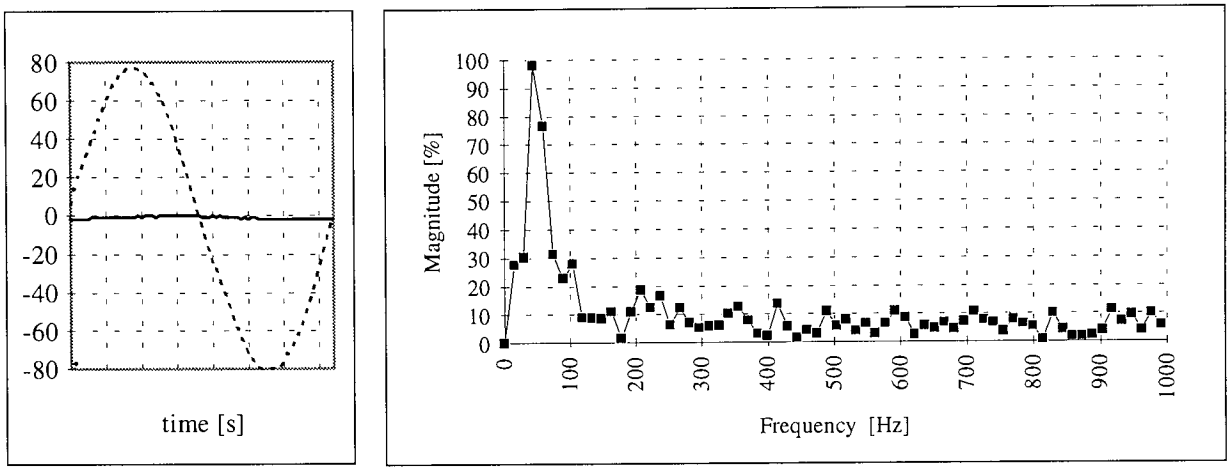

Fig 3.5 - Uncompensated transformer no load current and harmonic spectrum.

Taking the sampling error and the relative magnitude of the fundamental into consideration, it is evident that harmonics in the transformers' no load current are negligible. The low order harmonics are therefore a consequence of the compensating equipment and/or its interfacing. Low order harmonics will generally be present even in the uncompensated system on account of the peaked nature of the magnetising current required for a sinusoidal flux distribution, but appropriate phase terminal connections eliminate some of these (3rd, 6th, 9th, 12th ..) from the supply although they may exist in each phase winding.

3.4 LOW ORDER HARMONICS IN MULTI-PULSE OPERATION

3.4.1 - The switching deadband

Momentary discontinuous flow of currrent may occur due to the switching *deadband* i.e. the safety feature of a finite interval when both low side and high side power devices in a limb are off before the next device switches on. **Fig 3.6** shows the results of simulated impact of different sizes of the deadband on the total harmonic distortion (THD) of the supply current.

From **Fig 3.6**, the effect of the deadband is not very significant and experimental results seem to support this view. However, it was observed that the harmonic spectra for the values of deadband between 10μs and 1ms were generally much 'cleaner' i.e. fewer non zero components.

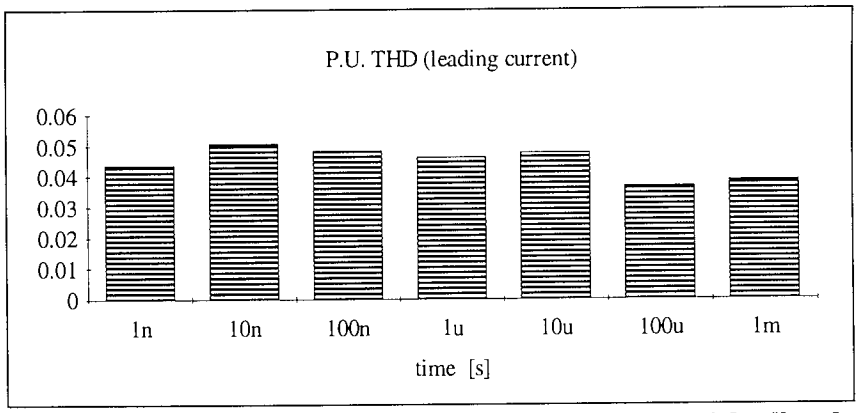

Fig 3.6 - THD for a leading current for different values of deadband.

3.4.2 - Imbalance in coupling inductances

Another contributor to the presence of the low order harmonics could be the differences in the sizes of the coupling reactances in the phases. Simulation suggests that a distortion of the current waveform occurs if the coupling reactors differ by as little as 5%.

3.4.3 - Imperfection in phase shift

By and large, deviation of the actual phase shifts from the desired is the most important cause of low order harmonics in the resulting supply current. Simulation of a transformer system with ideal phase shifts produces no low order harmonics below the expected values for either battery source or capacitor store. The voltages derived from the zigzag transformers used in the experiments were not exactly 15° apart as shown in **Table 4.6**. Indeed, it is often very difficult to obtain precise phase shifts with practical windings, more so in small size machines (kVA) on account of the variation of leakage inductances.

Hill [1995] suggests that further contributors to the presence of low order harmonics could include non-ideal characteristics of the bridge devices, non-ideal phase shifts in the three-phase supply and differences in the per phase effective resistance.

3.5 - SUMMARY

This chapter has described the topology and operation of the 24-pulse STATCON.

Some coupling requirements have been stated. The role of the zigzag transformers in deriving the required 12 phases from the standard three, and in providing the required coupling reactance by means of their leakage inductance has been discussed.

The fundamental requirements of the control system for such a system have been presented.

Experimental results from the laboratory model using zigzag parallel connected transformers and a bridge inverter of N-channel MOSFETs have been presented and explanations for non ideal system behaviour offered.

CHAPTER 4

SUPPLY COUPLING FOR A 24-PULSE STATCON

In general, a multiple-phase STATCON requires the appropriate number of phases to be derived from the standard three phase supply. This has implications on the complexity of the magnetic coupling. In the single phase case, a single transformer or even reactor will suffice. A three phase 6-pulse converter requires three single phase transformers or one 3-phase transformer, or three separate reactors to couple to the mains. Pulse numbers greater than six require a more complicated coupling transformer arrangement.

The purpose of this chapter is to discuss some conventional schemes of providing the required polyphase system of voltages with a view to identifying the relevant properties of the coupling and using these to establish similarities with, hence suitability of, the induction machine stator winding as an alternative.

4.1 - PHASE SHIFTING TRANSFORMERS

The conventional method of deriving multiple phase voltages from a three phase supply is to use appropriately wound and connected transformers. Suitability to inverter operation aside, there are a number of arrangements that will achieve the desired effect.

4.1.1 - Zigzag connected transformers

These are essentially three phase parallel or series connected transformers with a three phase secondary output which is phase shifted from the primary by some predetermined amount set by the turns ratios. For a 24-pulse system, the complete arrangement normally comprises four such units, each with some predetermined phase shift with respect to the primary supply phases.

In general, the elementary zigzag connection is formed from two windings in series, with the first winding on the same limb as the primary winding of say, phase A, and the second on the same limb as say, phase C, but with winding direction reversed. The turns ratios determine the phase shift and magnitude of the output [Norris, 1993, Brosan et al, 1965]. Example windings are shown in the schematics that follow.

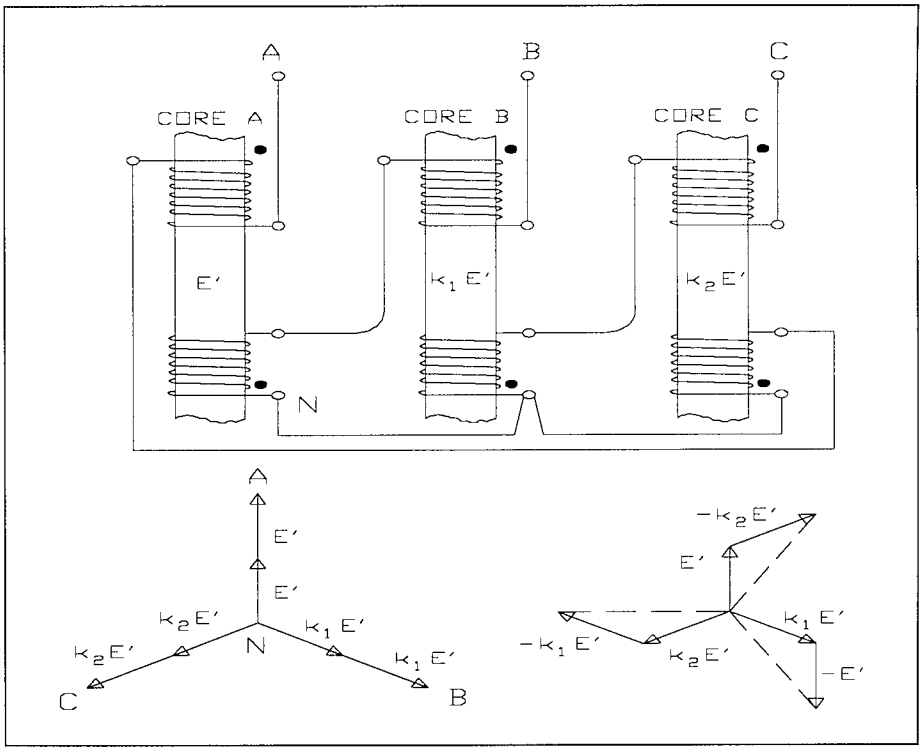

Fig 4.1 - Three phase zigzag connected windings and corresponding vector diagram.

Referring to **Fig 4.1**, if the voltage apparent across each winding is E', the coil voltages on limbs A, B and C may be written as E', k_1E' and k_2E' respectively where k_1 and k_2 are the factors that account for the phase shifts of the supply voltages. The phase to neutral voltage is the difference of any two of the voltages E', k_1E' and k_2E'. Thus, the phase A to neutral voltage V_A is such that :

$$V_A = E' - k_2E' = E'\left[1 - \left(-\frac{1}{2} + j\frac{\sqrt{3}}{2}\right)\right] \tag{4.1}$$

Thus:

$$V_A = \sqrt{3}.E'\left(\frac{\sqrt{3}}{2} - j\frac{1}{2}\right) = \sqrt{3}.E' \angle -30^\circ \tag{4.2}$$

V_B and V_C are found to be of similar magnitude at angles 120° and 240° respectively.

Other points to note about the zigzag connection, which may or may not be advantageous to converter opertation are that:

• For the same number of turns, the voltage produced by the zigzag connection is less than that for a star connection, where the two coils on a given core are simply joined in series. The star connection gives 2E' while the zigzag gives $\sqrt{3}$E'.

• As a consequence, for the same *line* voltage, the zigzag connection requires 15% more turns.

• If it is assumed that the leakage inductance of each phase winding is a function of the number of turns, then the zigzag connection has a higher leakage reactance for a fixed phase voltage.

• From an interfacing point of view, such as with a STATCON where the series reactance is a requirement, the increased leakage is a favourable feature of the zigzag connection.

The zigzag connected transformers shown above may be regarded as a specific form of the more general case of a phase shifting transformer system.

An m-phase system has, in general, m voltages of equal magnitude, phase displaced from each other by $2\pi/m$ radians. A two phase system is generally taken to be one with the two voltages in quadrature rather than anti-phase, and so is an exception to this rule.

Thus, if a transformer core has c magnetic cores carrying balanced phase fluxes $\phi 1$, $\phi 2$, ... ϕc, and a single turn is placed round each of the cores, then the c voltages in the turns effectively form a balanced c-phase system of voltages. By placing several windings on the cores and connecting these in a variety of ways such as the zigzag connections of **Fig 4.2**, different voltages at different phase shifts can be obtained. Of course, there are restrictions to the connections that can be made if phase balance is taken into consideration [Norris, 1993].

Brosan and Hayden [1965] discuss the effects of various parameters on the performance of three phase transformers.
The schematics that follow illustrate some possible connections of three phase transformers to produce twelve phases 15° apart. Uppercase A, B and C denote the primary terminals and the lowercase letters denote the secondary terminals.

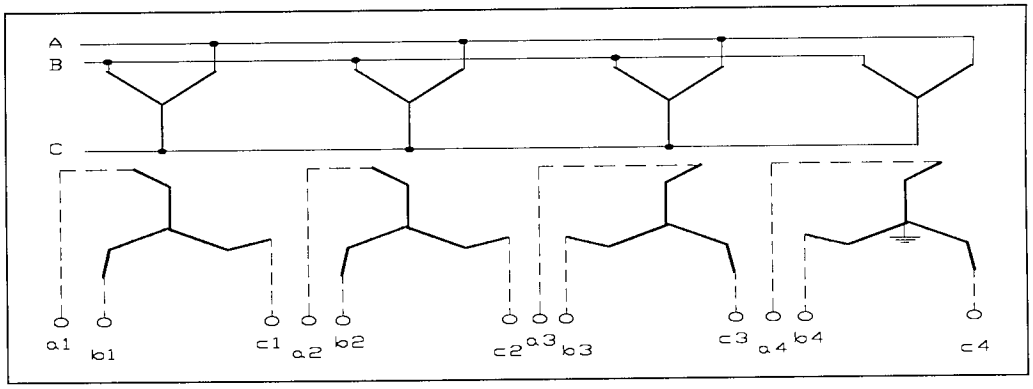

Fig 4.2a - Star and zigzag parallel connected transformers

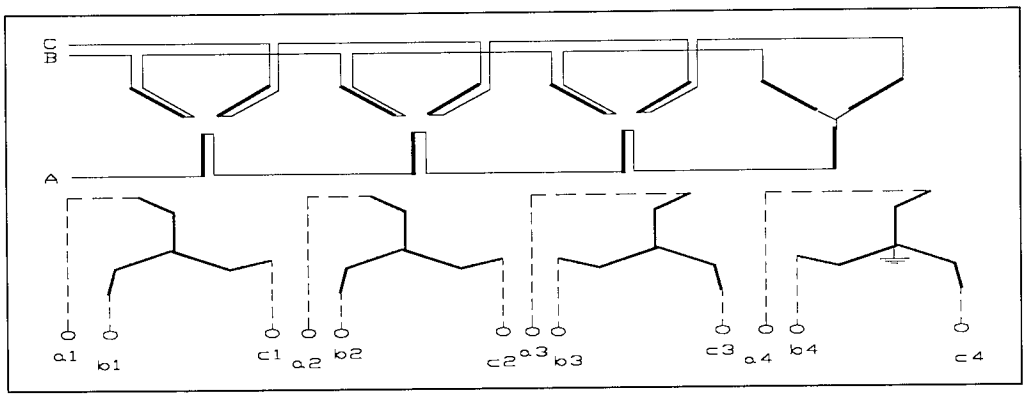

Fig 4.2b - Star and zigzag series connected transformers

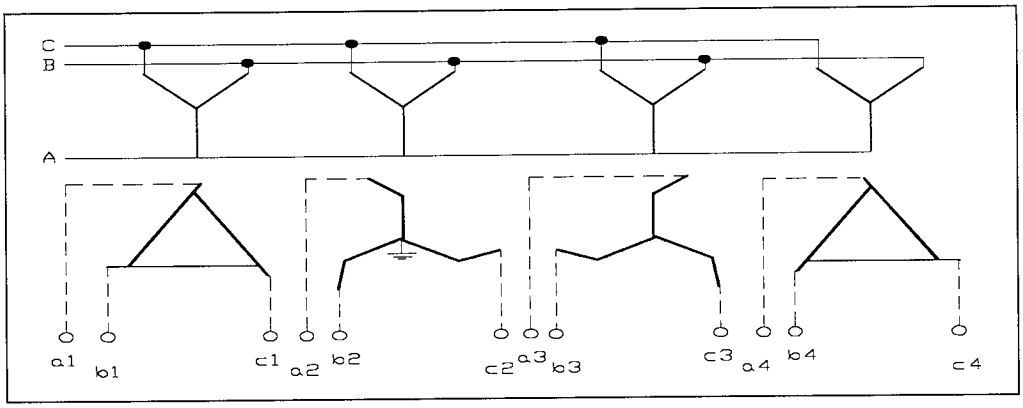

Fig 4.2c - Zigzag and extended delta parallel connected transformers

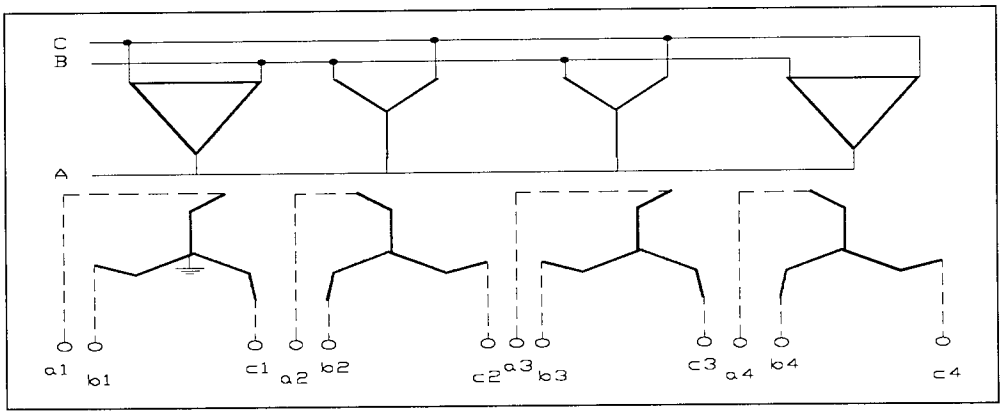

Fig 4.2d Star and delta primary connected transformers

Important features of the zigzag connections of **Fig 4.2** include the following::

- The complete assembly comprises four three phase transformers rather than a single multi-phase secondary output unit.

- Most of the transformers discussed can be used as suitable coupling between the power inverter bridge of a 24-pulse STATCON and the supply.

- The secondary features at least one star point to which a neutral connection is made. Only one transformer on the secondary has this connection. This is essential to the operation of the inverter because the neutral line voltage changes with the changing phase to neutral impedances as the inverter switches [Lander, 1987; Moltgen, 1984; Hill 1995]. The neutral connection on the secondary is also useful in preventing capacitive coupling of the windings from giving rise to high common mode voltages.

- In use with inverters, the transformer's leakage inductance is often sufficient to meet the coupling reactance requirements and is so designed.

4.1.2 - Star And Delta Secondary Transformers

The arrangement is normally used for HVDC inverters. Each of two three phase transformers produces three secondary phases.

The two sets of voltages are phase shifted by 30°. Note that the arrangement is such that the two sets are not exactly balanced - as is the case with a 60° phase shifted sets. This has implications on the performance of bridge rectifiers that may be connected to this system of voltages. It is usual for the star and delta to be on the primary rather than secondary side illustrated in **Fig 4.3**

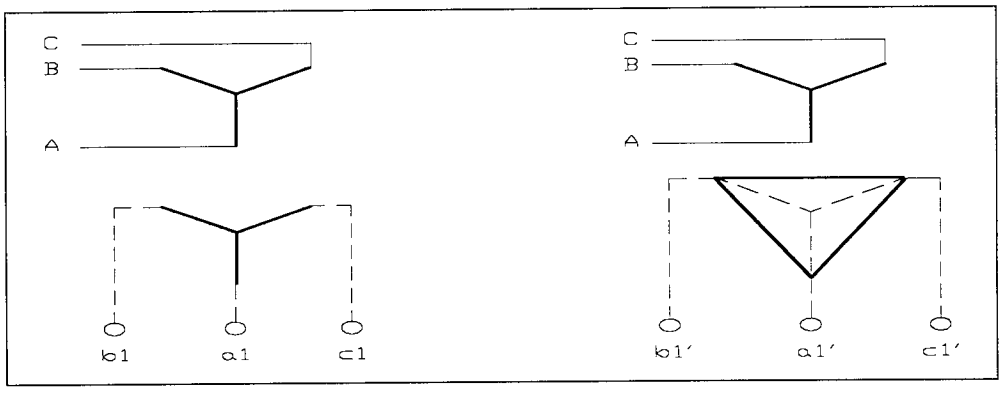

Fig 4.3 - Star and delta secondary transformers

4.1.3 - Ring Autotransformer

This is a remarkably different type of transformer arrangement in that there is no distinct secondary winding. The interconnection of windings described for zigzag transformers earlier is extended to several windings on multiple cores, and the desired phases are tapped off at the connection points between coils which themselves make up the primary winding. The winding is very similar to the stator winding of induction motors and this discussion is left until polyphase voltages from stator windings are described.

There are other transformer systems that will achieve phase shifting [Norris, 1993; Brosan et al, 1966] and only a few have been mentioned here.

4.1.4 - Notes on Phase shifting Transformers

A characteristic feature of all the transformers is that they have a distinct secondary winding, except the ring auto-transformer described in section 4.1.3 above. This particular difference is of significance to the proposed coupling and becomes evident when leakage inductances are discussed in chapter 6.

4.1.5 - The neutral voltage

In use with inverters, connection of the neutral is of significance. It is explained in a later chapter that the required form of excitation current for an induction machine (and the transformer is one such machine) is non-sinusoidal for sinusoidal flux distribution to result.
When transformers are connected in the manner described for the zigzag transformers above and sinusoidal current applied, the resulting flux is flat topped i.e. contains a prominent third harmonic. The flux induces a similar voltage in the secondary winding. The third harmonic components of the induced emf in the transformers are in phase and cause the potential of the neutral point to vary at third-harmonic frequency. If the neutral points of the transformers were connected together, then the third harmonic becomes evident in the supply phases [Slemon et al, 1980]. Indeed, triplen harmonics would be apparent in the phase if the neutrals were secured (connected together). In use with inverters therefore, the secondary neutrals are not connected together.

4.2 THE 24-PULSE STATCON WITH ZIGZAG COUPLING

In building the 4kVA model, the connection of **Fig 4.2d** was adopted and the transformers wound for a specific leakage inductance. N-channel MOSFETS were selected as the switching device on account of the simplicity of their gate drive requirements, and their general availability at economic prices in the stated power range. Chapter 7 gives further detail.
Four 3-phase transformers were manufactured to specification (section 3.3) by a commercial vendor. The no-load phase shifts measured on the secondaries are given in **Table 4.4** below.

Phase	a1	a2	a3	a4	b1	b2	b3	b4	c1	c2	c3	c4
Nominal	-22.5	-7.5	+7.5	+22.5	97.5	112.5	127.5	142.5	-142.5	-127.5	-112.5	-97.5
Actual	-21.0	-7	+10	+24	94	114	130	146	138	-127	112	-95

Table 4.4 - Nominal and actual phase shifts of experimental zigzag transformers

The resultant inverter output waveforms cannot be observed physically, since summing of the effects of individual units occurs in the transformers. The MOSFET voltage waveforms however, are accessible, but care needs to be exercised in interpreting the results on account of the behaviour of the neutral potential. It is therefore important to specify the measurement reference point as explained below.

The voltage beween one secondary phase and neutral was observed, as was the voltage between the same point and the capacitor ground. For practical reasons, the phase c4 was chosen and measurement done as shown in **Fig 4.5**. These particular waveforms were chosen for inclusion in this discussion because of differences observed with the proposed stator winding.

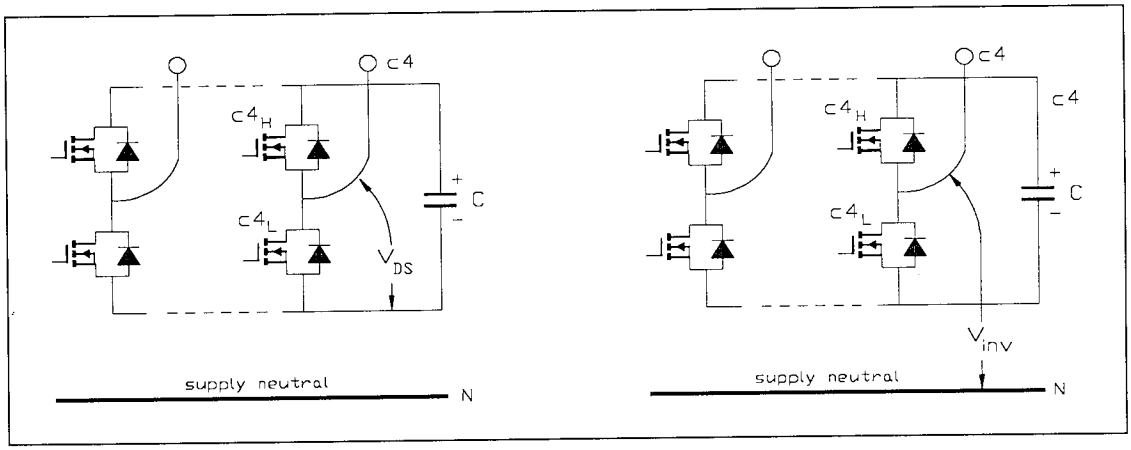

Fig 4.5 - MOSFET V_{DS} voltage and inverter output V_{inv} measurement points

V_{DS} is a square wave with superimposed ripple while V_{inv} appears as shown in **Fig 4.6**.

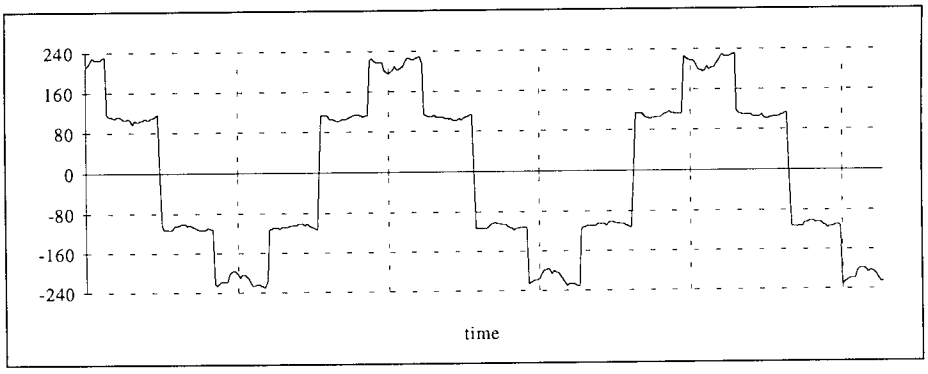

Fig 4.6 - Voltage between secondary phase and supply neutral

Similar waveforms are observed in all other limbs provided their particular neutral point on the associated transformer is used as reference. Thus, the waveforms on the bridge side of the supply tend to be distorted by the third harmonic variations in the neutral potential shown in **Fig 4.7** (experimental).

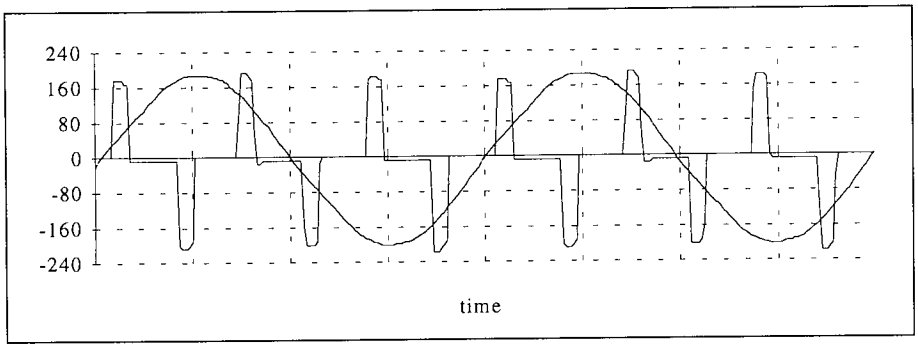

Fig 4.7 - Voltage between two secondary neutral points

The slant in the waveform is due to oscilloscope signal acquisition circuitry used and may be ignored. The results are consistent with simulation. Note that the magnitude scale is approximate, and the neutral point tends to rise to higher voltages depending on firing angle.
An alternative reference for the bridge-side waveforms is some point within the capacitor half way between the positive and negative d.c. rails. **Fig 4.8** shows how this point, termed the *bridge reference* in this thesis, could be realised in practice.

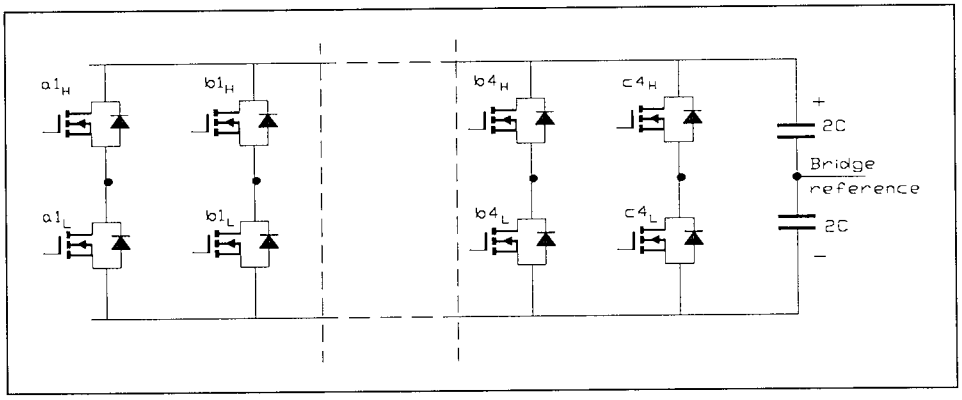

Fig 4.8 - Bridge reference point

The capacitor voltage is shown in **Fig 4.9** for the various power factors.

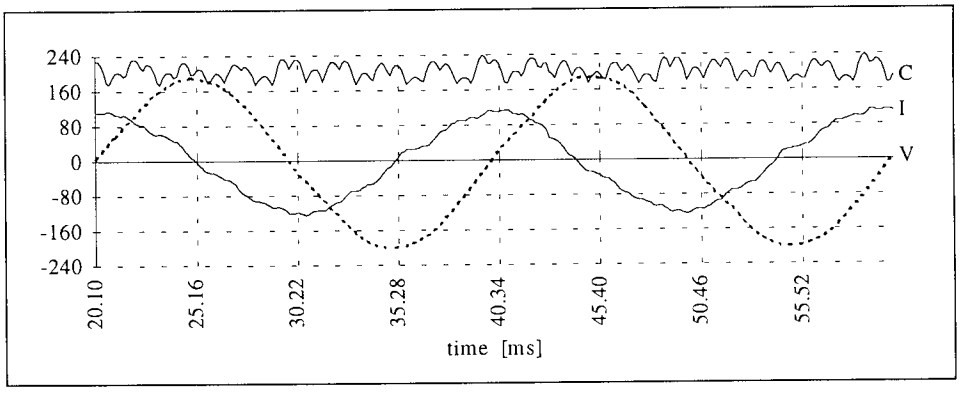

Fig 4.9a - Capacitor volts, supply voltage and current - leading

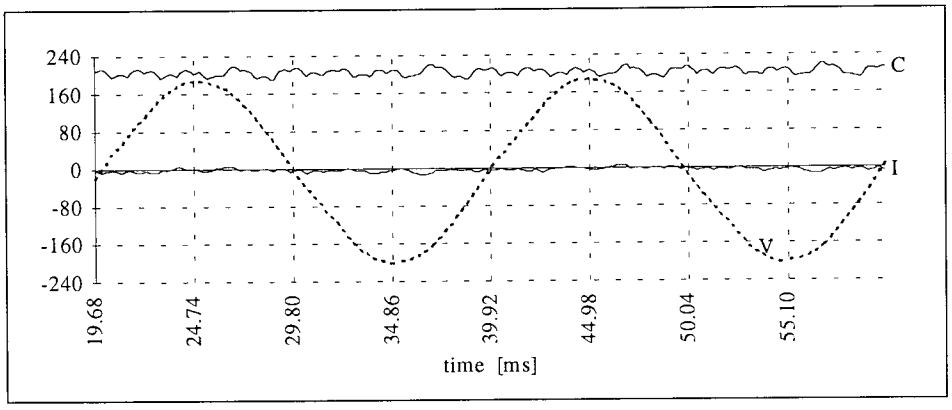

Fig 4.9b - Capacitor volts, supply voltage and current - unity power factor

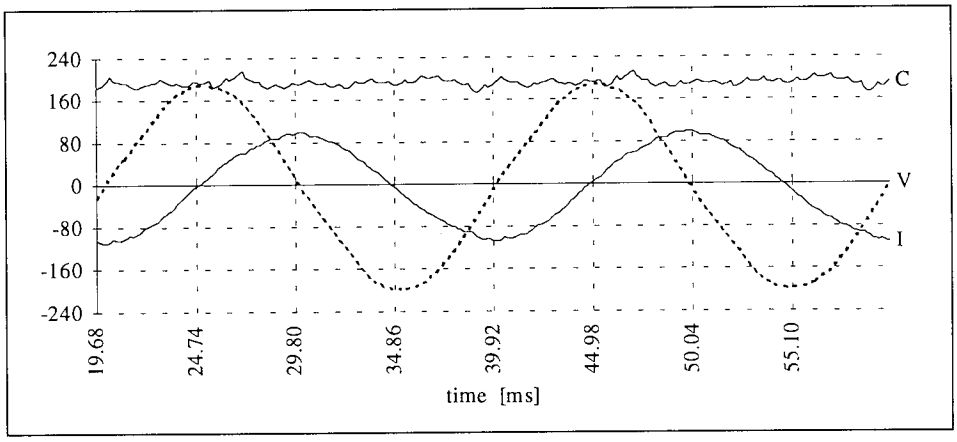

Fig 4.9c - Capacitor volts, supply voltage and current - lagging

See **Fig 6.16** for more realistice relative magnitudes of the capacitor and supply voltages. The capacitor has superimposed above its average dc value, a 24-pulse ripple characterised by peaks or troughs for leading and lagging power factors respectively. The actual magnitude of the ripple depends on the size of the capacitor; decreasing with larger size capacitors.

4.3 COUPLING REQUIREMENTS

In principle therefore, the STATCON should perform as required if the magnetic coupling meets the following list of requirements :

---

(1) ***provide the required coupling impedance*** which, electrically, must appear as :

(a) a series inductance and

(b) a low series resistance,

the values of which must be within the specification of the system resonance ratio.

---

(2) ***derive a system of polyphase voltages from a three phase supply***, and the resulting polyphase system must be such that all voltages are:

(a) phase shifted by the desired amount (15° for 24-pulse operation) and

(b) of the same magnitude referenced to the neutral, even under load.

---

(3) ***provide for bi-directional flow of reactive power between compensator and supply*** to enable the compensator to both generate and absorb reactive power as required.

---

(4) ***enable harmonic neutralisation by superposition of wave harmonics*** and so facilitate cancellation of the harmonics generated in the individual sections of the bridge.

The criterion 2(b) requires that the source of the polyphase voltages is a low output impedance system whose output voltage remains constant under load, otherwise unequal voltages result.

The absence of a distinct secondary winding may affect the availability of leakage inductance required for a coupling reactance, and this has direct implications on using a stator winding as the coupling. However, suitably wound, the stator, and in principle the ring autotransformer discussed above *may* provide an adequate coupling as long as the leakage inductance meets the criterion (1) above. The alternative would be to use additional external reactors.

4.4 SUMMARY

This chapter discusses the coupling requirements for a 24-pulse STATCON and identifies the transformer as the generally accepted method.

Different transformer connections and topologies have been discussed in brief to show that the required transformer arrangement is not unique. Of course, some are better suited to the application than others. **Fig 4.10** below is a photograph of the zigzag connected transformers used in obtaining the results presented in this chapter. The unit with a connected secondary neutral is visible on the left.

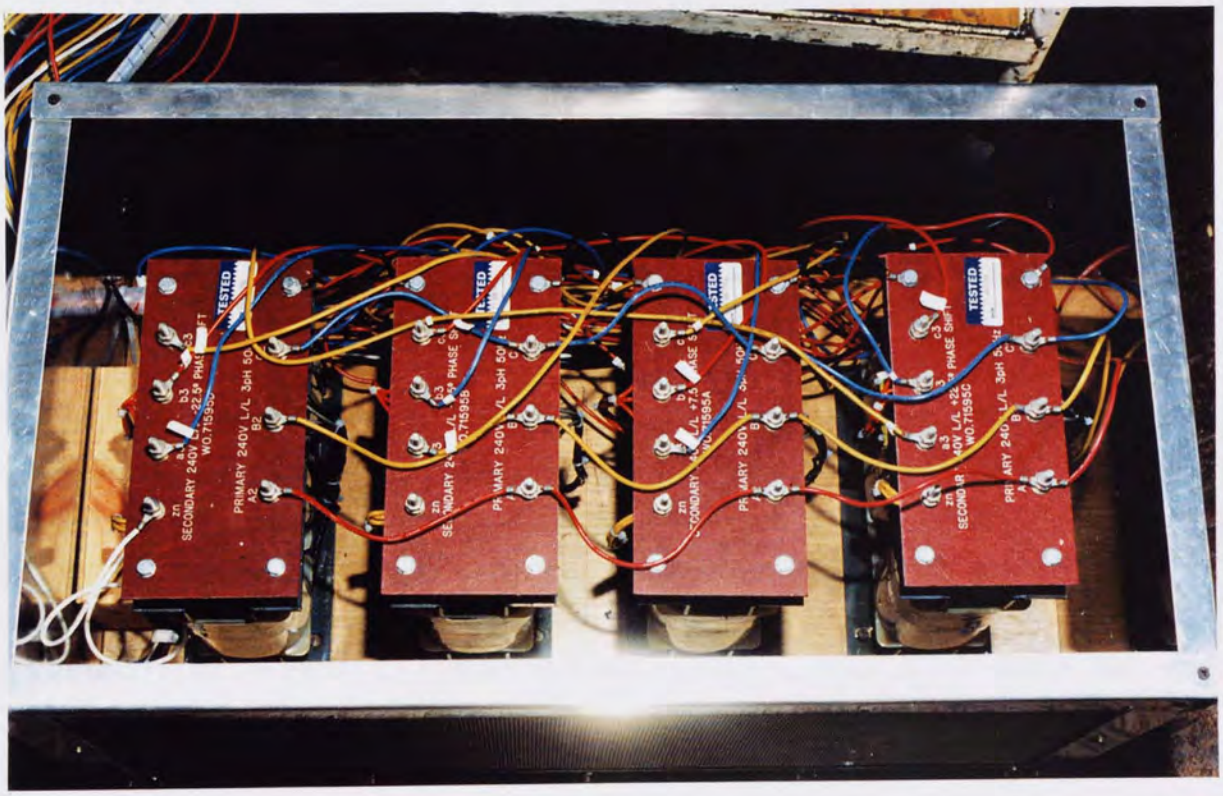

Fig 4.10 - Zigzag parallel connected transformers.

A list of the criteria that need to be satisfied by any selected coupling has been given and is referred to in later chapters.

CHAPTER 5

THE THREE PHASE CAGE ROTOR INDUCTION MOTOR

Chapter 1 lists some examples of sub-unity power factor systems and states that a high percentage are induction motor driven equipment [Longlund et al, 1984; Chalmers, 1990]. The lagging power factor has been cited as one of the machine's major disadvantages.

To date, the static capacitor remains the most popular form of power factor correction, but alternatives are still being investigated. Some seek to apply the power factor correction equipment externally while others seek to embed power factor correction within the machine design itself. There are advantages and disadvantages with either approach.

Induction motor design is an intricate process involving several trade-offs. These often include the efficiency, power factor and torque. The intended application itself has implications on the speed, physical geometry and size of the machine [Cotton, 1934]. Very often, post design improvement of any one of these by way of altering any of the fundamental design parameters such as winding size, type, material, connection, machine size, rotor type and coil arrangement causes a decline in a second parameter. Examples of this are the Wanlass Winding and Unity Plus Winding [Umans, 1989; Zipse, 1990; Medarametla et al, 1992] that quite plausibly, sought to introduce power factor correction at the elementary level by using additional windings and capacitances in the stator winding solely for this purpose. While power factor improvement was achieved, the machine efficiency and torque were inadvertently reduced. Independent researchers attributed the decline in efficiency to a decrease in the winding volume participating in the production of mutual flux, and attributed the claim to an unfortunate synonymous regard for efficiency and power factor.

This attempt acknowledges the difference between power factor and efficiency and seeks to minimise the disturbance to the fundamental design parameters. However, this has not been entirely possible, and the various modifications are presented in this thesis, together with an assessment of the impact on the machine performance.

This chapter discusses the various aspects of the induction machine of relevance to the proposed application and explains the background concepts that were taken into consideration in designing and building the motor used for laboratory experiments.

5.1 INTRODUCTORY NOTES

Knowledge of the types of 3-phase induction motor, classified by the type of rotor winding, is assumed. Broadly classified, these include:

- ***The wound rotor***

  - in which a polyphase winding of the same number of poles as the stator winding is present on the rotor. The ends of the winding are brought out to slip rings where appropriate external resistors can be connected to alter the machine characteristics.

- ***The cage rotor***

  - in which no distinct rotor winding exists, but rather, a cage like frame of conducting bars embedded in a solid structure and shorted at the ends by end rings. The bars may be straight or skewed, of circular cross section or more complex shapes.
    Main advantages of this type of motor are that it is:
    - cheap- a consequence of the simple manufacturing requirements
    - robust- a consequence of the rugged construction of the rotor
    - reliable - the low maintenance requirements due to the absence of slip rings

- ***The solid rotor***

  - in which the rotor is a solid iron structure. This is a less common type of motor but apart from good mechanical strength, has the advantage of facilitating high starting torques and has better thermal capacity to withstand high currents for short periods of time. It is also cheaper to build than the cage rotor [Chalmers et al, 1980,1981].

The Induction motor, whatever its rotor type has only one source of excitation, and that is the main three phase connection to the supply. Thus all the machine's active and reactive power demands have to be met by the same supply.

The active power demands of the machine are related to the load, internal and rotational losses while the reactive power demands are a direct consequence of the machine's magnetisation requirements, furnished by the magnetising current which flows in quadrature with the induced emf and lags it by 90°.

5.2 - CHARACTERISTICS OF THE EXCITATION CURRENT

The *magnetising current* is one of two components that make up the *excitation current*. The other component is in phase with the induced emf and so gives rise to real power dissipation. It is the *core-loss current* and accounts for the iron losses.

Of the two, the magnetising current is generally much larger and so the excitation current as a whole lags the induced emf by nearly 90°. **Fig 5.1** illustrates this.

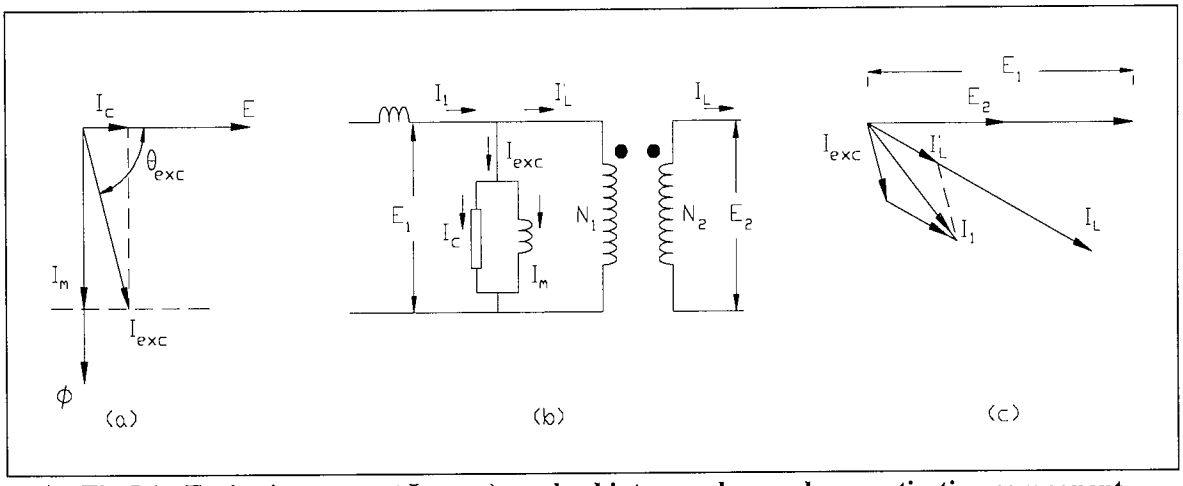

Fig 5.1 - Excitation current I_{exc} **a) resolved into core loss and magnetisation component**
b) in transformer equivalent circuit
c) in transformer current phasor diagram

A characteristic of the excitation current is that it is peaked rather than sinusoidal, and this is a requirement if the air-gap flux is to be sinusoidal [Kemp, 1934; Brosan & Hayden, 1966]. This waveform is a consequence of the non-linear relationship between the current and flux, defined by the iron's hysteretic B-H loop. The shape of the magnetisation current is shown for an example B-H loop assuming a sinusoidal flux distribution.

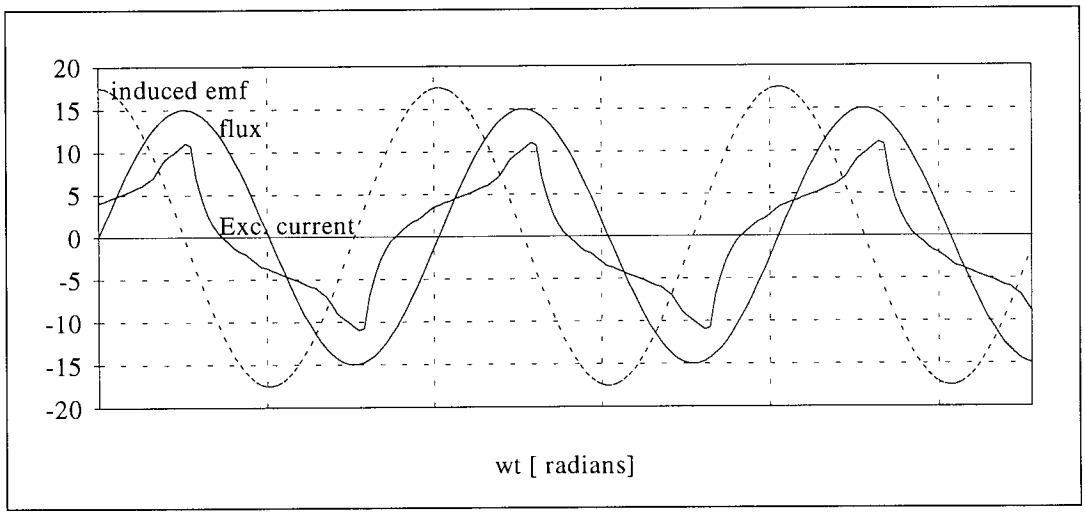

Fig 5.2 - General shape of excitation current required to produce sinusoidal flux in iron

The peaked form of the current suggests the presence of harmonics and these are evident in the spectral chart of **Fig 5.3** below for the example excitation current of **Fig 5.2** assumed at 50Hz.

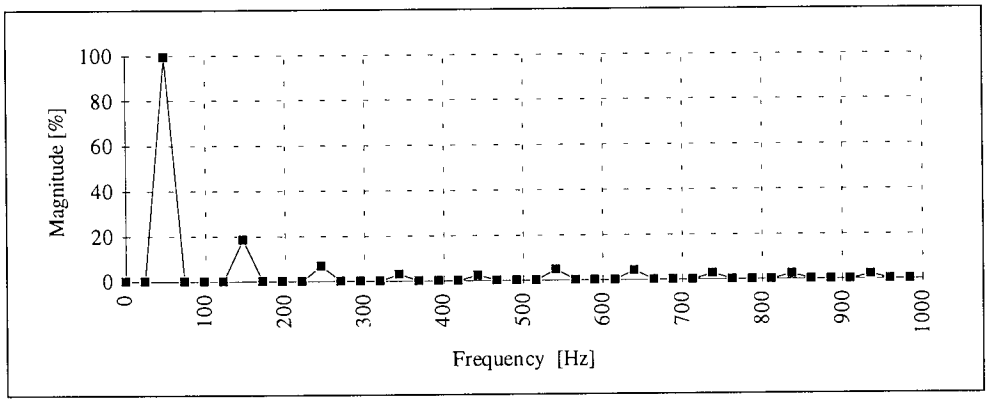

Fig 5.3 - Spectral chart of example excitation current.

Fig 5.3 shows that the excitation current has a number of odd harmonics and that the third is the most prominent. This is generally true.

A sinusoidal magnetisation current gives rise to a flattened-top flux distribution, which induces a similar emf in the linked circuit. The implications are generally less severe when the harmonics are present in the current rather than the induced voltage [Brosan and Hayden, 1966, Chapt 6]. Some of these are as follows:

5.2.1 Current harmonics

- Increased heating of machine windings due to the circulating harmonic currents in the copper. This effect can be rather serious in zigzag connected transformers.
- Increased iron losses due to the change in the flux waveform, which in turn affects the iron losses.

5.2.2 Voltage harmonics

- Increased voltage stress in the insulation. This can be quite serious and affects the voltage rating of the machine.

As stated, the authors argue that a greater amount of trouble is experienced with harmonic voltages than harmonic currents, and that it is usual to tolerate the effects of the harmonic currents to ensure sinusoidal flux and voltage waveforms.

Since the induction machine draws all its active and reactive currents from the same supply lines, the harmonics of the excitation current must affect the overall supply current. However, this depends on the phase connections of the load. For instance, when the primaries of identical transformers are connected in delta, no third harmonic is present in the supply currents since the phase currents are the *differences* of the phase to phase winding currents. However, the harmonic currents are present in the windings and do circulate within the delta.
The conclusions to be drawn from this discussion are that:

- the magnetisation current is responsible for the lagging power factor of an induction machine; certainly so under no-load conditions. Under load, the leakage reactance is a major contributor to this parameter.
- the *required* form of excitation current is not sinusoidal
- the presence of low order harmonics will depend, amongst other factors, on the terminal connections of the load (e.g transformer).

5.3 - INDUCTION MOTOR POWER FACTOR

The operating power factor of an induction motor depends on a number of variables which include the machine rating, number of poles, speed, and load [Chalmers, 1990; Brosan et al, 1966]. However, a common feature of the effect of these variables is the associated relative increase in the active power component which therefore increases the *ratio* of the active power to the apparent power, hence power factor. A compensator on the other hand brings about an actual *reduction* in the absolute size of the reactive component. Also, the amount by which each of these variables affects the power factor differs. Example graphs for the speed, rating and loading are shown in **Fig 5.4** below.

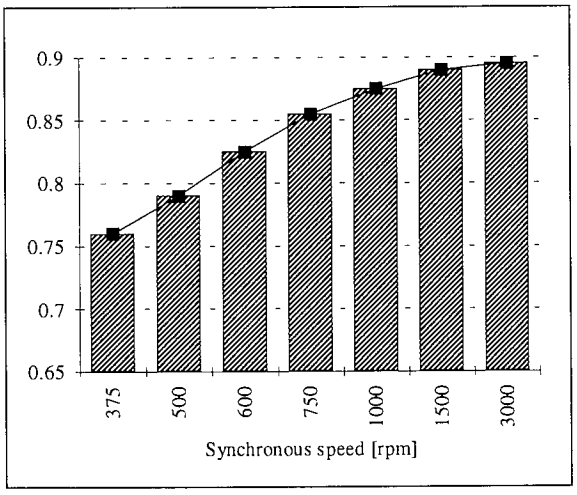

Fig 5.4a - Power factor v/s synchronous speed curve

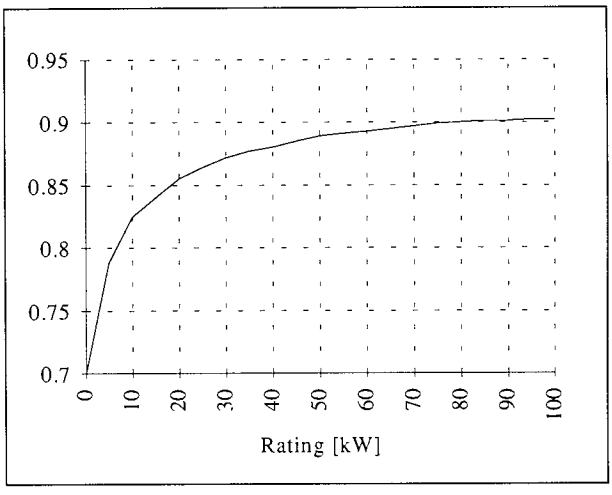

Fig 5.4b Power factor v/s rating curve

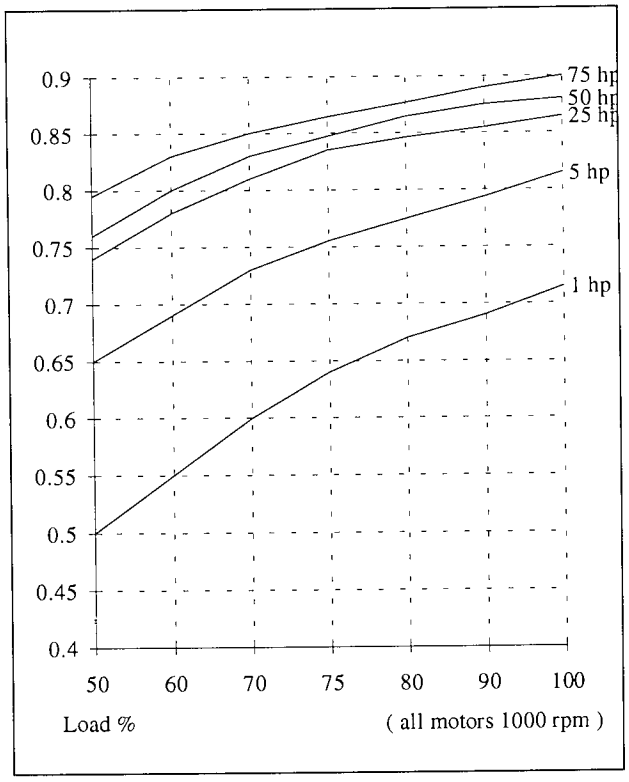

Fig 5.4c Power Factor v/s load

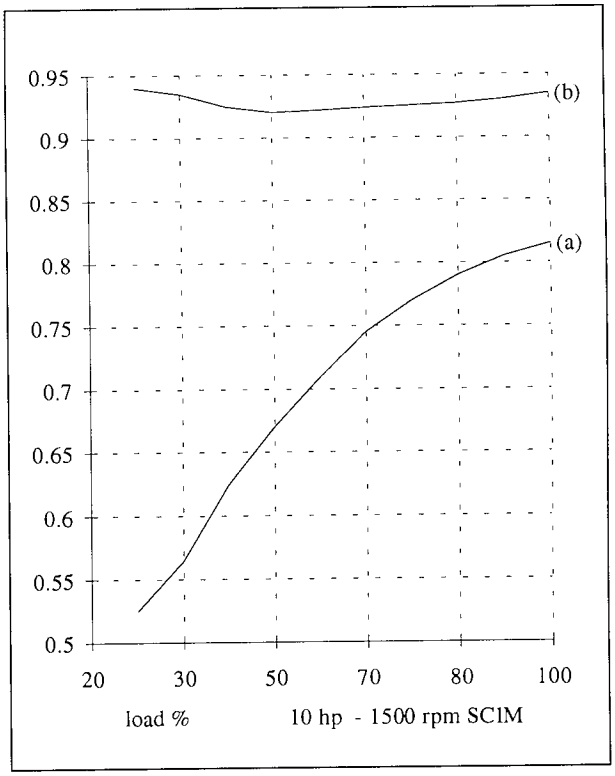

Fig 5.4d PF v/s load. - (1) uncompensated (2) 3kVAr capacitor connected

5.3.1 - Power Factor Correction

In order to improve the power factor of an induction machine, it's reactive power requirements have to be known. Once the kVArs are established, the size of the compensator can then be decided upon. If it is desired to use static power capacitors, then there are several methods available for the correct sizing.

Using static capacitors, it is not often that the power factor of an induction motor would be improved all the way to unity because of the following:

- cost of the required kVAr required increases rapidly approaching unity PF.
- the required capacitor size is perilously close to one that could give rise to self excitation of the machine if isolated from the supply as a unit, often leading to winding damage.
- the amount of cost saving realised in improving the PF from say 0.9 to 1 is not as motivating as that realised in improving from say 0.8 to 0.9.

Thus, in general static capacitors are often used to improve the power factor to close to, but not quite, unity.

Post machine-design calculation for P.F. correction is relatively straightforward. Let the power vector diagram shown below represent the machine's initial conditions:

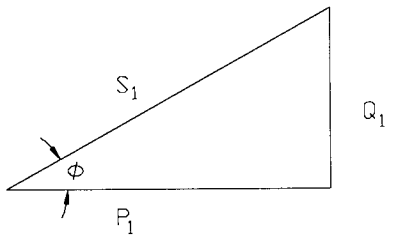

Initial conditions

Active power = P_1, Apparent power = S_1, Reactive power = Q_1, Power factor = PF_1

$$PF_1 = \cos\phi_1 = \frac{P_1\ [kW]}{S_1\ [kVA]} \tag{5.1}$$

$$\tan\phi_1 = \frac{Q_1[kVAr]}{P_1[kW]} \tag{5.2}$$

Corrected conditions

Active power = P_2, Apparent power = S_2, Reactive power = Q_2. Power factor = PF_2
$P_1 = P_2$ since there is no alteration to the active power

$$PF_2 = \cos\phi_2 = \frac{P_1\ [kW]}{S_2\ [kVA]} \tag{5.3}$$

$$\tan\phi_2 = \frac{Q_2\ [kVAr]}{P_1\ [kW]} \tag{5.4}$$

Thus, required kVAr from the compensator is Q_{cmp} and is given by:

$$Q_{cmp} = Q_1 - Q_2 = P_1.\tan\phi_1 - P_1.\tan\phi_2 \tag{5.5}$$

whence:

$$\underline{Q_{cmp} = P_1(\tan\phi_1 - \tan\phi_2)} \tag{5.6}$$

There are several ways to calculate the required kVA and most of these involve the use of tables [Longlund et al, 1984].

5.4 WINDING TYPES

A.C. Stator windings in general, can be constructed in one of two ways; as *single* or *double* layer windings. Knowledge of these is assumed. Double layer windings permit the use of chorded coils. The advantages of using short pitch coils i.e reduced end-turn length and reduced space harmonics, outweigh the disadvantages [Cotton, 1934; Fitzgerald at al, 1992] and this fact is assumed in this discussion, by adopting a short pitched coil double layer winding. **Fig 5.5** illustrates the main disadvantage of the chorded coil.

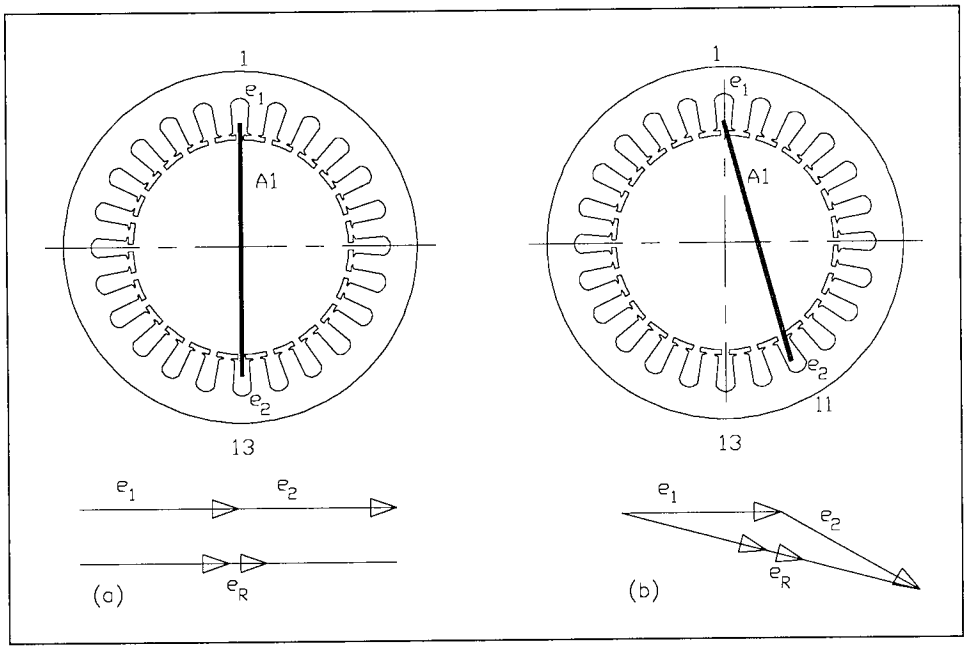

Fig 5.5 - emf vector addition for (a) Full pitch coil and (b) short pitch coil

Referring to **Fig 5.5**, e_1 is the emf induced in the coil side in the first slot, and e_2 that induced in the coil side in the second slot. For a full pitch coil, these emf's are equal and opposite and so are additive around the coil as shown in the vector diagram of **Fig 5.5a**. The coil of **Fig 5.5b** is chorded by two slots and spans only 150 of the 180 degrees required for full pitch. Such a coil is said to be short pitched by 30°. The resultant of the two emf's in the coil sides is shown in the vector diagram of **Fig 5.5b**. The chorded coil has a smaller resultant emf, an effect accounted for by the chording factor, k_C, given by:

$$k_c = \sin\left(\frac{\lambda}{\lambda_p}.\frac{\pi}{2}\right) \qquad (5.7)$$

λ is the number of slots spanned by the coil, and λ_p the number of slots required for full pitch.

Unless otherwise stated, a single winding path is assumed i.e. no alternative parallel paths exist and all coils in a phase are series connected.

5.5 MACHINE WINDING INDUCTANCES

In this section, expressions are derived for the tapping point voltages from an induction motor stator winding. In order to do this, expressions for the flux in the machine air gap and for the self and mutual inductances between the current carrying coils are established. It is normal to treat the machine on a per phase basis, to which the standard equivalent circuit is applicable, but this approach cannot be used here because the voltages required are those between individual coils.

Consider a 24-coil double layer lap wound stator and suppose each coil to be of N-turns and chorded by 30° i.e. spans 10 out of 12 slots required for full pitch. **Fig 5.6** shows the stator and one such coil.

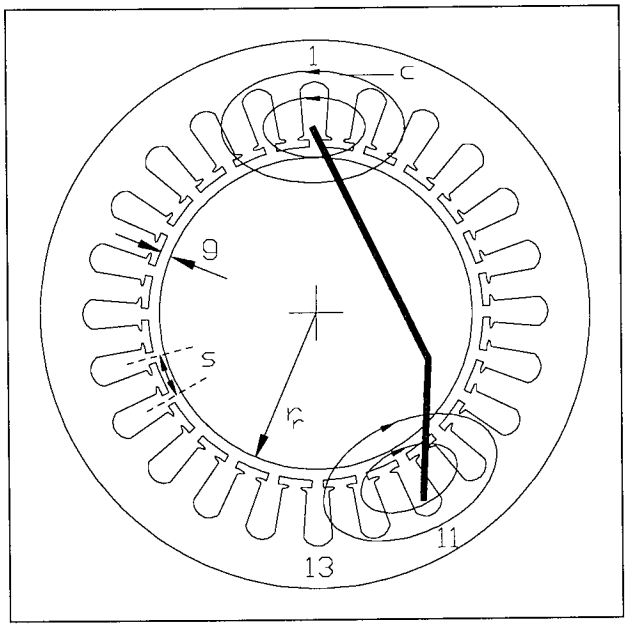

Fig 5.6 - A 24 slot DLL winding showing one coil (*la*1) chorded by 30° with sides in slots 1 and 11.

Let the following be defined thus:

g - air gap width
r_r - rotor radius
r - air gap radius = r_r+ ½ g
s - slot spacing at distance r
c - closed contour line of flux
l - axial length of air-gap
a - *la*1 slot span clockwise
b - *la*1 slot span anticlockwise
Q - number of stator slots

Suppose that the coil *la*1 of N turns carries some current i and that the relative permeabilities of the stator and rotor material are such that all the reluctance of the magnetic circuit is effectively in the air gap. The magnetic flux density distribution due to the coil *la*1 will be as shown in **Fig 5.7**. The slots are assumed narrow hence the abrupt change of B at the slots. Also shown are examples of coils linked by both Ba and Bb (*la*2, *la*3 ..) and those linked only by B_b (lb4, lb5 & lb6)

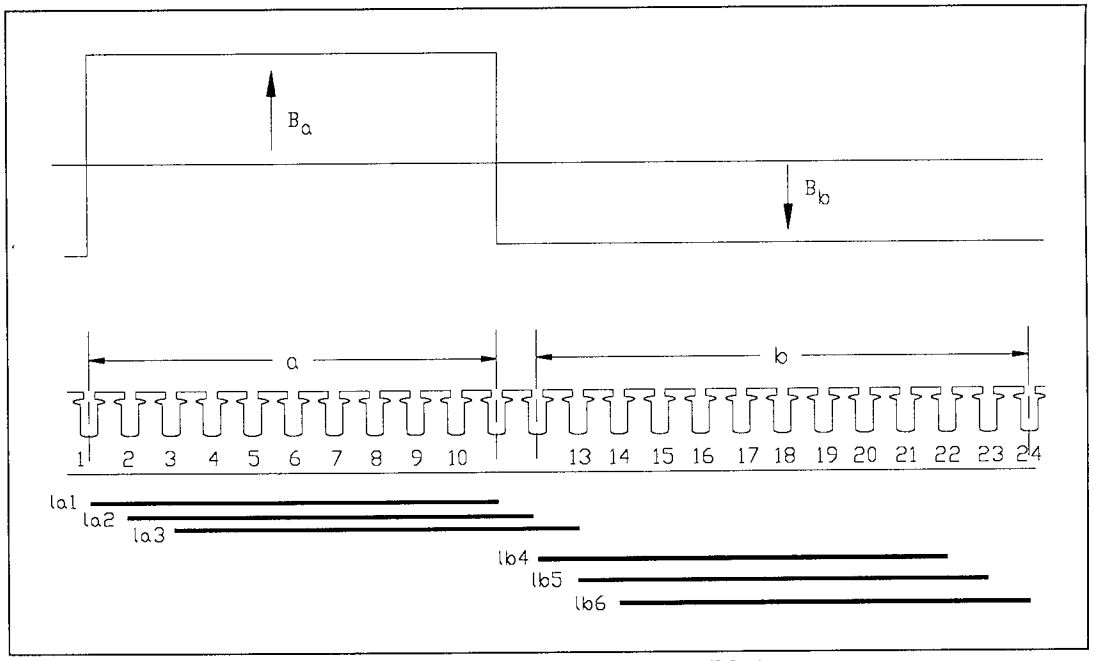

Fig 5.7 - Magnetic flux density distribution due to the coil la1.

5.5.1 Stator Coil Self Inductance L_c

The flux ϕ_a giving rise to B_a must be equal to the flux ϕ_b giving rise to B_b. If A_a is the area of the coil seen by the air gap in the clockwise direction and A_b that seen in the anticlockwise, then:

since $\phi_a = \phi_b = \phi$, it follows $B_a.A_a = B_b.A_b$ (5.8)

But $A_a = l \times s \times a$ and $A_b = l \times s \times b$, whence:

$$B_b = B_a \frac{a}{b} \tag{5.9}$$

The magnetic field intensity H produced by the current i flowing through the N turns is such that:

$$H = H_a + H_b = Ni \tag{5.10}$$

For uniform g, H is related to B by the general expression :

$$B = \mu_o.H/g \tag{5.11}$$

Thus:

$$Ni = \frac{Ba.g}{\mu_o} + \frac{B_b.g}{\mu_o} \tag{5.12}$$

Substituting for B_b :

$$B_a = \frac{N.i.\mu_o}{g} . \frac{b}{a+b} \qquad (5.13)$$

The flux ϕ is given by $\phi = B_a.A_a = B_a.s.l.a$

Substituting for B_a gives:

$$\phi = \frac{\mu_o.l.s.N.i}{g} . \frac{ab}{a+b} \qquad (5.14)$$

By definition of self inductance, $Li = N\phi$, from which $L = N\phi/i$.
Thus:

$$L = \frac{\mu_o.l.s.N^2}{g} . \frac{ab}{a+b} \qquad (5.15)$$

In expressions involving the air-gap width g, the value is slightly different from the average mechanical separation g_m of the rotor and stator members. The air gap from a magnetic circuit view point tends to be somewhat larger than g_m by a factor κ, of between 1.0 and 1.1. This is the Carter effect and the resulting dimension is called the effective air-gap [Brosan et al 1966, Matsch, 1977]. Thus:

$$g_m = g/\kappa \qquad (5.16)$$

Also, at high currents, the magnetic circuit may saturate. The expressions for the inductances described here are then only approximations because the linear relationship between the magnetic field intensity H and the flux density B ceases to hold. A constant k_i is introduced in the denominator of the expressions for self and mutual inductances to account for saturation of the iron.
With these considerations made, the expression for the self inductance of the coil becomes:

$$L = \frac{\mu_o.l.s.N^2}{g.k_i} . \frac{ab}{a+b} \qquad (5.17)$$

5.5.2 Stator coil to coil Mutual Inductance M_β - Case a

Consider a second coil such as l*a*3 in **Fig 5.7** which overlaps the coil l*a*1 and so has a certain fraction of its total area linked by the flux ϕ_a and the rest by ϕ_b. Let β be the clockwise displacement of this coil measured in slots (see that $\beta = 2$ for the coil l*a*3)

The flux linking such a coil due to the coil l*a*1 is such that

$$\begin{aligned}\phi &= B_a A_{a-\beta} - B_b A_\beta \\ &= B_a.s.l.(a-\beta) - B_a \frac{a}{b}.s.l.b \\ &= B_a.s.l.\left(a-\beta\left(\frac{a+b}{b}\right)\right)\end{aligned} \tag{5.18}$$

Substituting Eqn 5.13 in 5.18 for B_a gives the flux ϕ as

$$\phi = \left(\frac{\mu_o.l.s.N.i}{g.k_i}\right).\left(\frac{ab}{a+b}-\beta\right) \tag{5.19}$$

The mutual inductance M_β between such a coil and the coil *la1* is therefore given by

$$\underline{M_\beta = \left(\frac{\mu_o.s.l.N^2}{g.k_i}\right).\left(\frac{ab}{a+b}-\beta\right)} \tag{5.20}$$

5.5.3 Stator coil to coil Mutual Inductance $M_{\beta'}$ - Case a

Now consider a third coil such as lb5 in **Fig 5.6** which does not overlap the coil l*a*1 and is linked only by the flux ϕ_b.

The flux ϕ due to the coil l*a*1, linking such a coil is given by $\phi_a A_a - \phi_b A_a$

Since the area linked by ϕ_a is zero, it follows that $\phi = -\phi_b A_a$

Thus:

$$\phi = -\frac{\mu_o.s.l.N.i}{g.k_i}.\frac{a^2}{a+b} \tag{5.21}$$

The mutual inductance $M_{\beta'}$ between such a coil and the coil l*a*1 is therefore given by

$$\underline{M_{\beta'} = -\frac{\mu_o.s.l.N^2}{g.k_i}.\frac{a^2}{a+b}} \tag{5.22}$$

5.5.4 - The slot displacement s

The slot displacement **s** will be taken to be the chord length between the centres of two adjacent slots at the air gap radius r (see **Fig 5.6**). The mechanical angle between the centres of adjacent slots is $2\pi \div Q$ and $Q = a+b$. Thus:

$$s = \frac{2\pi r}{a+b} = \frac{2\pi r}{Q} \tag{5.23}$$

5.5.5 The rotor

The rotor inductances have been treated rather differently. The concept of a winding magnetic axis is the key to establishing the rotor self and mutual inductances.

In general, a sinusoidally distributed phase winding exhibits a single magnetic axis and for the purpose of analysis can be treated as though it were a single coil. The self inductance of such a coil, due to the air-gap flux, is L_{ph} given by:

$$L_{ph} = \frac{4}{\pi}\mu_0 \cdot \left(\frac{2k_W N_{ph}}{n_p}\right)^2 \cdot \frac{lr}{g} \tag{5.24}$$

Where:

n_p is the number of poles
k_W is the winding factor
N_{ph} is the total series turns per phase
l is the axial length of the air gap
r is the radial length of the air gap
g is the air gap width

The mutual inductance M_{ph} between one such distributed winding and another, whose magnetic axis is at some angle θ is such that M_{ph} is a maximum when the coils are aligned i.e. $\theta = 0$, and a minimum when the coils are in quadrature i.e. $\theta = \pi/2$. For the general angle θ therefore, M_{ph} is a function of θ given by:

$$M_{ph} = \frac{4}{\pi}\mu_0 \cdot \left(\frac{2k_{W1} N_{ph1}}{n_p}\right) \cdot \left(\frac{2k_{W2} N_{ph2}}{n_p}\right) \cdot \frac{lr}{g} \cdot \cos\theta \tag{5.25}$$

where suffixes 1 and 2 relate to the first and second winding parameters respectively.

The cage rotor is generally less straightforward in analysis or design compared to the wound rotor. Appendix A shows the derivation of expressions for the inductances between the rotor

bars and the stator coils, and between rotor bars. It also shows that the cage rotor can be treated as a polyphase winding with the following quantities:

$$N = N_r = 1/2,\ m = m_r = 2Q_r/p \text{ and } k_w = k_{wr} = 1 \tag{5.26}$$

m is the number of phases and k_w is the winding factor, explained in the next section.
The rotor rotates at some angular velocity ω_r, and for a machine with n_p poles connected to a supply of frequency f is such that:

$$\omega_r = \frac{4\pi f}{n_p} \qquad [\text{radians/s}] \tag{5.27}$$

The mutual inductance between the rotor bars and the N-turn stator coil of concern is therefore a periodic function of time and is given, from appendix A, by:

$$M_{ar} = \left(\frac{2\mu_0 . l . r . N}{g . k_i . n_p}\right).\frac{\sqrt{2ab}}{a+b}.\cos(\theta_0 + \omega_r t) \tag{5.28}$$

The mutual inductance M_{rr} between rotor bars at angular separation θ_r can be readily deduced from Eqn 5.25. Thus:

$$M_{rr} = \frac{4}{\pi}\mu_0 . \left(\frac{2k_{wr}N_r}{n_p}\right).\left(\frac{2k_{wr}N_r}{n_p}\right).\frac{lr}{g}.\cos\theta_r \tag{5.29}$$

Since $N_r = 1/2$, it follows that the mutual inductance between rotor bars, due to the air gap flux is given by:

$$M_{rr} = \frac{4\mu_0 . l . r . k_{wr}^{\ 2}}{\pi . n_p^{\ 2} . g}.\cos\theta_r \tag{5.30}$$

Thus, the mutual inductance between rotor bars is a cosine function of their angular separation.

These analyses were carried out primarily for the purpose of developing a simulation model for the induction machine stator winding. In general, the rotor plays no part in the phase shifting properties of the stator winding and can be ignored for this particular purpose. However, it does affect the magnitude of the supply current (transformer action of induction motor) and distorts the voltage waveforms slightly when running.

5.5.6 - The Stator Coil Inductance Constant - L_o

L_o is introduced here merely to simplify the expressions and calculations of the self and mutual inductances in the stator winding. It's units are Henries, but it has no practical significance.
It has been shown that:

$$L = \frac{\mu_o.l.s.N^2}{g.k_i}.\frac{ab}{a+b},\ M_\beta = \left(\frac{\mu_o.s.l.N^2}{g.k_i}\right).\left(\frac{ab}{a+b}-\beta\right)\ \&\ M_{\beta'} = -\frac{\mu_o.s.l.N^2}{g.k_i}.\frac{a^2}{a+b}$$

It follows that a constant L_o can be defined to reduce the expressions to direct functions of the parameters a and b. Thus:

$$L_o = \frac{\mu_o.l.s.N^2}{g.k_i} = \frac{\mu_o.l.2\pi r.N^2}{g.k_i.(a+b)} \qquad (5.31)$$

whence:

$$L = L_o\frac{ab}{a+b} \qquad M_\beta = L_o\left(\frac{ab}{a+b}-\beta\right)\ \& \qquad M_{\beta'} = -L_o.\frac{a^2}{a+b} \qquad (5.32)$$

5.5.7 - The Coil Induced emf.

As a first step towards establishing the induced emf's, let the rotor effects be ignored.
For any coil such as $la1$, the voltage induced can be written in terms of the self and mutual inductances of the coil and every other coil in the stator winding. If the coil has some resistance R_1 and carries current i_a, then in general, for 8 coils per phase the induced emf e_1 is given by:

$$e_1 = i_aR_1 + L\frac{di_a}{dt} + M_{a1a2}\frac{di_{a2}}{dt} + M_{a1a3}\frac{di_{a3}}{dt}....+M_{a1c8}\frac{di_{c8}}{dt} \qquad (5.33)$$

Note that Eqn 5.33 assumes constant inductance and therefore ignores iron effects.
Now in the absence of any electrical load connected to the tapping points, the current through all the coils in the 'a' phase is the same, and the same applies to the other phases. Thus:

$$\begin{aligned} e_1 = i_aR_1 &+ \frac{di_a}{dt}\left(L + M_{a1a2} + M_{a1a3}....+M_{a1a8}\right) \\ &+ \frac{di_b}{dt}\left(M_{a1b1} + M_{a1b2}....+M_{a1b8}\right) \\ &+ \frac{di_c}{dt}\left(M_{a1c1} + M_{a1c2}....+M_{a1c8}\right) \end{aligned} \qquad (5.34)$$

Or, more concisely:

$$e_1 = i_a R_1 + \sum_{n=1}^{8} M_{a_1 a_n} \frac{di_a}{dt} + \sum_{n=1}^{8} M_{a_1 b_n} \frac{di_b}{dt} + \sum_{n=1}^{8} M_{a_1 c_n} \frac{di_c}{dt} \qquad (5.35)$$

where M_{a1a1}, the mutual inductance between the coil $la1$ and itself, is taken to refer to the coil self inductance L. If the rotor were taken into account, e_1 would become:

$$e_1 = i_a R_1 + \sum_{n=1}^{8} M_{a_1 a_n} \frac{di_a}{dt} + \sum_{n=1}^{8} M_{a_1 b_n} \frac{di_b}{dt} + \sum_{n=1}^{8} M_{a_1 c_n} \frac{di_c}{dt} + \sum_{n=1}^{Q_r} M_{a_1 lr_n}(\omega_r t) \frac{di_{lr_n}}{dt} \qquad (5.36)$$

The time dependency of the mutual inductance between stator coil and the Q_r rotor bars is noted by expressing the quantity as a time function of the rotor angular velocity ω_r in the last term.

There is one such expression for the voltage across each coil, and assuming the coils identical and the currents sinusoidal (di/dt is a sinusoidal quantity), the induced emf's in each coil are equal but phase displaced by some amount.

5.5.8 - Phase voltage and current

If E is the induced voltage in each *phase* winding and i_a, i_b and i_c are the phase currents, then this voltage will be divided between the resistive and inductive components of the phase winding impedance. This may be expressed as:

$$E = i_a \cdot \sum_{n=1}^{8} R_n + \sum_{n=1}^{8} L_n \frac{di_a}{dt} + \sum_{n=1}^{7} \sum_{m=n+1}^{8} M_{a_n a_m} \frac{di_a}{dt} + \sum_{n=1}^{8} \sum_{m=1}^{8} M_{a_n b_m} \frac{di_b}{dt} + \sum_{n=1}^{8} \sum_{m=1}^{8} M_{a_n c_m} \frac{di_c}{dt} \qquad (5.37)$$

i.e.

$$E = V_{\text{resistive drop}} + V_{\text{self inductance}} + V_{\text{phase a mutual}} + V_{\text{phase b mutual}} + V_{\text{phase c mutual}}$$

The phase current lags the phase voltage by some angle φ, so that if i_a is the phase 'a' current of peak magnitude I_o, then, assumed sinusoidal,

$$i_a = I_o \sin(\omega t - \varphi)$$

The currents i_b and i_c in phases b and c respectively can therefore be described by:

$$i_b = I_o \sin(\omega t - \varphi - 2\pi/3) \qquad \& \qquad i_c = I_o \sin(\omega t - \varphi + 2\pi/3)$$

Each coil voltage can therefore be computed, and so too the tapping point to neutral voltages. A computer spreadsheet was used to compute and plot the voltages shown in **Fig 5.8** for one

such analysis on a 24-coil DLL stator winding using example values of Q=24, a = 10, b = 12, k_i = 1, g=0.3mm, N=35, l=76mm and r=35mm. The phase pattern of **Fig 5.8** was obtained for phase *a* only. The time axis has been scaled to represent angular measure in degrees for ease of measurement.

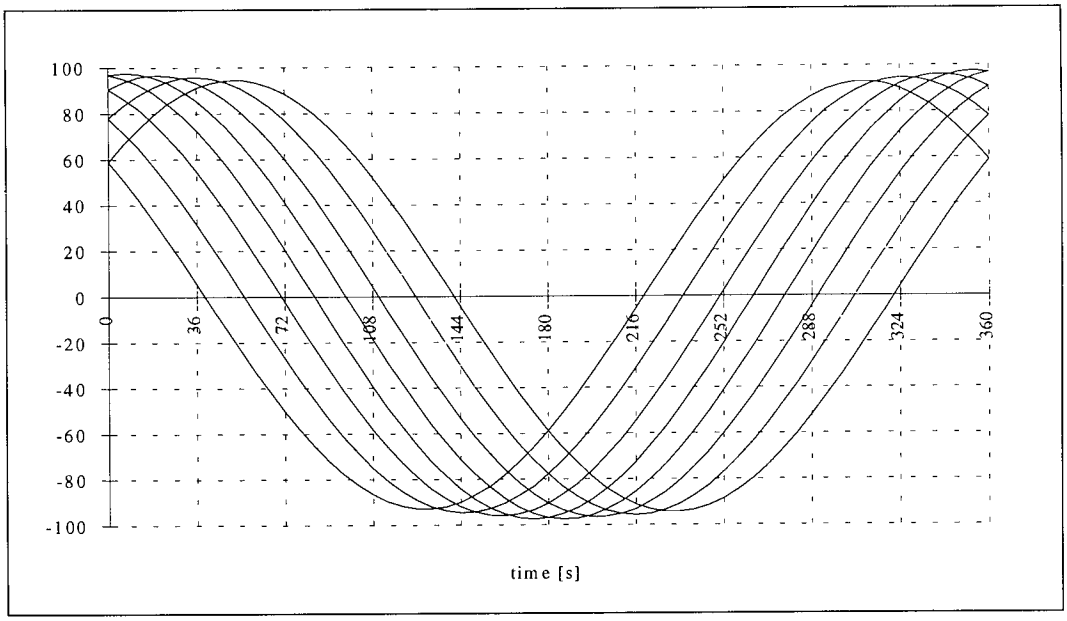

Fig 5.8 - Phase 'a' voltages derived from equation 5.35 with example values.

Note that the voltages of **Fig 5.8** are those *across* each coil rather than measured from a common reference. The phase shifts are therefore independent of phase connections (star or delta) although the magnitudes will be proportional to the applied volts, being greater for a delta connection when the applied volts are equal to the phase-to-phase. The phase shifts are the same and equal to the slot angle. The assumption that a sinusoidal flux distribution exists in the air-gap is justified rather than invalidated when rotor effects are taken into consideration c.f. amature reaction [Fitzgerald et al, 1992].

The conclusion to be drawn from this analysis is that **the stator winding behaves as a source of polyphase voltages whose phase shifts are fixed by design.**

The mutual inductances between any two coils remains the same for either star or delta connections. It should therefore be possible to model the machine winding inductances, and then specify different types of connections to observe the effects of such changes.
Rotor effects have been ignored but experimental results suggest that the approximations are good.

5.6 WINDING DISTRIBUTIONS

This section of the thesis discusses the coil arrangement within the stator and introduces the associated terminology and vector algebra for the induced emf's.

A double layer lap winding for a three phase stator features an equal number of coils per phase. These are normally distributed evenly around the stator periphery, so that each phase occupies an equal number of slots under each pole. Thus, a 24 slot machine wound for 4-pole operation will feature 24/3 = 8 slots per phase arranged such that there are 2 under each pole. The slots under a pole belonging to the same phase are termed a *pole phase group*.

As before, define:

Q = total number of slots
n_p = number of poles
m = number of phases
q = number of slots per pole per phase

and see that for Q = 24, n_p = 4 and m=3, q = 24/(3×4) = 2.
A 4-pole machine has an equivalent 720° i.e. angle per pole (180) × total poles. The **slot angle,** τ is the electrical angle between two adjacent slots and is such that:

$$\tau = \text{Total electrical degrees / total slots} = (180 \times n_p) / Q \qquad (5.38)$$

The emf's in the coil sides of the same phase in adjacent slots are displaced by τ. The number of parallel paths is of significance here but is ignored for the time being. A 48-slot stator wound for 4-pole operation therefore features a slot angle of 15°.

Fig 5.9 is a schematic of one phase of a 24 slot DLL stator wound for 3-phase 2 pole operation and featuring N-turn coils short pitched by 30°. Their interconnection to form a phase winding is also shown.

Let l*a*1 be the first coil in slot 1, with the first side labelled 1 at the top in slot 1 and the second side labelled 1' at the bottom in slot 11.

The voltages induced in each coil *side* add up as illustrated in **Fig 5.5b**. Addition of the resultants of each of these coils to give the phase voltage requires that the slot angle and the direction of winding are taken into consideration.

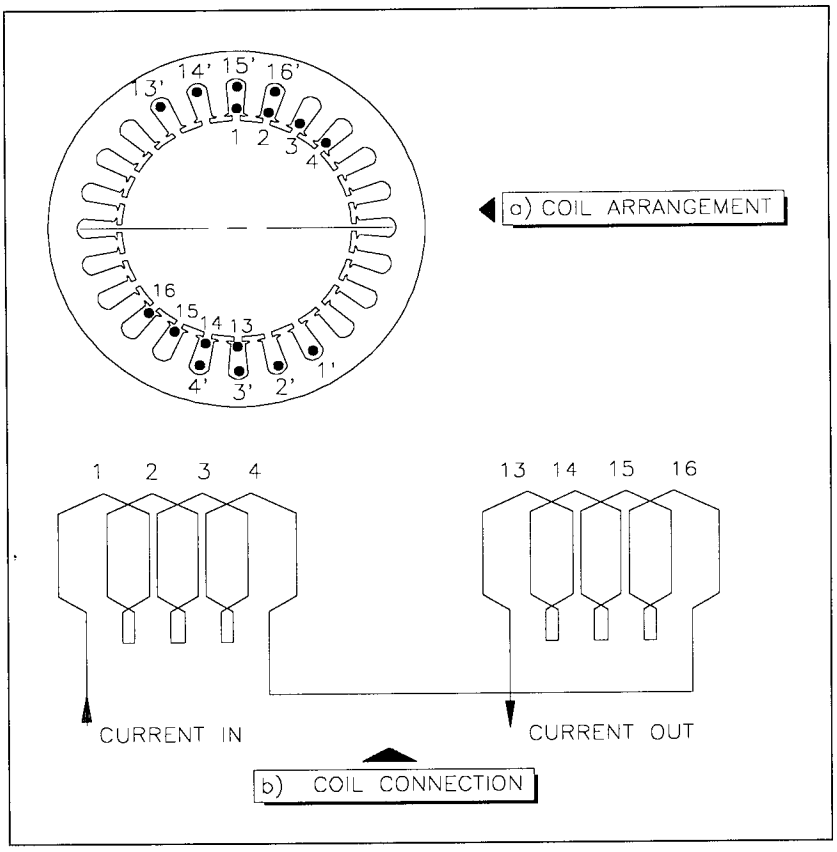

Fig 5.9 -

Conventional 24 slot stator winding for 3-phase 2-pole operation showing:

a) Coil arrangement in stator slots (1-1' is one coil)

b) Coil connections

Thus, if the resultant emf of the coil la1 is taken as the reference at 0°, then the angles at which the rest of the coil emf's occur can be deduced directly from **Fig 5.9**. The coils in slots 1, 2, 3 and 4 have emf's at angles 0, 15, 30 and 45° and the coils in slots 13, 14, 15 and 16 have emf's at angles -180, -195,-210 and -225°. The flux under the second pole is opposite to that under the first, so the winding under the second pole reverses as shown to ensure that the emf's in the coils are additive rather than opposing. The vector diagram is shown in **Fig 5.10**.

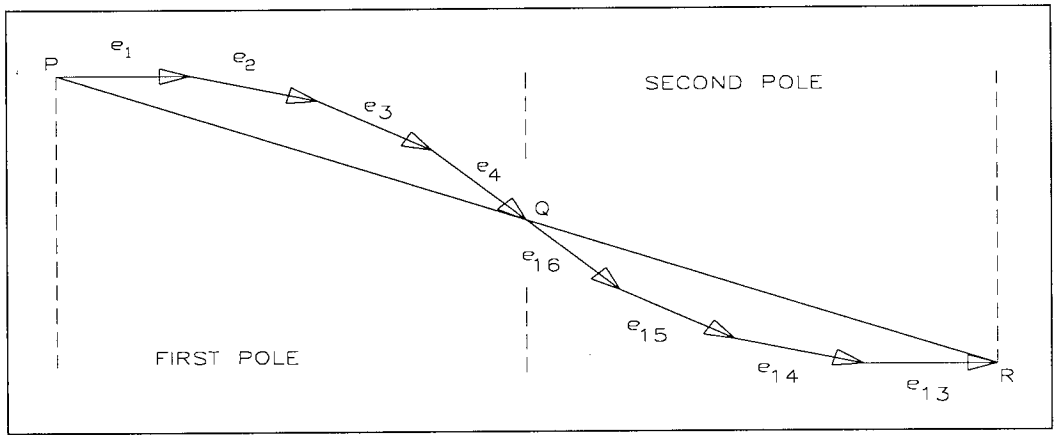

Fig 5.10 - Vector addition of coil voltages in a phase

Referring to **Fig 5.10**, the resultant **PQ** of the voltages under the first pole only is called the *pole group emf.*

The overall resultant **PR** is the phase voltage and equals the terminal voltage applied.

In general, the phase shifts are repeated under a pole pair and therefore, the total number of *unique* phase shifts equals those under a pole; i.e. q. As there are 180° under a pole, and the slots under a pole are equally divided amongst the three phases, each phase necessarily occupies 60°. This type of winding, characterised by the 60° maximum phase shift under a pole, is referred to as a *60° pole phase group winding*, or simply a *60° winding*.

The emf's in this band constitute the unique phase shifts available per phase, and are wholly contained within this band of 60°. Thus, doubling the number of poles to 4 to get a total of 720° electrical doubles the slot angle from 15° to 30° but halves the number of slots per pole per phase (q) from 4 to 2.

In general therefore, for a fixed number of slots, the more poles in the winding, the less the number of unique phase shifts and the greater the slot angle.
Also, for a three phase winding in general, whatever the connection and pole phase group, the supply is connected to the coils in the slots at angles 0, 120° and 240°. All other connections are referenced to these.

The 60° winding is the normal type of winding found on machines and is referred to throughout this text as the *conventional* winding. It is described here because a modification to the pole phase group has been found necessary in the proposed application.

In order to meet the coupling requirements listed in section 4.3, equipotential voltages are required, with the same phase shift between successive tapping points.

The terminals of the phase winding can be connected in either star or delta for three phase operation. Each connection gives rise to a different system of polyphase voltages, and these are discussed in this chapter.

5.6.1 - Star connection

Fig 5.11 is the vector diagram of **Fig 5.10** with the voltages between coils shown for star operation . The neutral point is labelled '0'.

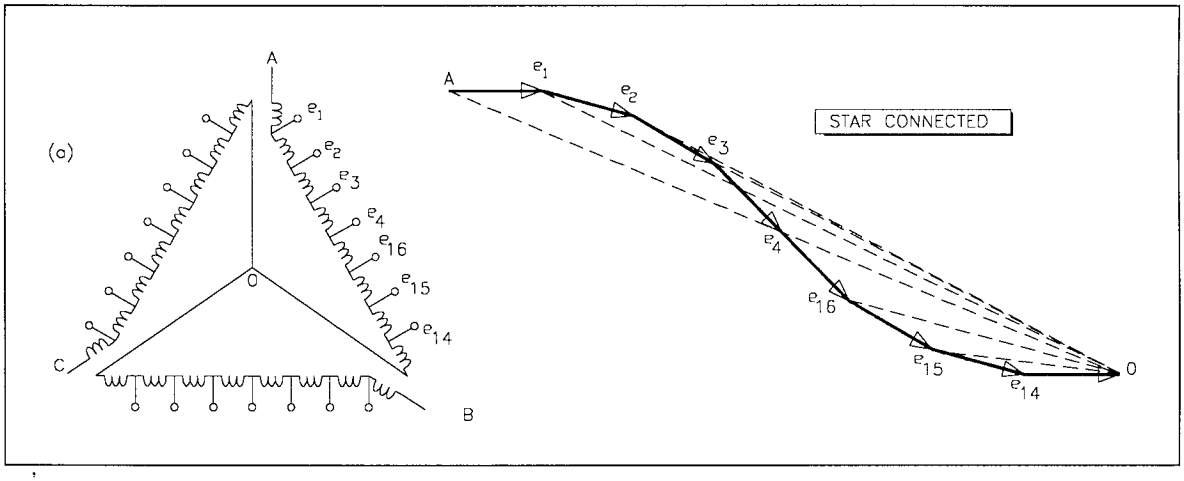

Fig 5.11 Star connected 24-coil stator and vector diagram of coil voltages in phase A.

The vector **0A** is the applied voltage between terminal A and the neutral, and each of the vectors $\mathbf{0e_n}$ for the values of n shown as subscripts represent the tapping point to neutral voltages. The vectors are drawn to scale, and it should be apparent, even in the absence of mathematical analysis, that the magnitudes of the voltages are unequal. The phase shifts are also unequal as can be seen comparing $\angle\mathbf{e_2 0 e_3}$ and $\angle\mathbf{e_1 0 A}$. Thus, in general, **a star connected winding is not suitable for interfacing to the proposed STATCON**

5.6.1 - Delta connection

Consider now the diagram of **Fig 5.12** in which the same winding is connected for delta operation. The vector **AB** represents the phase to phase voltage between the terminals connected to the supply phases A and B.

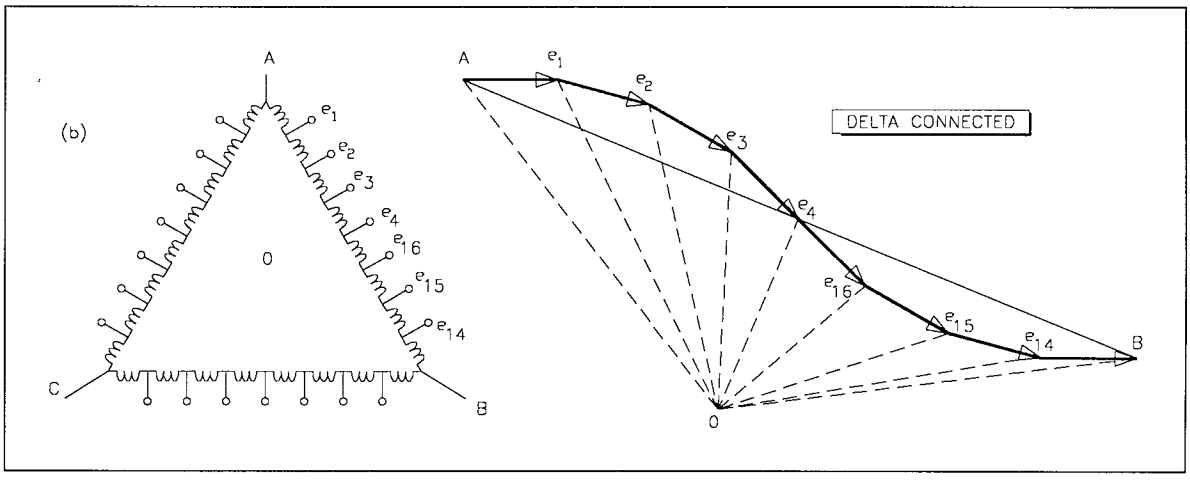

Fig 5.12 Delta connected stator and vector diagram of coil voltages in phase A (Limb AB)

- $\angle\mathbf{A0B} = 120°$, which is the angle between any two of the supply phases
- Each of the vectors $\mathbf{0e_n}$ represents the tapping point to neutral voltage
- $|\mathbf{0A}| = |\mathbf{0B}|$, which is the supply phase to neutral voltage

- The magnitudes of the voltages are unequal e.g. $|0A| > |0e_2| > |0e_4|$
- Although there is a general improvement in the phase shift pattern compared to the star connected winding, the phase shifts are still unequal.

The magnitudes and phase shifts of these voltages can be computed from the geometry. The results of **Fig 5.12a** for a star connection and **Fig 5.12b** for a delta connection are repeated in **Fig 5.13** below as sinusoids.

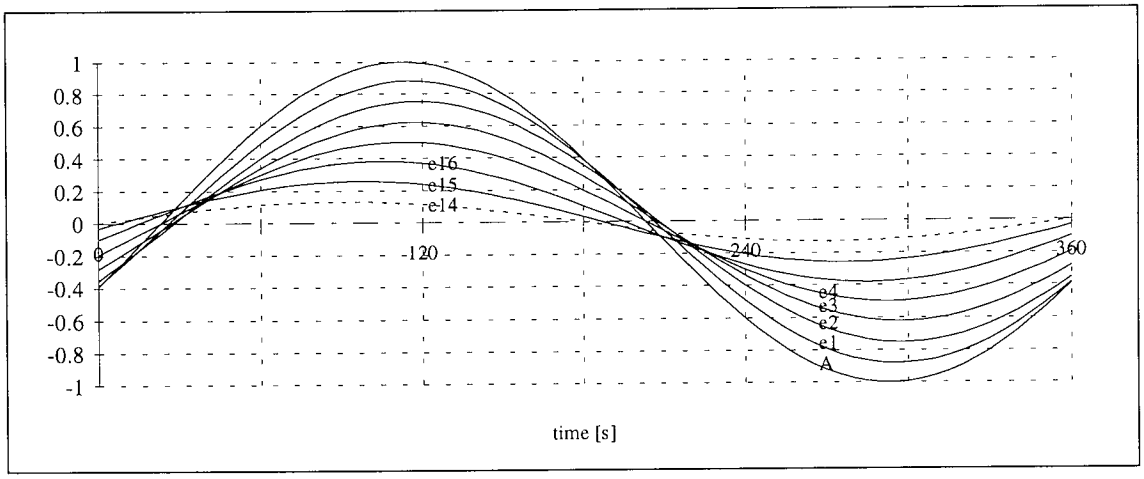

Fig 5.13a - Phase A voltages from a star connected 60° phase spread winding

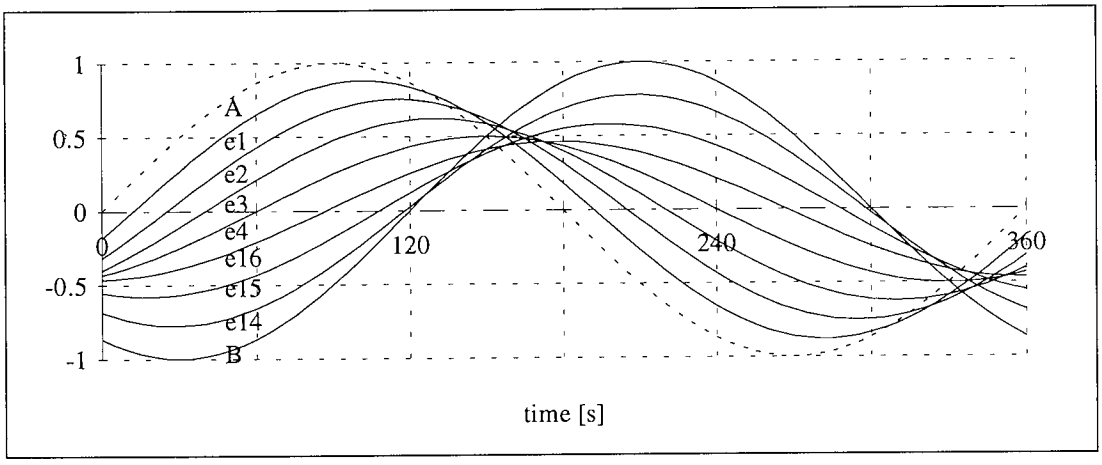

Fig 5.13b - Phase A voltages from a delta connected 60° phase spread winding

The general conclusion to be drawn from the observations of **Fig 5.12** is that a 60° winding, does not yield a system of equipotential voltages phase shifted by the same amount and is therefore unsuitable for interfacing to the proposed STATCON.

It *may* be possible to alter the topology of the STATCON to suit a 60° winding, hence the term 'proposed', but such a design is outside the scope of this discussion.

5.7 THE 120° POLE PHASE GROUP WINDING

From the previous descriptions, it should be evident that the required system of voltages is one whose vector diagram has all tapping points lying along the circumference of a circle, centre 0, so that all the magnitudes are equal (circle radius) and all the phase shifts are equal.

Such a phase shift pattern can be obtained from a delta connected stator in which, for a two pole machine, all the coils belonging to a phase occupy successive slots. **Fig 5.14** shows such a winding for a 24-slot stator connected for 3-phase 2-pole operation.

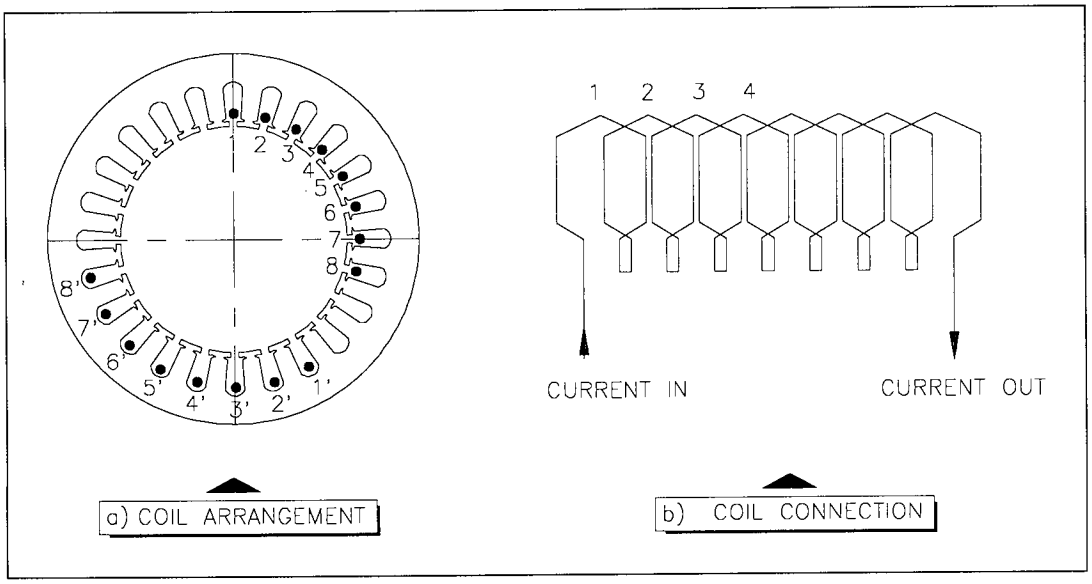

Fig 5.14 - 24-coil stator wound for 3-phase 2-pole operation, 120° phase spread

The phase shown occupies 2/3 rather than 1/3 the slots per pole, hence spans 120 out of the 180° electrical. The delta connection and vector diagram are shown in **Fig 5.15.**

The key differences between this winding and that of **Fig 5.9** are as follows:

- All coils are placed in consecutive slots so that the angle between any two adjacent coils is the same.

- The vectors lie along the circumference of a circle, so, not only are the coil voltages equal but so are their potentials with respect to the neutral as shown.

Note from **Fig 5.15** that differences in the coil emfs will lead to differences in angles with respect to the neutral point. This of significance and is explained in chapter 8.

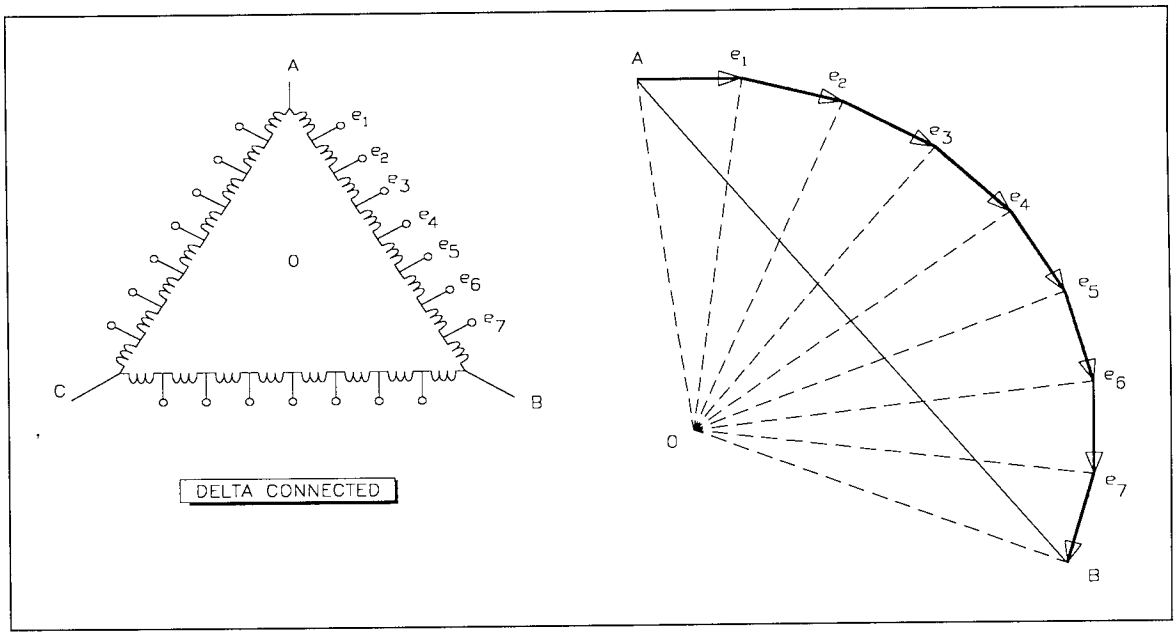

Fig 5.15 - Delta connection diagram showing all tapping points and the associated voltages

5.8 - INITIAL ASSESSMENT OF WINDING AS COUPLING

From the preceding sections, it may be concluded that the stator winding of **Fig 5.14** satisfies all the conditions listed in section 4.3 except for the coupling impedance. Thus:

- The winding produces equipotential voltages, appropriately phase shifted as required.
- Transformer action within the winding makes the stator tapping points low output impedance voltage sources. Compare this with potential divider action.
- The winding does in general, permit bidirectional flow of reactive power between the compensator and the supply and so should meet this requirement adequately.
- The winding, like that of a transformer, also provides a linear medium for harmonic cancellation (evident in the production of a sinusoidal air-gap flux distribution).

In altering the winding connections to achieve the desired phase pattern, the fundamental machine design has been altered. The implications are that the resultant of the phase group, vector AB in **Fig 5.15**, is less than that of a conventional winding such as that of **Fig 5.12**. This is a consequence of the change in the winding *distribution*, which, in computations of fluxes and similar, is accounted for by the **distribution factor k_D**, generally given by:

$$k_D = \frac{\sin(q.\tau/2)}{q.\sin(\tau/2)} \qquad (5.39)$$

For the 120° winding, q = 2/3 rather than 1/3 the slots under a pole. Thus, if q_1 and q_2 be the slots per pole per phase for the 60° and 120° windings respectively, then $q_2=2q_1$.

The chording factor k_C, accounting for induced emf reduction due to *short pitching* coils, and the distribution factor k_D above, accounting for induced emf reduction due to the modified *coil connections* are normally combined into a single parameter called the winding factor, $\mathbf{k_w}$, mentioned earlier in discussing rotor inductances. Thus:

$$k_w = k_D \times k_C. \tag{5.40}$$

Note however, that the reduction in the total induced emf AB in **Fig 5.15** is a consequence of the reduced distribution factor rather than chording factor and can be quantified as follows:

Let k_{D1} and k_{D2} be the distribution factors for the 60° and 120° pole phase group windings respectively. As stated above, $q_2 = 2q_1$. Also, the slot angle τ is such that $q_1 \times \tau = 60°$ for a 60 degree phase spread.

Percentage reduction in distribution factor is $\frac{k_{D1}-k_{D2}}{k_{D1}}\times 100$:

But:

$$\frac{k_{D2}}{k_{D1}} = \frac{\sin(q_2.\tau/2)}{q_2.\sin(\tau/2)} \div \frac{\sin(q_1.\tau/2)}{q_1.\sin(\tau/2)} = \frac{q_1.\sin(q_2.\tau/2)}{q_2.\sin(q_1.\tau/2)} \tag{5.41}$$

Thus:

$$1-\frac{k_{D2}}{k_{D1}} = 1-\frac{q_1.\sin(2q_1.\tau/2)}{2q_1.\sin(q_1.\tau/2)} = 1-\cos(\tau/2) \tag{5.42}$$

whence

percentage reduction in induced emf = 1-cos(30°) = 13%

Thus:

the 120° pole phase group winding has a poorer winding factor than the conventional winding, hence reduced induced emf's per phase and associated quantities.

5.9 - SUMMARY

This chapter discusses the Induction motor and explains the lagging power factor as being due to the magnetising current, a component of the excitation current.

The peaked nature of the waveform of the excitation current is explained and its role in the production of a sinusoidal flux distribution.

Induction motor stator windings are discussed with a view to establishing a suitable winding type for the intended application.

The machine winding inductances are described and expressions for the flux, self and mutual inductances per coil, and the induced emf's are derived and used in modelling the winding for the purpose of simulation. The rotor winding is described in brief. Appendix A gives further detail.

A suitable winding configuration to produce the desired system of voltages at the stator tapping points is established. It is a delta connected winding with a 120° pole phase group distribution. In the process, it is stated that:

- a star connected winding is unsuitable,
- a conventional winding featuring a 60° pole phase group is unsuitable and
- the change in distribution from the conventional winding incurs a 13% reduction in the magnitude of induced emf, hence related parameters.

Of the four coupling requirements listed in section 4.3, the modified stator winding is seen to meet three adequately i.e. all but the provision of the required coupling impedance.

CHAPTER 6

STATCON-STATOR WINDING INTERFACING

This chapter discusses the coupling design considerations and system sizing in brief. The design procedure is given further treatment in appendix B.

The per phase equivalent circuit of the induction motor is shown in **Fig 6.1**. The rotor is assumed to be of the cage type, hence the shorting link on the rotor (secondary) side of the circuit.

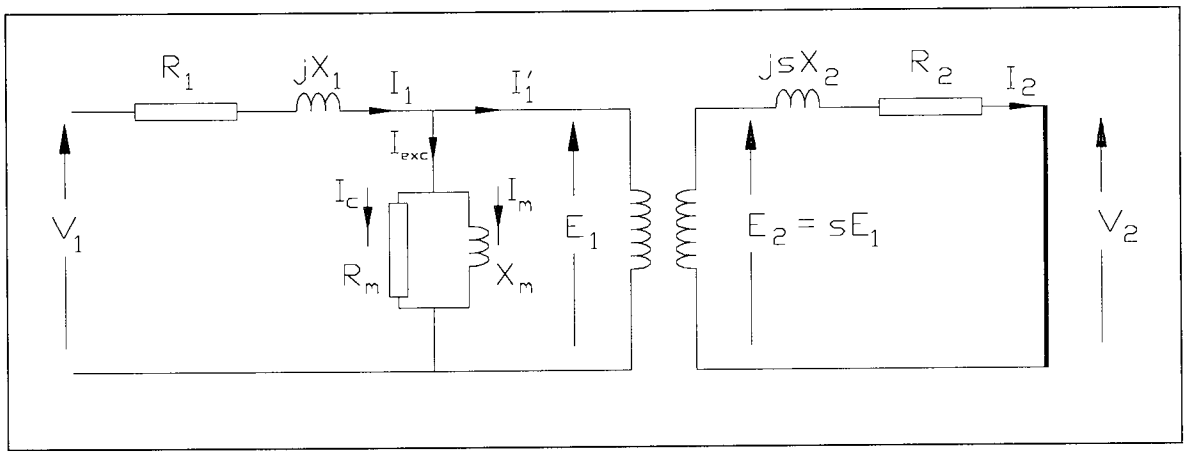

Fig 6.1 - Per phase equivalent circuit of an induction machine

In general, the stator leakage reactance of an induction machine, shown as jX_1 in **Fig 6.1** above, is greater than that of an equivalent size transformer (VA) on account of the higher leakage fluxes around the air-gap. High values of X_1 would be a desirable feature in interfacing with a STATCON which requires the leakage inductance for a coupling reactance. However, in the case of a zigzag transformer coupling, the terminals across which the voltage V_1 is applied (see **Fig 6.1**) are those of a *phase* winding and the leakage reactance X_1 is that due to the total per phase leakage flux. This is not so in the proposed scheme since the leakage reactance available to each phase connection from the STATCON is only a fraction of the total.

Also, since it is proposed to connect the compensator to tapping points between stator coils rather than the entire phase winding, the leakage inductance that would be seen by any phase connection from the bridge is likely to be mainly due to the end leakage flux.

6.1 - COUPLING IMPEDANCE

In order to connect a STATCON phase to the particular tapping point with the desired phase shift, some reactance is required, which, as stated in chapter 4, must appear electrically as a series inductance for the stated reasons.

Unlike the zigzag transformers of chapter 4 however, there is no distinct secondary winding present to provide the coupling leakage reactance. The required connections are as shown in **Fig 6.2** below.

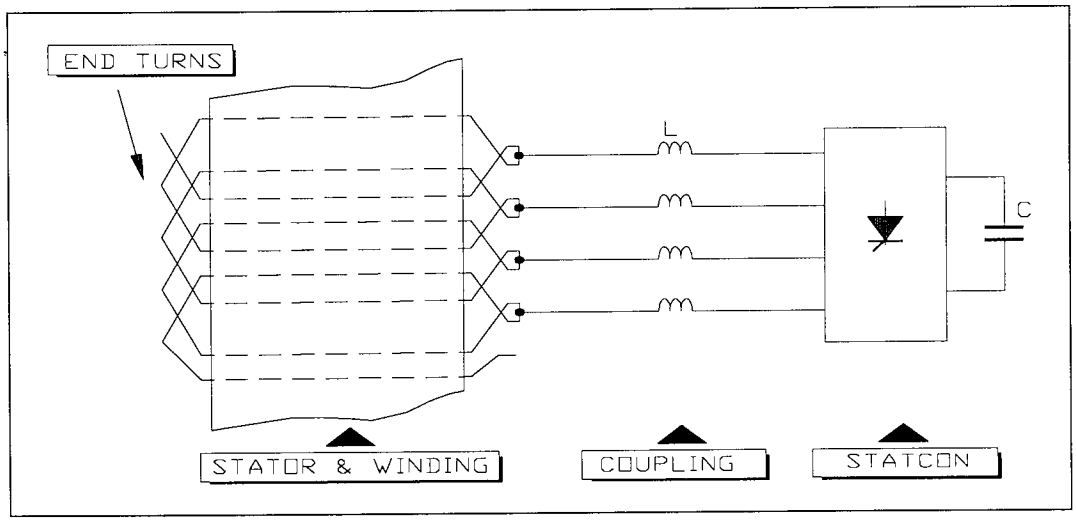

Fig 6.2 - Connected system showing required location of coupling reactance.

The coupling inductance L in **Fig 6.2** can probably be realised in one of two ways.

a) Direct coupling to the winding tapping points, relying on the winding leakage flux to provide sufficient inductance in the connecting leads.

b) Use of external reactors.

6.1.1 - Coupling by Leakage Inductance

Coupling leads are used to connect the stator phases to the magnetic coupling. If sufficient inductance were somehow introduced into these leads, then this requirement would be adequately met without the need for external reactors. Such a mechanism is likely to involve leakage fluxes and these are discussed next.

The flux produced by the coils in the stator winding does not all follow the intended path, which is to cross the air gap and link the rotor circuit. The flux that does is termed **mutual flux** and goes towards creation of the machine torque.

Some of the flux however, is termed leakage flux because it does not link the stator and rotor circuits as required. This leakage flux gives rise to a leakage reactance, which itself is made up of a number of components [Brosan & Hayden, 1966; Cotton, 1934; Alger, 1969] that include the following:

6.1.1.1 - Tooth-top leakage

This is the flux emanating from one tooth of the stator or rotor member and linking the adjacent teeth of the same member without crossing the air gap. It can be quite large in some machines.

6.1.1.2 - Zigzag leakage

For any two teeth on the stator and rotor displaced by some distance x (between their centres say), there will be between them an MMF which is a function of the displacement x.

6.1.1.3 - Overhang (End-turn) Leakage

While expressions for the tooth-top and zigzag leakage fluxes are available, the exact calculation of overhang leakage is rather difficult on account of the complicated geometry of the windings beyond the confines of the slot. In general, the shape of the end-windings, the effects of adjacent coils and phases, and the effects of stator and rotor circuits on each other should be accounted for. Calculations based on machine geometry are unreliable, and so empirical formulae are used instead.

The following components of leakage flux are generally of small magnitude and are often ignored in most analyses.

6.1.1.4 - Incremental Reactance

This results from the saturation of the iron in the leakage paths. It is greatest at no load and decreases as the current increases.

6.1.1.5 - Harmonic leakage reactance

Also called the *belt* or *differential* leakage reactance. This is due to differences that may exist in the stator and rotor mmf's. Such imbalance gives rise to harmonic fluxes which rotate at their own synchronous speeds and so cause a reactive voltage drop in the stator fundamental frequency component. The harmonic leakage is zero in cage induction machines since the rotor currents respond exactly to the stator mmf.

6.1.1.6 - Skew Reactance

This leakage reactance is present only if the rotor slots (bars) are skewed. Skewing decreases the induced voltage in a rotor conductor, i.e. appears to reduce the mutual flux compared to the total stator flux which has the same effect as increased stator leakage. Nevertheless, it is used to reduce parasitic torques and noise [Matsch, 1977].

6.1.1.7 - Peripheral Leakage Reactance

There are components of the leakage flux that exist wholly within the coil and do not enter the stator or rotor iron at all. These give rise to the peripheral leakage reactance, and the flux exists circumferentially round the air-gap without making contact with either the stator or rotor iron. Its magnitude depends on the ratio of the gap length to pole pitch. It is negligible for most machines and will be treated as thus in this discussion.

The performance of an induction motor is influenced by the leakage reactance. It is generally desirable in these machines that the leakage flux is minimised. Thus, while the zigzag transformers can be wound for sufficiently large leakage reactance to provide the coupling impedance, this would not be adviseable in the case of rotatating induction machines.

The tooth-top, zigzag and overhang leakage fluxes are normally the ones of concern and are accounted for in the design. Most text books on induction machine design give methods of calculating these as accurately as possible given the complexity of determining the overhang leakage as stated earlier [Matsch, 1977; Brosan et al, 1966; Cotton, 1934 ; Alger, 1969].
From **Fig 6.2**, it should be apparent that the only component of leakage flux that can link a conductor connected to the tapping point is the overhang or end turn leakage. This is illustrated in **Fig 6.3**.

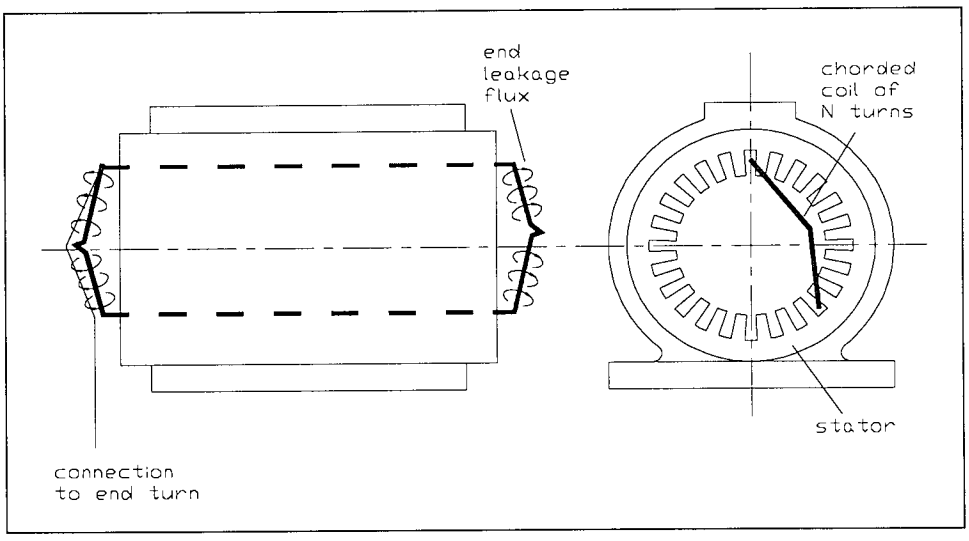

Fig 6.3 - Illustration of end turn leakage flux linking connecting lead.

Alger [1969, Chapt 7] discusses the end-turn leakage flux in some detail and concludes with a simplified expression for the total end leakage reactance x_e due to both stator and rotor as:

$$x_e = 4\times10^{-6}\times 7f.m.2r.\frac{(k_w.N_{ph})^2}{(a.n_p)^2}(\frac{\lambda}{\lambda_p}-0.3) \qquad [\Omega/\text{phase}] \qquad (6.1)$$

where:

- f is the supply frequency in Hz,
- λ/λ_p the winding pitch,
- k_w the winding factor
- r the air gap radius and
- m the number of phases
- n_p the number of poles
- a the number of parallel paths
- N_{ph} the per phase series turns.

Assuming the supply sinusoidal, the leakage inductance L_e responsible for x_e is

$$L_e = \frac{x_e}{2\pi f} = \frac{4\times7\times10^{-6}\times m.r}{\pi}.\left(\frac{k_w N_{ph}}{a n_p}\right)^2(\frac{\lambda}{\lambda_p}-0.3) \qquad (6.2)$$

x_e is shared equally between stator and rotor whence the stator end leakage inductance L_s is :

$$L_s = \frac{L_e}{2} = \frac{4\times7\times10^{-6}\times m.r}{2\pi}.\left(\frac{k_w N_{ph}}{a n_p}\right)^2(\frac{\lambda}{\lambda_p}-0.3) \qquad (6.3)$$

From appendix A, the per phase inductance L_{ph} of the stator winding due to the air gap flux was given as

$$L_{ph} = \frac{4}{\pi}\mu_0\left(\frac{2k_w N_{ph}}{a n_p}\right)^2\frac{lr}{g} \qquad (6.4)$$

The ratio of the end leakage inductance to the main inductance is therefore given by:

$$\frac{L_e}{L_{ph}} = \frac{0.7m.g}{32\pi l}.(\frac{\lambda}{\lambda_p}-0.3) \qquad (6.5)$$

and for m=3:

$$\frac{L_e}{L_{ph}} = \frac{2.1g}{32\pi l}.(\frac{\lambda}{\lambda_p}-0.3) \qquad (6.6)$$

For g =0.3mm, l=76mm, λ = 10, λ_p = 12 $\underline{L_e / L_{ph} \approx 4.5\times10^{-5}}$ (6.7)

L_e is the end leakage flux per phase. This value has to be halved to get the per phase end leakage on one end of the machine. Further, the resulting value has to be divided by the square of the number of coils per phase to get the per coil end leakage inductance. In general therefore, while it may be possible to obtain some inductance in the connecting leads due to the end leakage flux, the value is much less than that required to effect meaningful reduction in the size of the storage capacitor on the bridge, or realise the level of harmonic reduction required of the coupling reactance. Further:

- It would not be possible in practice to couple a connecting lead so that it is linked by *all* the leakage flux intended.

- For maximum inductance, the leakage flux lines would have to be normal to the plane of the connecting lead. This would be difficult to achieve in practice.

- Inductance is proportional to the square of the number of turns. A connecting lead is in essence half a turn.

Thus, the coupling inductance realised by relying on the leakage flux from the machine is unlikely to be adequate for the intended application, especially in small machines.

This point is revisited in the concluding chapter and in appendix A, section 02.

6.1.2 - Coupling by External Reactors

If additional external inductors or transformers are used, then the required value of L can be achieved quite accurately by design [Ferrari, 1975]. Of course there is the penalty to pay, that bulky and potentially expensive components are being introduced, and this is probably the single most notable draw back in the entire scheme. However, given the limitations of dependency on leakage inductance as a coupling impedance, the use of external reactors becomes inevitable. Hill [1995, Chapt 3] discusses the possibility of reducing the number of coupling reactors in a similar topology by moving them to the primary side of the supply, where only three phases are present, but argues that the harmonic performance deteriorates.

6.2 - GENERAL DESIGN PROCEDURE

6.2.1 - Machine Stator and Winding

The requirement was to design a three phase stator winding suitable for interfacing to a 24-pulse STATCON. It was also desirable that the resulting machine be as small as possible for reasons of cost and safety.

- A 24-pulse STATCON requires 12 phases at 15° shifts.
- These 12 phases are to be derived from the main 3-phase supply, therefore each of the three main phases must give rise to 4 phases at 15° shifts.
- The total number of unique phase shifts per stator phase is equal to the number of coils per pole per phase.
- It can be shown that the smallest machine that will give the desired phases and meet all the constraints of a delta connected winding featuring 120° pole phase groups has 24 slots and is connected for 2 poles. The machine features a single coil between tapping points.

Such a winding is shown in **Fig 6.4** with all possible tapping points labelled.

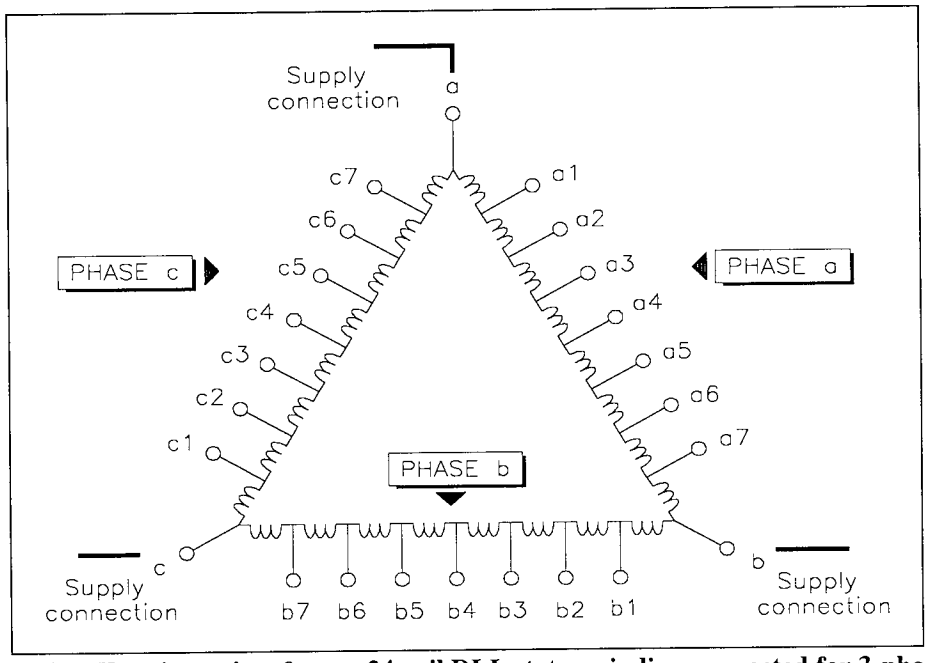

Fig 6.4 - Tapping points from a 24-coil DLL stator winding connected for 3-phase 2-pole delta operation.

Note from **Fig 6.4** the general nomenclature adopted for the phase to phase voltages.

The coil arrangement is identical to that shown in **Fig 5.14**, repeated here in **Fig 6.5** for ease of reference.

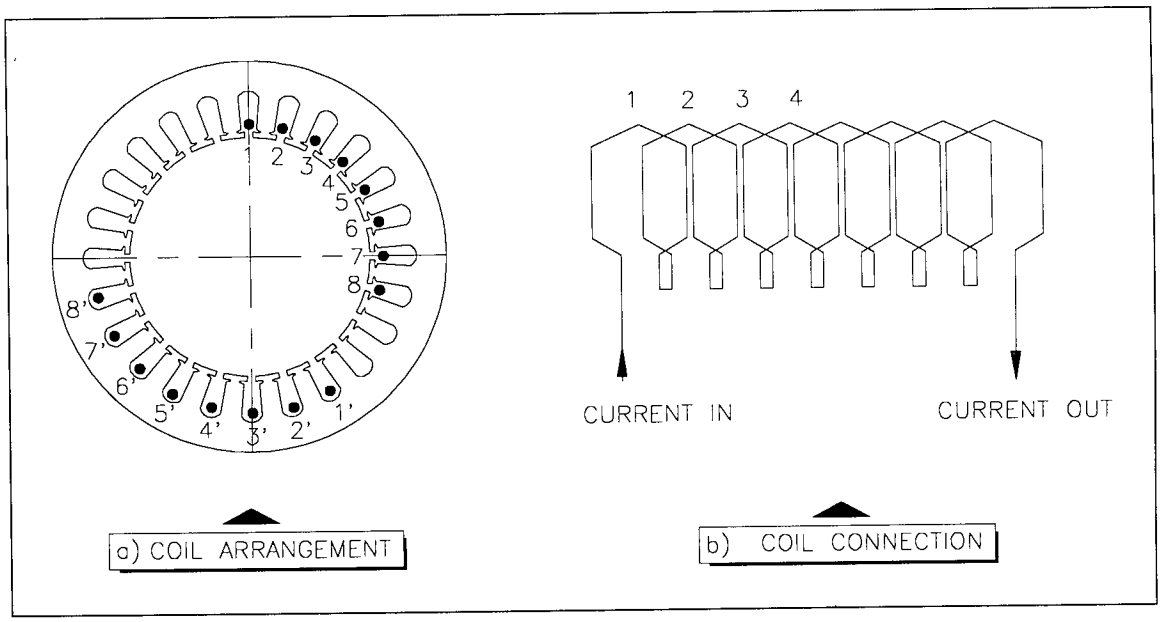

Fig 6.5 - 2-pole, 24 slot coil arrangement for 120° pole phase groups (one phase shown)

The vector diagram is identical to that of **Fig 5.15**.

The above design requires that all the coils per phase be assigned to consecutive slots along the stator periphery and connected in series. This is unique to the 2-pole connection whose electrical degrees are equivalent to the mechanical degrees around the stator member.

Higher pole numbers can also meet the requirement but require a different connection. This is explained next to complete the discussion.

6.2.2 - Design for Pole Numbers Greater Than 2

If it is desired to connect a machine for a number of poles greater than 2, then there are certain aspects of the connection to be considered.

Consider again a 24-slot stator winding and suppose it is required to run as a 3-phase 4-pole motor with 120° pole phase groups. There are two ways in which the this can be achieved.

(1) A series winding with a single path

Fig 6.6b shows the connection diagram for a single winding path in which all the coils in the phase are series connected. **Fig 6.7a** shows the vector diagram.

(2) A winding with two parallel paths

Fig 6.6c shows the connection diagram for two parallel paths. There are effectively two separate sections of the winding fed from the supply. The vector diagram is shown in **Fig 6.6b**

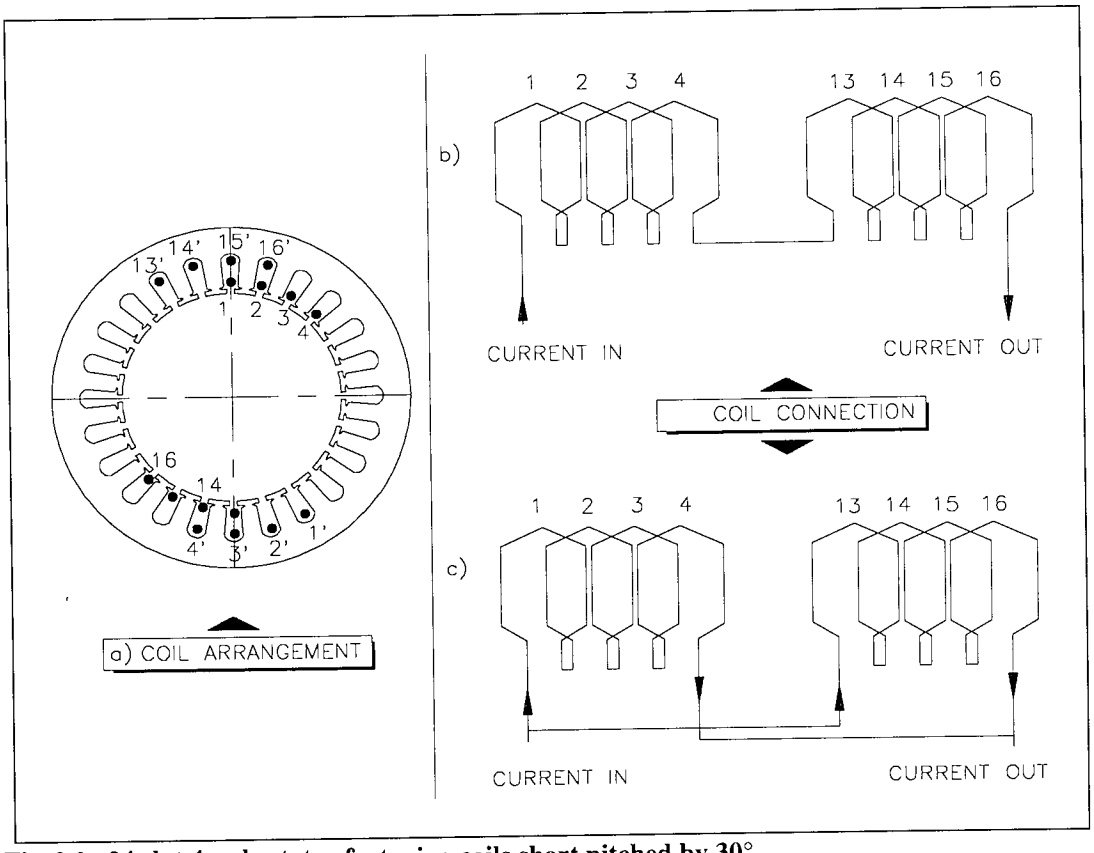

Fig 6.6 - 24 slot 4-pole stator featuring coils short pitched by 30°.
a) - Coil arrangement for 120° pole phase groups
b) - Coil connection for single path
c) - Coil connection for two parallel paths

Fig 6.7 below shows the vector diagrams for $a = 1$ and $a = 2$.

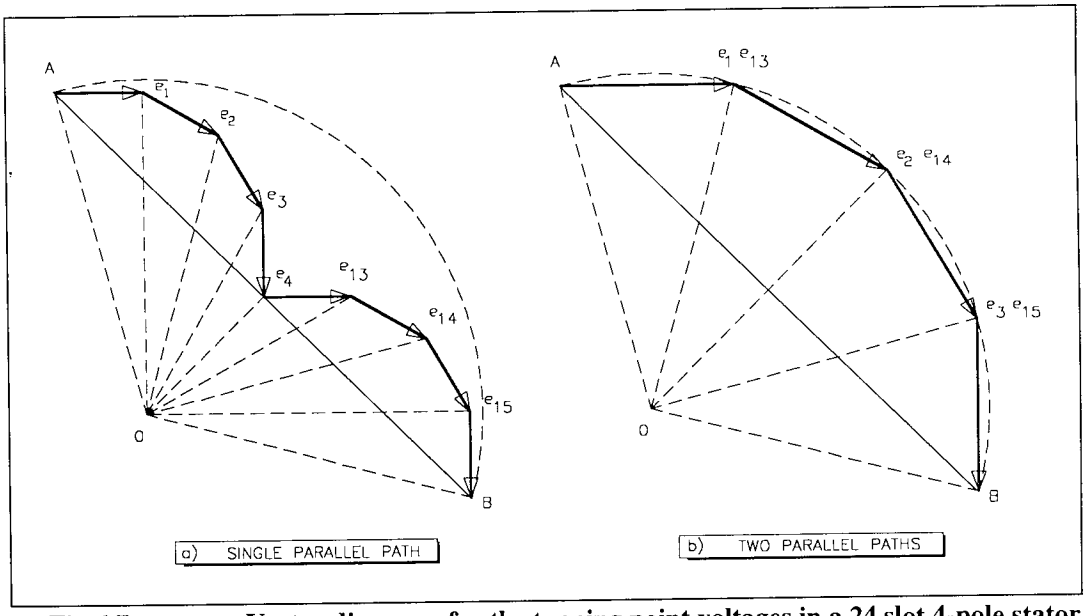

Fig 6.7 - Vector diagrams for the tapping point voltages in a 24 slot 4-pole stator winding wound for a) a single path and b) two parallel paths.

The following observations can be made from **Fig 6.6** and **Fig 6.7**

- The coil arrangement stays the same irrespective of the number of parallel paths.
- Unlike the 60° winding of **Fig 5.10**, there is no reversal of winding direction in connecting for more than a single parallel path
- For a single path, although the phase shift between tapping point voltages is the same and of the required magnitude, the voltages are not equipotential.
- Adaptation of a given winding from a single to two or more parallel paths reduces the winding resistance by a factor equal to the number of parallel paths.

Thus, to interface a 4-pole machine to a 24-pulse STATCON requires that the 2 parallel path connection is adopted, and that the number of stator slots is doubled to 48, to give, for a 120° phase spread, 8 slots per pole per phase, hence the required 15° between phases as before.

In general, to connect to the STATCON as proposed, a n_p-pole machine requires that the winding features as many parallel paths as there are pole pairs.

6.2.3 - STATCON Parameters and sizing

The required kVA rating of the STATCON may be deduced from the no load kVA of the machine. This can be done by calculation or by measurement and influences the size of the coupling reactance and hence the resonance ratio k.

There are essentially two design parameters of concern in sizing the machine and STATCON.

6.2.3.1 - kVAr rating

The STATCON rating in kVAr is related to the kVAr rating of the machine. The latter is itself a function of the magnetising current and it is shown in appendix B that:

$$Q_{IM} = \frac{m.E^2 k_i.g}{16\mu_o.l.r}\left(\frac{an_p}{k_w N_{ph}}\right)^2 \qquad (6.8)$$

where:

Q_{IM} is the total reactive power of the machine, assumed constant

E is the induced emf assumed equal to the applied voltage

k_i is a constant that accounts for saturation of iron

l, r and g are the effective air gap dimensions as before

N_{ph} is the total series turns per phase

Leakage reactances affect this parameter significantly when the machine is loaded, but will be ignored for the present and no-load conditions assumed.

The total reactive power generated or absorbed by a p-pulse STATCON at some firing angle α is given by

$$Q_m = -k_p\left(\frac{p}{6}\right).\frac{V_m^{\,2}}{X_L}.(q1 + q2\frac{\sin 2\alpha}{2\beta}) \qquad (6.9)$$

where:

V_m is the peak value of the tapping point voltage (assumed sinusoidal)

X_L is the reactance of the coupling inductance L at fundamental frequency

q1 is the normalised value of the reactive current at $\alpha = 0$.

q2 is a constant related to the active power in the STATCON

α is the delay or firing angle

k_p is a scaling factor accounting for differences in coupling topologies.

Thus, the compensator rating is given by $Q_m = Q_{IM}$. (6.10)

6.2.3.2 - Energy storage components

If it is assumed that the leakage inductance of the stator winding can be made sufficiently large, or some means devised whereby external reactors are not required and the coupling inductance is realised from the machine's main and/or leakage flux, then the coupling reactance becomes a function of the machine winding inductances. Whatever its form, let L_e be the value of coupling inductance.

Expressions for the parameters k and M determining the threshold values of the energy storage components in the STATCON were given in chapter 2. It was mentioned that they are functions of the pulse number and topology of the magnetic coupling. For the proposed scheme, simulation and experimentation showed that the values of the energy storage components computed were too low. This has been attributed to the air gap in the magnetic circuit whose effect is to reduce the magnetising reactance. It is therefore suggested at this stage that the expression for k given earlier for a transformer coupling be modified to include a scaling factor λ_G to account for the increase in magnetisation current requirements. Thus, if k_{IM} is the modified value of k, then:

$$k_{IM} = \sqrt{\frac{\lambda}{\lambda_G}.\frac{X_C}{X_L} - \beta^2} \qquad (6.11)$$

In this expression, all quantities other than λ_G are as defined for 24-pulse STATCONs assuming a *parallel* transformer connection. Thus, $\lambda = 8/3$.

Also

$$L = \frac{1}{\lambda_G}\left(\frac{\lambda}{(k_{IM}^2 + \beta^2).\omega^2.C}\right) \qquad \text{if C is known, or} \qquad (6.12)$$

$$C = \frac{1}{\lambda_G}\left(\frac{\lambda}{(k_{IM}^2 + \beta^2).\omega^2.L}\right) \qquad \text{if L is known} \qquad (6.13)$$

Simulation suggests that a suitable value of λ_G is 0.1

This subject is given further treatment in appendix B.

6.2.4 - Coupling winding considerations

The required phase shift pattern is shown in **Fig 3.2**.

It should be apparent from **Fig 6.4** that based on phase shift only, there are a number of tapping point combinations that would give the required system of voltages. The expected phase shifts at each tapping point are given in **Table 6.7** below which also helps clarify the naming convention adopted for different tapping combinations in the discussion that follows.

Table 6.7 - Tapping point phase shifts for delta connected 24-coil 2-pole stator

Tap	*a*	*a*1	*a*2	*a*3	*a*4	*a*5	*a*6	*a*7
Shift[°]	0	15	30	45	60	75	90	105

Tap	b	b1	b2	b3	b4	b5	b6	b7
Shift[°]	120	135	150	165	180	195	210	225
						(-165)	(-150)	(-135)

Tap	c	c1	c2	c3	c4	c5	c6	c7
Shift[°]	240	255	270	285	300	315	330	345
	(-120)	(-105)	(-90)	(-75)	(-60)	(-45)	(-30)	(-15)

For the purpose of comparison, the combinations were named after the *first* phase shift of the selected combination, with the supply '*a*' phase taken as reference 0°. For example, the combination involving c6, c7, *a*, *a*1 was referred to as the -30° group while that comprising *a*1, *a*2, *a*3, *a*4 was referred to as the +15° group. The combinations are shown in **Fig 6.8.**

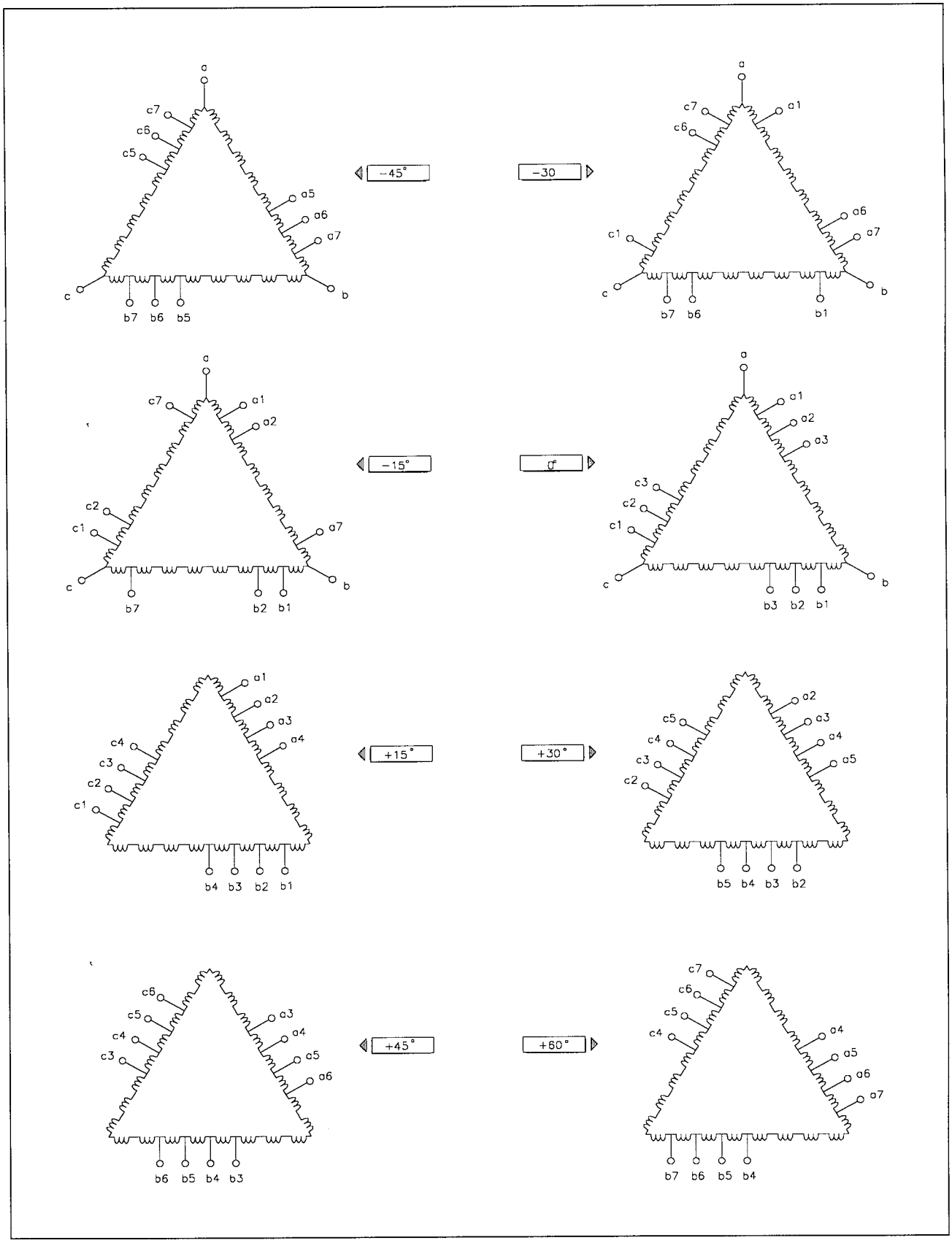

Fig 6.8 - tapping point combinations for a 24 coil 2-pole stator connection

Simulation of the complete model using external reactors for L and *measured* values of coil resistances was conducted for all the unique combinations for a fixed firing angle and the results revealed a difference in the harmonic content of the supply *current*, which was manifest in the waveshape and peak values. The -60° was eliminated by inspection and the results are not included. The low order harmonics are also shown.

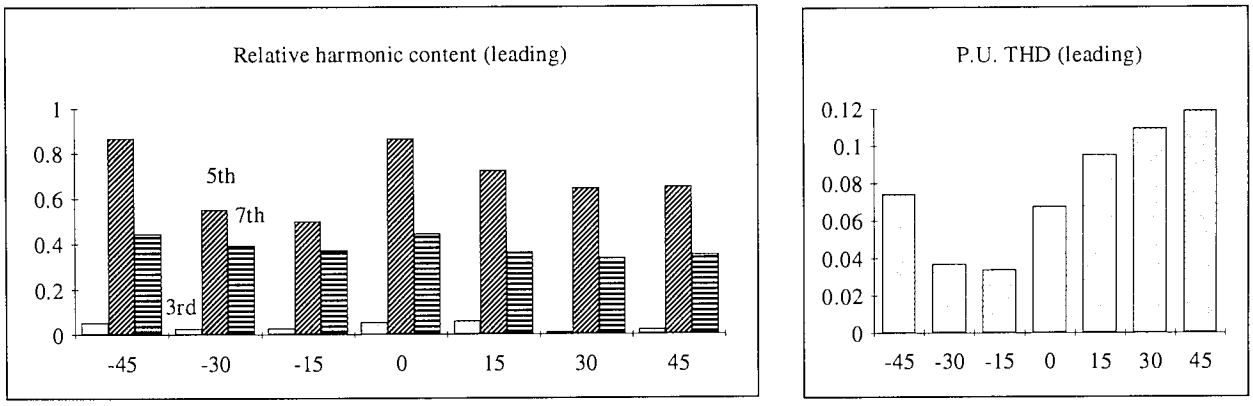

Fig 6.9a - p.u. THD for leading current for different tapping point combinations

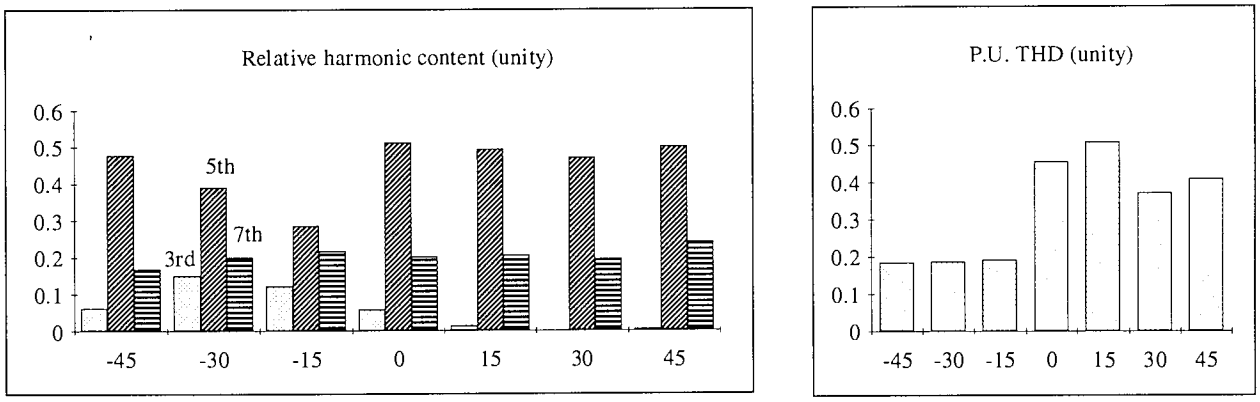

Fig 6.9b - p.u. THD for unity PF current for different tapping point combinations

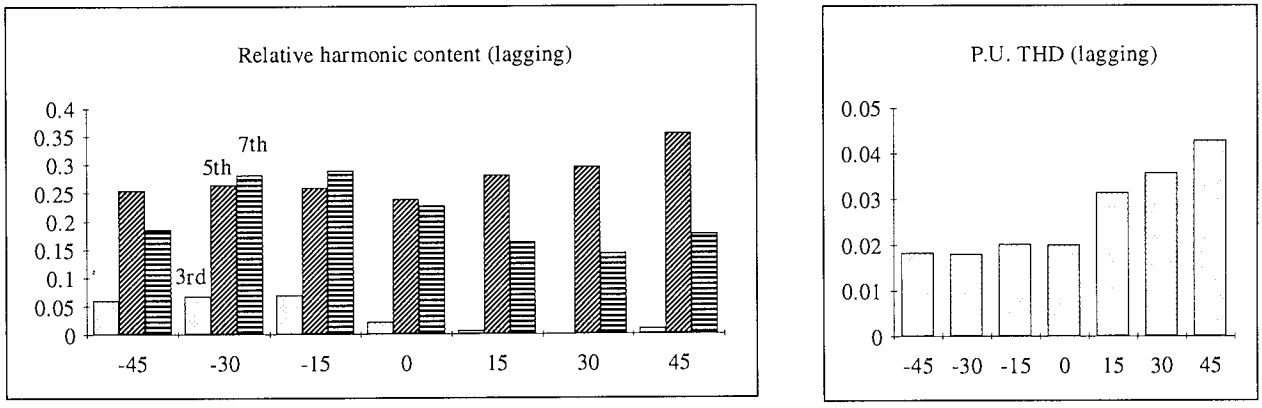

Fig 6.9c - p.u. THD for lagging current for different tapping point combinations

Note that all references to harmonics and harmonic distortion in the discussion that follows relate to the phase currents rather than voltages.

The total harmonic distortion was chosen as the measure of goodness in this application. Even so, a group which gives the least value of THD at leading power factor is not necessarily the best at lagging power factor, and comparing the p.u. THD of the groups at -30° and -15° for leading and lagging power factor operation supports this.

It should be apparent from **Fig 6.9** that the groups at -30° and -15° give the least THD at any power factor. The -30° tap group was chosen because of its good performance at all power factors, but there were only marginal differences with the -15° tap group. Also apparent is a prominent 5th harmonic, which is suspected to a be consequence of imperfect phase shifts of the tapping point voltages as a consequence of voltage drop due to coil resistances as explained in chapter 5. No low order harmonics are observed when perfect phase shifts and equipotential voltages are specified.

Selection of the tapping combination was the first step in meeting the requirements of the coupling in that it establishes the source of polyphase voltages which meet the conditions of equipotential and equal phase shift as required.

As explained in the preceding chapter, the voltage at each tapping point is a function of the coil self inductance and the coil's mutual inductance with each and every coil in the winding. Thus, the voltage at a tapping point is essentially a result of transformer rather than potential divider action and so the tapping points behave as low output impedance sources. Also, the STATCON bridge circuit by virtue of the high voltage across its d.c. rails is a high input impedance system seen from the supply side. It is important that connection of an electrical load to the tapping points does not cause loading of the winding i.e. lowering of the tapping point voltage.

The consequences of loading the winding would be that:

- excessive current would flow through the coils
- the rectifier section of the converter would fail to function as a proper multiple pulse system as a result of reduced voltage at some tapping points therefore rendering the diodes connected to them permanently reverse biased by those at higher potentials.

6.3 - THE MODELLED SYSTEM.

The MOSFETs were modelled as digitally controlled analog switches with antiparallel diode as shown in **Fig 6.10**.

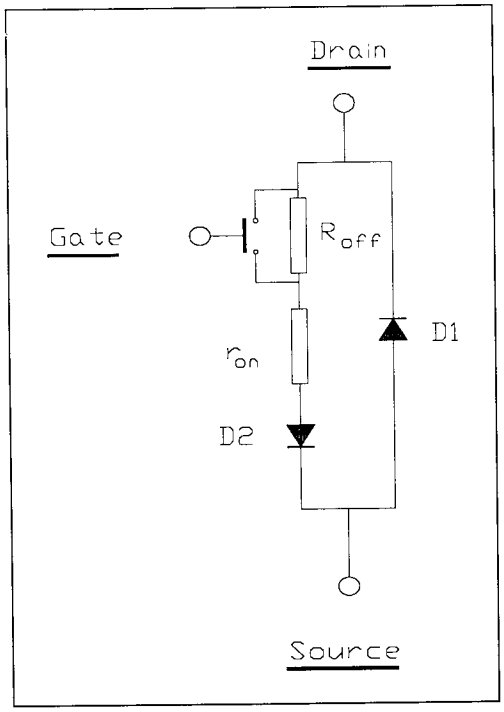

Fig 6.10
Simple model of MOSFET used in simulations.

It will be seen that:

- In the on state, the MOSFET appears as a small resistance r_{on} in series with a diode D2, which models the turn-on threshold voltage and unidirectional current flow through the device

- In the off state, the MOSFET appears essentially as a very large resistor R_{off}, to model any drain-source leakage that may exist in the device.

Also:

- The digitally controlled switch permits specification of turn-on and turn-off times. These were selected to model the switching deadband (section 3.4.1).

The snubber in the physical circuit was not included in the model to speed up the simulation process but was included later for validation.

The control was modelled as four composite systems of the digital logic circuits of gates and clock sources shown in **Fig 6.11**. Three such units in parallel form a single six-pulse bridge. The appropriate number of these were grouped to model any ρ-pulse bridge. Thus, four were used to model a 24-pulse STATCON.

In **Fig 6.11**:

- Clk1 is a digital clock of specifiable frequency (f) and delay (α).
- G1, G2 and G3 are logic gates specified to have zero propagation delay.
- Q_H and Q_L are the high side and low side MOSFETs respectively.
- c1_p and c1_n are the connections for the storage capacitor, while w_1 is the phase connection. *Enable* is the bridge start-up on/off control parameter.

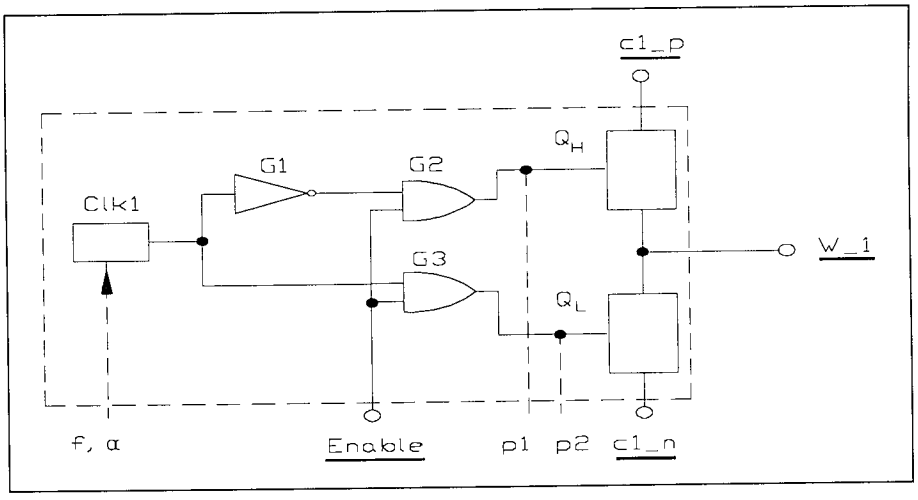

Fig 6.11 - Elementary control logic for one limb of a 6-pulse bridge

The points p1 and p2 in **Fig 6.11** were included to monitor the digital control signals. This was made possible by the mixed signal simulation capability of the software used* .

The synchronisation was modelled as a digital bit pattern generator so that the MOSFETs could be enabled and disabled at specified times by setting or resetting the *Enable* connection shown This was useful in observing transients when switching MOSFETs on or off at different times and voltage levels. It was instrumental in producing the simulation results of appendix B.

The machine was modelled as a delta connected system of identical inductors of some value of self inductance calculated as shown in chapter 5. Only 80% of this value was used in specifying the mutual inductances between the coils. The remainder modelled the leakage. Measured values of coil resistance were specified model the copper losses. For model validation, a star connection was specified and the model behaviour was consistent with the theory of chapter 5.

The rotor winding was not included although the presence of the rotor iron was implied in calculating mutual inductances between coils. The currents expected are therefore those that would be observed if rated voltage at rated frequency were applied to the winding with a blocked rotor.

The coupling coils were specified as external linear inductors with a small finite series resistance. No mutual coupling between the main winding and the coupling coils was specified.

Fig **6.12** shows the complete system as modelled, excluding the three phase 4-wire supply which has been omitted for clarity.

* Saber Version 3.4

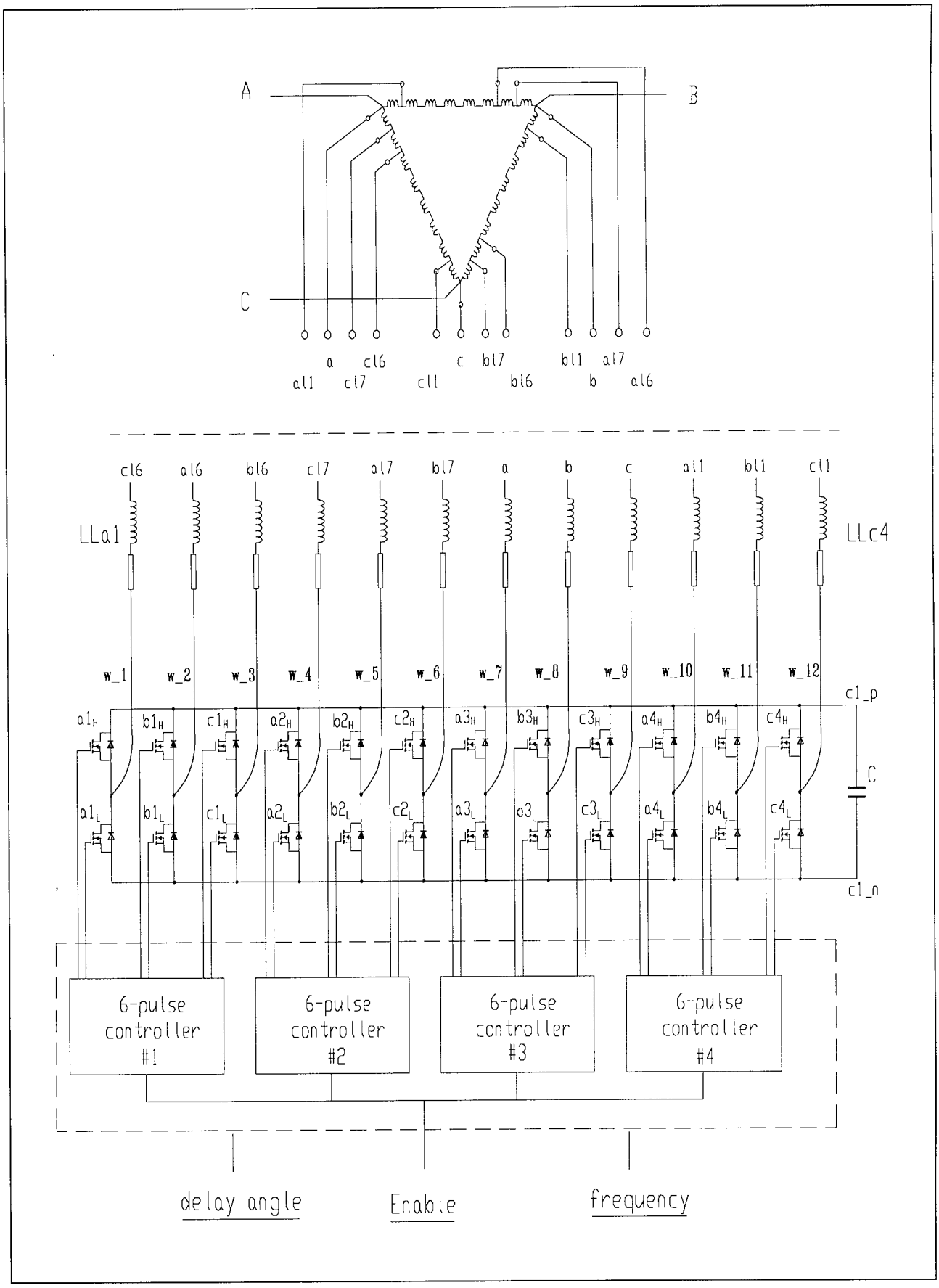

Fig 6.12 - Complete schematic of 24-pulse STATCON connected to 24-coil stator

Notes on Fig 6.13

- The links between the tapping point connections and the coupling reactors have been labelled rather than drawn in to enhance the clarity of the schematic.

- The zero reference used was the three phase supply neutral. There are however no connections made to the neutral, as is the case in the practical system. The supply phases connect to points A, B and C as shown.

- Each of the coupling reactors, examples of which are the two labelled LL*a*1 and LLc4 are identical and have a value of L. The series resistance shown is specified as an integral part of the inductor i.e. copper winding resistance.

The specification of an Electrodrives™ D90S[1] Motor was used for the design parameters. Specifically, the following were given:

Electrodrives D90S Three Phase Cage Rotor induction motor

• No. of stator slots Q	24
• No. of stator coils	24
• Turns per coil N	35, SWG 24
• Winding type	Double Layer Lap
• Connection Type	Delta
• Number of poles	2
• Rated voltage	230V rms phase/phase
• Rated power	1.5kW
• Air gap width g	0.3mm
• Air gap radius r	35mm
• Air gap axial length l	76mm

Table 6.13 - Simulated Machine parameters list

The machine was reconnected for 120° pole phase groups, and the appropriate tapping points made accessible at the terminal box as shown in the photograph of **Fig 6.18**.

The no load voltages and currents are discussed next.

[1] BS 5000, BS 4999

6.3.1 - Simulated machine winding voltages and currents

Viewed closely, the voltages of **Fig 6.14** show a slight reduction in the peak value of the tapping point phases closest to the centre of the phase belt. This is a consequence of the leakage inductance and winding resistance. As stated in chapter 5, differences in magnitude also affect the phase shifts of the derived waveforms, and these in turn affect the performance of the STATCON in terms of harmonic reduction. In general however, the phase shift pattern will be seen to be consistent with the theory of chapter 5.

The currents through the stator coils are sinusoidal, and each coil in a limb of the delta connection carries the same current. The magnitudes as shown are inaccurate since the rotor is not modelled as a rotating inductance giving rise to a back emf which causes a reduction in the supply current. However, experimental results show that the general waveshape is the same.

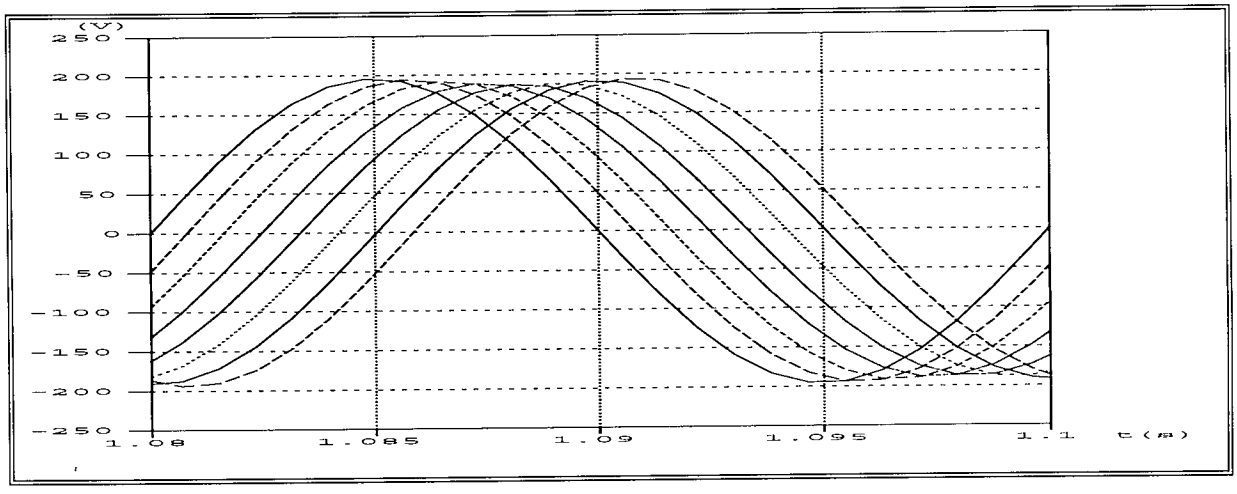

Fig 6.14 - Phase A steady state voltages - pre-switching

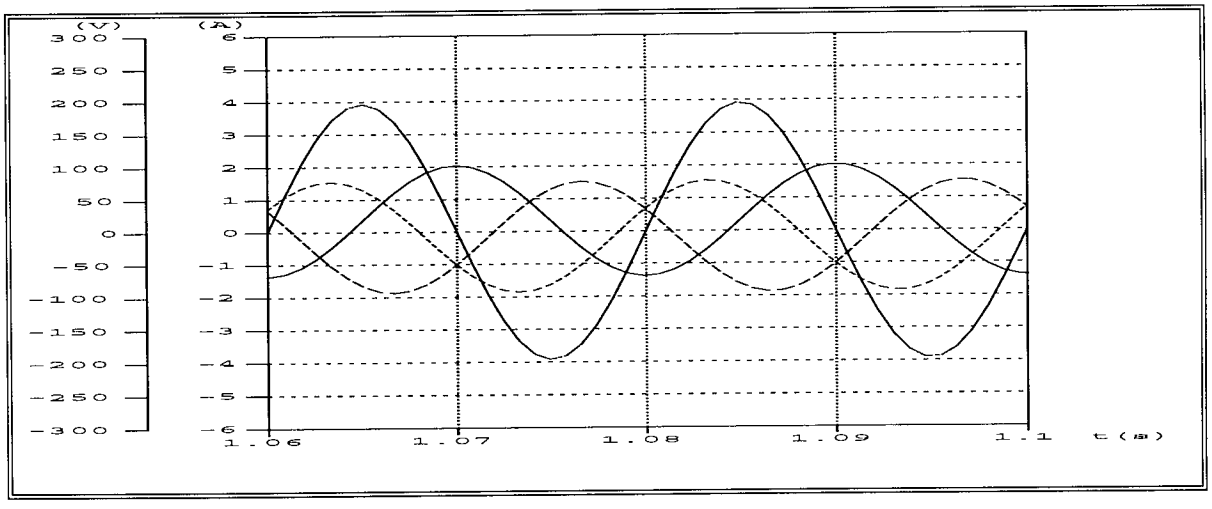

Fig 6.15 - Line currents and reference voltage - steady state. - Inverter not switching

6.3.2 - Simulated supply currents and capacitor volts

Appendix B discusses the form of the no load currents at different points in the winding. Only selected *no load* simulation results are shown here for later comparisons with the experimental.

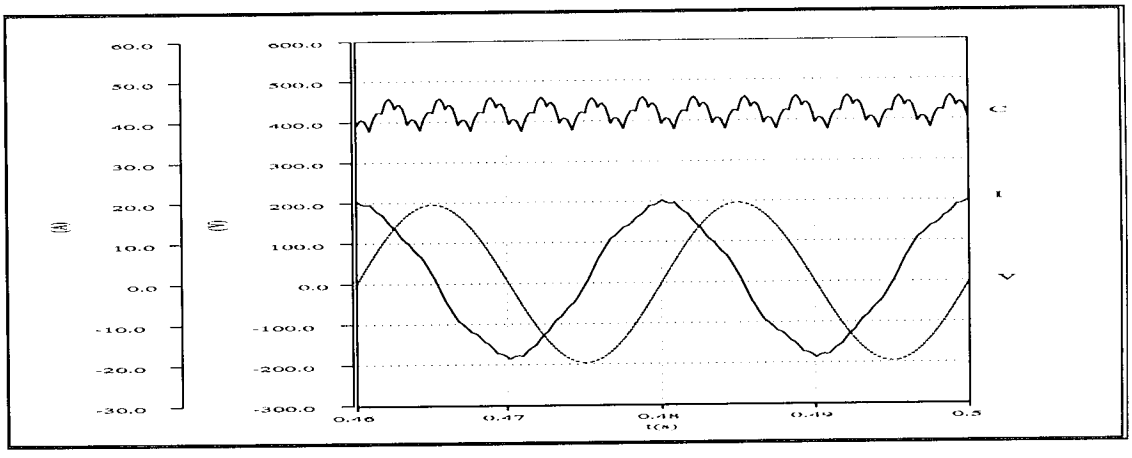

Fig 6.16a - Capacitor volts, supply volts and current - leading power factor (α=1).

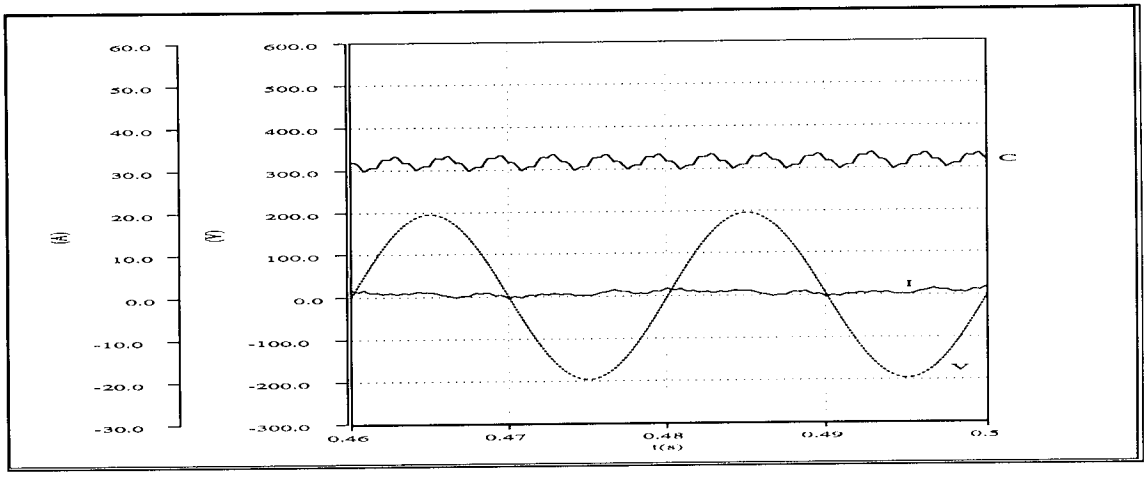

Fig 6.16b - Capacitor volts, supply volts and current - unity power factor (α=0.075).

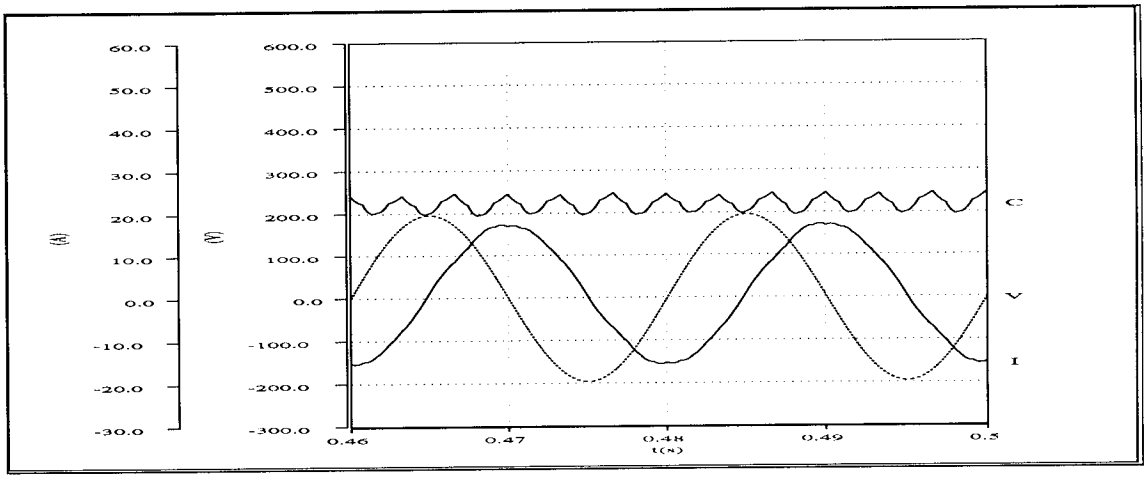

Fig 6.16c - Capacitor volts, supply volts and current - lagging power factor (α=-1).

Note that 'Supply volts' refer to the phase to neutral volts. The capacitor waveforms will be seen to be similar to those observed with conventional (zigzag) transformers.

6.3.3 - Simulated inverter bridge voltages

As stated in chapter 4, observation of the inverter output voltage requires that the reference point is specified because of the behaviour of the supply neutral and bridge reference with respect to each other as shown in **Fig 4.7** for the zigzag transformer coupling. **Fig 6.17a** shows the simulated bridge reference to neutral waveform. The inverter to neutral output waveform is therefore as shown in **Fig 6.17b**, while the same point, observed with respect to the bridge reference, is the regular rectangular wave of **Fig 6.17c**.

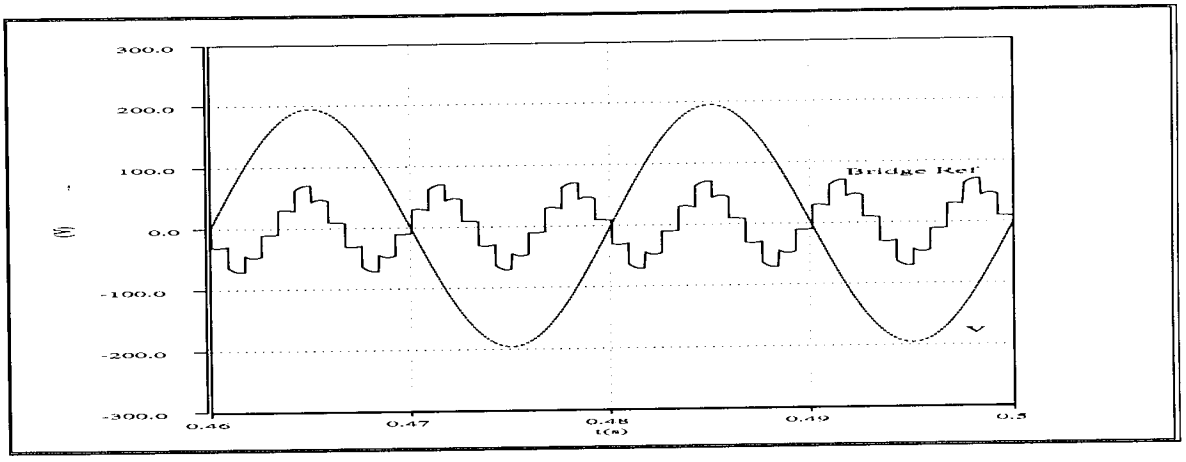

Fig 6.17a - Bridge reference to neutral voltage.

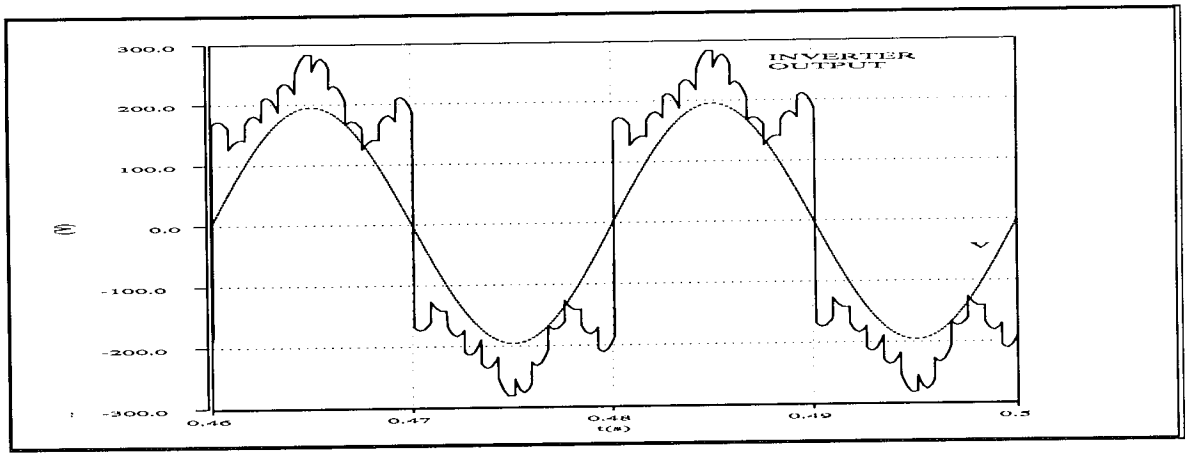

Fig 6.17b - Inverter output voltage taken across one MOSFET and supply neutral.

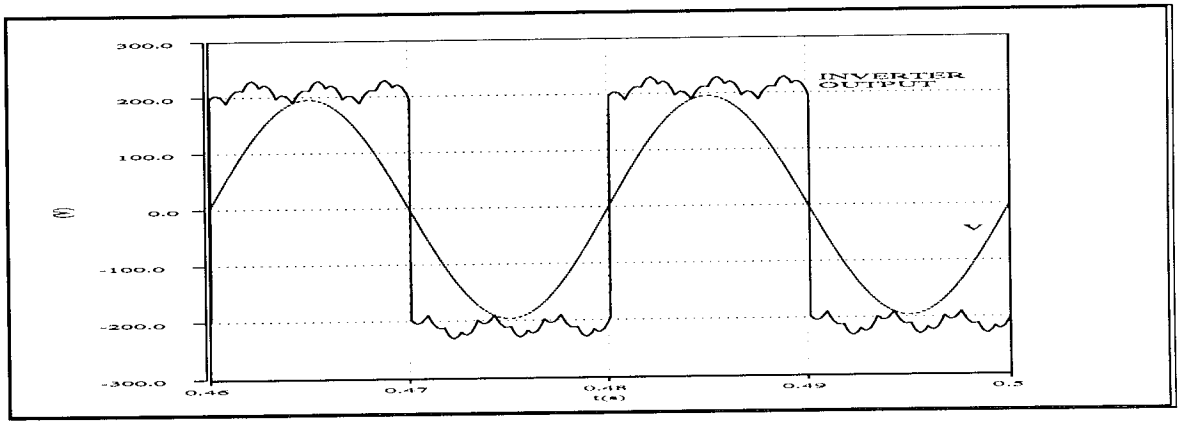

Fig 6.17c - Inverter output voltage taken across same MOSFET and bridge reference.

6.4 - SUMMARY

Practical aspects of the machine design and implementation have been discussed. The major limitation of inadequate coupling reactance has been explained and the need for external reactors justified. It cannot be stated conclusively from this investgation if a motor with adequate coupling reactance can be designed.

Simulation results of a 24 slot 3-phase double layer lap wound 2-pole delta connected motor with 120° pole phase groups have been presented to show how the complete system meets the coupling requirements. The simulation is approximate in that rotor effects have been ignored, although the presence of the rotor iron has been implied. The results suggest that the winding, configured as described, will facilitate the control of reactive power in the supply over a continuos range of the power factor between leading and lagging.

Simulated inverter voltages are similar to those observed with the zigzag transformers, implying the STATCON's general behaviour is affected little by topology of the magnetic coupling which meets the conditions listed in section 4.3.
Fig 6.18 is a photograph of the induction machine showing the multiple phase connectors for the coupling reactors (bottom left) and for the STATCON (bottom right). One reactor is partly visible in the top right hand corner.

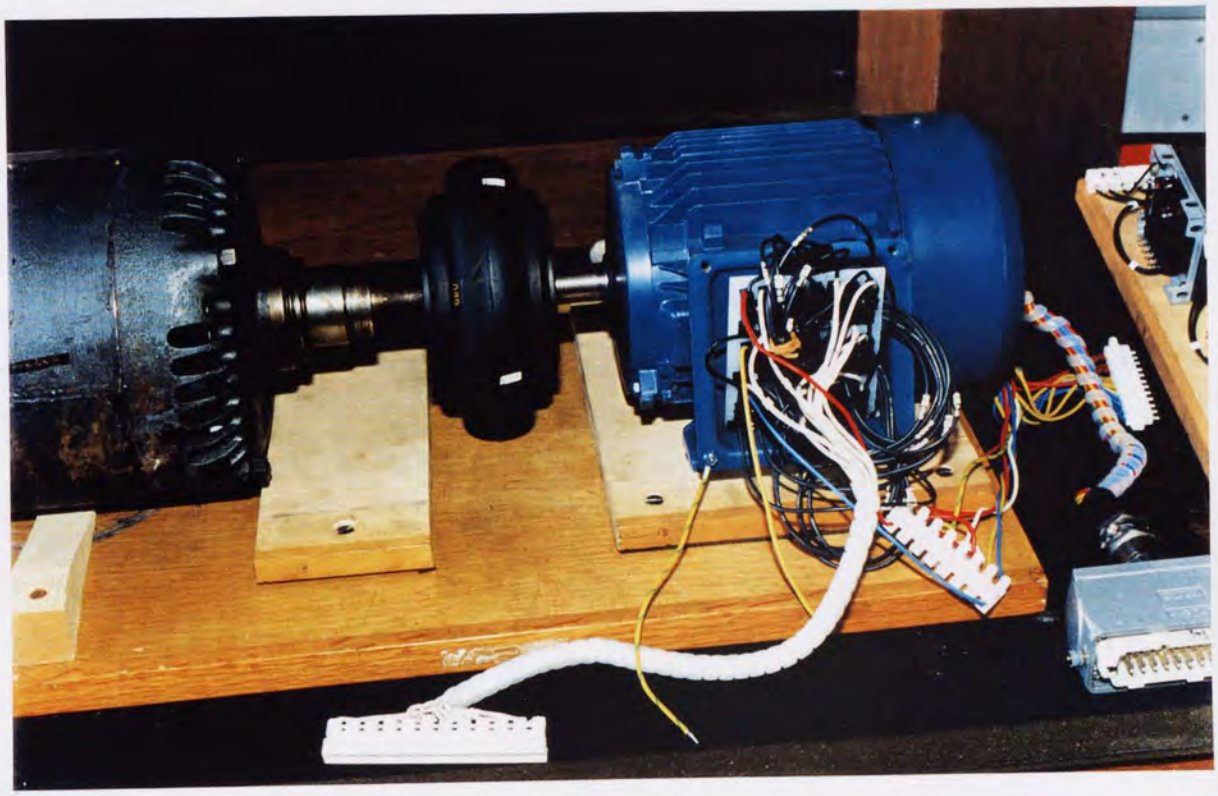

Fig 6.18 - Induction machine and multiple-phase connectors for reactors and STATCON.

CHAPTER 7

A 24-PULSE STATCON CONTROL SYSTEM

This chapter describes in some detail the control system that was used in the experimental model of the 24 pulse STATCON.
While a purely digital or analog/digital hybrid could achieve the same effect, there are certain advantages in using software based systems. These include:

- Ease of adaptation to different modes of operation.
- Presettable parameters that would otherwise require hardware modification.
- Artificial intelligence and programmable fail safe.
- Control parameter tuning by software.
- Automatic data capture, storage and processing (if required).

Purely hardware based systems often offer superior performance in terms of speed, but a properly designed hybrid circuit can make optimal use of both software and hardware.

The control circuit was initially designed for use with three MC8051 microcontrollers for minimum component count and ease of shielding against electromagnetic interference (emi), but availability of a suitable emulator proved difficult, and so the software core was ported to a 80386 PC™ platform with an intermediate expansion slot interface card.

Even so, a modular approach was adopted in the design so that any microprocessor or microcontroller circuit could be used. This was achieved by separating the processor specific hardware from the generic. In this manner, changing over from a desktop computer to an embedded microcontroller configuration requires only that a small circuit board with the microcontroller(s) duplicates the essential functions of the computer and provides the necessary interface.

The control circuit diagram is the subject of appendix C.

7.1 - GENERIC CONTROL DESCRIPTION

The basic requirement of the controller is to produce a system of switching signals that are of the correct timing and phase shift to switch the converter devices as required. An additional requirement is for these signals to respond to a control instruction i.e. delay angle. The requirements list was therefore outlined thus:

(1) - Synchronisation

A zero crossing signal from one primary supply phase to provide the required frequency tracking and locking and to act as a general synchronisation signal.

(2) - Frequency tracking

A phase locked loop type system to generate a spply frequency dependent pattern of switching signals for the inverter

(3) - User Interface

A means of accepting user input to control set points.

(3) - Feedback

Measurement of phase angle as VArs or Power Factor. Some schemes use voltage comparisons between inverter output and capacitor voltage.

The control strategy was derived from the control block diagram of **Fig 7.1**. The final circuit inevitably features higher functionality because of the prototype nature of the work in hand requiring sufficient observability and flexibility.

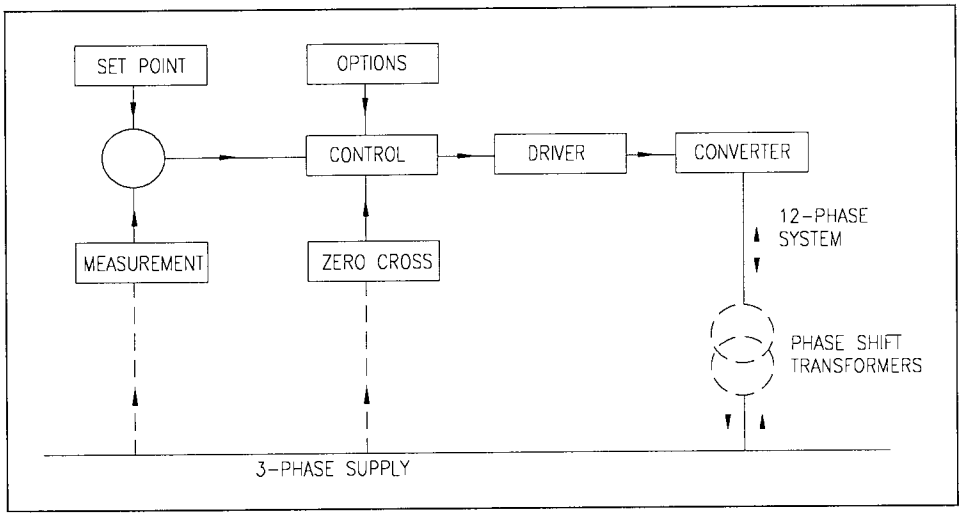

Fig 7.1 Basic control block diagram

7.1.1 - Set point

The computer keyboard was used to enter the set point for test purposes, but the primary means was by way of a console mounted potentiometer as shown in **Fig 7.2**.

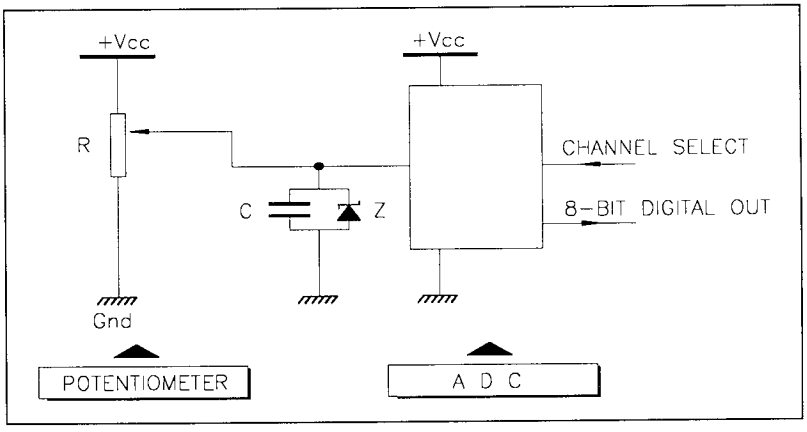

Fig 7.2 - Analog set up of setpoints

The capacitor C is connected between the input and ground as shown to suppress high frequency transients when the slider moves. A zener diode is connected in parallel with the capacitor to clamp the input signal to the maximum 5V allowed. All ADC inputs were zener protected but channels assigned to waveform capture excluded the capacitor to prevent unwanted filtering and phase shifting.

7 1.2 - Measurement

Commercial linear transducers (with meters) were employed to measure power factor and/or VArs. The devices connect to the three phase supply and output a linear -10V to +10V d.c. equivalent. Linear optical coupling was used to scale and level shift this signal to the required 0-5V for ADC compatibility. The circuit is shown in **Fig 7.3**.

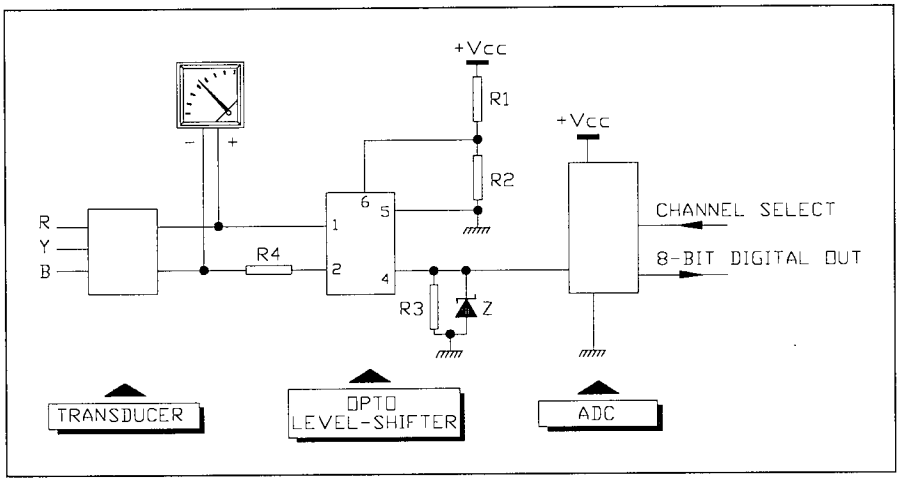

Fig 7.3 - Linear optical isolator in level shifting application

The ADC was configured for 0-5V FSD and all number systems (signed or unsigned raw binary) were implemented in the software.

Signals of 50Hz and above were converted differently. The circuit of **Fig 7.4** was used to scale and level-shift such signals to the required voltage levels.

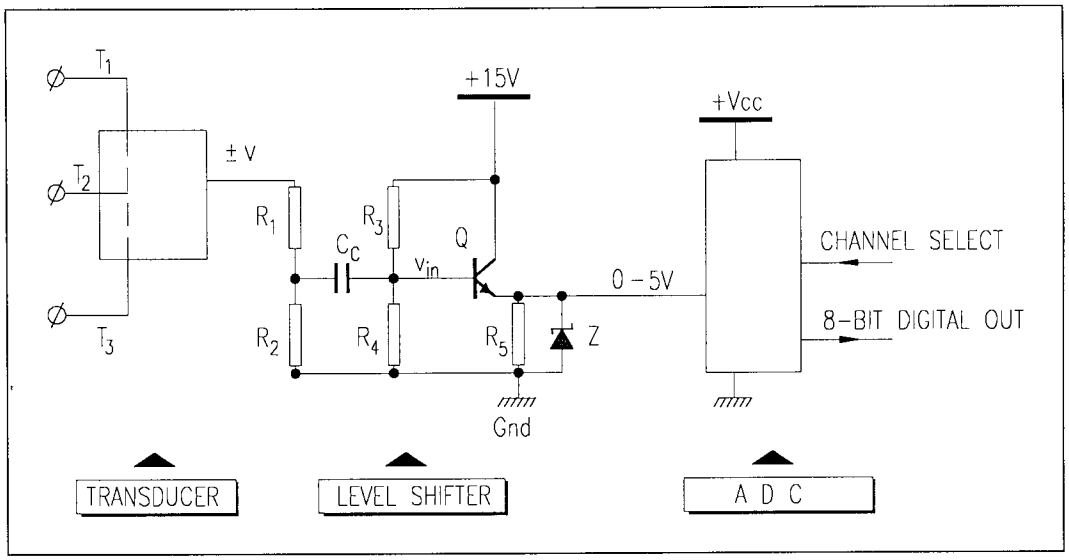

Fig 7.4 - Analog signal conditioning for digital conversion

Referring to **Fig 7.4**, the signal from the primary transducer is scaled to ±2.5V d.c. by the potential divider comprising resistors R1 and R2. The capacitor C_c couples the signal to the base of the NPN transistor Q which is connected as an emitter follower, biased by resistors R3 and R4, which set the base to about 3.2V so that the emitter is at about +2.5V; half way along the 0-5V scale. Thus, an input signal v_{in} in the range -2.5V to +2.5V appears as 0 - 5V at the output, conforming to the acceptable range for the ADC. The resistor R5 limits the transistor collector current as required.

7.1.3 - Options

The options that were made available to the user can be grouped into two:

Software-enabled options - selectable in response to prompts at start up. These include preferences such as plotting of graphs on the screen and presetting the starting phase as explained in section 7.8. These options were intended primarily for use with the computer rather than microcontroller version of the control circuit.

Hardware-enabled options - facilitated by push buttons on the operating console. These were used to set up the control loop and switching modes.

Fig 7.5 shows the circuit that was designed to implement a push button toggle function.

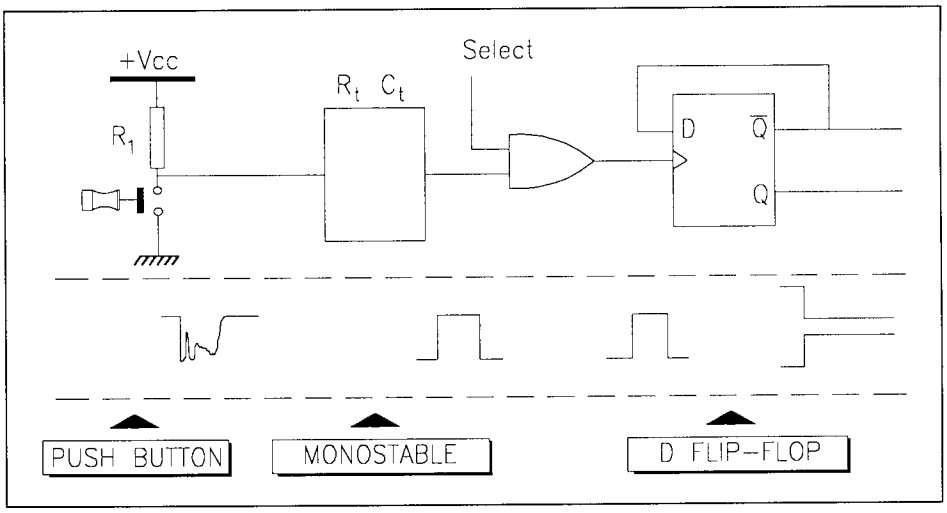

Fig 7.5 - Circuit of contact debounced toggle switch enabled by software

When the push button shown is activated, it connects one end of resistor R_1 to ground. This appears as a negative step at the input to the retrigerrable monostable multi-vibrator, which outputs a pulse of fixed duration determined by the external RC circuit shown, thus eliminating mechanical contact bounce effects of the switch. The output from the monostable is connected to one input of a 2 input AND gate. The other input, labelled 'select' in **Fig 7.5**, is controlled by software and only when set to logic '1' are pulses from the monostable allowed through to the D type flip flop which toggles its output thus effecting the setting and resetting of selections by the user as required. Sketches of signals at various points in the circuit, in response to the push button closing, are shown. 'Select' is assumed set to logic '1'.

This circuit has been used for selection between open and closed loop control and between 180 and alternate switching modes.

7.1.4 - Zero Cross

The zero crossing signal derived from the primary red phase (by choice) is probably the single most widely used throughout the hardware and software to provide a means of measuring the supply *fundamental frequency* (which all derived switching signals must track) and the real-time signal that synchronises the entire switching circuit and therefore eliminate all potentially cumulative error in switching times. As thus, noise on the signal could easily lead to erroneous switching and is potentially disastrous. Extensive measures were taken to rid the signal of the spurious transitions often observed with OP-AMP comparator based zero cross detectors.

- At the primary level, transient suppression capacitors were connected across the three phase supply to the equipment, and across the single phase power supply to the electronics.

• At the secondary level an optically coupled Schmitt trigger with a logic level output has been used. The circuit is shown in **Fig 7.6** . ZX_1 and ZX_2 are two such triggers.

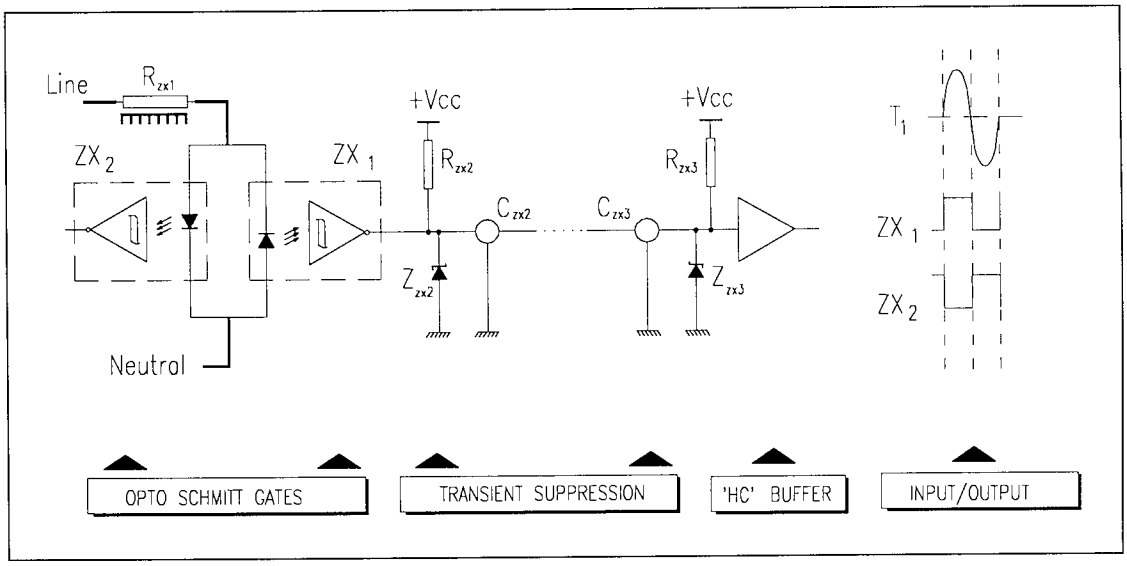

Fig 7.6 - Optically isolated schmitt trigger used in zero cross detection

The trigger ZX_2 is connected in anti-parallel to ensure that the reverse breakdown of the first trigger is not exceeded. It was advantageous to use the output from the first detector, which is in phase with the supply, because the polarity was that required to operate active low and active high inputs of connected devices, and the software also followed a logical philosophy in that the signal was representative of the original sinusoid. A heat sink-mounted high wattage series resistor Rzx1 provides the required current limiting for the detector.

• At the tertiary level, the control program was written to treat the received zero-cross signal judiciously. Thus, after the initial frequency computation, any subsequent measurement that would otherwise cause a significant change in the derived switching frequency is repeated twice to make certain that the perceived change in frequency is genuine. Further code was included to monitor for total loss of the zero crossing signal by means of a 'watchdog timer' which times out if the expected zero crossing transition does not occur within a specified time. This feature limits the bandwidth of the control system but is useful in orderly isolation of the equipment should a problem occur.

During commissioning, it was discovered that the equipment was rather prone to tripping on high current or current surges. The trip-protection was effected by a semiconductor circuit breaker, specifically, the AZ R10A (see **Fig 7.9b**) by Klockner Möeller™ whose performance was very satisfactory. The general speed of MOSFET switching and inherent current limiting (r_{ds}) limits the effectiveness of fuses as protective devices.

The tripping was traced to spikes induced in the zero cross. These were observed in the signal's positive and negative half cycles. The solution implemented is described next.

7.1.4.1 - Positive half cycle spikes

Two zener diodes and two transmission line transient suppressers, type NFV610 were used as shown in **Fig 7.6.** The zener diodes were sized so that they were conducting all the while the zero crossing signal was in its positive half cycle, thus eliminating their response time. Specifically, 3V9 types were used with 'HC' CMOS which has a V_{ih} parameter of 3.15V. The resistors were sized large enough to prevent excessive current through the devices or the zero crossing detector output transistors and low enough to prevent what is in effect the transmission line from possessing too high an impedance as this makes it susceptible to noise pick-up. The result was much improved performance.

7.1.4.2 - Negative half cycle spikes.

To establish the source of interference, suitably sized Nickel Cadmium batteries were used to power the control circuit while the computer was powered directly from a UPS. Spikes were still observed on the scope but some were common mode noise picked up by the scope leads. RF interference was therefore confirmed present prompting the use of earthed aluminium cases. Higher stabilisation was achieved.

Further, suitably sized pull up resistors (4k7 for 5V HCT and TTL) were introduced into the circuit on all long transmission lines between the computer and the control circuit, and between the latter and the signal acquisition board. An even higher degree of stabilisation resulted and it was generally possible to run the equipment for hours problem free at maximum absorption or generation.

7.2 - POWER CONVERTER

The choice of power semiconductor inevitably dictates the type of driver, and the nature of the switching signal i.e. whether pulsed or sustained. The Power MOSFET was chosen for the model primarily because of the ease of control, fast switching speed and similar turn on and turn off times. **Fig 7.7** shows a generic 24-pulse bridge and **Fig 7.8** shows the circuit details of each switch. A snubber was connected as shown.

Specifically, the device type STH15NA50 was used with snubber values of C_s = 100nF, Rs = 47Ω and type IN4004 diodes (D_s). BZX15 gate to source zener diodes were used and twisted vane heat sinks rated for 7.1°C/W were attached to each power device.

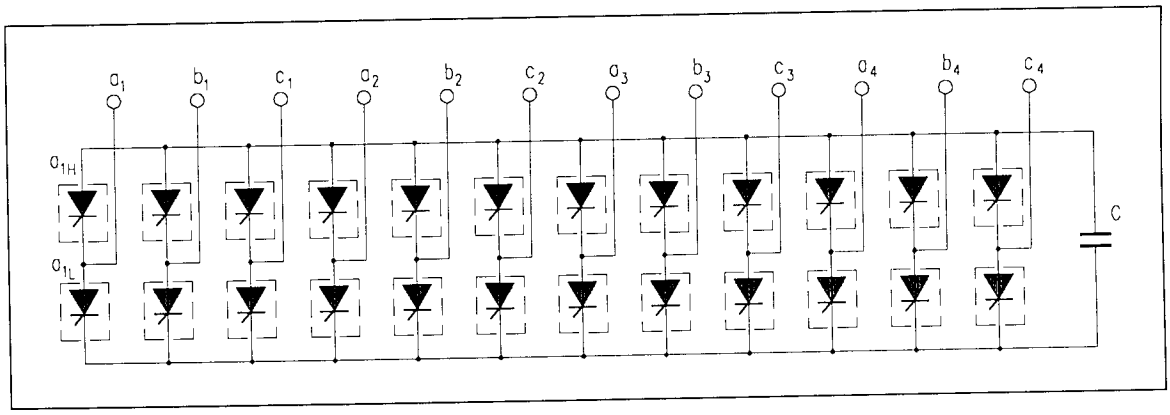

Fig 7.7 - 24-Pulse bridge connected to common capacitor

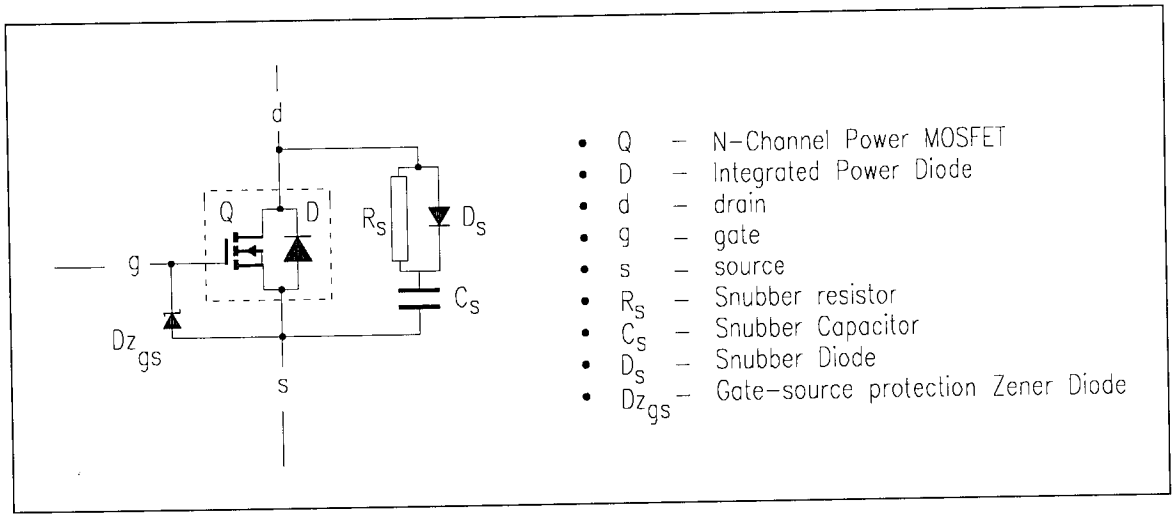

Fig 7.8 - Detail of each circuit element of the 24-pulse bridge

7.2.1 - Circuit connections

In **Fig 7.7,** the terminals labelled *a*1, b1, c1 e.t.c are the connections to the multiple phase voltages from the magnetic interface. The gate of each of the MOSFETs connects to the driver circuit via an external gate resistor Rg shown later in **Fig 7.9**.

7.2.2 - The gate-source zener diode

Referring to **Fig 7.8,** a zener diode Dz_{gs} is shown connected between gate and source. It was introduced as a consequence of problematic operation during the commissioning stages of the model when it was discovered that transients in the gate source voltage (v_{gs}) exceeding the MOSFET rating for this parameter were mostly responsible for device failure. MOSFET failure was observed to reduce significantly with the inclusion of the diode. Also, whenever a problem did occur, it was usually the diode rather than the MOSFET that failed.

7.2.3 - The snubber circuit

The snubber is an important feature of the power electronic circuit typified by the bridge of **Fig 7.7**. However, precise sizing was not done in the model and values were chosen based on simple calculations derived from the earlier 6-pulse model. The power rating however, is switching frequency dependent and higher ratings are required for higher frequencies such as in PWM applications.

7.2.4 - Power MOSFET Protection

- The reverse breakdown voltage of the MOSFET was designed for by sizing the MOSFET itself for the intended application voltage. A safety factor of between 1.5 and 2 was included.

- The MOSFET gate to source breakdown voltage was accounted for by use of the zener diode Dz_{gs} described above. Devices with a higher rating of this parameter were tested but the particular model was observed to posses longer turn off than turn on times. This led to problems of simultaneous conduction at high power levels.

- Drain current is ideally monitored within each limb by low loss circuitry. Devices such as the HEXSENSE™ power MOSFET by International Rectifier® are ideally suited to this. They feature additional output terminals which provide a scaled down linear equivalent of the drain current. However, this feature loses some of its advantages in switching applications where the current is non continuous. Also, while monitoring of individual currents in the bridge would probably be a worthwhile feature in a large power application, it is not cost effective in the model. Thus, drain current limiting was designed for by slightly oversizing the MOSFET.

Protection of individual devices in the bridge must be such that the whole bridge benefits, rather than just the device of concern. This is because isolation (for instance) of a single MOSFET interferes with the entire switching pattern giving rise to large surges of current which could subsequently lead to more damage.

7.3 - THE POWER MOSFET DRIVERS

The specific driver chosen for the model was the INT200/INT201 pair of **Fig 7.9**. This configuration was deemed preferable to that of a single module (dual or hex driver) from an economical view point so device failure requires only half the driver replaced. The absence of connections to the high voltage rail was an attractive feature.

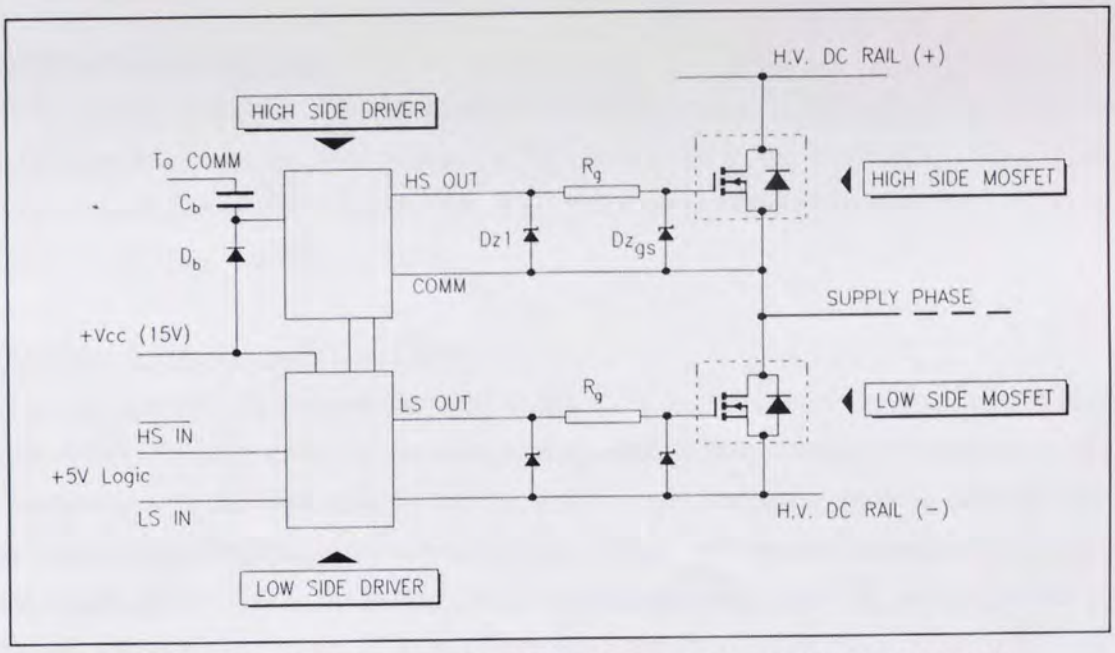

Fig 7.9a - MOSFET drive based on the INT200 low side and INT201 high side pair

In **Fig 7.9a**, the resistor R_g is the external gate drive resistor. It is normally in the range 10 to 100Ω with lower values giving rise to generally faster operation on account of the increased rate of charge and discharge of the associated capacitances [Horowitz et al, 1995]. **Fig 7.9b** shows the photograph of the driver circuit. Also visible in the top right hand corner is the semiconductor circuit breaker mentioned in section 7.1.4.

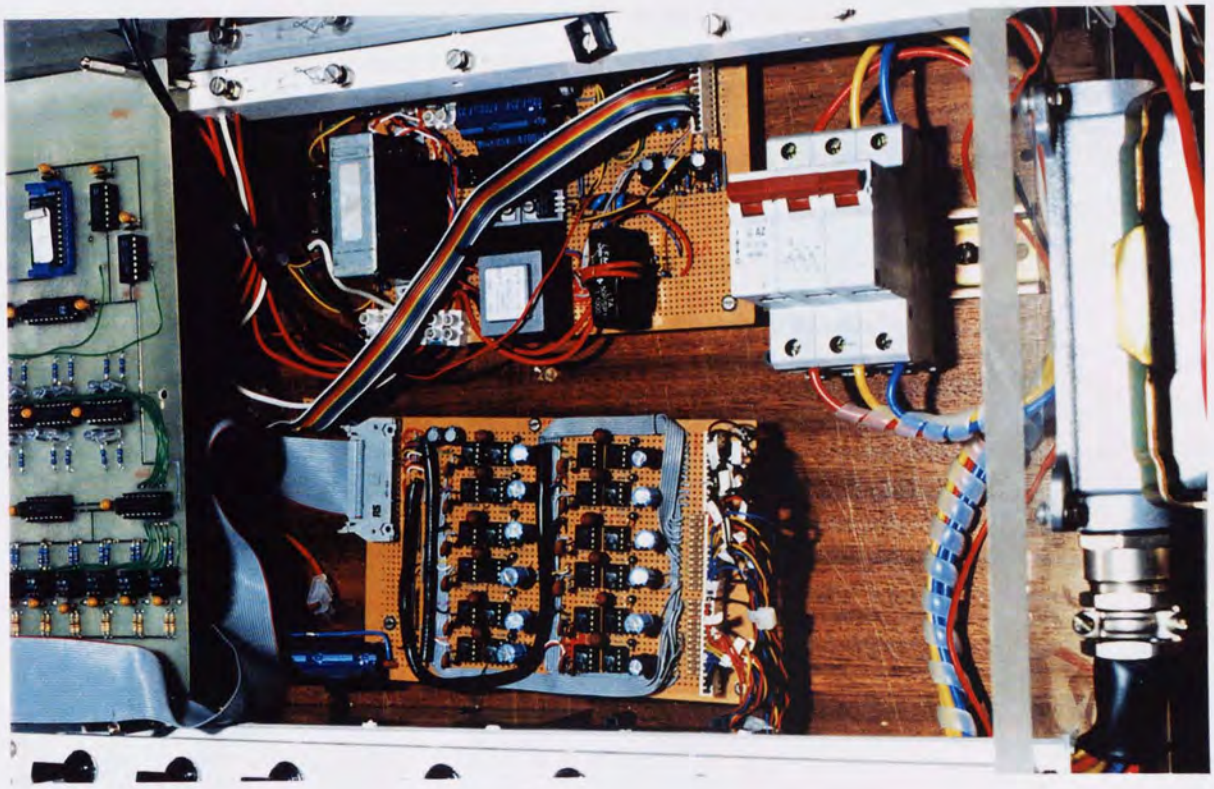

Fig 7.9b - MOSFET driver circuit (bottom centre) used in model.

7.3.1 - Driver configuration

Across the output and common (reference) of each driver is a zener diode, Dz_1 in **Fig 7.9a**, which clamps the output to 15V even in the presence of high common mode voltages. It was observed in practice that Dz_1 protected the driver but not the MOSFET because of resistor R_g. The zener diode Dz_{gs} was then included.

7.3.2 - Driver Features and Operation

The low side driver is the control chip that receives 5V logic control signals for both high and low side MOSFETs. The driver ignores requests to switch both devices on simultaneously and communicates with the high side driver by coded high frequency pulses. The drivers also feature undervoltage lockout in the event the gate voltage belows an acceptable minimum.

The high side driver uses a bootstrap circuit comprising the diode D_b and capacitor C_b to provide the required gate drive. It is therefore not connected to the high voltage d.c. rail. C_b determines the maximum duration over which the gate drive can be sustained without the capacitor discharging and therefore depends on the switching frequency, thus imposing a limit on the operating bandwidth. Sizing C_b requires data sheets. For the model, a capacitor capable of sustaining the gate drive for at 2/3 a cycle at 50Hz was used. This introduces some safety factor and extends the lower limit of the operating bandwidth.

7.4 - Interlocking & Isolation

To prevent simultaneous conduction of two devives in a limb:

- the MOSFET drivers ignore requests to switch on both devices simultaneously,
- logic gates with specially connected RC circuits to delay turn on have been used and
- the switching pattern has a deadband when both devices are held in the off sate.

Fig 7.10 shows the interfacing between the control electronics and the MOSFET drivers.

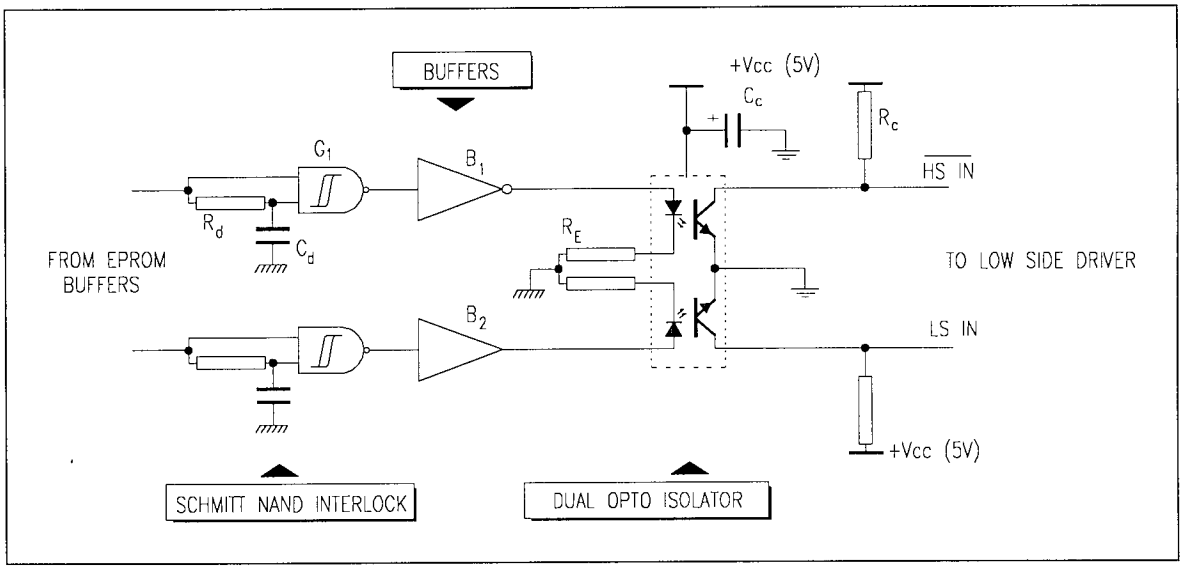

Fig 7.10 Switching interlock and isolation between control and MOSFET drivers

The opto-isolators of **Fig 7.10** provide the required ground and high voltage isolation between the low voltage and high voltage electronics. The particular devices used feature open collectors and so require the pull up resistors R_c. The isolators are consequently inverting. The +5V supply shown (Vcc) is separate from the supply that powers the control electronics.

The capacitor C_c provides local decoupling and voltage support per device and is connected across the supply and ground pins on the transistor side of the isolator. It was discovered during test operation of the model that when the number of opto-isolators connected to the **Vcc** supply was large, the voltage required support and the switching effects of the devices were apparent in the supply. Thus, the capacitor C_c is not featured in the manufacturer's application notes.

The buffers B1 and B2 provide two important functions.

- They are driver specific in that they are either inverting or non inverting depending on whether the signal they carry is for the high side driver or the low side driver. In this manner, all circuitry prior to this stage is generic and assumes logic '1' turns a device on while logic '0' turns a device off.

- They provide the necessary current drive for the diode half of the opto-isolator which would otherwise have to be sourced by the preceding logic gates (e.g. G1).

The gate G1 is a NAND gate with schmitt trigger characteristics to provide some hysterisis and so prevent the gate from responding to noise transients at the inputs. The function of the RC circuit (R_d and C_d) is to create some delay in any turn-on requests from the controller, while turn-off requests are honoured immediately. The input with the RC circuit will be referred to as the delayed input in the brief explanation that follows.

Only when both inputs are high does a NAND gate's output switch to low. It should be evident that all control requests arrive immediately at the undelayed input. Logic '0' at this input, required to turn the associated MOSFET off, immediately causes the output to switch to logic '1' (subsequently arriving as the appropriate request at the MOSFET) irrespective of the state of the delayed input.

A logic '1' from the controller, required to turn the associated device on, also arrives immediately at the undelayed input, but the output stays at logic '1' because the delayed input is still at logic '0'. The MOSFET driver therefore sees no change in request initially. It should be apparent that the RC circuit constitutes a first order low pass filter whose response to a step

input (logic signal) of size V_o is such that the output v_{out} behaves as shown in **Fig 7.11** and is described by:

$$v_{out} = V_o(1 - e^{-t/R_d C_d}) \tag{7.1}$$

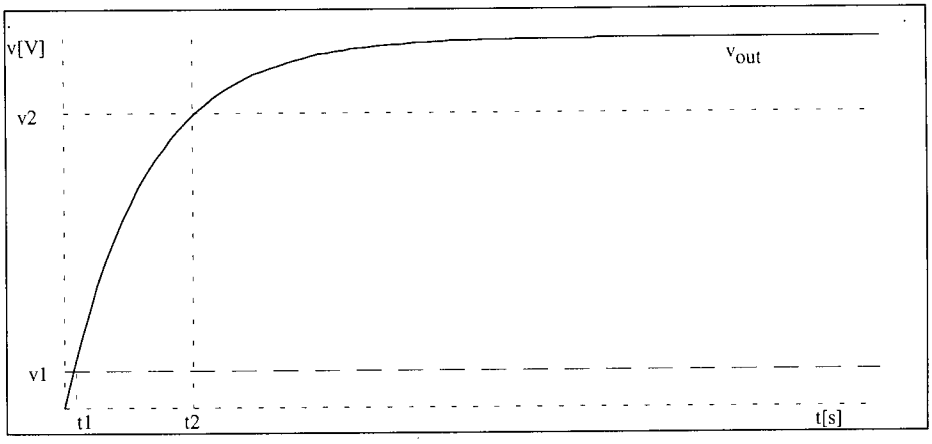

Fig 7.11 Delay circuit time response to positive going step

In **Fig 7.11**, the following are defined as follows:

v1 - maximum input signal that is reliably interpreted as logic '0' (v_{il})
v2 - minimum input signal that is reliably interpreted as logic '1'(v_{ih})
t1 - time when v_{out} = v1
t2 - time when v_{out} = v2

The requirement was that the duration t2 - t1 gives the required switching delay. As the rise time is independent of the fundamental switching frequency this arrangement imposes further limitations on the operating bandwidth of the equipment i.e. reduces the upper cut off frequency. 5V 'HC' CMOS with v1 = 0.3V and v2 = 3.15V was used. 'HCT' and TTL logic families have smaller bands of v2-v1 and would not be suited to this application.

R_d is a metal film resistor chosen for its closer tolerances compared to the less expensive carbon film types. Polystyrene capacitors were chosen for C_d to offer good precision and significant stability over the operating temperature range.

7.5 - THE CONTROLLER

7.5.1 - Switching Pattern Generator

Fig 7.12 shows the functional circuit diagram of the switching pattern generator.

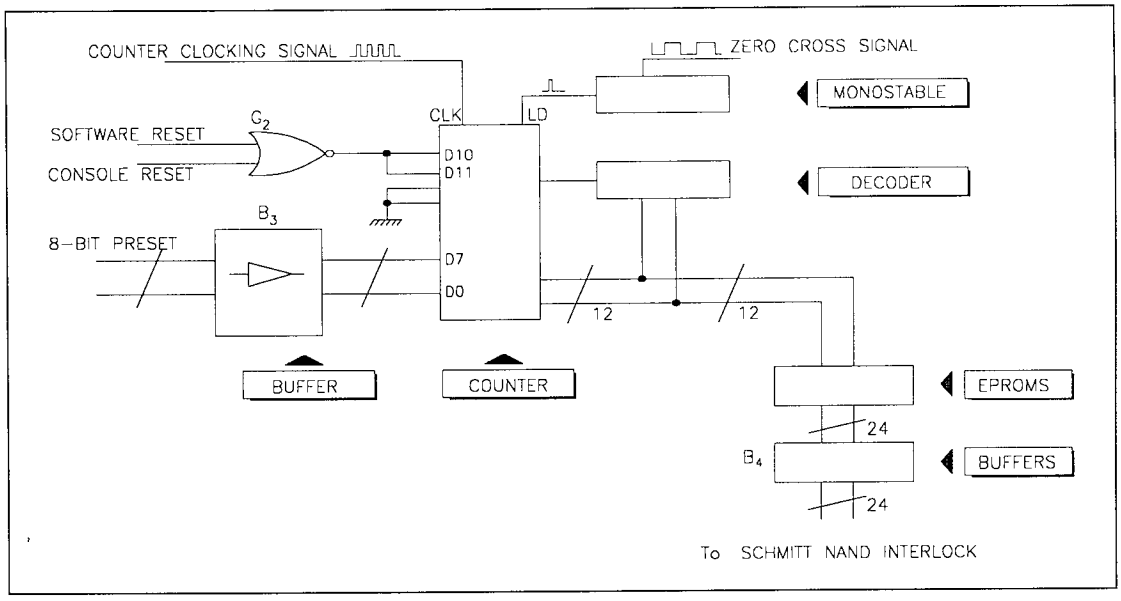

Fig 7.12 - EPROM based MOSFET switching pattern generator

Referring to **Fig 7.12** above, the buffers B4 provide the interface between the EPROMs and the schmitt NAND gates of **Fig 7.10**, providing the current to drive the latter's RC delay circuits.

There are three 4K, 8-bit EPROMs, each dedicated to the four phases derived from each of the three main phases. Since there are two MOSFETs per phase (high and low side), there are 8 MOSFETs controlled by each EPROM. The EPROMs are clocked at some frequency f_c which is a multiple of the fundamental frequency of the supply and is such that the EPROMs step through 2400 (explained in section 7.6) addresses in one cycle of the fundamental. **Table 7.14** summarises the action of one of the EPROMs.

7.5.1.1 - Counter Operation

The EPROM address lines are connected to the outputs of a 12-bit synchronous counter. The counter itself is clocked at frequency f_c mentioned above. The basic procedure is that the computer measures the fundamental period and divides this into the required eras. The resulting quotient is the interval to clock the counter.

7.5.1.2 - Decoder Operation

In normal operation, the EPROM addresses are restricted to the first 2400 stages (0- 2399) by a decoder which detects the pattern 2399 on the EPROM address lines and sets up the counter to reset to stage 0 at the next clock pulse.

7.5.1.3 - Monostable Action

To prevent switching frequency error from accumulating, the zero cross signal is used to force the counter, hence EPROMs into synchronism. The mechanism involves an edge triggered monostable which outputs a narrow pulse (~100ns) on every positive edge of zero cross. This output activates the counter load operation which immediately sets its outputs equal to the preset. This action forms the basis of delaying or advancing the switching signals because a change in the preset causes the counter to load a different value and so synchronise to a different point in the EPROM address space.

7.6 - PRE-SWITCHING CONTROL

Prior to switching , the MOSFETs are held in an off state awaiting synchronised start up, even if the counter is running. Alternatively, the ENABLE control on the Buffers B4 may be used to achieve this, but in practice, it was discovered that the unsecured buffer outputs responded to noise, triggering some drivers. Use of the EPROMs proved much more reliable. Hardware and/or software reset forces the counter to some stage between 3072 and 3373 depending on the preset. The software then sets the counter preset to 11111110 binary rather than 111111111 binary to prevent false activation of the particular decoder used. The action of the first EPROM is summarised in **Table 7.14** explained as follows:

- **STAGE** is the counter value which corresponds to the specified EPROM address. The counter loops from stage 0 to 2399 before forced back to stage 0 by the decoder.

- **ANGLE** is the stage equivalent in degrees in one cycle of the fundamental..

- **PATTERN** refers to the bit pattern stored in the EPROMs, hence the state of each MOSFET at a given stage. 1 implies a device is on. Thus for example, when the first red phase, *a*1, crosses zero from its negative half cycle, its associated low side device (H) switches off and the high side (L) on. The complete bit pattern at this instant would be as shown in **Table 7.13** below. The highlighted phase is the focus of **Table 7.14**.

Table 7.13 - EPROM bit pattern as phase a1 crosses to positive half cycle

EPROM #3 - Blue Phase								EPROM #2 - Yellow Phase								EPROM #1 - Red Phase							
c4		c3		c2		c1		b4		b3		b2		b1		*a4*		*a3*		*a2*		*a1*	
L	H	L	H	L	H	L	H	L	H	L	H	L	H	L	H	L	H	L	H	L	H	L	H
1	0	1	0	1	0	1	0	1	0	1	0	1	0	1	0	1	0	1	0	1	0	0	1

Table 7.2 - Explanation of EPROM switching patterns

STAGE	ANGLE	PATTERN ($a4_L$ - $a1_H$)	COMMENTS
0	0	10101000	$a1_L$ switches off
1	0.15	10101000	Devices $a1_H$ and $a1_L$ off
2	0.3	10101001	$a1_H$ switches on
...	.....	.....	
99	14.85	10101001	
100	15	10100001	$a2_L$ switches off
101	15.15	10100001	$a2_L$ and $a2_H$ off
102	15.3	10100101	$a2_H$ switches on
...	.....	.....	
150	**22.5**	10100101	Sync stage. May not coincide with sync. signal
151	22.65	10100101	
150	**22.5**	10100101	Suppose Sync signal occurs here. Forces pattern to jump to
151	22.65	10100101	sync stage
152	22.8	10100101	
153	22.95	10100101	
...	.....	10100101	
200	30	10000101	$a3_L$ switches off - Sync stage #2. *May* occur before signal
201	30.15	10000101	$a3_L$ and $a3_H$ off
202	30.3	10010101	$a3_H$ switches on - Sync. signal forces pattern to sync. stage
200	30	10000101	$a3_H$ switches off
201	30.15	10000101	$a3_L$ and $a3_H$ off
202	30.3	10010101	$a3_H$ switches on
...	.....	.....	
299	44.85	10010101	
300	45	00010101	$a4_L$ switches off
301	45.15	00010101	$a4_L$ and $a4_H$ off
302	45.3	01010101	$a4_H$ switches on
...	.....	.....	
1200	180	01010100	$a1_H$ switches off
1201	180.15	01010100	$a1_H$ and $a1_L$ off
1202	180.3	01010110	$a1_L$ switches on
....	.....	.....	
1300	195	01010010	$a2_H$ switches off
1301	195.15	01010010	$a2_H$ and $a2_L$ off
1302	195.3	01011010	$a2_L$ switches on
....	.....	.....	
1400	210.0	01001010	$a3_H$ switches off
1401	210.15	01001010	$a3_H$ and $a3_L$ off
1402	210.3	01101010	$a3_L$ switches on
....	.....	.....	
1500	225.0	00101010	$a4_H$ switches off
1501	225.15	00101010	$a4_H$ and $a4_L$ off
1502	225.3	10101010	$a4_L$ switches on
....	.....	.....	
2399	359.75	10101010	2399 detected by decoder - Counter resets on next pulse
2400	360	00000000	
....	.....	.....	
3072		**00000000**	Minimum preset in RESET state
....	.....	**00000000**	*If counter running, addresses cycle here in RESET state*
3327		**00000000**	Maximum Preset in RESET state
....	.....	.....	
4095	.....	**00000000**	Maximum EPROM stage - unused

Notes on Table 7.14

Assume operation with the zigzag transformers so that the first phase occurs at -22.5° with respect to the primary red phase. The initial preset to effectively place the zero cross signal at +22.5° is required. With 2400 stages per cycle, each represents 0.15°. A phase shift of 22.5° is thus equivalent to 22.5/0.15 = 150.

An example is shown in **Table 7.14** when the EPROM is assumed to reach the synchronisation stage of 150 too early. The actual signal is assumed to occur two stages later and forces the switching pattern back to 150. This produces no change in the MOSFET states since the bit pattern at stages 150 and 152 is the same.

A second example is shown to highlight a potential problem. Assume synchronisation is required at stage 200 and suppose, as before, that the EPROMs reach this stage too early. The low side MOSFET $a3_L$ in phase $a3$ switches off. The deadband stage at 201 ensures both $a3_H$ and $a3_L$ are off to allow for extinction of the current in $a3_L$. At the next stage, 202 , the high side MOSFET $a3_H$ switches on. However, this coincides with the actual synchronisation signal which forces the EPROMs back to stage 200. In this transition, the switching pattern skips the deadband at 201, and the result is a simultaneous request for switch off of $a3_H$ and switch back on of $a3_L$. This may lead to a shorting of the high voltage d.c. rails. Of course, one possible solution is to widen the deadband.

Synchronisation may occur at the 'wrong' time on account of noise and any voltage fluctuations that may cause the detector to activate slightly before or after the expected instant. It is therefore not sufficient to rely on the EPROM deadband alone and it was for this reason that the NAND schmitt triggers were included in the design. They ensure that all requests, spurious or not, are subject to some deadband. However, it was observed that the equipment with the schmitt triggered NANDs alone was less stable than the combination involving the EPROM deadbands. The effect of the deadband on the supply current was simulated and the results have been shown in section 3.4.1. A net deadband of about 50μs based on experimental trials was decided upon, with 30μs in the NAND gates and about 20μs in the EPROMs.

7.7 - COMPUTER INTERFACE

A digital I/O card designed for an expansion slot of an IBM® compatible PC™ was used to interface the control circuit described above to the computer. It's essential components are two 8255 peripheral interface adapter chips (PIAs) and a single 8253 timer chip. Each 8255 chip features three 8-bit ports, A, B & C which can be configured for all input or all output, and port C for mixed input and output. Thus, a total of 48 digital I/O lines was available. These were assigned as shown in **Table 7.15**.

I.C.-PORT	CONFIGURATION	ASSIGNMENT
PORT 1A	All outputs	8 LSBs on Counter Preset for phase initialisation and delay angle control
PORT 1B	All outputs	Bit 0 - User Select enable Bit 1 - Buffer Tristate Bit 2 - Control limiting indicator Bit 3 - Synchronous start (Bits 4-7) - unused
PORT 1C	4 output / 4 input	Bit 0 - 2 - Timers control Bit 3 - All enable Bit 4 - 6 - Timers outputs Bit 7 - Zero crossing signal
PORT 2A	All inputs	Unused
PORT 2B	All inputs	ADC data bus
PORT 2C	4 output / 4 input	Bits 0-4 ADC address and control Bit 5 - Console start/reset Bit 6 - Console open/closed loop selection Bit 7 - switching mode selection

Table 7.15 - Computer Interface card I/O assignment

The choice of pin assignments was made with control software optimisation in mind, an example being the allocation of the four LSB's on Port 2C to the ADC address and control lines. Device control can therefore be achieved with simple logical AND and OR to clear the channel address, set up the new one, and enable the device without changing the output port address (Port 2C). Although the time saving is small, the code is optimal, especially for waveform capture sampling operations where hardware set up delay can lead to errors in phase relationships. **Fig 7.16** is a schematic showing the interface card and the associated input and output signals.

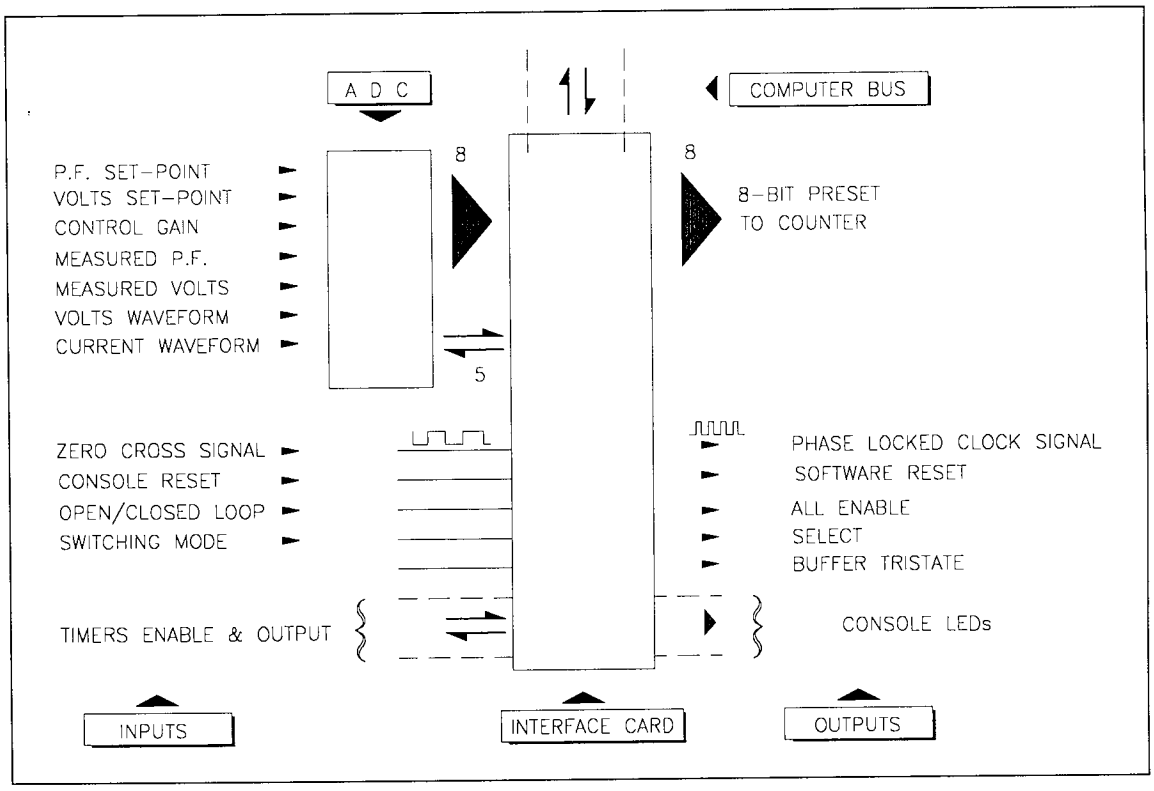

Fig 7.16 - Computer interface card input/output connections

The Interface card has one 8253 integrated circuit which features three independent 16-bit timers running at some fixed frequency upto 4MHz. An external 3MHz clock was used for this purpose. The timers count down but are software programmable for at least 5 modes of operation. They were assigned the following tasks:

- *Timer T0* - configured as software strobe and used to time the fundamental period.
- *Timer T1* - used to provide the phase locked clocking signal to run the counter. T1 was configured as an auto-reloading square wave generator.
- *Timer T2* - used in waveform sampling routines and in frequency measurement watchdog functions. T2 is general purpose and reconfigured during run time as required

7.8 - SYSTEM OPERATION

7.8.1 - Phase initialisation at start up

At start up, the user is prompted to enter the relative location of the first phase, in degrees. This is -22.5° for the transformers and -30° for the induction motor. The required preset is then computed and stored. A small error in the precision of the zero-cross signal exists as a consequence of the finite voltage drop of the detector - a characteristic of all light emitting diodes. The error depends on the size of the current limiting series resistor. It is accounted for by adjusting the preset accordingly. The software sets the first phase in such a way that equal negative and positive swings of the delay angle may be possible. A list of 'hot keys' is displayed and include options to toggle the sampling and plotting of waveforms on and off as required.

7.8.2 - Interface card initialisation

Each pin on the interface card is assigned its input or output function, and the timers are configured appropriately. The initial states of the outputs are also set at this time and these include enabling the buffers, the timer gates, reset activation and the EPROM counter preset is set to maximum so that all MOSFETs are off on power up.

7.8.3 - Control hardware initialisation

The user is now asked to power up the control circuit. This procedure is necessary to prevent the interface card from 'latching' when the external circuit is powered up. Once this is done, the software proceeds to initialise all hardware by performing what are termed 'dummy read/write' operations on the ADC and similar devices. All the channels on the ADC are then read in sequence and displayed graphically.

7.8.4 - Zero cross signal processing

The user is asked to power up the three phase supply while the secondary voltage is set to minimum. The zero-cross signal is derived from the variac primary red phase to neutral terminals and so becomes available. Upon user confirmation, the software proceeds to check for the existence of the zero crossing signal and displays the ADC values read. Although not all the displays are useful, this action presents an easy way of monitoring the health of ADC. Absence of the zero-cross signal is relayed to the user.

7.8.5 - Initial frequency measurement

Frequency measurement involves the use of two timers. The first, T0, does the actual timing while the second, T2 acts as a watchdog timer and so prevents the software from waiting indefinitely in the event of loss of the zero crossing signal, or if the frequency is too low. In normal operation, frequency is calculated and displayed in Hertz.

7.8.6 - EPROM output initialisation

The EPROM address counter is preset to decimal 254 while the software RESET signal is held high. The EPROMs are therefore in the off states of **Table 7.14.**

7.8.7 - User options and set point initialisation

The 'select' is activated to enable the user to preset the setpoints, choose the control *loop* required i.e. closed or open, and select the switching *mode* desired. Upon user confirmation of completion, the 'select' is disabled and options read into memory. Subsequent change in options as a result of noise or user action has no effect, thus preventing large step changes in control.

7.8.8 - Synchronised start of switching

The initial computations of the required EPROM clock rate follow. The fundamental frequency is measured while the reset state is maintained active. Once accomplished, the user is then prompted to activate the console START when ready. Pushing the button deactivates the hardware RESET signal but as synchronisation cannot be guaranteed, the software reset is maintained high until a positive going edge of zero cross is detected. This is not entirely necessary if the three phase voltage is zero, but simulation suggests severe transients may occur if not. At the appropriate instant, the software reset is deactivated and the MOSFETs begin to switch accordingly.

7.8.9 - Delay angle control

Once switching has began, the output voltage may be increased and the control set point varied.

The software features two routines for handling open and closed loop control. In either case, it is assumed that the relationship between the delay angle and the reactive power absorbed or generated is linear [Hill, 1995]. The size of the delay angle was restricted to the range -7.5° to +7.5° based on simulation results. This range was wider than the ±4° required for maximum generation and absorption at rated voltage to enable reasonable performance at low voltage.

7.8.9.1 - Operation

Referring to **Table 7.14**, suppose the initial preset is 150 as before, corresponding to a starting phase of -22.5°. While the EPROMs are cycling in their active address space, stage 150 coincides with the reference positive going zero crossing (zero cross ensures this). If it is then desired to change the delay angle to say 0.75° *post* zero cross, this is equivalent to causing reference zero cross to occur *earlier* in the switching sequence. Since each stage in the EPROM address space represents an equivalent 0.15°, five stages are required to change the delay angle by 0.75°. A *reduction* in the preset from 150 to 145 will achieve the desired effect.

7.8.9.2 - The Open Loop Control algorithm theory

Let α_{min} and α_{max} be the minimum and maximum *permissible* delay angles respectively, in degrees, and N_{eprom} the number of EPROM active pages in one cycle of the fundamental and suppose the control variable, ε, to be restricted to the 8-bit range 0 through 255.The basic requirement is that the full range of the control variable corresponds to full range variation of the delay angle between the α_{min} and α_{max}. This is shown graphically in **Fig 7.17a** below.

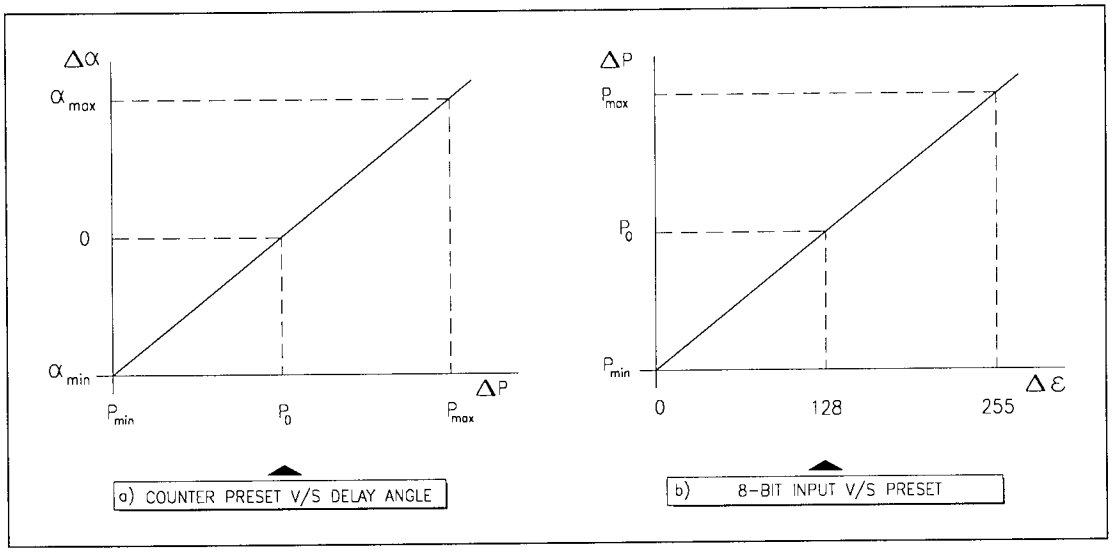

Fig 7.17 - Relationships between control parameters as implemented in software

From **Fig 7.17**, the preset P v/s input ε is a straight line whose equation is:

$$P = \frac{2}{255}\left(\frac{\alpha_{max} \times N_{eprom}}{360}\right).\varepsilon + \left(P_o - \frac{\alpha_{max} \times N_{eprom}}{360}\right) \qquad (7.2)$$

where P_0 is the initial preset corresponding to a delay angle of 0°

For α_{max} = 7.5°, N_{eprom} = 2400, the equation simplifies to:

$$P = \frac{100}{255}\varepsilon + (P_o - 50) \qquad (7.3)$$

The 8-bit preset limits the values of initial preset P_0 which cannot be less than 0, nor greater than 255. In the model, these limits are such that $-7.5 \geq P_0 \geq -40°$. Open loop control therefore translates the set point directly into the required preset i.e. ε = set-point.

Thus:

$$P = \frac{2}{255}\left(\frac{\alpha_{max} \times N_{eprom}}{360}\right) \times setpoint + \left(P_o - \frac{\alpha_{max} \times N_{eprom}}{360}\right) \qquad (7.4)$$

7.8.9.3 - The Closed Loop Control Algorithm

Closed loop control requires that the set-point is compared with the measured value, and the error processed accordingly. The size and sign of the error determines the amount and direction of corrective action. The control parameters require careful tuning for acceptable damping, overshoot and steady state error.

The maximum permissible change in the preset is set to correspond to the occurrence of maximum error. This is shown graphically in **Fig 7.18**.

The control philosophy is that zero error gives rise to zero corrective action and maximum error gives rise to maximum corrective action.

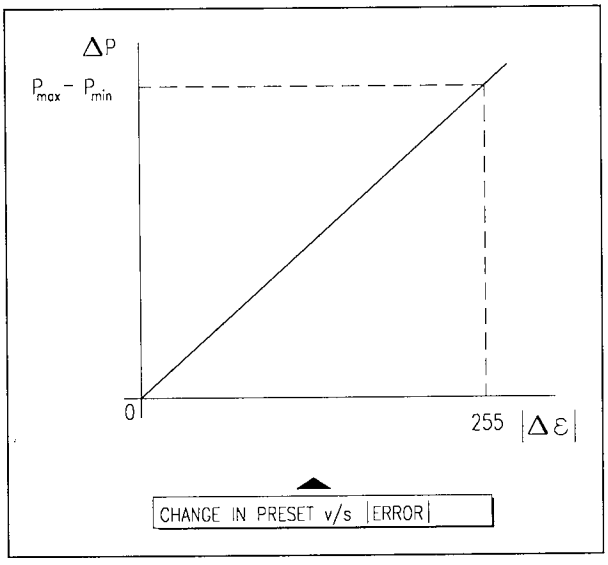

However, the absolute value of the preset itself needs to be confined to the permissible range of angles between α_{max} and α_{min}.

Change in preset is:

$$\Delta P = \frac{(P_{max} - P_{min})}{255} \times \text{error} \qquad (7.5)$$

Fig 7.18 - Graph of change in preset v/s absolute error

P_{max} and P_{min} are defined as before for Open Loop control. Thus, if the error is defined as ε = setpoint - measurement, and if P_{t-1} is the previous value of the preset, currently active, then the new preset, P_t, is given by:

$$P_t = P_{t-1} + 2\left(\frac{\alpha_{max} \times N_{eprom}}{360 \times 255}\right).\varepsilon \qquad (7.6)$$

assuming $|\alpha_{max}| = |\alpha_{min}|$

For the implemented values of $\alpha_{max} = 7.5°$ and $N_{eprom} = 2400$,

$$P_t = P_{t-1} + (100/255) \times \varepsilon \qquad (7.7)$$

These particular values of the control algorithm make it insensitive to changes in the error of less than 3 LSB's. This gives the control system sufficient immunity from 'chatter' when the error fluctuates by small amounts about zero at the required steady state value of the preset.

However, it also implies finite steady state error and reduced control resolution. Integral control can be included to minimise the steady state error. A gain factor K may also be used, leading to the expression:.

$$P_t = P_{t-1} + (100/255) \times K \times \varepsilon \qquad (7.8)$$

Closed loop control response of the STATCON has not been investigated fully and the control gain has been made available as variable input to the system from the console.

7.8.9.4 - Delay angle Limiting action

The algorithm, as implemented, rounds off non integer values of the preset to the nearest whole. Where the computed preset exceeds the stated limits, the software clamps the output to the limiting value and activates an indicator.

7.8.9.5 - Changing delay angle

When a change in the counter preset is required, the negative going edge of the zero cross-signal is detected and the change in preset effected immediately after. This prevents simultaneous presetting and loading of the counter thus eliminating potentially erroneous loading by giving the data sufficient settling time. The positive going edge then loads the new preset.

7.8.9.6 - Closed Loop Control Compensation

It was observed in practice that when the STATCON was left to operate at a fixed firing for an extended period (about 1 hour) in open loop mode, the generated or absorbed reactive power exhibited net drift from the set point. This suggests that open loop is unsuitable, and simple proportional control probably inadequate. In order to eliminate the steady state error, a PI controller would be required [Dorf, 1995].

7.8.10 - Phase Locked Loop action

In order to track frequency changes accurately and so maintain synchronism, the period of the zero crossing signal is measured at most once every three cycles depending on whether or not the waveform sampling and display options are enabled. Frequency measurement which would lead to a change in the timing interval, is repeated twice in rapid succession before implementation. In this manner, the software safeguards against the effects of spurious or noisy zero crossing.

The timing uses a 16 bit counter running at 3MHz, so for an idealised 50.00Hz the value accumulated by the counter should be 60000. This, divided over the 2400 eras gives a value of 25. In general, the count is not exactly 60000, and division by 2400 gives a quotient between 24.5 and 25.5. It would require complex coding to process the fractional part of the quotient, and would take up virtually all the processor's time. Thus, a rounded off value is computed which will lead to the EPROM address counter gaining or losing a few stages over one cycle. This error is potentially cumulative, and it is for this reason that the zero crossing signal itself is used to force synchronisation of the counting sequence. A hardware based PLL would also require this synchronisation mechanism due to quantisation errors.

The counter T1 generates the clocking signal for the counter and is auto-reloading, requiring activation only once for fixed frequency operation. This leaves the computer free to process the delay angle and other requirements. In the event of the computer 'hanging', the counter continues to run so supervised reset can be done without the equipment running out of synchronism.

7.8.11- Waveform Sampling and processing

The software spends most of it's time checking for reset requests, tracking frequency changes and set point variations in that order. When none of these requires servicing, the voltage and current waveforms are sampled together with an additional third channel to which may be connected an extra signal such as the inverter output or capacitor voltage.
The software was optimised for speed by using efficient instructions and sampling all three channels together. The sampling frequency is limited by processor speed, hardware set up and access times and the ADC conversion times.

Performance on a 20MHz 80386 system was satisfactory if the number of cycles was less than 4 and no more than 500 samples per channel. Thus, for the normal application the equipment is intended for, the hardware limitations can be ignored. The sampling frequency was set to about 3 times the fundamental in order to capture the high frequency distortions observed in the current waveform.

7.8.11.1 - Waveform and Spectral Display

The program samples the three waveforms specified and plots them to the screen using direct video memory access for maximum speed. The fundamental control parameters are then checked soon after and serviced as required. The waveform selected for spectral analysis is then processed and the harmonic spectrum displayed.

7.8.11.2 - Sampled data storage

Sampled data may be stored to disk for off-line processing. This is done by pressing the 'S' key on the keyboard. The sample is read directly from memory into an automatically named file and appears as a three column ASCII table of voltage, current and the thirdchannel. The files may be are numbered sequentially, but overwritten if the program is restarted and storage requested. The 'experimental results' in this thesis were stored as such and then processed using an off-line spreadsheet.

7.8.12- Software or Hardware Reset

Any of the following conditions leads to a RESET of the equipment i.e. halting of the MOSFET switching:

- Pressing the ESC key during run-time
- Pressing the RESET button on the console
- 15V supply to the MOSFET drivers falling to below about 14.5V
- The 5V supply to the control circuit falling to below about 4.5V

The voltage monitoring functions are assigned to a voltage supervisor integrated circuit which generates the hardware reset pulse.

When active, the software runs a shut down routine which involves switching off the MOSFETs by setting the counter preset high as described earlier. The EPROM address counter is then deactivated. A hardware reset causes the EPROM address counter to shift to the all zeroes stages of the address space and so effects MOSFET isolation even before the software responds. The software proceeds to execute the systematic shut down soon after.

7.8.13 - LED Display

Generally, CMOS circuitry does not provide the sort of current drive required for l.e.d. displays. Integrated circuits featuring 4 Darlington pair transistors per device were used to interface the CMOS to the l.e.d.s.

7.9 - SUMMARY

This chapter describes a 24-pulse control circuit and its features as implemented

Power MOSFET protection and driver topologies have been explained and so too their need for adequate protection. A novel zero crossing detector has been described and the importance of noise immunity in the circuit as a whole explained.

The control software, its functions and structure have been described and also the manner in which effective time sharing strategies have been implemented on a basic operating system that does not support a multi-tasking executive. The complete program listing in Turbo C/C++ is given in appendix D.

Fig 7.19 is a photograph of the control circuit. The three devices in soft eject sockets at the top are the EPROMs. Immediately under them are three octal buffers, and under these are the NAND schmitt delay circuts. The large integrated circuit in a soft eject socket at the bottom left hand of the circuit board is the ADC. Ten of the twelve high side MOSFETs are visible at the bottom of the photograph just under the row of toggle switches.

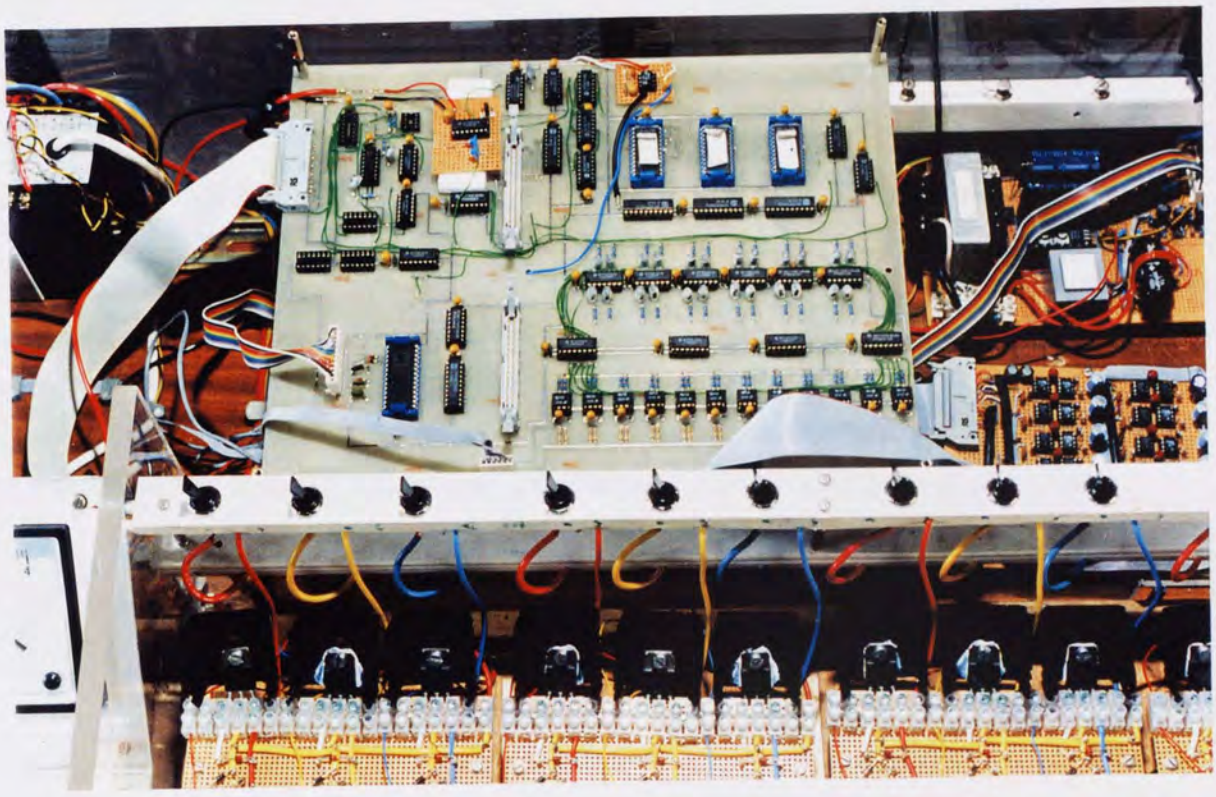

Fig 7.19 - Circuit showing the control hardware, drivers and MOSFETs.

CHAPTER 8

PERFORMANCE OF THE STATCON CONTROLLED INDUCTION MOTOR

8.1 - Introduction

This chapter presents the results of performance tests conducted on the motor and assesses the impact of the STATCON on the induction motor as a whole based on experimental data.

8.2 General performance parameters

The performance of an induction motor is characterised by six parameters:

- the starting current (inrush)
- the starting torque
- the pull out torque
- the machine efficiency
- the machine power factor
- the heating of the windings and iron

In this discussion, only the torque, efficiency and power factor are investigated.

8.3 D90S Performance Parameters

Detailed information about the performance of the conventionally wound D90S was supplied by the manufacturer based on results from purpose designed software[1]. The results have been presented and discussed in appendix A-03. However, for accurate comparisons, load tests would have to be performed on the conventional winding under the exact conditions that they were performed for the modified winding. The results in the appendix were included only as a general indication of trends and machine performance over a wider range of slip values.

[1] 4715 THREE PHASE INDUCTION MOTOR DESIGN PROGRAM - Version 1.2.1 © Copyright Electrodrives Ltd.

8.4 - Performance Comparisons

The diagram of **Fig 8.1** shows the experimental apparatus arranged for no load and load tests on the induction motor.

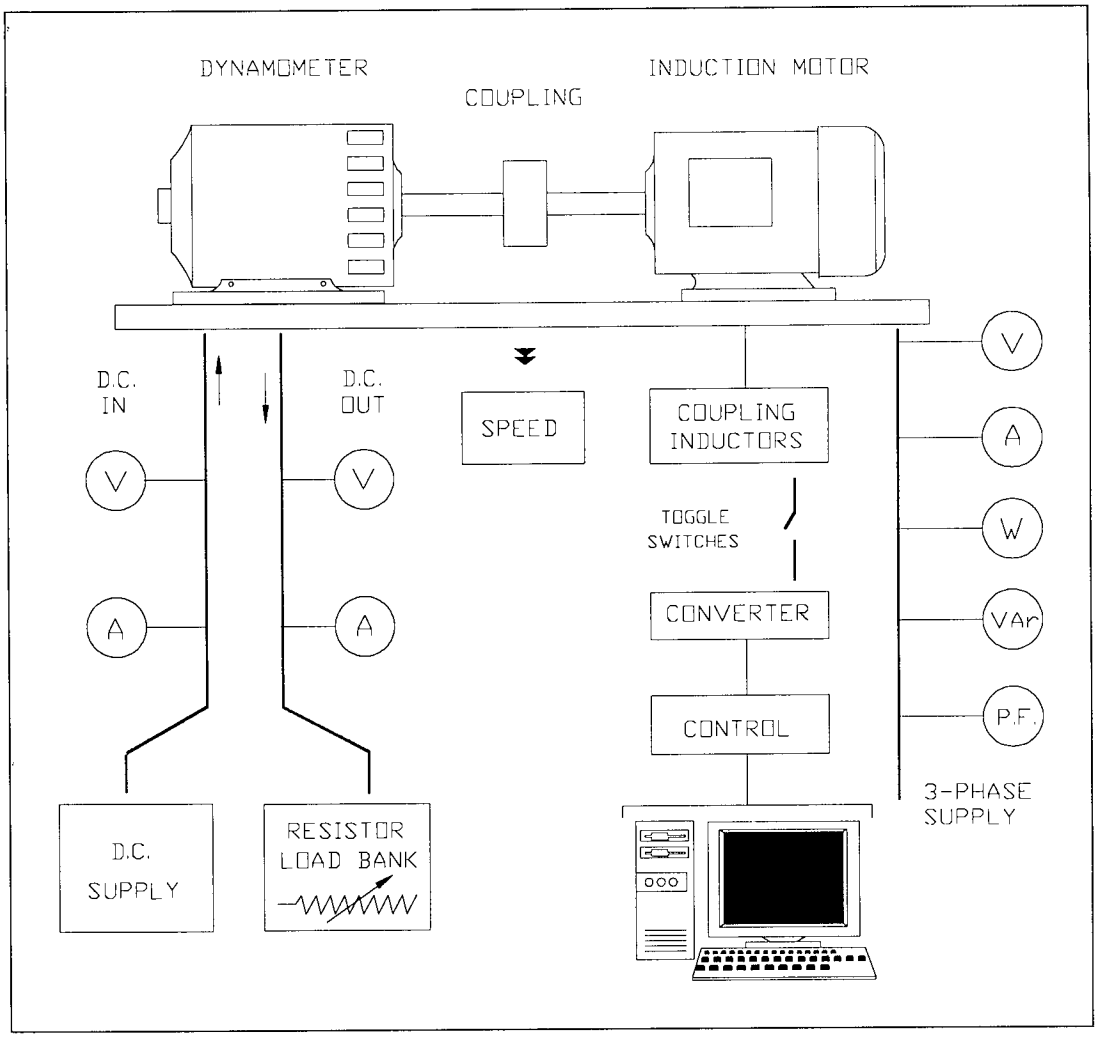

Fig 8.1 - Arrangement for load test experiments on induction motor

Referring to the diagram of **Fig 8.1**.

- The d.c. supply permits control of the output voltage and the excitation (field) current as required.
- The speed was measured using a stroboscope. Some error in accuracy of the given results is therefore to be expected.
- The toggle switches between the coupling reactors and the converter on the STATCON side were included to facilitate isolation of the bridge converter from the magnetic interface so that tests on the uncompensated system could be done.
- Values of delay angle were obtained directly from the computer.

Photographs of the experimental apparatus have been included in appendix C (**Fig C-10**).

8.4.1 - Experimental procedure

The load was adjusted by changing the value of the resistance connected across the d.c. output of the dynamometer. In general, the resistance was adjusted until a desired d.c. output current was observed, and measurements taken upto the rated value of the dynamometer, checking constantly that all operating parameters on the induction motor side were within acceptable limits. Key waveforms were also captured.

For each set value of the output current, the field current was adjusted to give rated output voltage until further change in field current was not possible. Beyond this current, the d.c output voltage was recorded as observed.

At each load setting, hence d.c. output current, all the induction motor parameters shown in **Fig 8.1** were recorded, as were the d.c. output voltage and current.

The product of the d.c. output voltage and current is a measure of the mechanical output power of the induction motor. This is not the best way to measure the mechanical output of the a.c. machine because of the d.c. machine losses and efficiency, but suffices for the *comparisons* intended since all measurement is subject to the same experimental conditions.

The product of the a.c. voltage and current gives the per phase total input power to the induction motor, applying the appropriate scaling to account for the delta connection. The total active power input is the product above further mutliplied by the power factor.

The developed torque is the developed mechanical power divided by the mechanical angular velocity ω_m of the rotor. The torque was thus calculated rather than measured.

8.4.2 - Tests on the uncompensated machine

To perform the tests on the uncompensated machine, the toggle switches of **Fig 8.1** were opened to isolate the machine from the converter. The coupling inductors were therefore on open circuit.

8.4.3 - Tests on the compensated machine

The toggle switches of **Fig 8.1** were closed, converter switching enabled and the three phase voltage raised to rated value by means of variac control with the induction machine on light load (dynamometer not energised). The firing angle was adjusted to give the desired power factor. At each load setting, it was ensured that the machine was running at unity power factor by means of the VAr meter (zero VArs) and power factor meter. The required change in firing angle was recorded.

8.4.4 - Experimental results

In **Fig 8.2**, the uncompensated curve is shown as a broken line.

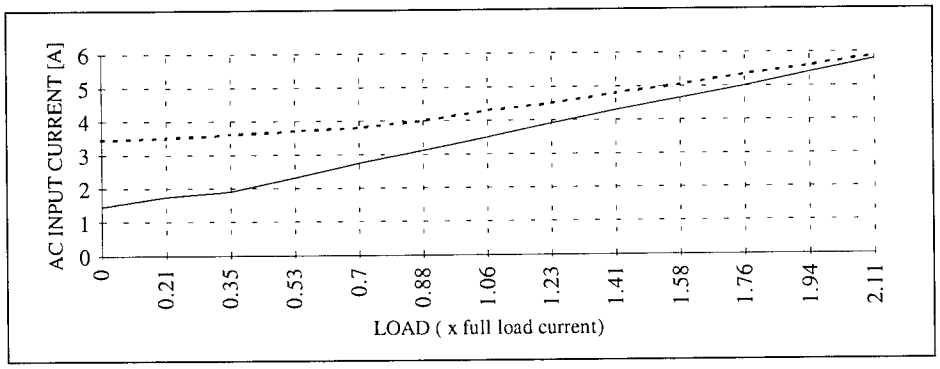

Fig 8.2a - Supply line current v/s load

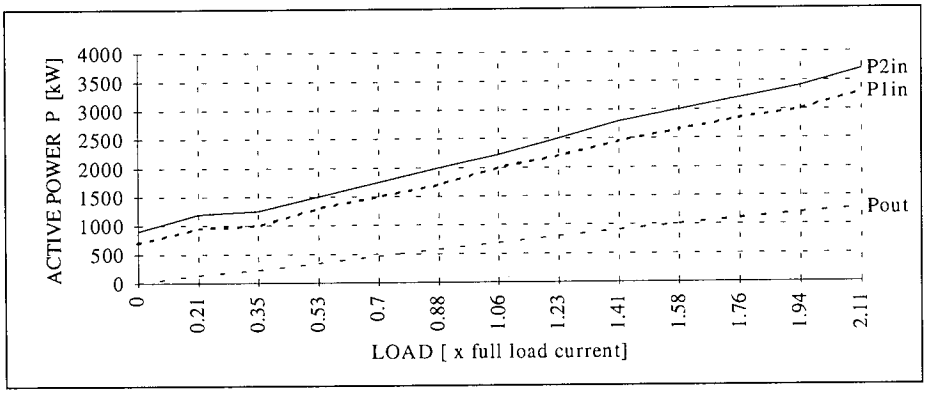

Fig 8.2b - Input and output active power v/s load

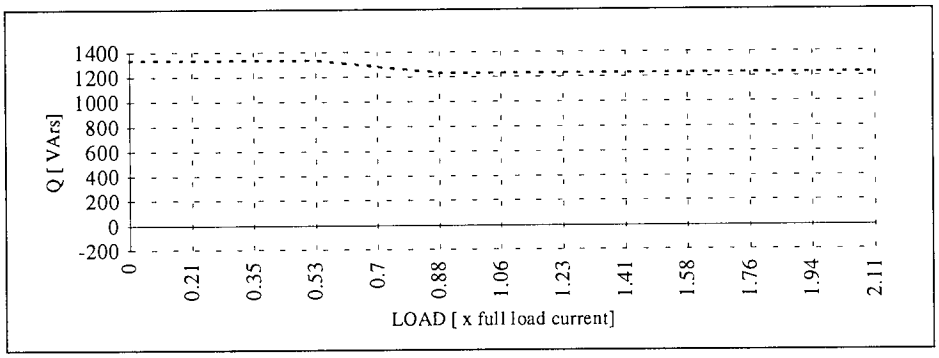

Fig 8.2c - Total Reactive power v/s load

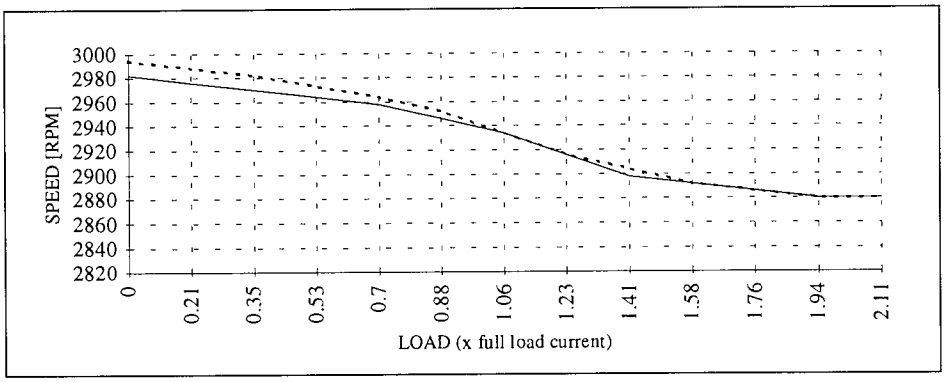

Fig 8.2d - Rotor speed v/s load

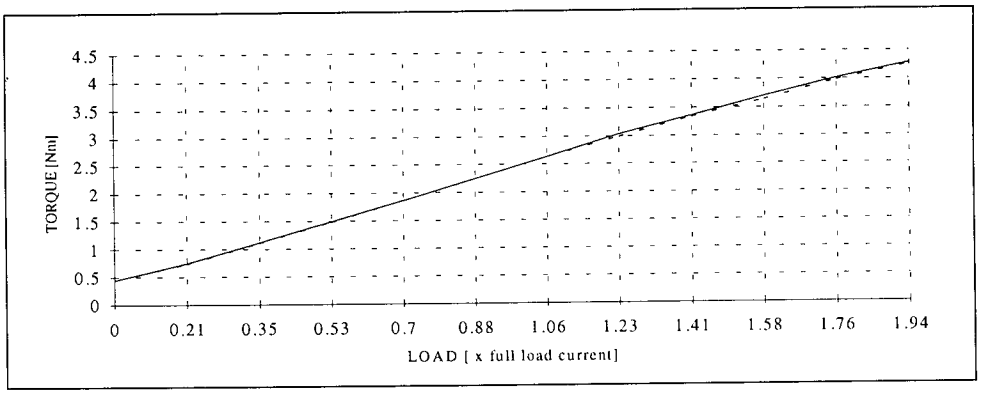

Fig 8.2e - Developed torque v/s load

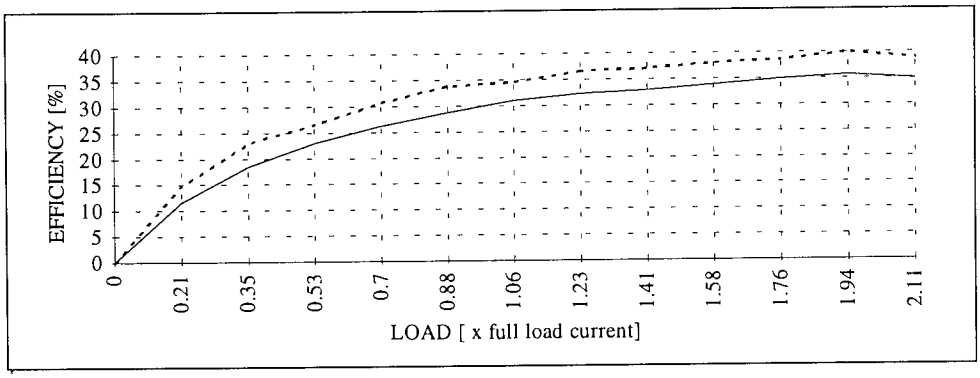

Fig 8.2f - Overall system efficiency v/s load

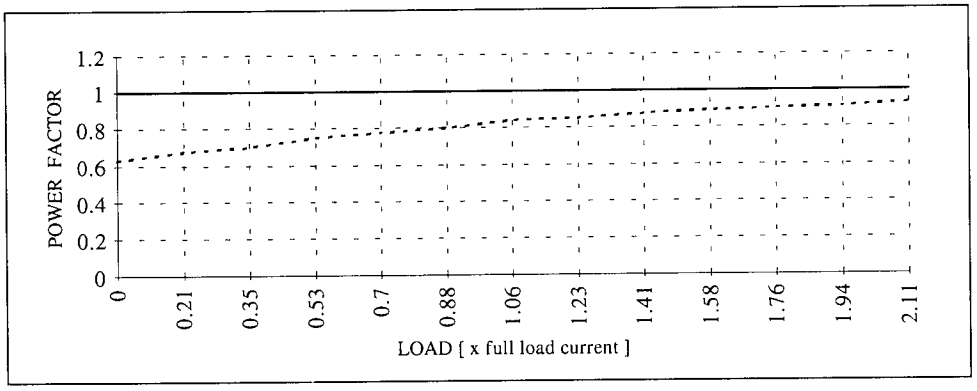

Fig 8.2g - Terminal power factor v/s load

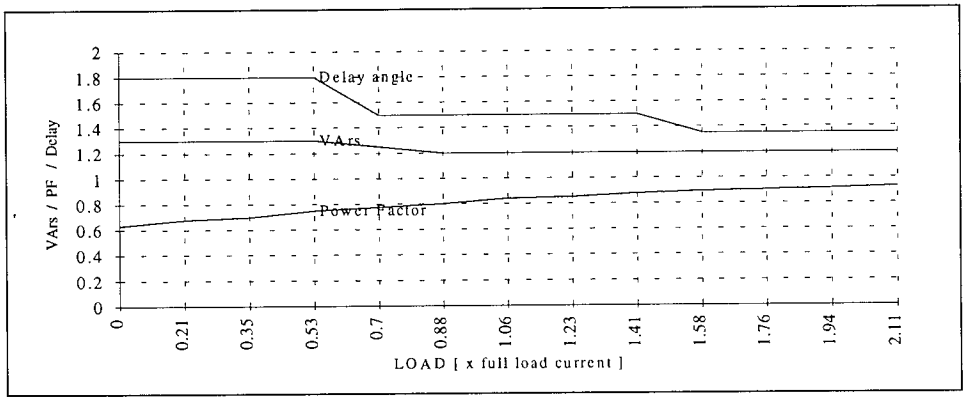

Fig 8.2h - Uncompensated motor kVArs & Power factor and delay angle [°] v/s load

8.4.5 - Notes on experimental results

The general overview reveals that over the slip range of concern, as the load increases:

- power factor improves
- a.c. line current increases
- the reactive power stays virtually constant
- the machine slows down
- the developed torque increases to meet the load demands
- the combined system (machine and STATCON) efficiency decreases

8.4.6 - A.c. Phase current

The total a.c. input current comprises the active and reactive components of the system. It is evident that at light load, when the ratio of the active power to the apparent power is low, the compensated machine draws much less current than the uncompensated system. This is because the total phase current for the compensated system represents the active component only. At higher load when the ratio of the active power to the apparent power increases, the two curves converge.

Fig 8.2a shows that in the range of speeds over which the load tests were performed, i.e. between slip values of 0 and 0.2, the a.c. phase current is between 0.4 and 1 p.u.

8.4.7 - Input and Output Active Power

In **Fig 8.2b**, for a given output power (labelled P_{out}), the compensated system is observed to have a higher power input than the uncompensated case. The curves of the input power, P_{in1} for the uncompensated case and P_{in2} for the compensated case are virtually parallel as expected since the effect of the STATCON is manifest only in the reactive component of the total intake power. The offset between the curves is an indication of the losses in the STATCON and magnetic coupling.

The losses in the STATCON are suspected to be largely due to the coupling reactors which, for the purpose of reduced size and low resistance, were chosen to be iron-cored rather than, ideally, air-cored. Iron losses are therefore present in addition to the copper losses in the winding. If the compensator losses are subtracted from the input power curve P_{in2}, it becomes evident that there is a significant reduction in the total power input in the compensated case. The measured active power at fixed load for the compensated and uncompensated cases revealed that the losses due to the compensator were approximately 250W. Assuming a nominal value of 200W to allow for possible losses in the machine itself due to the generated harmonics, the modified input and output power v/s load curve for a lossless compensator is shown in **Fig 8.3** below. Note that the output power curves for the two cases are concurrent.

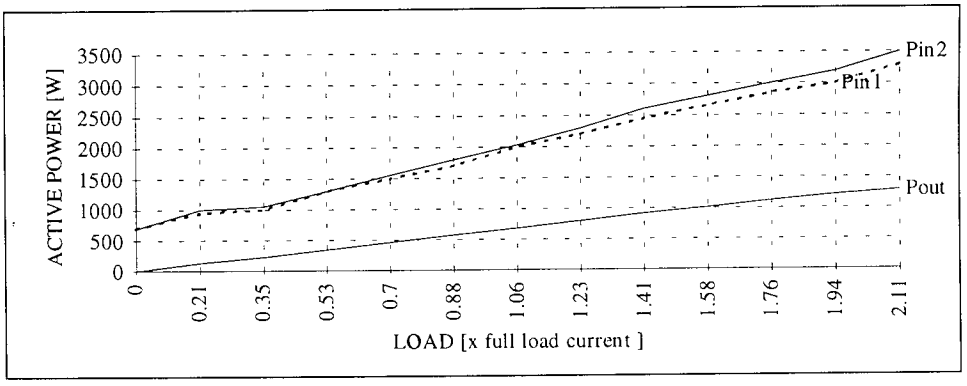

Fig 8.3 - Active power input and output assuming lossless compensator.

The curves P_{in1} (compensated) and P_{in2} (uncompensated) in **Fig 8.3** diverge with increasing load. This trait is also observed in **Fig 8.2b** and **Fig 8.2f**, and is a consequence of the non-linear variation of equipment losses with firing angle [Hill, 1995]. The difference in the input power has implications on the overall system efficiency and **Fig 8.4** below shows the modified plot of efficiency v/s load for the cases depicted in **Fig 8.3** above (lossless compensator). As before, the solid line represents the compensated case.

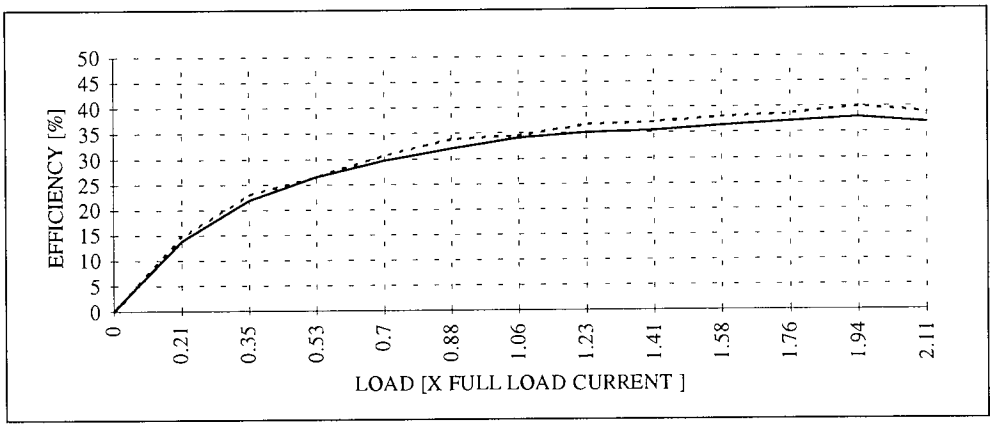

Fig 8.4 - Efficiency v/s load assuming lossless compensator

Clearly, in the limit as the compensator and coupling losses tend to zero, the efficiency of the compensated machine approaches that of the uncompensated machine. There is obviously need to minimise the compensator losses if the gain in power factor is to incurr minimal decline in overall system efficiency. This requires energy efficient coupling inductor design, preferably air-cored and of low winding resistivity (wire gauge), a suitable choice of power semiconductors and capacitor store, and a general system sizing that permits use of as small a firing angle as possible to achive the required compensation.

8.4.8 - Reactive Power and Power Factor

Fig 8.2c reveals that over a *limited* operating range, the reactive power stays virtually constant. This suggests that sizing of the compensator can be made quite accurately based on a *fixed* kVA requirement as was shown for power factor correction using capacitors in section 5.3.1.

However, over a wider range of slip values, the reactive power demand rises with load as shown in appendix A. The ability of the STATCON to generate and absorb a variable amount of reactive power over a continuous range implies it can cope with changing demand and emphasises the superiority of this scheme over fixed capacitor methods.

Also evident is the STATCON's ability to achieve precisely unity power factor over the entire operating range. **Fig 8.2h** shows that very little change in the delay angle is required to maintain unity power factor over the operating range shown.

8.4.9 - Developed Torque and slip

The primary purpose of the induction motor is to develop the torque required to accomplish a given task, and it is obviously advantageous if the machine can develop the required torque at maximum efficiency, but this is not always possible.

Fig 8.2d shows that the compensator has little or no impact on the slip at a given load. It can therefore be stated that over the range of concern, the STATCON has little effect on the developed torque. This is to be expected since the STATCON in general affects only the reactive component of current while the torque is related to the active component. This is consistent with the concepts discussed in chapter 1. **Fig 8.2e** shows the relevant torque v/s load curve.

However, there is a difference in the speed v/s load curves for the compensated and uncompensated cases suggesting that the machine develops a given torque at slightly different values of slip. The compensated machine develops a given torque at a higher slip. This is a consequence of the harmonic torques (braking) and is further discussed in section 8.5.6

8.4.10 - System efficiency and Compensator Losses

Fig 8.2f shows a decline in the system efficiency in the compensated case. Ideally, there should be no change in the machine efficiency, but this assumes a STATCON operating at 100% efficiency. Losses are present in the compensator itself and so the overall system efficiency will be seen to fall.

The motor efficiency itself, excluding the compensator, would probably be seen to be less than that of the uncompensated case because of the presence of braking torques which necessitate an additional active component of the a.c. input current. This however, has not been measured.

8.5 - WAVEFORMS

The waveforms of **Fig 8.5** were taken with the motor running light.

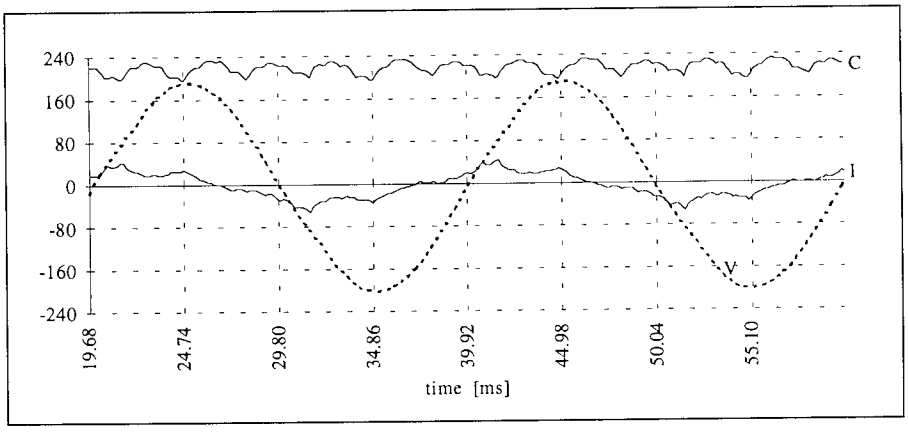

Fig 8.5a - Capacitor volts, supply volts and current - leading

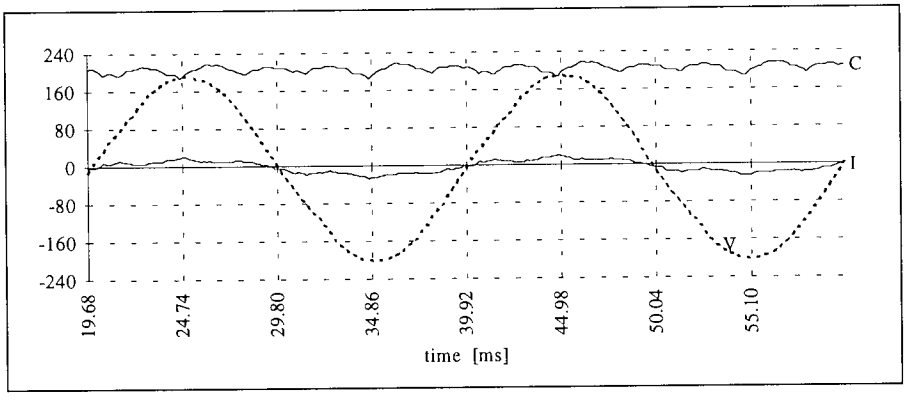

Fig 8.5b - Capacitor volts, supply volts and current - unity power factor

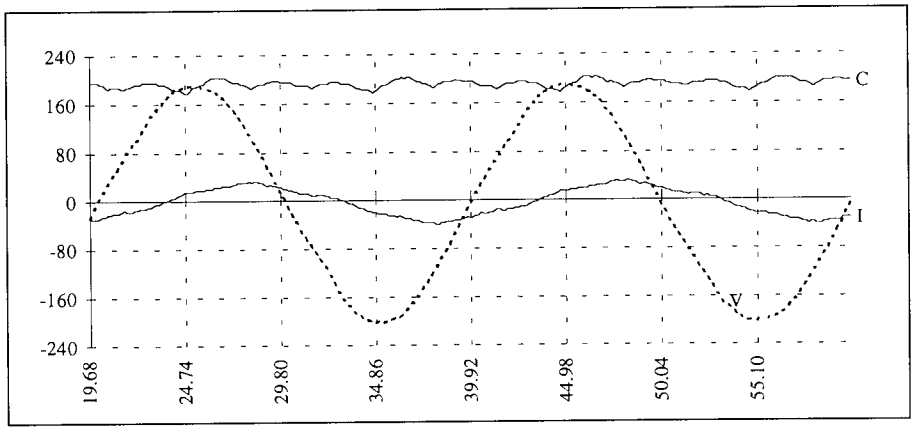

Fig 8.5c - Capacitor volts, supply volts and current - lagging

8.5.1 - Notes on Capacitor waveforms

The capacitor voltage waveforms are similar to those observed with the zigzag transformer coupling. There is also very close correlation between the simulated waveforms and those

observed in practice suggesting that the polyphase system of voltages as seen from the STATCON is essentially the same.

8.5.2 - Supply current characteristics

The lagging and unity power factor currents are practically sinusoidal. The effect of harmonics becomes evident as the current goes leading. The spectrum of **Fig 8.6** shows the harmonics present in the current at unity power factor.

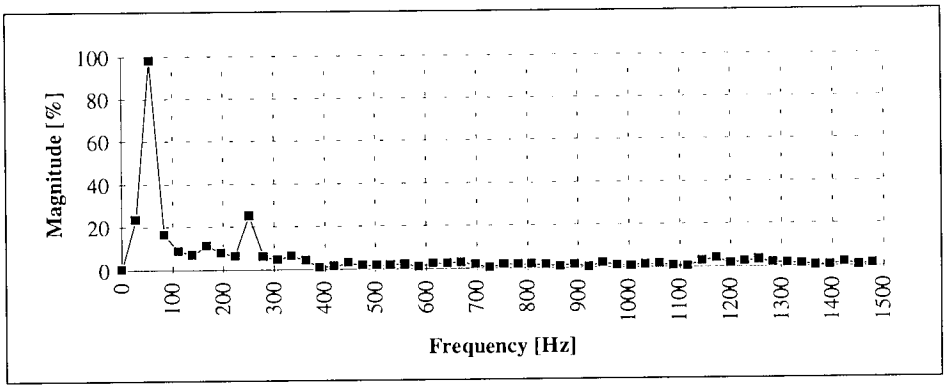

Fig 8.6 - Motor supply current harmonics for leading power factor operation

A prominent fifth harmonic of 25% the fundamental is observed in the current. As suggested in chapter 4, the most outstanding cause of low order harmonics is the imperfection in the phase shift of the multiple phase system of voltages as this reduces the effectiveness of the harmonic cancellation technique.

The polyphase system of voltages derived from the tapping points on the stator winding were measured and found to be non-ideal, with variances of between 5 and 12%. It was shown in chapter 5, (**Fig 5.16**) that the required system of multiple-phase voltages was one in which the relevant vectors lie along the circumference of a circle. The *magnitude* of the induced voltages (Eqn 5.33) needs to be identical for the angle between phases to be exactly 15°. The coil leakage inductances and resistances affect the magnitude of the induced voltages, hence the phase shift.
It is therefore difficult in practice to get all the coil inductances, mutual inductances, resistances and leakage inductances identical in a small machine of the size studied. Simulation suggests that the leakage inductance is the more important contributor to voltage differences.

The current waveform's sinusoidal quality was also observed for a load of 3 times the D90S rated full load current (overloaded). The results are shown in **Fig 8.7** below.

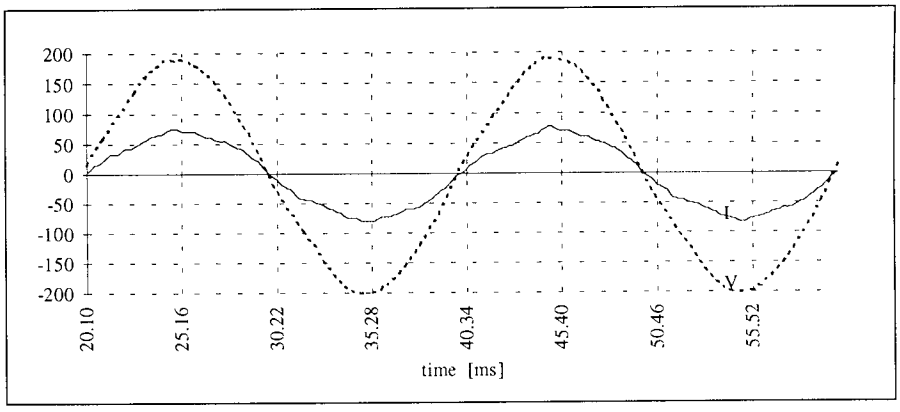

Fig 8.7a - Supply volts and current at 6 times full load - unity power factor

A spectral analysis of the current waveform reveals the presence of the fifth harmonic as before but of course at greatly reduced relative size. The third harmonic just evident in the no load unity power factor current is also noticeable.

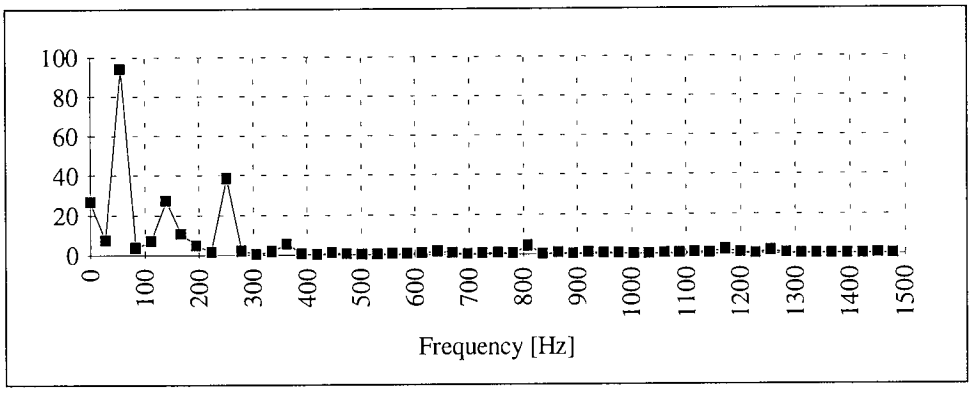

Fig 8.7b - Supply current harmonics at 6 times rated current..

The relative size of the fundamental was reduced in order to reveal the harmonics. The actual relative size of the 5th harmonic is 10%

The relative increase in the third harmonic compared to the fifth would suggest that a pulsating harmonic torque is also present, but of course, the relative size of the fundamental is such that the effect of the harmonics is negligible [Alger, 1969].

8.5.3 - The Inverter Output Waveforms

The form of the inverter output voltage per limb is the same as that observed with the zigzag transformers if the bridge reference point is used. If the supply neutral is used as the reference instead, then the effect of the third harmonic comes into play and the waveforms appear as shown in **Fig 8.8** for a lagging current. The neutral voltage responsible was shown in **Fig 6.17a**.

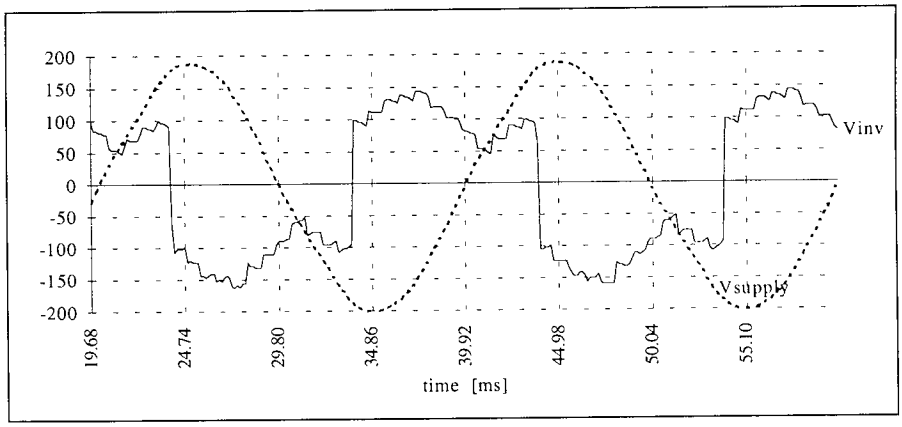

Fig 8.8 - Inverter phase to neutral waveform and supply volts - lagging power factor

8.5.4 - Coupling Coil Voltage

The waveform across a randomly selected coupling inductor was also observed. Apart from the relative size of the fundamental component, the general waveshape is the same for different delay angles. The voltage across the inductor, V_Z, is the difference between the square wave output of the inverter and the sinusoidal tapping point voltage. It is therefore the resultant of the harmonics of the inverter square wave when the fundamental component is greatly reduced.

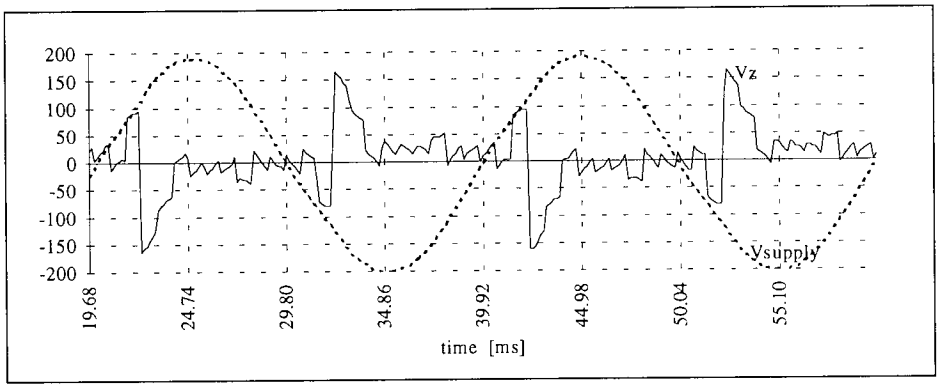

Fig 8.9a - Voltage across coupling reactor

The harmonic spectrum of the waveshape of **Fig 8.9a** is shown in **Fig 8.9b** below.

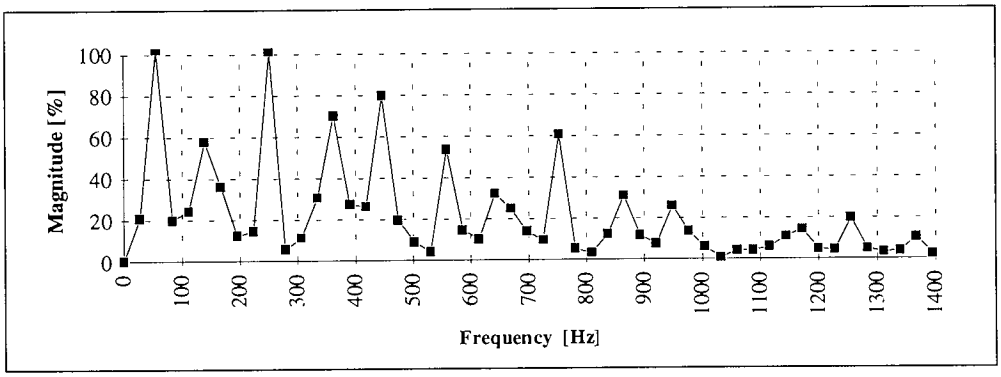

Fig 8.9b - Harmonic spectrum of voltage across coupling reactor

8.5.5 - The Tapping point voltage

The no-load voltage waveforms at the tapping points along the stator winding were examined for harmonics as distortion would suggest the presence of unwanted harmonics in the induced emf, hence the developed torque. **Fig 8.10a** shows one such waveform.

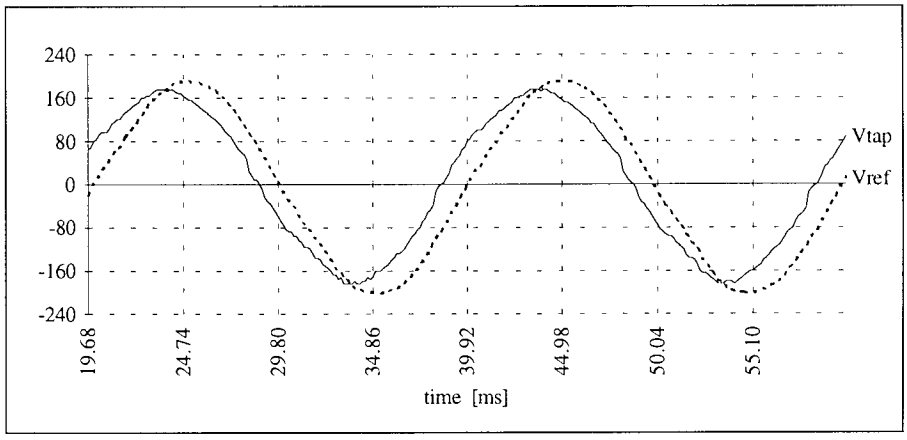

Fig 8.10a - Tapping point voltage shown for an arbitrary power factor.

In **Fig 8.10a**, Vref is the supply reference voltage and Vtap the tapping point voltage.

The harmonic spectrum for the voltage is shown in **Fig 8.10b** below, primarily to show the harmonics present.

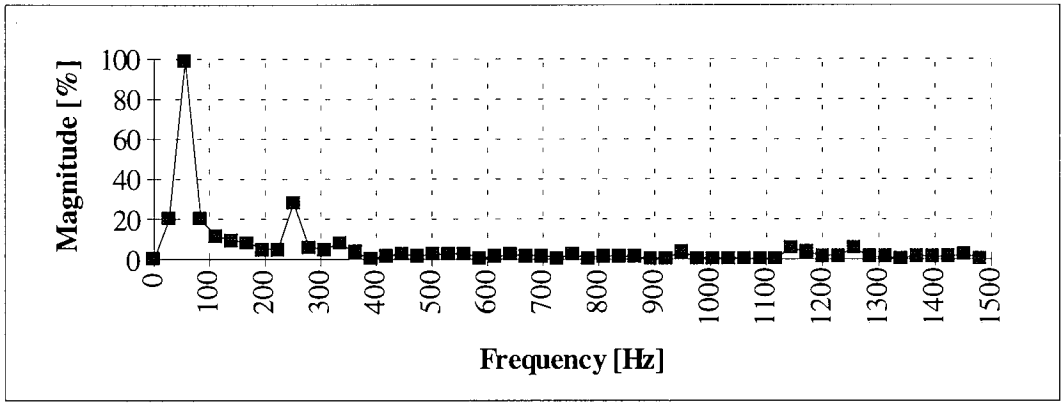

Fig 8.10b - Harmonic spectrum of tapping point voltage

While there appears to be good attenuation of a large number of the low order harmonics within the machine winding, the fifth is still present.

8.5.6 - Harmonic Torques

Kemp [1934] discusses the effects of different harmonics on the air-gap flux. It can be shown that the fifth harmonics occur 120° phase shifted on the fifth harmonic scale and therefore produce a rotating flux in the air-gap. However, the phase sequence is in opposition to that of the fundamental, implying the fifth harmonic produces a *braking* torque. The effect is therefore to slow down the rotor and this is evident in **Fig 8.2d** in which the uncompensated machine is seen to run at a slightly higher velocity for a given load, especially at light load. At higher load, the fundamental component of the stator current becomes much more prominent and tends to swamp the effects of the harmonics. The retardation in rotor speed due to the braking torques therefore becomes less significant.

On its own scale, the fifth harmonic gives rise to a uniform torque. However, viewed in relation to the fundamental component, the torque is seen to vary at 4th and 6th harmonic frequency, giving rise to a resultant torque which is non uniform, resulting in generally noisy machine operation.
The output power at a given load is similar, implying that the compensated machine is capable of developing a given torque, albeit at higher slip than the uncompensated machine.

By way of comparison, the seventh harmonic also produces a travelling flux but unlike the fifth harmonic, gives rise to a harmonic torque in the same direction as the fundamental.

8.5.7 - Aspects of Practical Operation and Noise Problems

Assume no load operation and that a *decreasing* firing angle is one which leads to a larger *lagging* effect.

The STATCON is set up to start switching at as near unity power factor as possible to prevent the flow of excessive currents at start up.
The three phase supply voltage is raised to rated voltage over which transition the machine draws the large starting current (the worse for the delta connection) of about 3 p.u. Chapter 10 discusses the possibility of effecting compensation for starting conditions. Just before the rotor begins to rotate, the iron-cored coupling inductors can be heard to rattle as the harmonic laden current flows. The uncompensated machine itself was not particularly noisy in operation.

Once the rotor accelerates the current drops to about 10% the starting value, depending on the operating power factor. The firing angle can be adjusted to achieve precisely unity power factor. Use of a power factor meter at no load proved erratic in the vicinity of unity power factor on account of the distorted form of the current. A VAr meter was found to be more stable.

As the firing angle is decreased to cause the STATCON to absorb reactive power i.e. to cause the supply current to lag the voltage, operation is less noisy as the fundamental component of the current becomes more prominent. As the delay angle decreases further, the noise level rises again on account of the large current flow through the coupling coils. The waveform however is of good sinusoidal integrity. If the delay angle is now increased so that the current tends towards unity power factor operation, the process reverses.

The current reduces in magnitude and reaches a finite non-zero value consistent with the machine and compensator losses. Further increase in the firing angle sees the current waveform, viewed on an oscilloscope, sidle at nearly constant magnitude from lagging to leading quadrature.

As the firing angle is increased further, the current grows in magnitude and leads the voltage. As for the lagging current, the coupling reactors become noisy at high values of the leading current, more so than for the lagging current.

Just audible over and above the noise of the coupling reactors is the motor itself, whose noise level certainly increases when the compensator is attached. This has been attributed to harmonic torques but has not been investigated fully.

8.5.8 - Supply Current Fluctuations

At large values of either leading or lagging current, especially with the machine lightly loaded, the current is seen to fluctuate rather noticeably on the connected ammeter. The VAr meter is also seen to follow these fluctuations. The wattmeter however, hardly fluctuates. Hill [1995] observes this phenomenon and suggests that fluctuations in the supply voltage and/or frequency may be responsible.

This is plausible explanation since a slight fluctuation on the supply voltage would cause a small change in the STATCON capacitor voltage, hence the inverter output, which in turn affects the amount of reactive current that is absorbed or generated, even for fixed firing angle. Similarly, fluctuations in the frequency give rise to change in the effective delay angle, and as has been explained (chapter 2), the STATCON is particularly sensitive to changes in the firing angle. The effect of a change in delay angle is a change in the generated or absorbed reactive power.

Thus, the STATCON effectively *amplifies* fluctuations in supply voltage magnitude and/or frequency, manifest in the amount of reactive power generated or absorbed at constant control system delay angle.

8.6 - SUMMARY

This chapter discusses experimental results of the compensated induction motor.

It is observed that the STATCON is capable of achieving precisely unity power factor within its operating limits.

It is also observed that over a narrow range of slip values, there is little change in the reactive power demand of the motor.

There is a fifth harmonic present in the supply current and the induced emf which gives rise to a rotating flux at fifth harmonic frequency. This is a braking torque which tends to slow the rotor down, forcing the machine torque/speed characteristic to shift in the direction of increasing slip so that for a given speed, the uncompensated machine develops a higher torque than the compensated machine.

The presence of a fifth harmonic has been attributed to imperfection in the phase shift of the multiple-phase voltage system derived form the stator winding, this in turn attributed to differences in the magnitude of the induced emf.

There is much improved power factor over the entire operating range of the machine or compensator (whichever reaches its limit first). Over the same operating range, there appears to be a modest improvement in the machine efficiency although for a small machine, the compensator losses can greatly affect this parameter.

The practical aspects of operation have been discussed. A noise problem due to harmonic currents through the iron-cored coupling reactors and harmonic fluxes in the machine air gap is described. Also, fluctuations observed in the supply current and reactive power generated or absorbed have been discussed.

CHAPTER 9

PERFORMANCE OF THE STATCON CONTROLLED INDUCTION GENERATOR

This chapter presents the results of tests performed on the machine to assess the effectiveness of the STATCON as a practical means of reactive power compensation for an induction generator.

9.1 - INDUCTION GENERATOR OPERATION

In order to behave as an induction generator, and induction machine requires that the stator winding is connected to a three phase supply, and that the rotor is driven above synchronous speed by some external mechanism such as a wind turbine.

At the time of writing, wind energy remains a rapidly growing and active area of research [R. Lynette, 1988; Mingzhou et al, 1995; Chen et al, 1995]. Not all wind energy schemes employ induction generators but those that do almost invariably feature some form of capacitor system connected across the terminals of the machine to provide the required compensation. Induction generator theory and operating principles are well established and the subject of a number of papers.

The conventional equipment set up is as shown in the single line diagram of **Fig 9.1** in which a turbine is shown coupled to an induction generator by means of a gear box. A capacitor is also shown connected to the supply terminals of the generator as required.

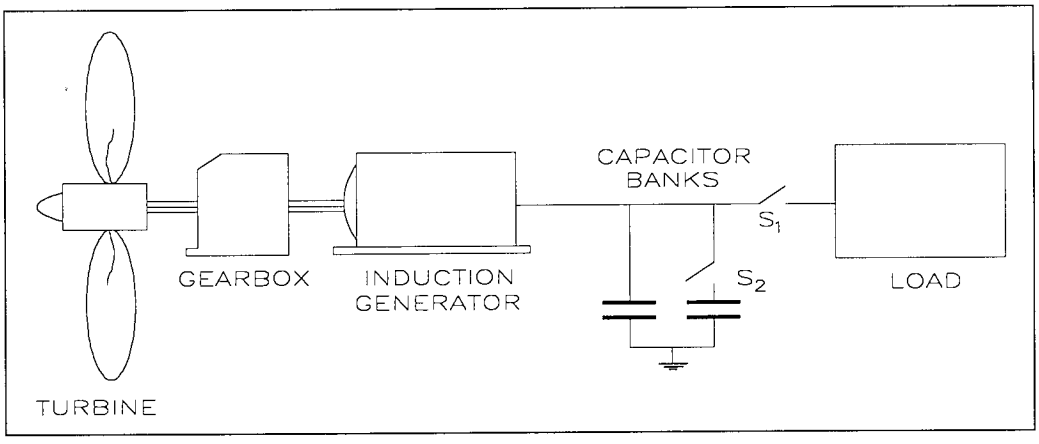

Fig 9.1 - Elementary induction generator set up

Nearly all the components depicted in **Fig 9.1** have been the subject of debate at one time or another.

9.1.1 - The Turbine

Turbine design has been a major consideration in the implementation of wind energy schemes involving induction generators. The sizes, number of blades and construction material are being further researched. The geographical activity of the intended site plays an important role in these considerations.

9.1.2 - The Gear Box

The type and size of gear box, and indeed whether one is required at all, has been the subject of debate but it would appear, at least at the time of writing, that there are notable advantages in schemes that dispense with the gear box altogether. Chen [1995] argues that the absence of a gear box implies smaller dimensions of the overall set up, lower cost, lower noise emission and lower system losses.

9.1.3 - The Generator

Induction machine performance can be changed quite significantly by altering any one of its basic design parameters. The machine is often designed to exhibit optimal performance in some aspect relevant to the application. Lipman [1988] discusses various types of generators and lists criteria employed in selecting the type (wind, diesel or both) for a given application.

9.1.4 - The Supply Link

The generator output can be connected directly to the supply if the output is at the same frequency. This often requires that fixed speed operation is employed. Alternatively, the generator output can be of any frequency (direct coupling variable speed operation), the output rectified to d.c. and then inverted back to a.c. at the supply frequency as required.

9.1.5 - The Capacitor

The capacitance shown provides the required power factor correction. Iinduction generators in general operate at very poor lagging power factors and the capacitor has been a popular choice of compensator. Different topologies for induction generator sets which include the use of saturable reactors and switched capacitors have been described by others [Lidgey et al, 1995].

A common feature of the schemes that seek to optimise the performance of the induction generator appears to be the requirement of some form of variable capacitance so that the excitation can be optimised for all machine operating points [Bolton et al, 1988]. This has been depicted by the switch S_2 in **Fig 9.1**.

The STATCON can behave as a variable capacitor, and applied successfully should be a worthwhile option to the static or switched capacitor in induction generator schemes.

9.2 - EXPERIMENTAL PROCEDURE

9.2.1 - Equipment setup

The experimental motor was connected as shown in the previous chapter for the load tests on the machine. The d.c. machine was connected to a variable speed drive as shown in **Fig 9.2** below. Appendix C shows photographs of the experimental apparatus (**Fig C-9**).

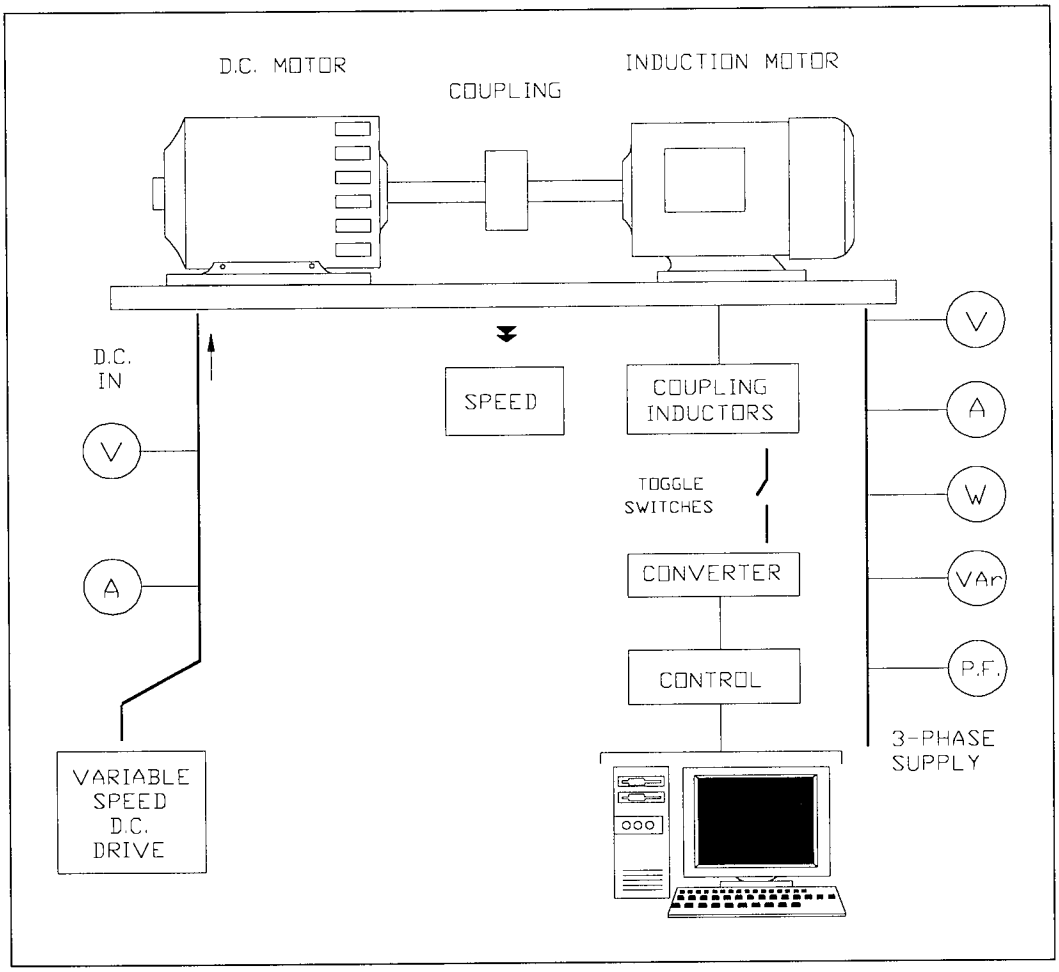

Fig 9.2 - Experimental set up for induction generator tests

As the induction motor was connected for two poles, its synchronous speed at 50Hz was 3000 rpm. The requirement that the machine be driven above synchronous speed to achieve generator action was a task involving a lot of care on account of the very high speeds involved.

The variable speed drive employed could only manage synchronous speed, so field weakening techniques were employed i.e. series resistance added in the field winding circuit to achieve higher speeds.

A centre 0 wattmeter was used to measure and monitor the direction of active power flow.

A centre 0 VAr meter was used to observe the reactive power flow on the a.c. side of the arrangement.

As before, a stroboscope was used to measure the speed of rotation of the coupled rotors.

9.2.2 - Test procedure

The d.c. machine was started first with the coupled induction motor not connected to the supply. The variable speed drive was set to maximum before the field weakening resistors were brought into play. The resistance was set so that the coupled system was running at about 5% above synchronous speed i.e 3150 rpm.

With the compensator disconnected, the induction machine was then connected to the three phase supply and the voltage raised to rated value. The speed, active power, reactive power and a.c. line current were noted. The a.c. supply volts were then reduced to zero and the STATCON switched into the circuit by closing the toggle switches of **Fig 9.2**. The voltage was again raised to rated value and the parameters of concern recorded. The d.c. motor was then adjusted so that the induction machine was generating as much power as it's rated value when operating as an induction motor.

The firing angle was then adjusted to control the amount of reactive power drawn by the generator from the three phase supply.

9.2.3 - General Observations

With the compensator unconnected, the induction machine was observed to generate power as required i.e. the centre 0 watt meter indicated a negative value suggesting that the direction of power flow had reversed. The machine was observed to draw about 1.0 p.u. reactive power from the supply.

With the compensator connected, the induction machine was observed to generate power as before. However, the reactive power could be varied by adjusting the firing angle, and indeed so over a wide range of leading and lagging power factors.

9.2.4 - Experimental results

9.2.4.1 - Measured values

The results are summarised in the bar graph of **Fig 9.3**. The power factor of the uncompensated generator was off-scale on the meter used and had to be determined from the sampled data as 0.36 with the generator absorbing reactive power from the supply.

The compensation was switched into the circuit without altering the settings of the variable speed d.c. drive. The induction machine was then observed to run at a slightly lower speed, suggesting the possible presence of braking torques as discussed in the previous chapter.
The delay angle was adjusted for zero VArs and measurements then taken.

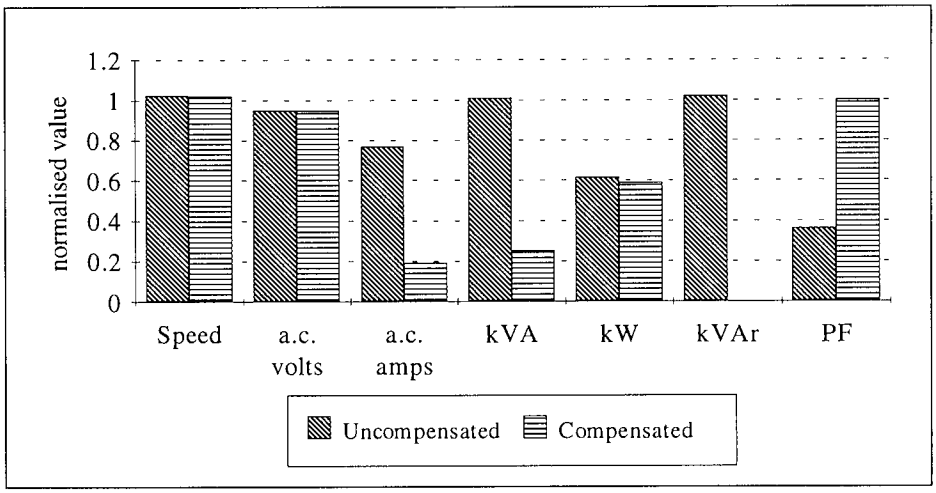

Fig 9.3 - Comparisons of the uncompensated and compensated induction generator.

9.2.4.2 - Waveforms

All waveforms were observed to be similar to those obtained with the induction machine running as a motor. They are included here to complete the discussion.

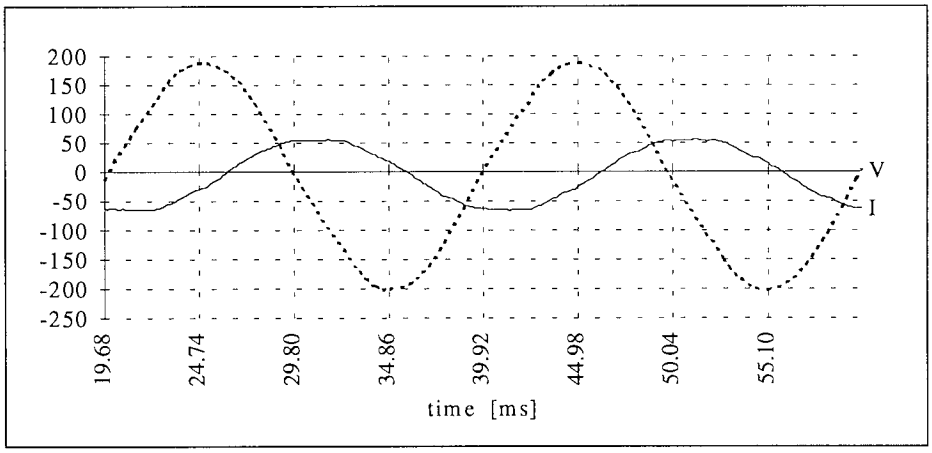

Fig 9.4a - Uncompensated generator supply voltage and current

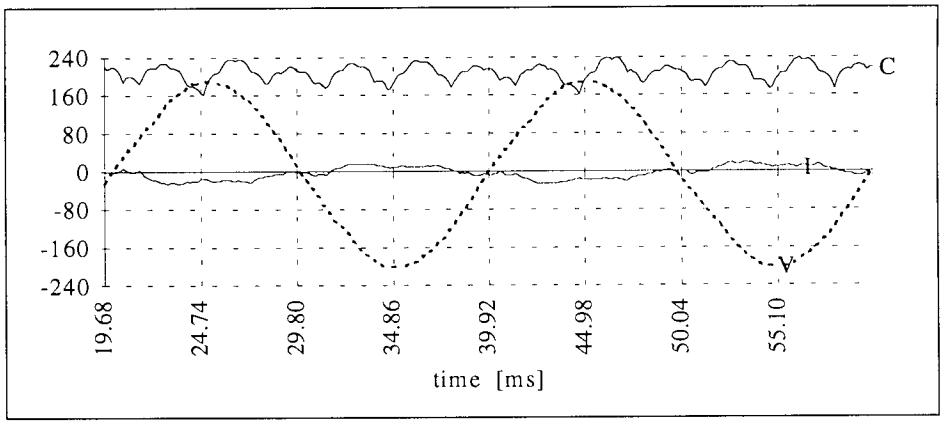

Fig 9.4b - Compensated generator supply volts and current. Capacitor volts also shown.

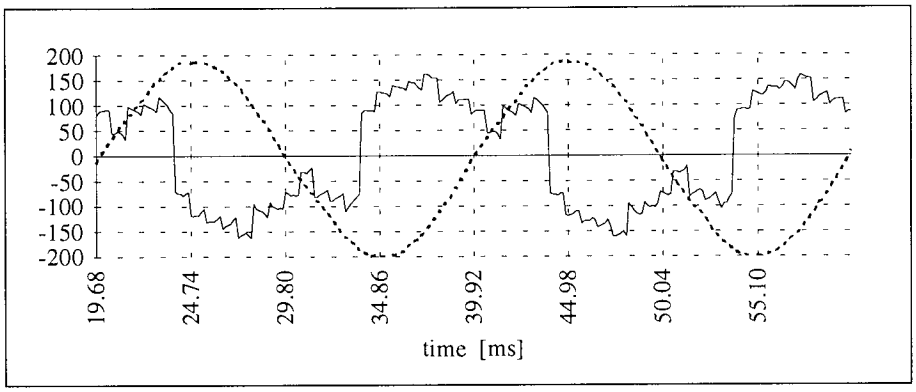

Fig 9.4c - Inverter output to neutral voltage for compensated generator.

The compensated generator current was analysed for harmonics and the results are shown in **Fig 9.4d** below.

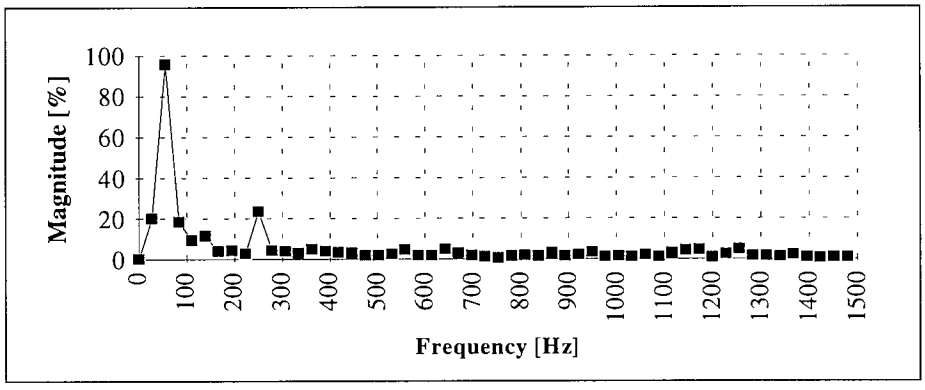

Fig 9.4d - Generator supply current harmonic spectrum

The harmonic spectrum for the uncompensated machine is relatively pure but features a seventh harmonic of about 0.2% the fundamental. The d.c. component is a consequence of imperfections in the data acquisition hardware and software and may be ignored.

9.3 - SUMMARY

The experimental results of this chapter show that the STATCON, connected as proposed, can function as a source of reactive power for an induction generator also rewound and connected as proposed.

Harmonics present in the system when the machine functions as a motor are also present when the machine functions as a generator. For the experimental machine, a fifth harmonic is observed and as discussed in the previous chapter, gives rise to a braking torque and possible losses in the machine.

CHAPTER 10

CONCLUSIONS AND PROPOSALS FOR FURTHER WORK

This thesis shows that a suitably connected stator winding can, in general, provide the required magnetic interface for a multiple phase reactive power compensator so that controlled power factor of the machine can result. Experimental tests show that the scheme works for both motoring and generating modes of operation.

The ability of the compensator to absorb or generate reactive power makes it a very good choice for use with induction generators.

10.1 - ADVANTAGES OF SCHEME

1) The absence of a complex transformer coupling to provide the required phase shift since this is accomplished by the winding itself.

2) Control of power factor over a continuos range between leading and lagging, hence the ability to operate at *precisely* unity power factor at any load within the limits of the machine and the compensator.

3) It has the potential to bring about some reduction in the starting current although the amount may not be significant on account of the relative magnitudes of the active and reactive components of this current. The STATCON rating would also be prohibitive.

4) It is independent of the machine rotor type and is therefore applicable to any induction machine with the appropriate stator winding.

5) The STATCON's ability to both generate and absorb reactive power implies it can be suitably controlled to avoid the self excitation problems observed with fixed capacitor schemes when the compensator and machine are isolated from the supply as a unit.

6) The use of external coupling inductors introduces some flexibility, in that the basic topology of the coupling can be altered and modified independently of the machine itself.

10.2 - DISADVANTAGES OF SCHEME

1) There is an observed reduction in overall system efficiency as a result of compensator losses and additional machine losses due to the generated harmonics.

2) There is need to wind the stator for 120° pole phase groups as opposed to the conventional 60°, resulting in a poorer winding factor.

3) There is need to wind the stator for multiple parallel paths to cater for pole numbers greater than 2.

4) External reactors are required if realistic reduction in the size of the energy store is to be realised, making the scheme bulky, lossy, and potentially expensive.

5) The range of values of power factor over which the machine operates in practice must be limited since the stator winding has to carry the resulting current.

6) There is an observed reduction in the developed torque for a given slip as a consequence of some of the inverter generated harmonics.

7) There is an increase in the audible noise in the coupling reactors and the machine itself, also a consequence of the generated harmonics.

10.3 - RELATED DEDUCTIONS

1) The form of magnetic interface for a multiple-phase compensator is potentially diverse but ideally features a discrete secondary winding so that the leakage inductance present provides the required coupling reactance. In this respect, the ring auto-transformer described in chapter 4 is probably not suitable for inverter operation.

2) There is need to optimise the winding of the magnetic coupling so that it provides a poly-phase system of voltages that approaches the ideal as closely as possible. The ideal coupling would feature:

- Accurate phase shifts and
- Coupling reactances each of which meets the minimum design value for a chosen value of M. The reactances need not all be of the same value as long as all those connected to phases 120° apart are.

10.4 - PRACTICAL CONSIDERATIONS

1) Provision of tapping point connections adds to the wiring requirements of the machine.

2) Provision of a power supply and cooling for the control and switching devices may introduce complexity in machine installation.

3) There is need to design as reliable a compensator as possible if it is to compete favourably with other established schemes and not bring into question the induction machine's noted attribute of reliability.

10.5 - DISCUSSION

The STATCON in principle, is the ideal reactive power compensator in that it is capable of absorbing or generating reactive power over a continuos range using a single control variable i.e. firing angle [Hill, 1995], has no moving parts, possesses a fast response time [Barry et al, 1995], is compact and inherently relocatable.

However, for the scheme proposed in this thesis, the requirement for external reactors implies a substantial increase in the overall size of the compensator and potentially, in the losses incurred and equipment cost, especially for high pulse numbers.

Still, the STATCON can adopt different forms depending on the complexity bias in the design. This is to say one can opt for a simple controller and complex coupling such as the zigzag connected transformers, or simpler coupling and a more complex controller such as required for most multi-level topologies.

For the intended application to power factor control in induction machinery, it would appear that as long as external reactors are required, the multi-layer topology is probably ideal since it requires no modification to the winding and uses only three coupling reactors. As stated, the control as a rule, is more complex.

To make the multiple phase STATCON truly competitive, further research into the possibility of reducing if not eliminating altogether the external inductors is priority. Simulation suggests that even a large machine with ample leakage reactance per coil may still require the external reactors if the coupling between the connecting lead and the leakage flux does not produce the required reactance.

10.6 - PROPOSALS FOR FURTHER WORK

10.6.1 - External reactors

Means of eliminating the requirement for external reactors are worth investigating. One technique would be to investigate the possibility of winding the connecting lead through any space that may be available in the stator slots to take advantage of some of the flux in the slot. This has the advantage that the number of turns need not be restricted to one but of course would have implications on the efficiency given that some stator volume potentially participating in the production of mutual flux is not being used. Optimum routing of the connector to take advantage of available flux is also a consideration.

10.6.2 - Harmonic reduction

It has been argued that non ideal characteristics of the multiple phase system of voltages derived from the machine stator winding has implications on the supply current harmonics, which in turn give rise to harmonic torques, whose effect depends on the harmonic. If it is desired to use the scheme as proposed, then ways of obtaining phase shifts closer to the ideal are required. A large number of slots per pole per phase may be of advantage in this regard.

10.6.3 - Noise Reduction

As the trend towards energy efficiency and environmental awareness grows, reducing the noise produced by motors in general has become an important area of research. The impact on audible noise due to compensator effects is therefore of significance. Clearly, this is nearly accomplished if the external coupling can be eliminated, and an added bonus of such an achievement would be the possibility of using higher pulse number STATCONs to produce even better harmonic elimination at low extra cost.

10.6.4 - Transient performance

This thesis has addressed what is essentially the steady state performance of the STATCON controlled induction machine. Simulation suggests that severe transients in the switching device voltages and machine currents can occur at start-up and shut down if the switching commences on line i.e. with rated three phase applied already and the capacitor charged. Investigation into the nature of these transients and appropriate start up and shut down procedures are required. The experimental apparatus took advantage of the reduced voltage starting techniques available (variacs).

10.6.5 - Closed loop control

The control software as implemented features routines for closed loop control. However, at the time of writing, the hardware to provide the necessary feedback signal has not been fully implemented for reasons of priority. As stated in the body of the text, fluctuations are observed in the current and reactive power, especially at high power levels. Hill [1995] observes similar behaviour and suggests that closed loop control may be able to eliminate this. Implementation of the closed loop control would also help to assess system dynamics when compared to other established schemes of reactive power compensation.

10.7 OPINION

There is considerable potential for use of the Converter Compensator as a practical means of power factor control for induction motors and induction generators, with implications on energy conversion and generation schemes. The method proposed in this thesis however will require refinement for adoption in a practical installation.

There are other methods of power factor correction such as the static capacitor. Choice between alternatives will involve weighing the advantages of the superior control and smaller capacitor sizes of the Converter Compensator against the disadvantages of the need for an alternative winding, possible requirement for external reactors and the effect of harmonics produced by the converter.

REFERENCES

R1 - STATCON TECHNOLOGY

Ashbrook, A. & Hill, J.E., December 1993. The Design & Performance Of A 1kVAr Voltage Sourced Inverter Type Advanced Static VAr Compensator Aston University Electric Power Group Internal Note FE/MEE/PGN/20/93, Birmingham, England.

Barry, N., Canny, D., September 1994. Performance Aspects Of A Three-Level Voltage Source Inverter For Induction Motor Drives. Proceedings Of The 30th Universities Power Engineering Conference. pp111-114, Greenwich, England.

Edwards, X., Mattern, X., Nannery, P. R. & Gubernick, X, October, 1988. Advanced Static Var Generator Employing GTO Thyristors. Journal Paper, IEEE Transactions on Power Delivery, Vol 3 NO. 4.

Gyugyi, L., Hingorani, N. G., Nannery, P. R. & Tai, N, 26th August - 1st September 1990. Advanced Static VAr Compensator Using Gate Turn-Off Thyristors For Utility Applications Cigré Paper 23-203, 1990 session, Paris.

Hill, J. E., February 1995. The Steady State Performance Of Converter Type Reactive Power Compensators. PhD Thesis, University of Aston in Birmingham, England,

Hill, J. E, Chileshe, C. M., Boardman, S. M. & Westrick, M. P., September 1994. Experimental Model Of A Harmonic Neutralised STATCON. Proceedings Of The 29th Universities Power Engineering Conference. pp338-341, Galway, Ireland,

Mori, S., Matsuno, K., Hasegawa, T., Ohnishi, S., Tekeda, M., Seto, M., Murakami, S. & Ishiguro, F, February 1993. Development Of A Large Static Var Generator Using Self Commutated Inverters For Improving Power System Stability. IEEE Transactions on Power Systems, Vol. 8, No. 1, pp371-377.

Norris, W. T., Hill, J. E., March 1995. 48-pulseConverter Compensator with Parallel Connected Transformers. Aston University Electric Power Group Internal Note FE/M&EE/EPGN/51/95, Birmingham, England.

R2 - POWER ELECTRONICS TECHNOLOGY

Lander, C. W., 1987. Power Electronics. 2nd Edition, McGraw-Hill Book Company Ltd., Maidenhead, England.

Moltgen, G., 1984. Converter Engineering - An Introduction To Operation And Theory Siemens Aktiengesellschaft, John Wiley And Sons.

Ramshaw, R. S., 1993. Power Electronics Semiconductor Devices. 2nd Edition, Chapman & Hall, London.

R3 - ELECTRIC MOTOR AND TRANSFORMER TECHNOLOGY

Alger, Philip R., 1970. Induction Machines. Second Edition, Gordon And Breac Science Publishers, New York.

Brosan, G. S., & Hayden, J. T., 1966. Advanced Electrical Power & Machines. Sir Isaac Pitman & Sons Ltd., London.

Chalmers B (Editor), 1984. The Motor Handbook. Butterworths.

Chalmers, B.J., Spooner, E., Abdel-Hamid, R.H., May 1980. Parameters of Solid-Rotor Induction Machines with Unbalanced Supply. IEE Proceedings, Vol 127, Part B, No. 3, [pp 174 - 182].

Chalmers, B.J., Spooner, E., Abdel-Hamid, R.H., Nov 1981. Single-phase Traction drive with Solid-Rotor Induction Motor and Synchronous Phase Converter. IEE Proceedings, Vol 128, Part B, No. 6, [pp 285 - 292].

Cotton, H., 1934. Design OF Electric Machinery. Oxford University Press, England.

Draper, A., 1972. Electrical Circuits - including Machines. Longman, England.

Fitzgerald, A. E.., Kingsley, C. J., & Umans, S. D., 1992. Electric Machinery. 5th Edition, McGraw Hill, London.

Ferrari, R. L., 1975. An Introduction To Electromagnetic Fields. Van-Nostrand Reinhold, USA.

Gray, C.B., 1989. Electrical Machines & Drive Systems. Longman Singapore Publishers, (Pte).

Hindmarsh, J., 1984. Electrical Machines And Their Applications. 5th Edition, Pergamon Press Ltd., Oxford, England.

Kemp, P., 1934. Theory Of Alternating Current Waveforms. Chapman & Hall, Ltd., London.

Laithwaite, E. R., 1966. Induction Machines For Special Purposes. Newness International Monographs on Electrical Engineering & Electronics.

Liwschitz-Garik, M., 1950. Winding Alternating Current Machines. D. Van Nostrand.

Liwschitz-Garik, M. & Whipple, C. C., 1954. A-C Machines. Vol II, 5th Edition, D. Van Nostrand.

Liwschitz-Garik, M. & Whipple, C. C., 1961. Alternating Current Machines. Second Edition, D. Van Nostrand.

Matsch, L., 1977. Electromagnetic & Electromechanical Machines. 2nd Edition, IEP - A Dun-Donnelly Publisher, New York.

Morgan, A. T., 1979. General Theory Of Electrical Machines. Heyden & Son Ltd.

Norris, W. T., December 1993. Ring Transformers With Multiphase Secondaries. Aston University Electric Power Group Internal Note FE/M&EE/EPGN/33/93, Birmingham, England.

Richardson, D. V., Caisse Jr., A. J., 1987. Rotating Electric Machinery & Transformer Technology. 3rd Edition, Prentice Hall, New Jersey.

Slemon G. R., Straughen A., 1980. Electric Machines. Addison Wesley Publishing Co.

R4 - REACTIVE POWER COMPENSATION TECHNOLOGY

Chileshe, C. M., September 1994. Power Factor Correction of Induction Motors Using Advanced Static Var Compensation. Proceedings Of The 30th Universities Power Engineering Conference. pp305-308, Greenwich, England.

Longlund, T., Hunt, T. W., & Brecknell, A., 1984. Power Capacitor Handbook. Butterworths, London.

Medarametla, X, Cox, X. & Baghzouz X. December 1992. Calculations & Measurements Of The Unity Plus 3-Phase Induction Motor. Journal Paper, IEE Transactions on Energy Conversion, Vol 7, No. 4, Dec 1992, pp 732-738

Miller, T. J. E.(Editor), 1982. Reactive Power Control In Electric Systems. John Wiley & Sons Inc, New York.

Moran, T. L., Ziogas, P. D., Geza Joos. July/August 1989. Analysis And Design Of A Novel 3-ϕ Solid-State Power Factor Compensator And Harmonic Supressor System.
IEE transactions On industry Applications, Vol. 25, No. 4, July/August 1989, pp 609-619.

Umans, S. D., September, 1989. AC Induction Motor Efficiency. Journal Paper - Proceedings of the 19th Electrical, Electronics & Insulation Conference, 25-28 Sept., 1989, pp 99 - 107.

Walker, M., 1924. The Control Of The Speed & Power Factor Of Induction Motors. Ernest Benn Ltd.

Zipse, D. W., 20 April - 3 May, 1990. Unity Plus Motor Winding Method - Advantages & Disadvantages. Journal paper - IEEE Industrial & Commercial Power Systems Technical Conference, 30 April - 3 May, 1990. Detroit, pp 111-118

R5 - WIND POWER & INDUCTION GENERATORS

Bolton, H. R., ABU-ADMA, M. A., 1988. Dynamic response of Isolated Induction Generator, Induction Motor Scheme For Wind Powered Borehole Pumping Applications. Proceedings of the 1988 10th BWEA Wind Energy Conference, London, Jan 22-24th, 1988. *Wind Energy Conversion* - Milborrow, D. J. (Editor). Mechanical Engineering Publications Ltd.
[pp 325 - 333]

Chan, T. F., 1993. Steady State Analysis Of Self-Excited Induction Generators. Paper approved for IEEE/PES 1993 Summer Meeting, Vancouver, BC, July 18-22, 1993.
Ref: 93 SM 355-8 EC

Chen, Z., Spooner, E., September 1994. A Variable Speed Permanent Magnet, Wind Turbine Generator And It's Control. Proceedings Of The 30th Universities Power Engineering Conference. pp517-520, Greenwich, England.

Lidgey, S.M.I, Moore, P.J., Passey, K.J., September 1994. Harmonic Reduction Of Saturable Reactor Controlled Induction Generators. Proceedings Of The 30th Universities Power Engineering Conference. pp482-485, Greenwich, England.

Lipman, N. H., 1988. A review Of Autonomous Wind/Diesel strategies. Proceedings of the 1988 10th BWEA Wind Energy Conference, London, Jan 22-24th, 1988. *Wind Energy Conversion* - Milborrow, D. J. (Editor). Mechanical Engineering Publications Ltd.
[pp 361 - 367]

Quarton, D. C., Fenton, V. C. (Editors), 1991. Wind Energy Conversion. Proceedings of the 1991 13th BWEA Wind Energy Conference. Mechanical Engineering Publications Ltd.

Horowitz, P, and Hill, W., 1995. The Art Of Electronics. Second Edition, Cambridge University Press.

Lynn, P. A., Fuerst, W., 1989. Introductory Digital Signal Processing With Computer Applications. John Wiley & Sons Ltd.

Vetterling, W. T., Teukolsky, S. A., Press, W. H., Flannery, B. P., 1992. Numerical Recipes In C. Second Edition, Cambridge University Press.

Yuen, C. K., Beauchamp, K. G., Robinson, G. P. S., 1982. Microprocessor Systems And Their Application To Signal Processing. Academic Press Inc., London.

APPENDIX A

ASPECTS OF THE CAGE ROTOR INDUCTION MACHINE

This appendix discusses the induction machine theory and has been subdivided into three main sections for ease of reference.

A-01 - CAGE ROTOR WINDING INDUCTANCES

Fig A-1 shows the magnetic flux density due to a single stator coil of N_c turns. It is a rectangular wave whose symmetry depends on the chording. The coils are generally arranged so that the resultant MMF distribution is as sinusoidal as possible. This minimises the flux harmonics. The flux distribution is as shown in **Fig A-1**, and the MMF may be described by

$$M = \frac{4}{\pi}(N_c / 2).i_a.\cos\theta \qquad (A1)$$

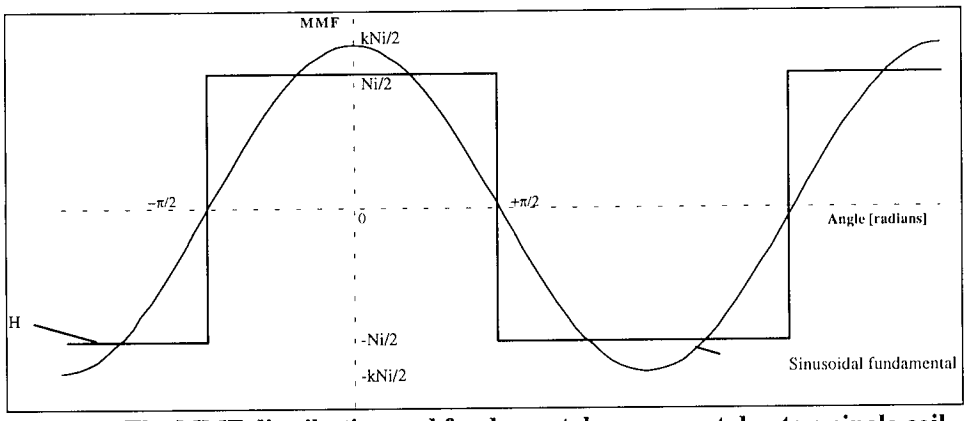

Fig A-1 - The MMF distribution and fundamental component due to a single coil.

The resultant MMF per phase for say, four slots per pole per phase is also a sinusoid as shown in **Fig A-2:**

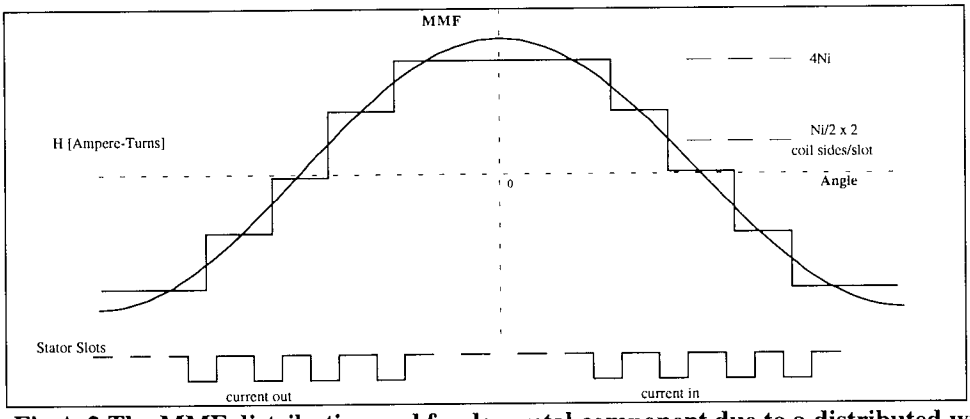

Fig A-2 The MMF distribution and fundamental component due to a distributed winding.

In general, the peak of the fundamental of the phase group is less than the scalar sum of the individual coil fundamentals. This is a consequence of the winding distribution, accounted for by the distribution factor k_D , which for a winding featuring q coils per pole per phase and slot angle τ is given by:

$$k_D = \frac{\sin(q.\tau/2)}{q.\sin(\tau/2)} \tag{5.39}$$

Chording also causes a reduction in the resultant emf induced in a coil as shown in **Fig 5.5**. It is a winding parameter called the pitch factor or chording factor, denoted by k_C and given by:

$$k_C = \sin\left(\frac{\lambda}{\lambda_p}.\frac{\pi}{2}\right) \tag{5.7}$$

Ignoring skewing, the winding factor k_w is the product of the distribution and chording factors and is given by:

$$k_w = k_D \times k_C \tag{5.40}$$

Thus, if N_{ph} is the total series turns per phase of the distributed winding, then the effective series turns, accounting for the reduced emf due to k_w becomes the quantity k_wN_{ph}. The resultant mmf M_{res} of the distributed winding therefore becomes:

$$M_{res} = \frac{4}{\pi}\left(\frac{k_wN_{ph}}{n_p}\right).i_a.\cos\theta \tag{A2}$$

Here, $4/\pi$ arises from the fourier analysis, n_p is the number of poles and i_a is the phase current

If i_a itself is sinusoidal, described by say, $i_a = I_O.\cos\omega t$, then the time maximum of the standing mmf wave described by M_{res} occurs when i_a is a maximum, i.e. $i_a = I_O$. If M_O is the maximum value of the MMF, then :

$$M_0 = \frac{4}{\pi}\left(\frac{k_wN_{ph}}{n_p}\right).I_0 \tag{A3}$$

and occurs in space at $\theta = 0$, at the instant when $i_a = I_O$.

Equations A1 and A2 are similar, and imply that a distributed winding with N_{ph} series turns and of winding factor k_w behaves as though it were a single coil of $k_w \times N_{ph}$ turns with a single magnetic axis and gives rise to a sinusoidal flux in the machine air gap.

In general, for an air gap of width g, the magnetic field intensity H is given by H = M/g

The maximum field intensity H_0 is therefore given by

$$H_0 = \frac{4}{\pi}.\frac{NI_0}{2g} \tag{A4}$$

and in general, $H = H_0 \cos\theta$ (A5)

The flux density B is related to the field intensity by $B = \mu_0.u_r$. H, where μ_0 is the permeability of free space and μ_r is the relative permeably of air (assumed equal to 1).

For an air gap of length l and radius r, the air gap flux, ϕ, is found buy integrating the product $B \times l \times r$ with respect to the angle θ. Thus

$$\phi = \frac{4}{\pi}\mu_0.\frac{Ni}{g}.l.r \tag{A6}$$

The N-turn coil carrying current i and linked by this flux will have a self inductance L given by:

$$L = \frac{N\phi}{i} = \frac{4}{\pi}\mu_0.\frac{N^2.l.r}{g} \tag{A7}$$

For a distributed winding, the self inductance L_{ph} due to the air gap flux is taken over a pole pair whence:

$$L_{ph} = \frac{4}{\pi}\mu_0.\left(\frac{k_w.N_{ph}}{n_p/2}\right)^2.\frac{l.r}{g} \tag{5.24}$$

and for *a* parallel paths in the winding becomes:

$$L_{ph} = \frac{4}{\pi}\mu_0.\left(\frac{k_w.N_{ph}}{a.n_p/2}\right)^2.\frac{l.r}{g} \tag{A8}$$

Thus:

$$L_{ph} = \frac{4}{\pi}\mu_0.\left(\frac{k_w.N_{ph}}{a.n_p/2}\right)^2.\frac{l.r}{g} = \frac{16\mu_0.l.r}{\pi.g}.\left(\frac{k_w.N_{ph}}{a.n_p}\right)^2 \tag{A9}$$

Let the subscripts '1' and '2' relate to two distributed windings linked by a common flux. The mutual inductance between the two is a function of the angular separation of their magnetic axes, θ, and is such that:

$$M_{12} = k\sqrt{L_1.L_2} = k.\frac{16\mu_0.l.r}{\pi.g}.\left(\frac{k_{w1}.N_{ph1}}{a_1.n_p}\right).\left(\frac{k_{w2}.N_{ph2}}{a_2.n_p}\right).\cos\theta \qquad (A10)$$

k is the coupling coefficient which will be assumed equal to 100% i.e. leakage ignored.
For balanced three phase operation, the windings, hence the terms in brackets, are identical.
Thus:

$$M_{12} = \frac{16\mu_0.l.r}{\pi.g}.\left(\frac{k_w.N_{ph}}{a.n_p}\right)^2.\cos\theta \qquad (A11)$$

This will be seen to be equivalent to the winding self inductance multiplied by the cosine of the angle between their magnetic axis. For a balanced three phase winding, cosθ = -1/2.
Fig A-3 illustrates this concept.

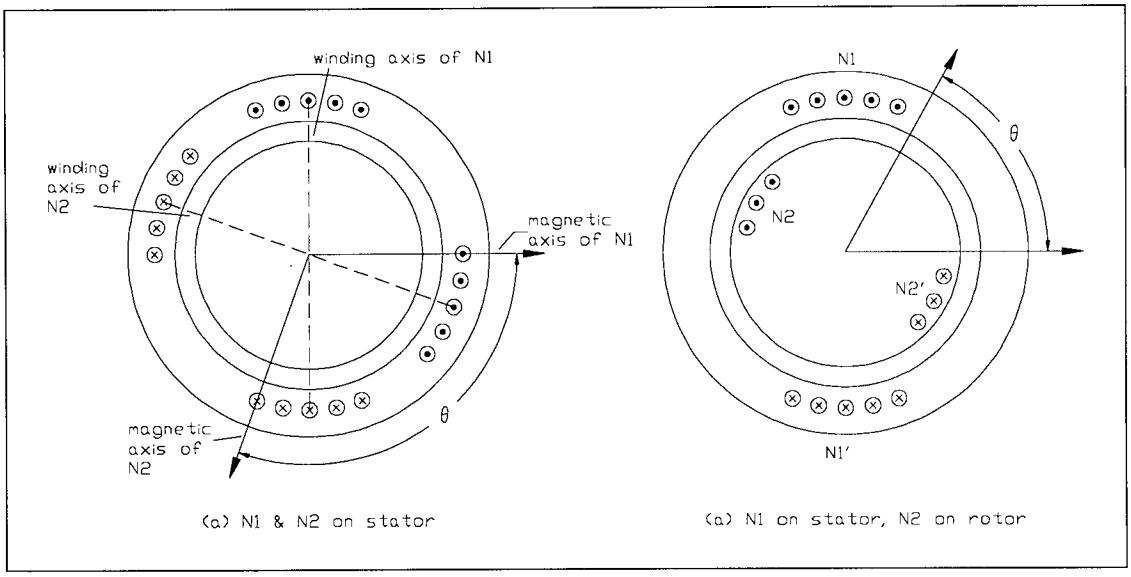

Fig A-3 - Distributed windings N1 and N2 with magnetic axes at angle θ.

Since the rotor winding is linked by the same flux, the expressions for the stator winding self and mutual inductances apply. However, the number of turns and phases on a squirrel cage winding are not straightforward and the subject of the next section.

A-02 - THE CAGE ROTOR AS POLYPHASE WINDING

Cotton [1934] gives a detailed account of the design procedure for a cage rotor while Liwschitz-Garik and Whipple [1961] give a comprehensive analysis of the cage rotor. Some of their important conclusions are as follows:

- the induction motor operates on the transformer principle and has a similar equivalent circuit
- Standstill of stator and rotor mmf waves with respect to each other is a necessary condition for the existence of a uniform torque in the machine
- The stator and rotor mmfs are at standstill with respect to each other, so the induction machine is able to produce uniform torque at any rotor speed.
- the induction motor when running, behaves as a transformer loaded with pure ohmic resistance

Consider therefore a 24-slot DLL stator winding connected for 3-phase 2-pole operation, and suppose the rotor to be a 15-slot squirrel cage of some finite skew factor. In general, for a cage rotor winding, $k_D = k_C = 1$. Thus, if k_S is the skew factor, it follows that $k_w = k_S$.

The stator and rotor members of such a machine are shown in **Fig A-4a**.

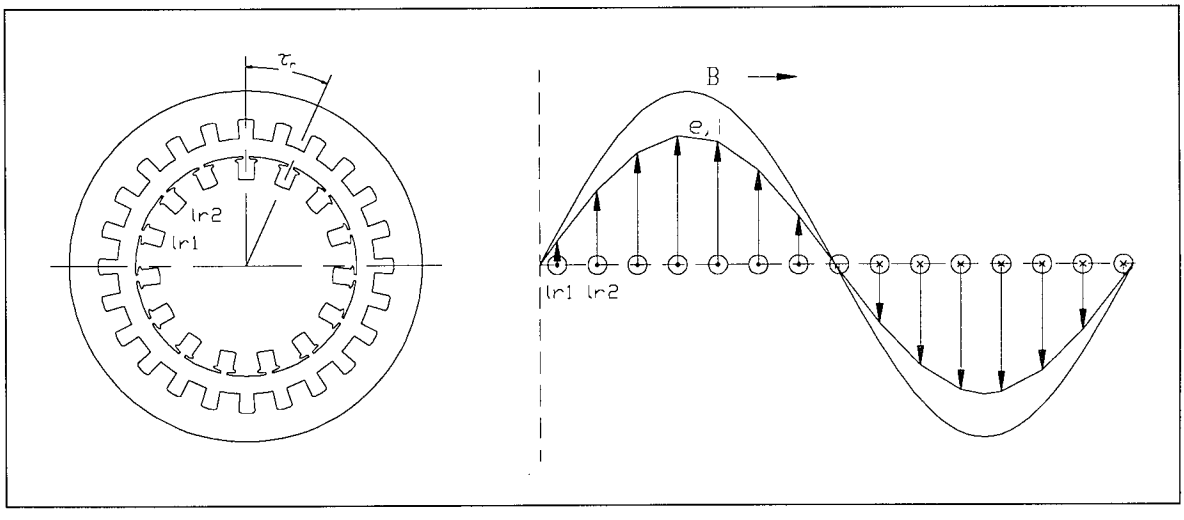

Fig A-4a Stator and rotor members **Fig A-4b - Development of poles by cage rotor**

Consider **Fig A-4b**. The rotating flux is sinusoidally distributed around the air gap as shown by the B curve. The flux moves at synchronous speed n_s while the rotor moves at some speed n in the same direction. With respect to the rotor, the flux therefore moves at a speed of n_s-n.
An emf e, will be induced in a conductor of length l travelling through a field of flux density B at velocity v. It is given by e = Blv from first principles (Faraday's law). Since B is sinusoidally distributed, it follows that the emfs induced in the individual bars will be of sinusoidal distribution as well. If it is assumed that $n \approx n_s$, i.e. $n_s - n \approx 0$, then the induced voltages and currents are in phase and **Fig A-4b** represent to another scale, the currents of the individual bars with the polarity shown. Since the number of poles of the flux wave is the same as that of the stator winding , the squirrel cage rotor produces the same number of poles as that of the stator. Thus, if the number of poles in **Fig A-4b** doubled, the B-curve would have two cycles over the same period shown, and the rotor emfs would react accordingly. Of course, for a large number of poles in the stator, the rotor needs to be designed with more slots.

Since B is a sinusoidal function of time, the emfs, hence currents, in the individual bars are also sinusoidal functions of time. As thus, they can be represented as phasors. **Fig A-5** is the required phasor diagram for the rotor bars of **Fig A-4**.

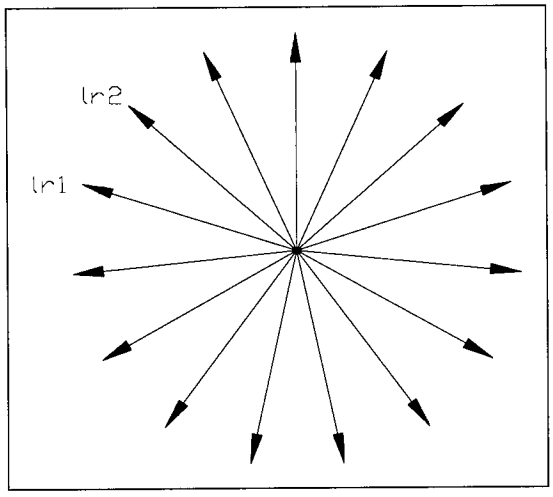

Fig A-5 - Phasor diagram of rotor bar emfs

The time angle between the phasors representing two adjacent bars is shown as τ and is equal to the mechanical angle between two bars, assumed symmetrically arranged, measured to the centre of the rotor as shown in **Fig A-4a**. Form **Fig A-5**, it is evident that the total number of phases is equal to the number of rotor bars [Liwschitz-Garik & Whipple, 1934; Matsch, 1977] Thus, the squirrel cage winding is a polyphase winding with as many phases as there are rotor bars, and as many poles as there are in the stator winding.

If Q_r is the number of rotor slots, then the number of phases is m_r simply given by

$$m_r = Q_r \tag{A12}$$

Now, a machine coil in general features two sides under opposite poles so that the emfs induced are equal and opposite and so additive around the coil. At any time, each rotor bar is under a single pole. Thus, the number of turns per phase, N_r, is such that

$$N_r = 1/2 \tag{A13}$$

The electrical circuit is still completed because of the end rings which connect together the ends of the bars.

The above expressions have been developed for a two pole motor and used in the body of the thesis. For a general number of poles p, the number of phases m_r becomes:

$$m_r = 2Q_r/n_p \tag{A14}$$

The expression for the mutual inductance is applicable to windings on the same member or to windings on different members as shown in **Fig A-3**. Thus, in Eqn A10, substituting the subscript r for the subscript 2 to represent the rotor winding, the mutual inductance between rotor bar and stator phase winding becomes:

$$M_{ph} = \frac{4}{\pi}\mu_0\left(\frac{2k_{W1}N_{ph1}}{n_p}\right).\left(\frac{2k_{Wr}N_{phr}}{n_p}\right).\frac{lr}{g}.\cos\theta \tag{A15}$$

Eqn A15 describe the mutual inductance between a phase winding on the stator and a phase (bar) on the rotor, assumed stationary, with their magnetic axes inclined at some angle θ. However, when the rotor rotates, the angle between its magnetic axis and that of any stator winding varies with time.

If the rotor rotates at some constant angular velocity ω_r, which, for a machine with n_p poles connected to a supply of frequency f is given by:

$$\omega_r = \frac{4\pi f}{n_p} \qquad [\text{ radians/s}] \tag{5.27}$$

then, every second, the angular separation between the rotor magnetic axis and any stator coil changes by ω_r radians. Thus:

$$M_{ar} = k_m \sqrt{\left(\frac{\mu_0 . l . s . N^2}{g . k_i} . \frac{ab}{a+b}\right)} \times \sqrt{\left(\frac{16\mu_0 . l . r . k_{wr}{}^2 N_r{}^2}{k_i . n_p{}^2 . \pi . g}\right)} . \cos(\theta + \omega_r t) \qquad \text{(A16)}$$

k_{wr} is the winding factor of the rotor, which, for a cage rotor winding is equal to the skew factor, and N_r the series turns per rotor phase is such that $N_r = 1/2$. Since the slot displacement s can be expressed in terms of the air gap radial length r from Eqn 5.23, it follows that M_{ar} simplifies to the more familiar form:

$$M_{ar} = k_m \frac{4\mu_0 . l . r . N . k_{wr} . N_r}{g . k_i . n_p} . \frac{\sqrt{2ab}}{a+b} . \cos(\theta + \omega_r t) \qquad \text{(A17)}$$

If it is assumed as before, that $k_m = 100\%$, then the expression further simplifies to:

$$M_{ar} = \left(\frac{2\mu_0 . l . r . k_{wr} . N}{g . k_i . n_p} . \frac{\sqrt{2ab}}{a+b}\right) . \cos(\theta + \omega_r t) \qquad \text{(5.28)}$$

The quotient in brackets will be seen to be a constant, so that the expression is of the general form :

$$f(t) = A.\cos(\theta + \omega_r t) \qquad \text{(A18)}$$

θ is the angular separation between the rotor bar magnetic axis and that of the stator coil of concern at some arbitrary time t = 0.

A - 03 - INDUCTION MOTOR PERFORMANCE PARAMETERS

Use of the equivalent circuit to predict induction machine performance is well established and the subject of numerous texts [reference section R3].

Computer software specifically designed for induction motor performance predictions taking into account the material properties of the rotor and stator was used to generate the results presented in this appendix. They refer to the standard D90S 3-phase induction motor.

Pre-modification parameter listing

Winding type	D.L.L.
Stator slots	24
Winding pitch	75% (i.e. slots 1-10)
Pole phase group	60°
Conductors per coil	35
Wire size	2×0.53mm
Mean length of turn	460mm
Winding resistivity	8.25×10^{-7} Ω/inch at 75°C
Stator core material	Newcore
Stator core length	76mm
Stator phases	3
Poles	2
Parallel paths	1
Rotor core length	76mm
Rotor bars	16
Rotor bar resistivity	1.46×10^{-6} Ω /inch at 75°C
Air gap radius	35mm
Air gap width	0.3mm
Air gap volume	$0.0167 m^3$
Phase connection	Delta
Supply voltage	240V line-to-line
Supply frequency	50Hz

Performance trends of unmodified winding

The following are the predicted results of the unmodified conventional 2-pole machine, to which reference has been made in chapter 8.

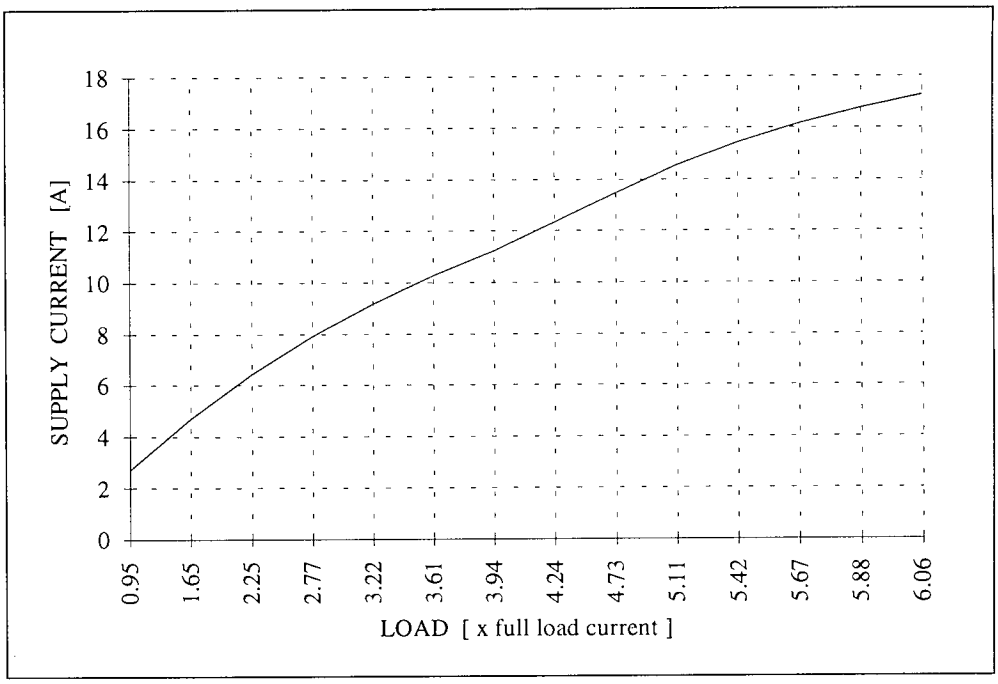

Fig A-6a - Supply phase current v/s load for conventional 60° winding

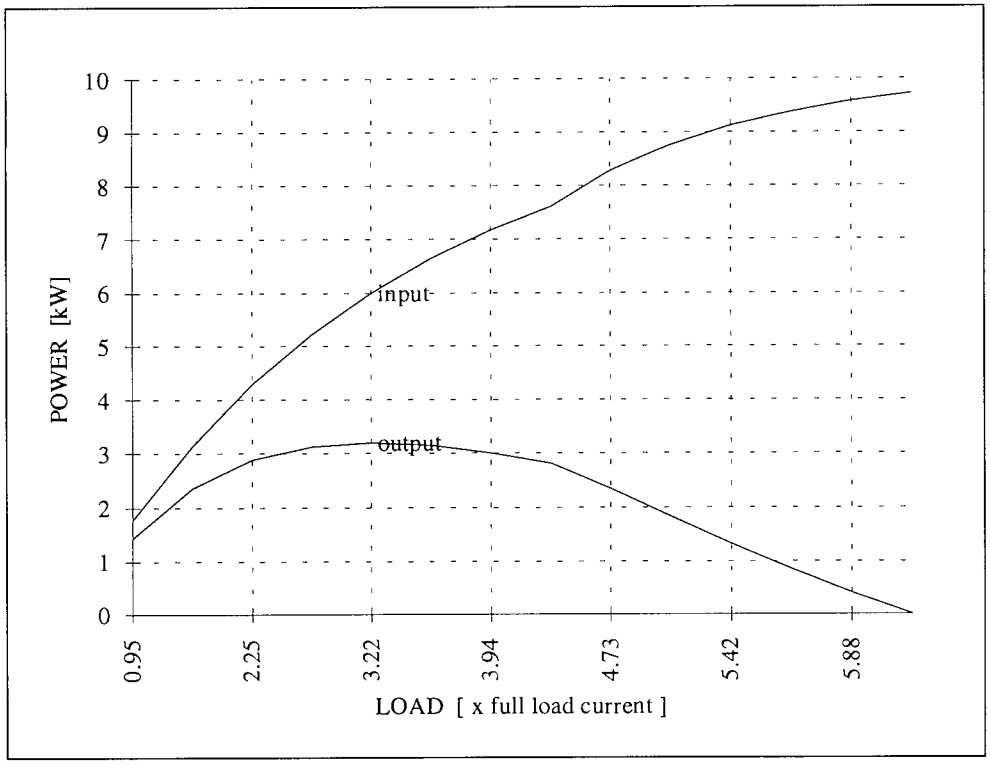

Fig A-6b - Active power input and output v/s load for conventional 60° winding

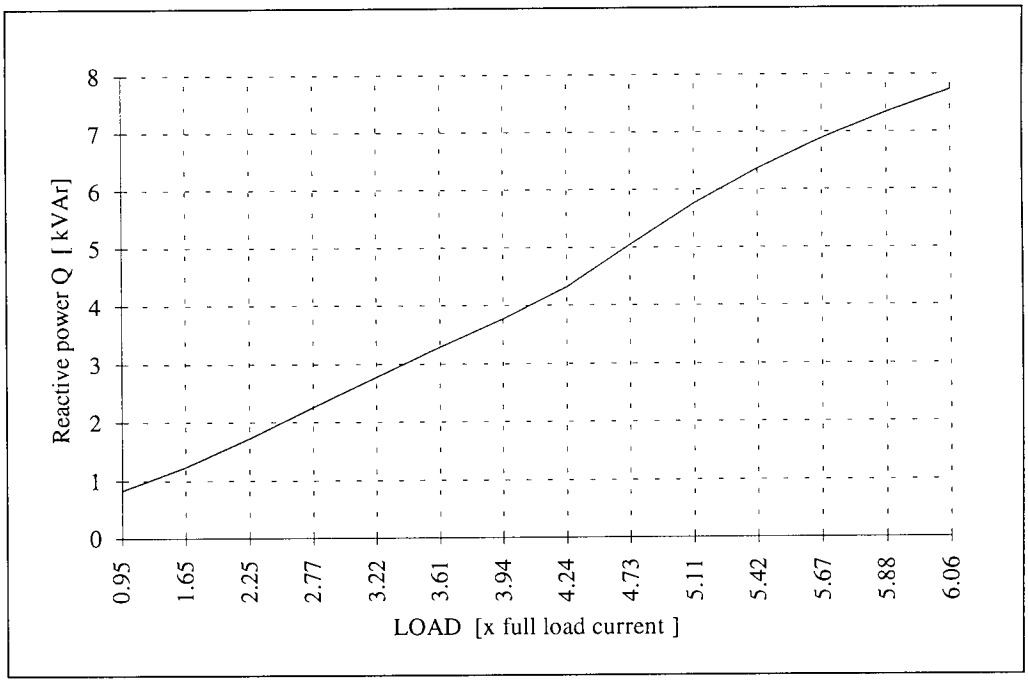

Fig A-6c - Reactive power v/s load for conventional 60° winding

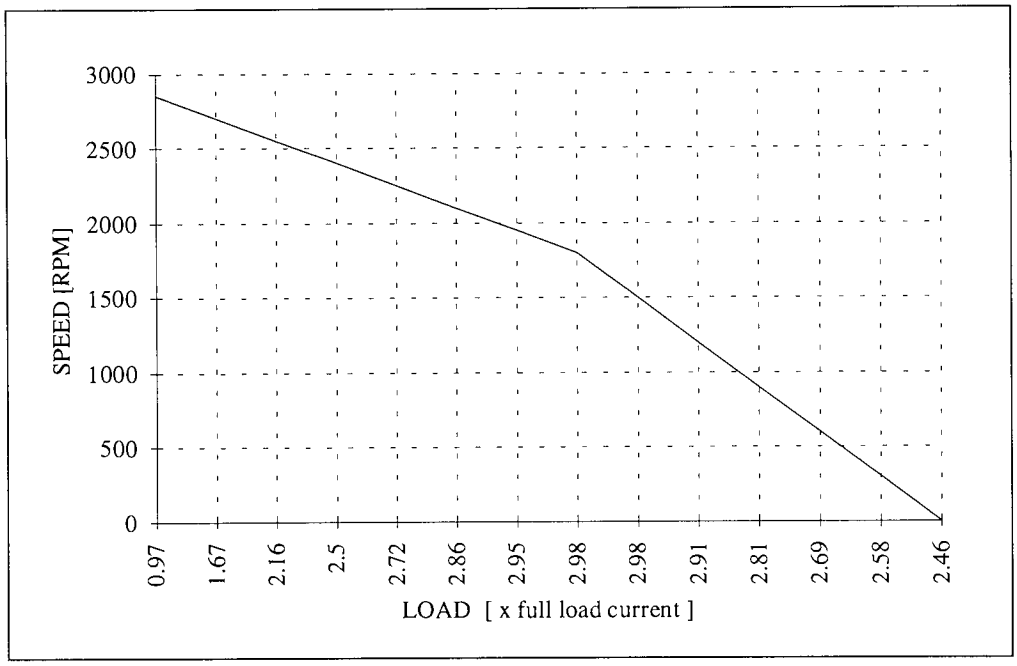

Fig A-6d - Rotor speed [RPM] v/s load for conventional 60° winding

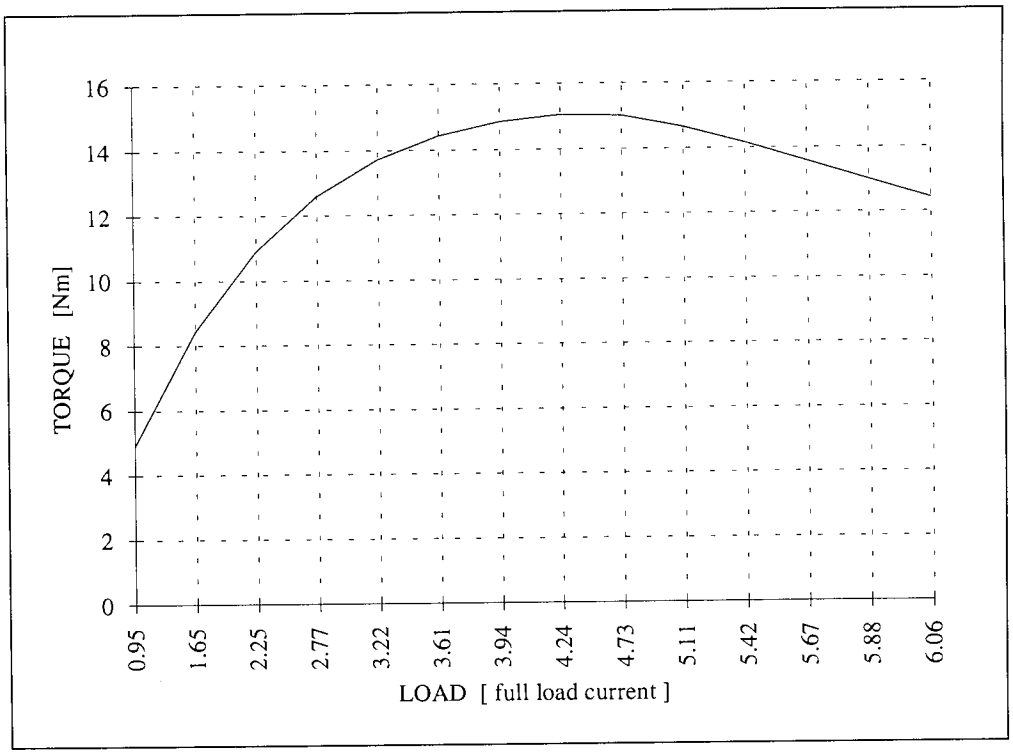

Fig A-6e - Developed torque v/s load for conventional 60° winding

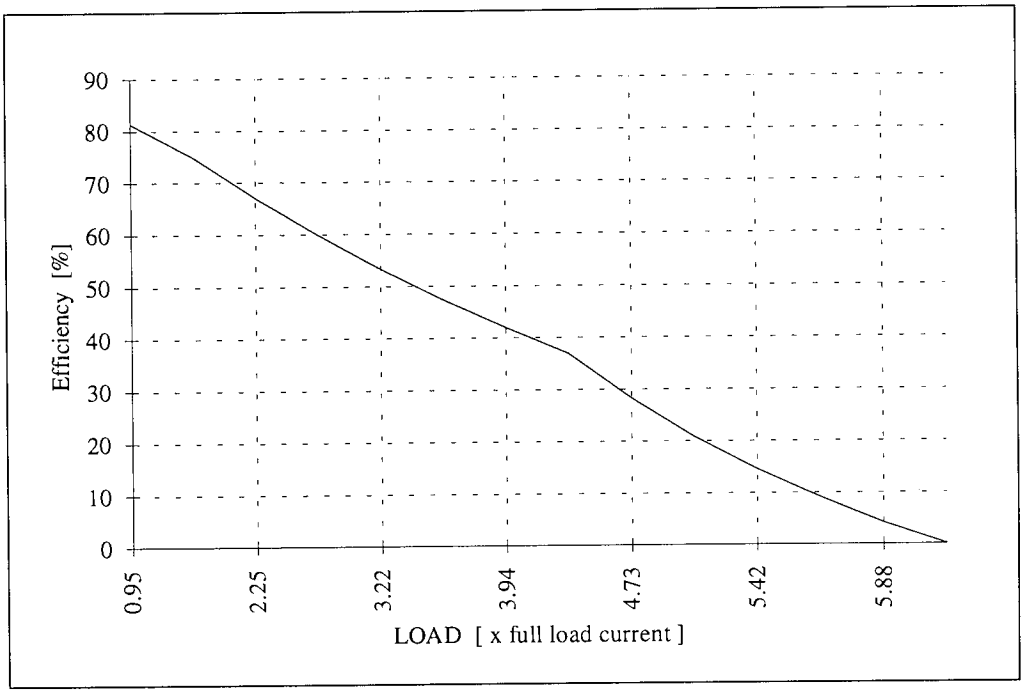

Fig A-6f - Machine efficiency v/s load for conventional 60° winding

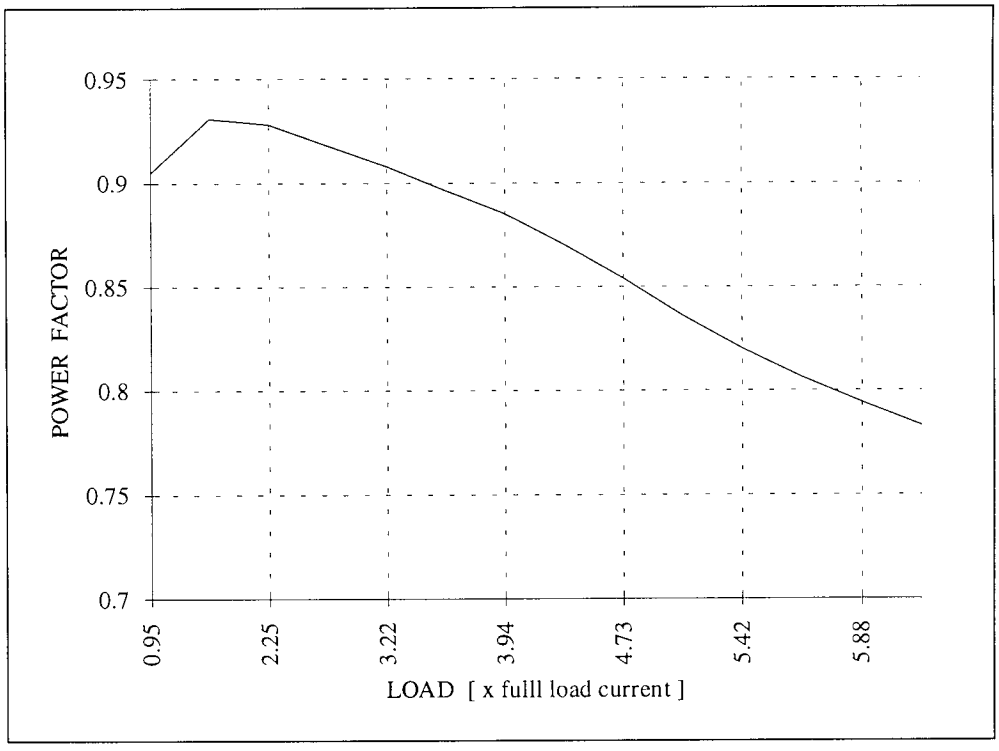

Fig A-6g - Terminal power factor v/s load for conventional 60° winding

Notes on the performance characteristics

An almost linear increase in the supply current as the load increases is observed. The machine full load current is 2.8A, occurring at a slip of about 0.08.

The machine full load torque is about 5.1Nm occurring at a slip of about 0.08 while its maximum torque is three times this value, but occurring at the higher slip of 0.4.

The machine power factor is observed to improve with speed and is a maximum value of about 0.93 at a slip of about 0.1. For maximum torque, the machine is expected to operate at a slip of 0.4, hence a power factor of 0.84. At this slip however, the supply current is expected to be six times the rated current and therefore imposes limitations on the thermal capacity of the machine.

At maximum torque, the machine efficiency is observed to be approximately 40%. This value increases to just under 80% at full load torque as is typical of induction motors.

Notes on comparisons with experimental results

Direct comparisons between the results of **Fig A-6** and the corresponding experimental values for the rewound machine described in chapter 8 require that caution is exercised in their interpretation for the following reasons:

- In the predicted results above, the applied voltage is the rated 240V phase to phase. The actual applied voltage in the experimental model could not be raised beyond about 230V. The applied voltage has direct bearing on the supply current and machine torque.

- The predicted results have been obtained for a wide range of slip values. Only a small range could be observed in practice within the full rating of both machine and compensator. Thus for instance, only a small change in reactive power was observed over the slip range of concern in the experimental model while it is evident from **Fig A-6c** shows that the reactive increases quite significantly with load.

- The predicted results were specified for standard test operating temperatures*. Accurate comparisons would require that the tests are performed under identical conditions ideally using the same measurement equipment.

Thus, sizing of the compensator requires that the operating range of the machine is known. Clearly, a machine intended for use over a wide slip range requires that the compensator is sized for the maximum reactive power observed at maximum load, if it is required that the machine operates at unity power factor over the entire range. This has implications on the size of the energy storage components in the STATCON.

* BS4999

APPENDIX B

ASPECTS OF THE COMPENSATED MACHINE

A design is specified for a 3-phase, double layer lap wound stator with 120° pole phase groups.

Let Q be the number of stator slots of the 3-phase machine with the following parameters:

N_c = turns per coil
q = coils per pole per phase
p = STATCON pulse number
n_p = number of poles
τ = slot angle

Slot angle considerations

• A p-pulse STATCON requires p/2 voltages phase shifted by π/p radians. This is the largest permissible value of the slot angle τ, since values smaller than π/p simply imply tapping points with more than a single coil between them so that the combined angle gives the required phase shift. A necessary condition of the winding is therefore that:

$$\tau \leq \pi/p \qquad \text{(B1)}$$

Coil distribution considerations

Let a be the number of parallel paths given by $a = n_p/2$. The number of series coils per parallel path per phase therefore becomes $Q/(a \times m)$. The winding is arranged in the slots as per convention, except that the number of coils per pole per phase changes from q_1 to q_2, where:

$$q_1 = Q/(m \times n_p) \qquad \text{and} \qquad q_2 = 2q_1 = 2Q/(3 \times p)$$

For each parallel path, the connections are such that all the q_2 coils belonging to a phase under a pole are in series and the last coil connects to the next supply phase. The q_2 coils thus connect between two supply phases and therefore span 120° as required, giving the slot angle as:

$$\tau = \frac{\pi/3}{q_2} = \frac{\pi}{3 \times q_2} = \frac{\pi}{3 \times 2 \times q_1} \qquad \text{(B2)}$$

Fig B-1 below shows one phase of a 72-slot 6-pole delta connected winding.

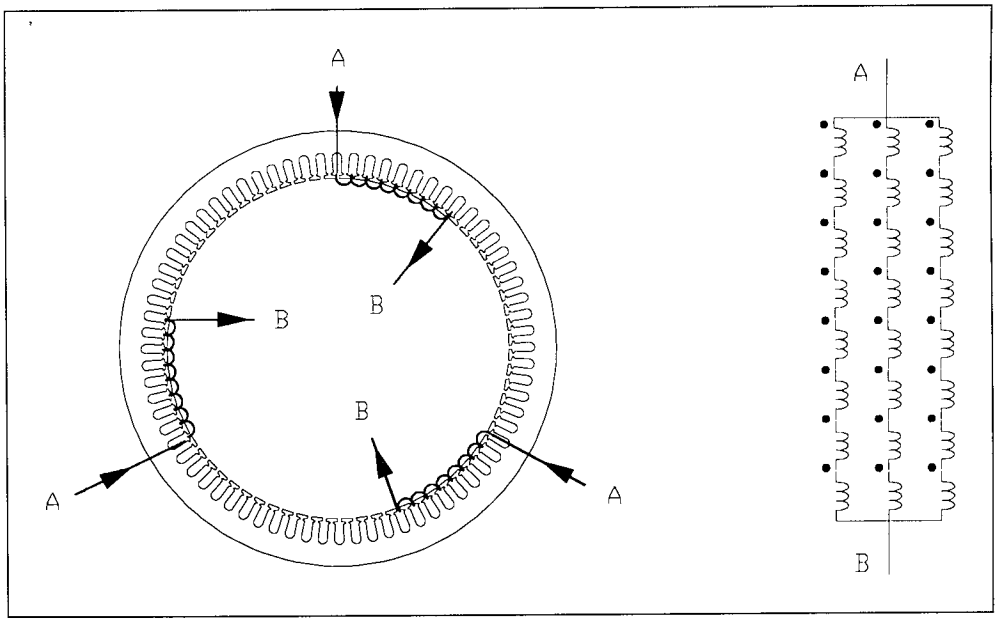

Fig B-1 - One phase of 72-slot 6-pole machine wound for 120° pole phase groups and 3 parallel paths.

For the example winding shown, the slot angle is 15°, implying the largest pulse number STATCON that can interface as proposed is 24.

The requirement for more than a single parallel path in order to facilitate interfacing to the compensator implies reduced resistance per phase.

The phase shifts obtained from a given winding are repeated under each pole. Thus, for *a* parallel paths, there are *a* voltages at the same angle of phase shift. Also, the total number of unique phase shifts derived per supply phase is necessarily equal to q_2.

Tapping Point considerations

Simulation suggests that the choice of tapping points is not restricted to those under the same pole. Thus, for 24-pulse operation, the 0° and 45° phases can be derived from the first pole phase group while the second and third provide the 30° and 15° phases respectively. The tapping point combination itself affects the harmonic performance (chapter 6).

Inductance calculations

As a result of the air-gap flux, mutual inductance exists between each and every stator coil and between stator and rotor winding, and between rotor windings. It has been shown that the self inductance of any stator coil is given by:

$$L_C = \frac{\mu_o . l . s . N^2}{g . k_i} . \frac{ab}{a+b} \qquad (5.17)$$

Since a+b = Q, and s = 2πr/Q:

$$L_c = \frac{\mu_0 . l . (2\pi r) . N^2}{g . k_i . Q} . \frac{ab}{Q} = \frac{2\pi . \mu_0 . n_p . l . r . N^2}{g . k_i . Q^2} . ab \qquad \text{(B3)}$$

Assuming only the *end* or *overhang* flux leakage can give rise to a coupling reactance in the connecting leads, the parameter of concern is the per phase end leakage inductance of the stator winding, given by:

$$L_e = \frac{4 \times 7 \times 10^{-6} \times m \times r}{\pi} . \left(\frac{k_w N_{ph}}{a n_p} \right)^2 \left(\frac{\lambda}{\lambda_p} - 0.3 \right) \qquad \text{(6.2)}$$

Since L is proportional to N^2, it follows, assuming each coil contributes equally to the various components of leakage, that the total *end* leakage flux per coil, L_{ec}, is such that:

$$L_{ec} = \frac{L_e}{(Q/m)^2} = \frac{4 \times 7 \times 10^{-6} \times m^3 \times r}{2\pi Q^2} \left(\frac{k_w N_{ph}}{a n_p} \right)^2 \left(\frac{\lambda}{\lambda_p} - 0.3 \right) \qquad \text{(B4)}$$

Assume the connecting lead links all the end leakage flux. L_{ec} is then the value to be used in computations of the STATCON parameters, and also gives an indication of the size of the machine required to meet a given M and k. From Eqn 6.5, the ratio of the end leakage inductance to the total inductance per phase is:

$$\frac{L_e}{L_{ph}} = \frac{0.7 m . g}{32\pi l} . \left(\frac{\lambda}{\lambda_p} - 0.3 \right) \qquad \text{(6.5)}$$

Machine sizing considerations

In design, if L_{ec} is set to some predetermined value that meets the choice of k in sizing the STATCON, the self inductance of the coil that will give this value of leakage can be deduced. The magnetisation reactance x_M per phase for a uniform air gap machine is given by:

$$x_M = \frac{16 \mu_o . l . r}{k_i . g} . \left(\frac{k_w N_{ph}}{a n_p} \right)^2 \qquad \text{(B5)}$$

Thus, the magnetisation current I_M is given by:

$$I_M = E / x_M \qquad \text{(B6)}$$

The induction machine (subscript IM) total magnetisation volt amperes Q_{IM} are the product of the applied volts (assumed equal to the induced volts) and the magnetisation current. Thus:

$$Q_{IM} = mE.I_M = m\frac{E^2}{x_M} = mE^2\frac{k_i.g}{16\mu_0.l.r}\left(\frac{an_p}{k_w N_{ph}}\right)^2 \qquad (6.8)$$

Compensator sizing considerations

The compensator will be required to provide at least Q_{IM} VArs to achieve unity power factor operation of the machine.

The generic form of the sizing parameter k described in chapter 2 is:

$$k = \sqrt{\lambda\frac{X_C}{X_L} - \beta^2} \qquad (2.12)$$

Simulation and experimentation suggest that larger values of the energy store are required with a stator winding interface. A second factor λ_G has therefore been incorporated in the expression for the parameter k to give:

$$k_{IM} = \sqrt{\frac{\lambda}{\lambda_G}.\frac{X_C}{X_L} - \beta^2} \qquad (6.11)$$

In the absence of exact analyses of the STATCON and stator winding system, conclusive statements on the form of the expressions for k and reactive power generated or absorbed by the compensator cannot be made. The behaviour of the system however, is summarised in the simulation results of **Figs B-2, B-3** and **B-4** in which the pulse number of the STATCON is changed dynamically to observe the effect on the capacitor voltage and supply current. Apart from the pulse number, all other parameters, including the delay angle are fixed.

The simulation was initially conducted for a set of values optimised for 24-pulse operation with the zigzag connected transformers. This implies that the value of M is potentially too small for lesser pulse numbers. Over the time scale shown in **Fig B-2**, the system switched as a 6-pulse unit, then as a 12-pulse unit and finally, as a 24-pulse unit.

Identical parameters were then used with the stator winding coupling, and it was observed, as shown in **Fig B-3** that the value of M was too small, even for 24-pulse operation.

Finally, values optimised for 24-pulse operation with the stator winding were used and it is evident from **Fig B-4** that the same values suffice for both 6 and 12-pulse operation though not

optimally, suggesting further that in use with the stator winding coupling, the change in energy storage components for different pulse numbers is less than that seen with the transformers.

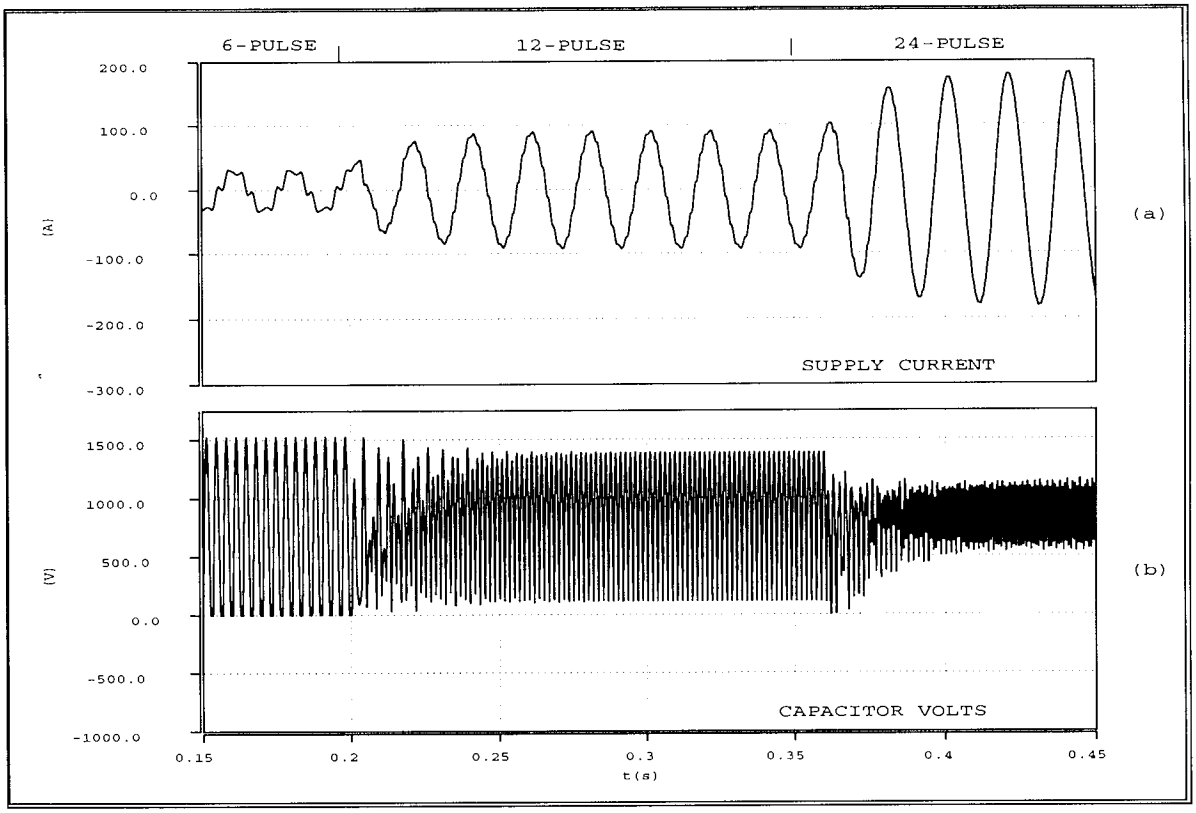

Fig B-2 - Effect of pulse number for fixed L and C - zigzag transformer coupling.

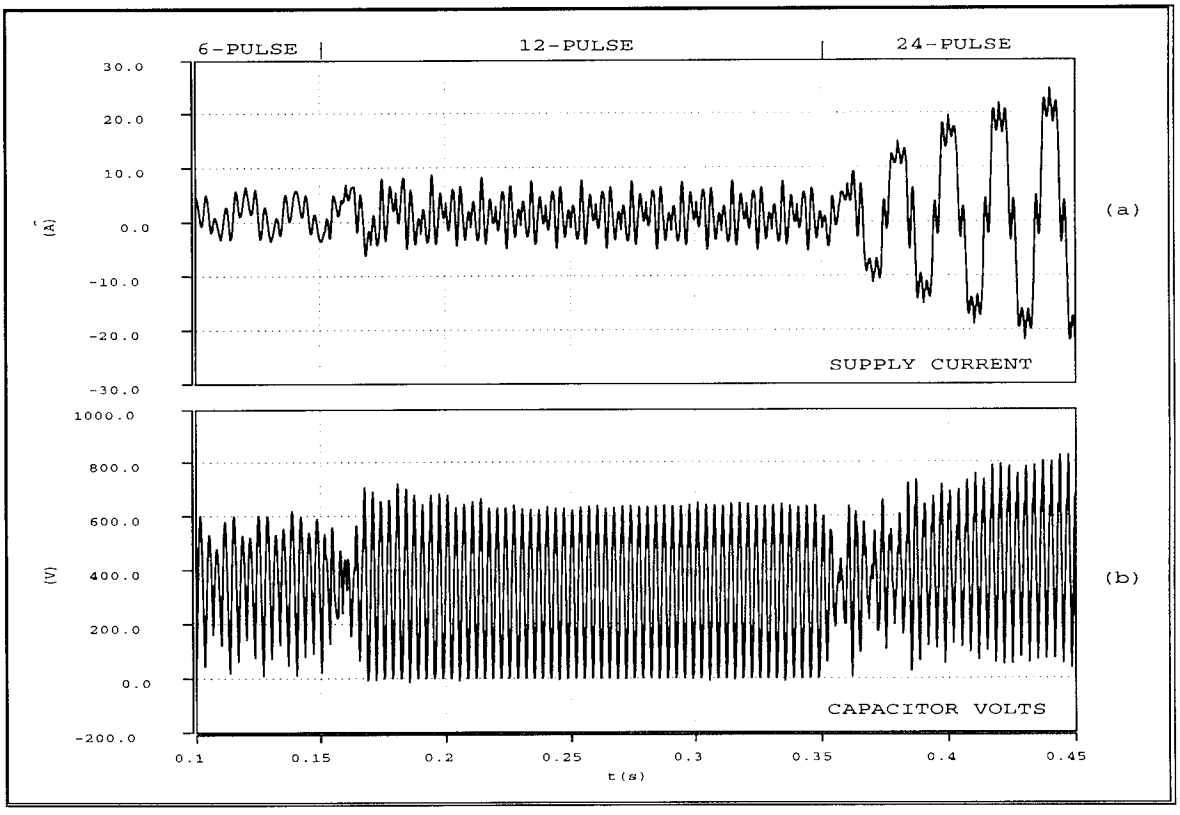

Fig B-3 - Effect of pulse number for same fixed L and C - stator winding coupling

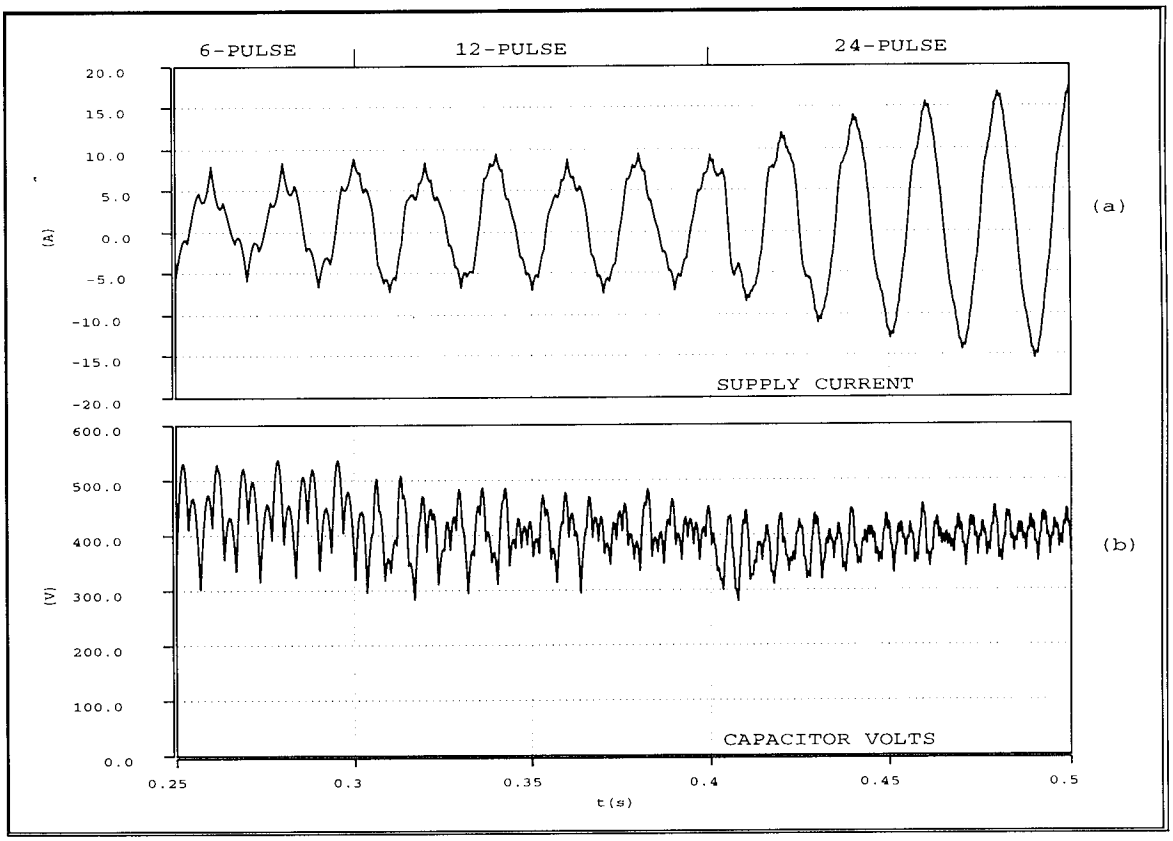

Fig B-4 - Effect of pulse number for fixed L and C, optimised for 24-pulse operation - stator coupling.

From the simulation results above, it should be evident that the topology of the magnetic coupling between the supply and the bridge has significant impact on the STATCON performance parameters. Thus, the expressions for the reactive power and sizing parameter k given in this thesis are only approximations.

Of course, for 6-pulse operation, the parameters for the zigzag connected transformer coupling and the stator winding coupling using external reactors are the same, since in the latter case, the combined system is effectively one in which a conventional STATCON is connected at the terminals of the machine.

Let the following be defined thus:

X_L is the reactance of the coupling reactor.

V_m is defined as the peak of the secondary output voltage. From chapter 5, the tapping point voltage is essentially the same as the applied voltage, whence $V_m = E\sqrt{2}$.

q1 is defined as the normalised value of Iq, the reactive current when the delay angle $\alpha = 0$.

q2 indicates the dependence of variation of real and reactive currents with delay angle α.

Hill [1995] gives the general form of the current I_q for a p-pulse STATCON as:

$$I_q = \left(\frac{p}{6}\right).\frac{V_m}{X_L}.(q1 + q2.\alpha) \qquad (B7)$$

The form of the graphs of q2 and q1 v/s M is shown in **Fig B-5** below. The values indicated are consistent with three phase 6-pulse behaviour with zigzag connected transformer coupling.

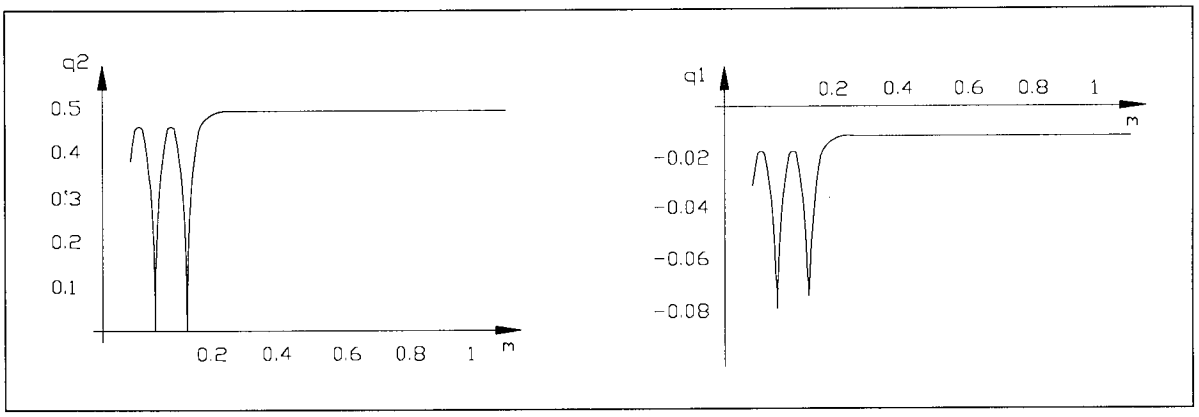

Fig B-5 - Graphs of q1 and q2 for 6-pulse operation with transformer coupling.

In general q2 varies little with pulse number, and so by inference, q2 may be set to 0.5. The reactive power Q_m generated or absorbed by the STATCON is itself given by

$$Q_m = -k_p\left(\frac{p}{6}\right).\frac{V_m^{\,2}}{x_L}.(q1 + q2\frac{\sin 2\alpha}{2\beta}) \qquad (6.9)$$

where k_p is a pulse number dependent constant accounting for topological differences in the coupling. Thus, in terms of reactive power:

$$Q_m = Q_{IM}. \qquad (6.10)$$

From the expression for k, the values of C and L may be determined. In this application, it would be logical to establish the size of the coupling reactor, L_{ec}, and then deduce the size of storage capacitor required. Thus:

$$C = \frac{1}{\lambda_G}\left(\frac{\lambda}{(k_{IM}^{\,2} + \beta^2).\omega^2.L_{ec}}\right) \qquad (6.13)$$

Assuming linear variation with pulse number, $\lambda_G \approx 1.3 - \frac{p}{20}$ (B8)

Thus, for 6-pulse operation , $\lambda_G = 1$ and for 24-pulse operation, $\lambda_G = 0.1$

Currents in Compensated Winding

Consider the diagram of **Fig B-6** shown for a 0° tapping combination.

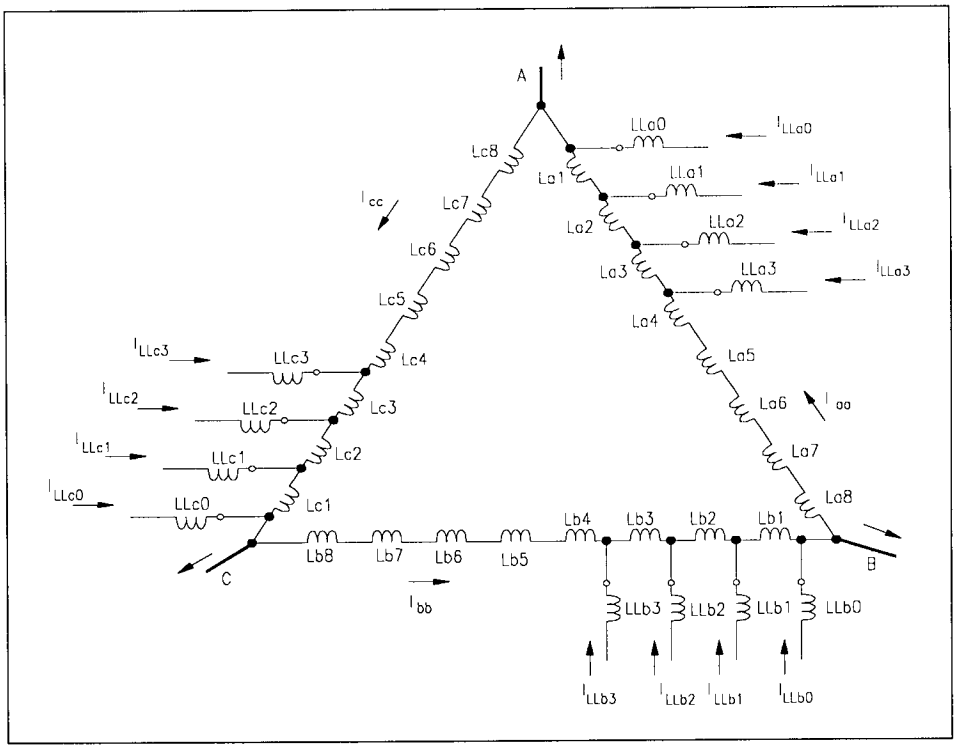

Fig B-6 - Currents in compensated stator winding

The form of the currents in any limb of the delta can be estimated if it is assumed that each inverter section outputs a rectangular wave and the tapping point voltage, v_{tap}, is sinusoidal.

Each reactor such as LL*a*0 (top right) in **Fig B-6** therefore couples a square wave on the inverter side to a sinusoidal voltage on the stator side. Ignoring capacitor ripple, the inverter voltage V_{inv} may be expressed in terms of its fourier series, which, ignoring the d.c. term is given by:

$$V_{inv} = \sum_{n=1}^{\infty} \frac{V_i}{(2n-1)} . \sin((2n-1)\omega t) \qquad \text{(B9)}$$

V_{tap} is phase shifted from V_{inv} by the firing angle α. Thus:

$$V_{tap} = V_s . \sin(\omega t + \alpha) \qquad \text{(B10)}$$

The voltage across the coupling reactor, V_z, is the difference between the inverter voltage and the tapping voltage. Thus:

$$v_z = V_i \sin\omega t - V_0 \sin(\omega t - \alpha) + \sum_{n=2}^{\infty} \frac{V_i}{2n-1} . \sin((2n-1)\omega t) \qquad \text{(B11)}$$

v_z therefore features a reduced fundamental component whose size depends on the firing angle α, and odd harmonics starting with the third. The current through the inductor is the voltage across it divided its impedance Z_L. Thus:

$$I_{LC} = I_L = \frac{v_z}{Z_L} = \frac{v_z}{R_c + j\omega L_c} \qquad \text{(B12)}$$

whence:

$$I_L = \frac{v_z}{\sqrt{(R^2 + \omega L^2}} . \frac{1}{(\cos\varepsilon + \sin\varepsilon)} \qquad \text{(B13)}$$

and as before, $\varepsilon = \tan^{-1}(R / \omega L)$ (2.11)

Fig B-7 shows the associated waveforms for leading power factor operation.

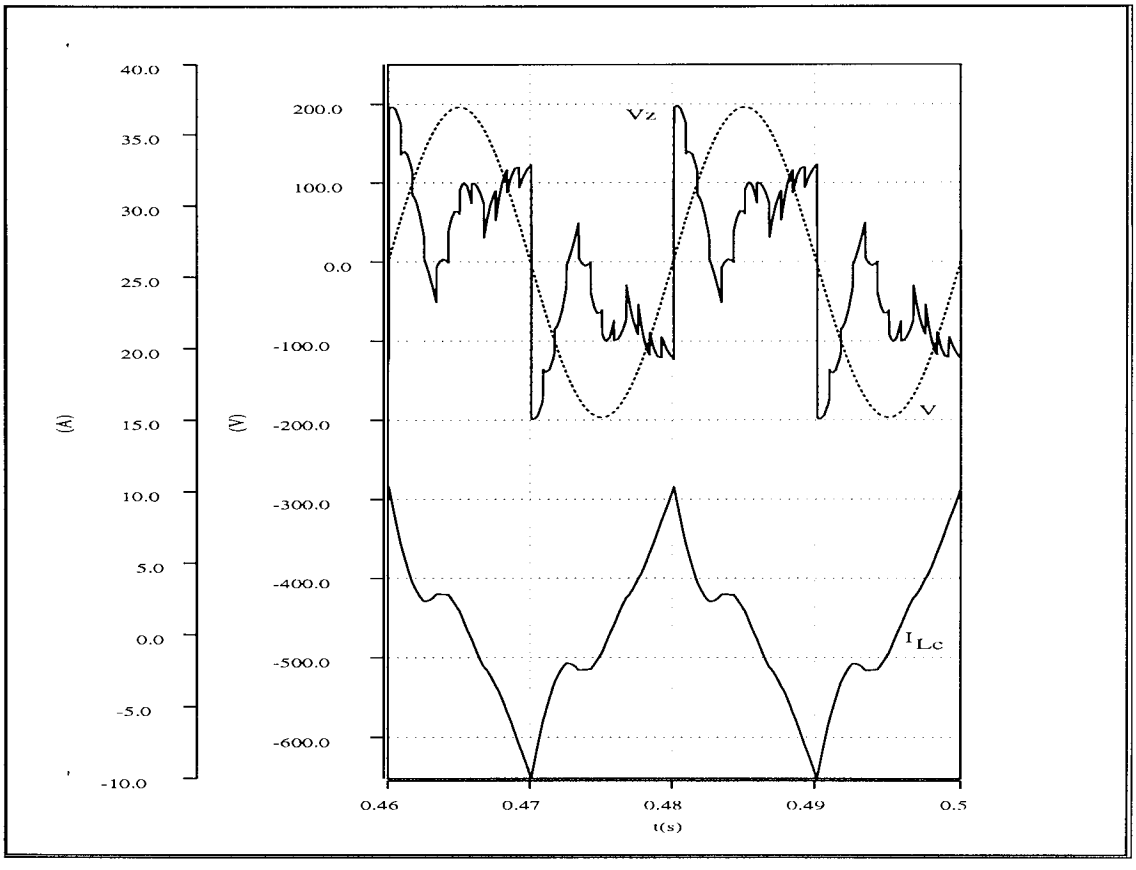

Fig B-7 - Simulated coupling coil voltage and current waveforms.

From a fourier series expansion, the fundamental component of the inverter square wave is given by $(4/\pi)V_C$ where V_C is the capacitor voltage. Thus, the fundamental component of the voltage across the inductance is V_L, given by:

$$V_L = \frac{4}{\pi} V_C \sin \omega t - V_{tap}.\sin(\omega t - \alpha) \qquad \text{(B14)}$$

The phasors of **Fig B-8** depict generation and absorption for arbitrary values of delay angle α .

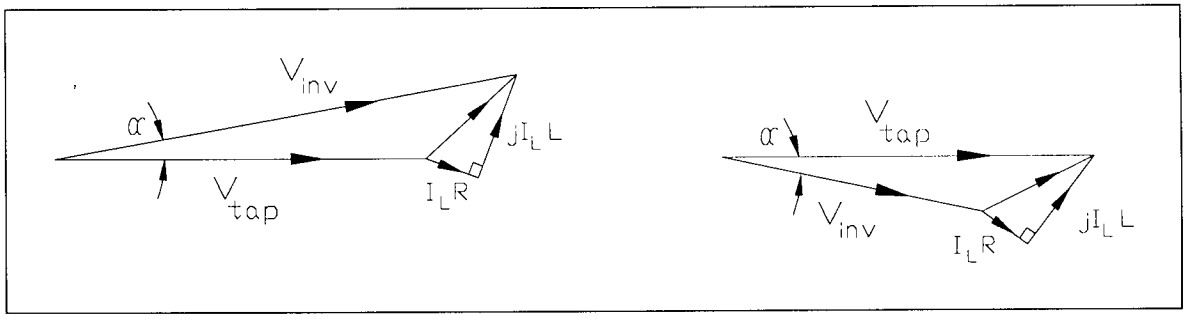

Fig B-8 - Phasors showing the tapping point and inverter output fundamentals for leading and lagging values of delay angle

The fundamental component of the current through the coupling reactor is:

$$I_{Lo} = -\frac{V_{tap} - V_{inv}\cos\alpha}{Z_L}\cos(\omega t + \varepsilon) + \frac{V_{inv}\sin\alpha}{Z_L}\sin(\omega t + \varepsilon) \qquad \text{(B15)}$$

Suppose a situation where the STATCON is injecting just sufficient current into the stator winding for unity power factor operation.

The total current supplied by the STATCON then just equals the magnetisation current of the machine. In principle therefore, the section of the STATCON shown provides the *per phase* magnetisation current.

The total current supplied by the STATCON at fundamental frequency is therefore the vector sum of the phasors in each limb of the bridge. Since these currents are $2\pi/\rho$ radians phase shifted for a ρ-pulse compensator, the total injected current I_{inv} is given by:

$$I_{inv} = \sum_{n=1}^{n/2m} I_{Lo}.\sin(\omega t + (n-1)(2\pi/p)) \qquad \text{(B16)}$$

From Eqn B5 and B6, the per phase magnetisation current is given by:

$$I_M = E/x_M = \frac{E.k_i.g}{16\mu_0.l.r}.\left(\frac{a.n_p}{k_w.N_{ph}}\right)^2 \qquad \text{(B17)}$$

whence, for unity power factor, $I_{inv} = I_M$ (B18)

Current Waveforms

Refer to **Fig B-6** and let I_{BA} be the current between the supply terminals B and A. See that:

$$I_{BA} = I_{aa} + I_{LLa3} + I_{LLa2} + I_{LLa1} + I_{LLa0} \qquad (B19)$$

where each of the currents (shown in Fig B6) is a phasor.

Fig B-9 shows these currents and their summation to give the phase to phase current I_{BA}. **Fig B-9f** shows that the resultant current is not the same as the phase current. This is to be expected since the current I_A requires that the current in the branch of the delta with the coil Lc8 is summed vectorially with the current I_{BA}. Thus:

$$I_A = I_{BA} + I_{Lc8} = (I_{aa} + I_{Lc8}) + I_{LLa3} + I_{LLa2} + I_{LLa0} \qquad (B20)$$

But $I_{c8} = I_{cc}$, whence:

$$I_A = (I_{aa} + I_{cc}) + I_{LLa3} + I_{LLa2} + I_{LLa0} \qquad (B21)$$

Assuming balanced three phase operation, $|I_{aa}| = |I_{cc}|$ and the two are phase shifted by 240°.

The currents I_B and I_C in the other two supply lines are equal in magnitude to I_A but phase shifted by 120° and 240° respectively. All other currents in the winding have appropriately phase shifted counterparts in the phase discussed above.

Kemp [1934] discusses the behaviour of harmonics of three phase winding connections and explains that some harmonics that may be present in the phase to phase current such as I_{BA} above do not appear in the phase current such as I_A. In summary, a third harmonic in the phase to phase current does not appear in the phase current unless the neutral point is secured. The fifth harmonic appears in both phase to phase and supply phase currents.

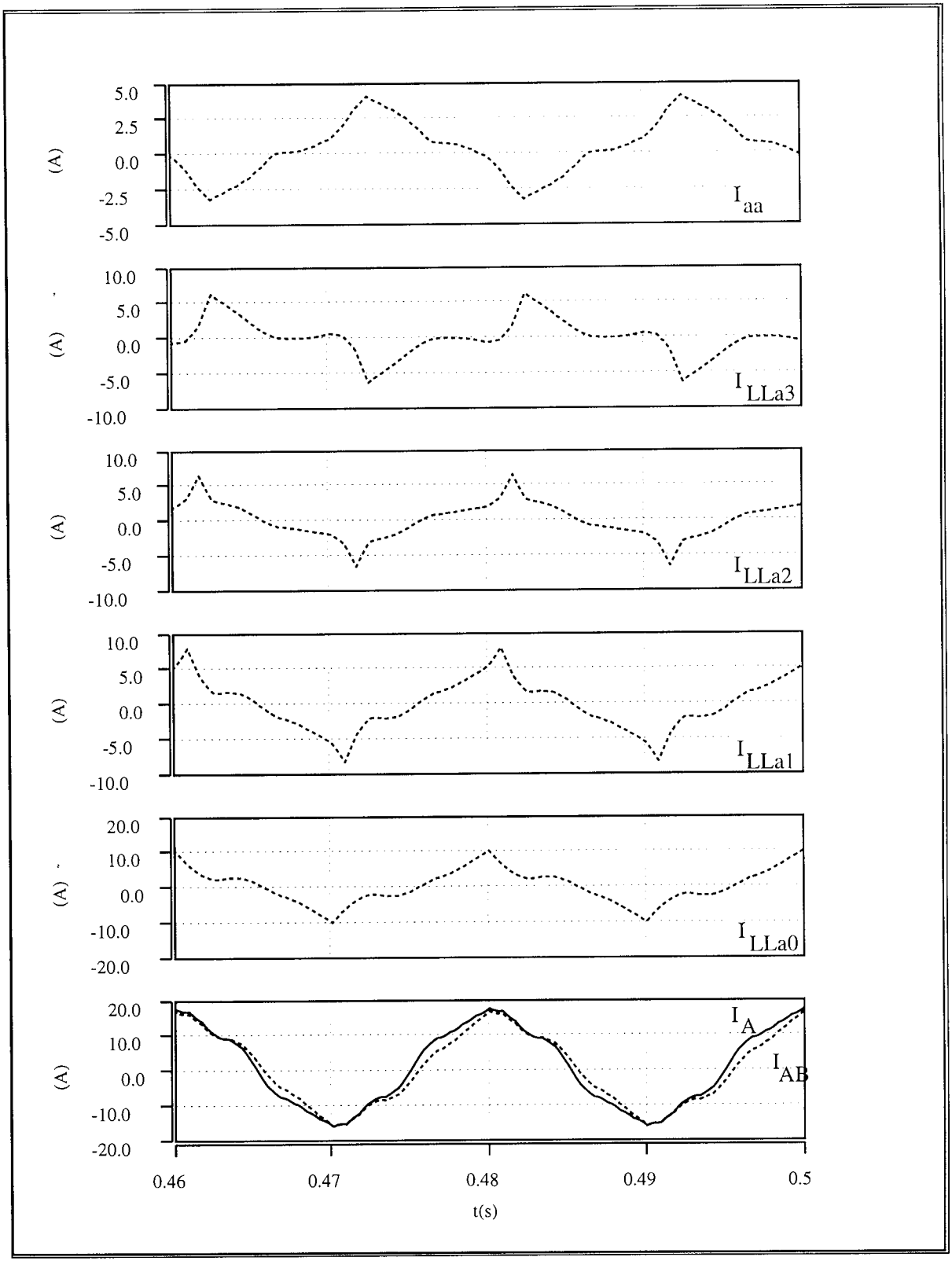

Fig B-9 - Machine and coupling coil currents and their vector sum.

Assumming balanced operation, all other currents in the delta can be deduced from symmetry.

APPENDIX C

CONTROL SYSTEM HARDWARE

This appendix gives the circuit diagram of the control system used. The functionality has been described in chapter 5.

Notes:

- All power supply decoupling comprises a parallel combination of two capacitors. These are
  (1) 0.01μF disc ceramic
  (2) 10μF, 15V, solid tantalum

- Each l.e.d has a 2.2kΩ carbon film, 0.25W resistor connected in series

- Each push button connects across one end of a 10kΩ resistor and ground. Where better noise immunity is required, e.g. RESET push button, a 2.2kΩ pull up resistor is used instead.

- All points on the PC connectors feature 4.7kΩ pull-up resistors for better noise immunity. The ribbon connectors from the computer are passed through a ferrite clamp for protection against radiated electromagnetic interference.

Original Circuit design:	C. M. Chileshe
Current Revision No.:	3
Revised by:	C. M. Chileshe & M. A. Higlett

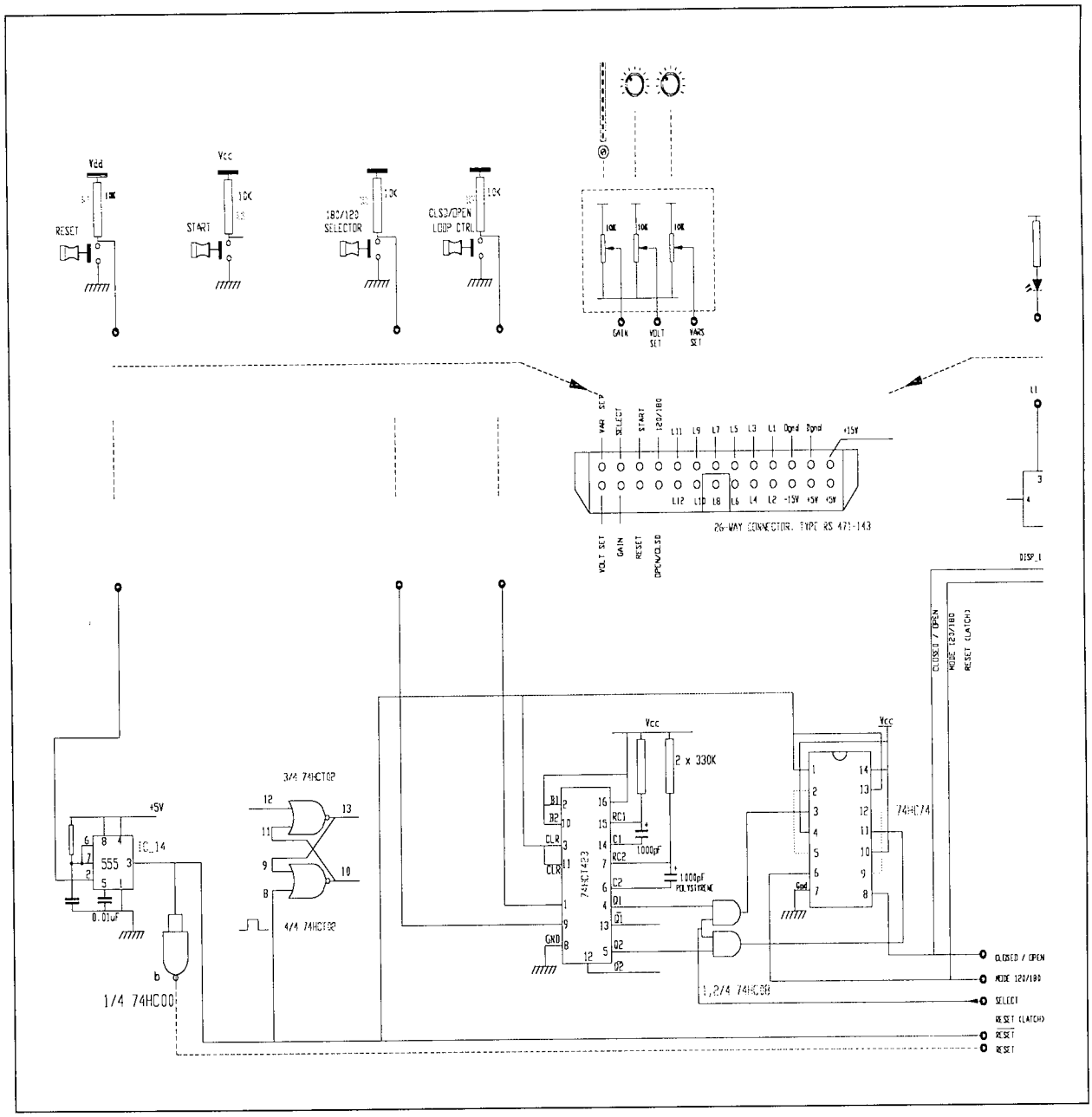

Fig C-1 - Console interface.

The push buttons shown are console mounted.

The potentiometers are of two designs:

- Single turn featuring integral knob with pointer.
- Multi-turn recessed, for accurate gain control. A bar graph display was included.

The RESET and START push button have the effect of setting or resetting the S-R flip flop. The RESET pulse is generated by a 555 monostable which subsequently replaced the MAX708 voltage supervisor on account of the latter's sensitivity to voltage dips, giving rise to nuisance reset pulses.

The D-type latch generates a clean pulse for monostable control while the AND gate disables or enables transmission of pulses.

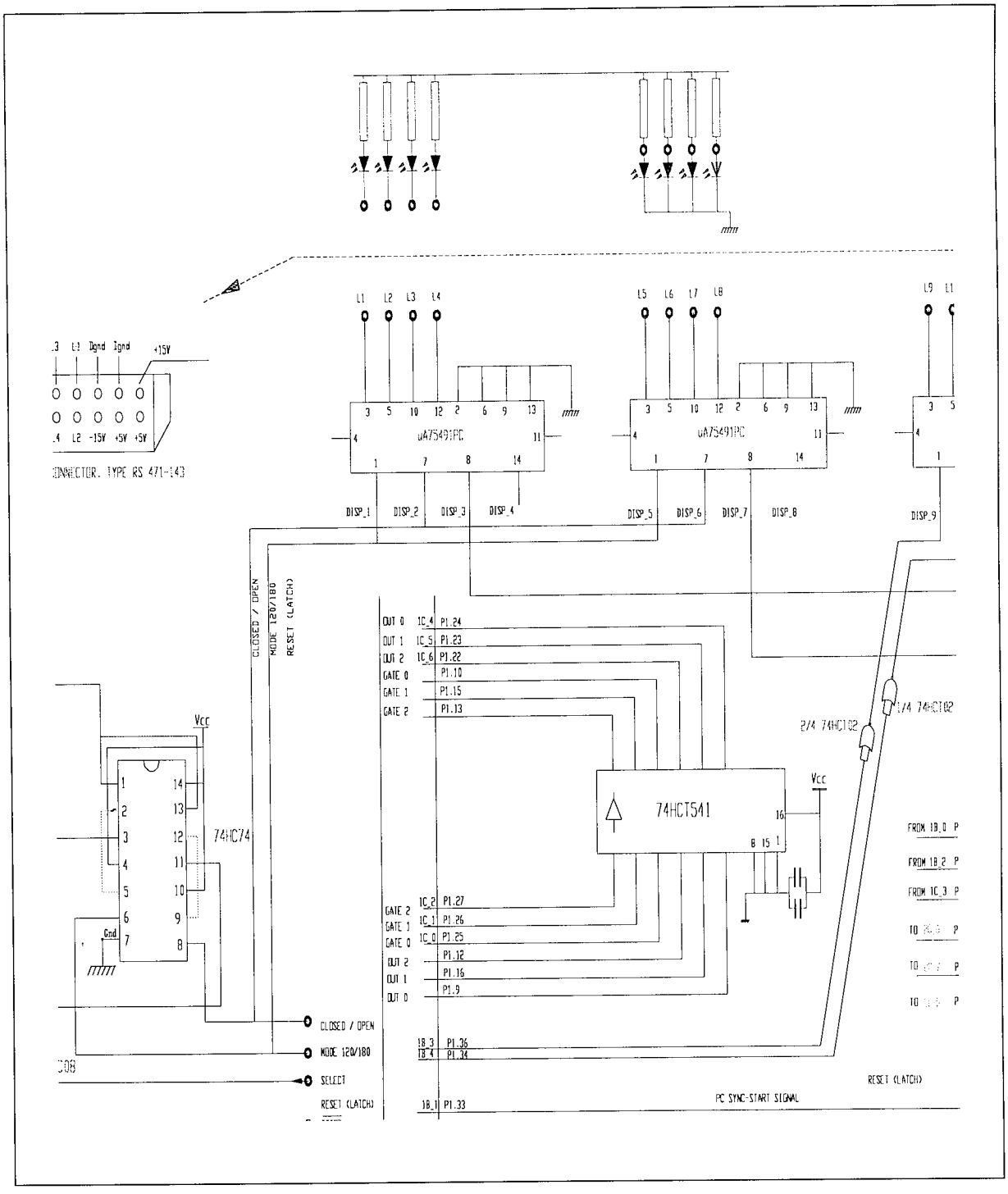

Fig C-2 - Console display

The CMOS to l.e.d. drivers are in essence four darlington pair transistors per chip with open collector outputs. All l.e.d.s feature 2.2kΩ series resistors and are console mounted. As shown, some l.e.d.s are switched on by a high signal on the collector output, some by a low signal output. All emitters are grounded.

The 74HCT541 device shown buffers signals from the computer which are required to run back into the same. Examples are timer gates and outputs.

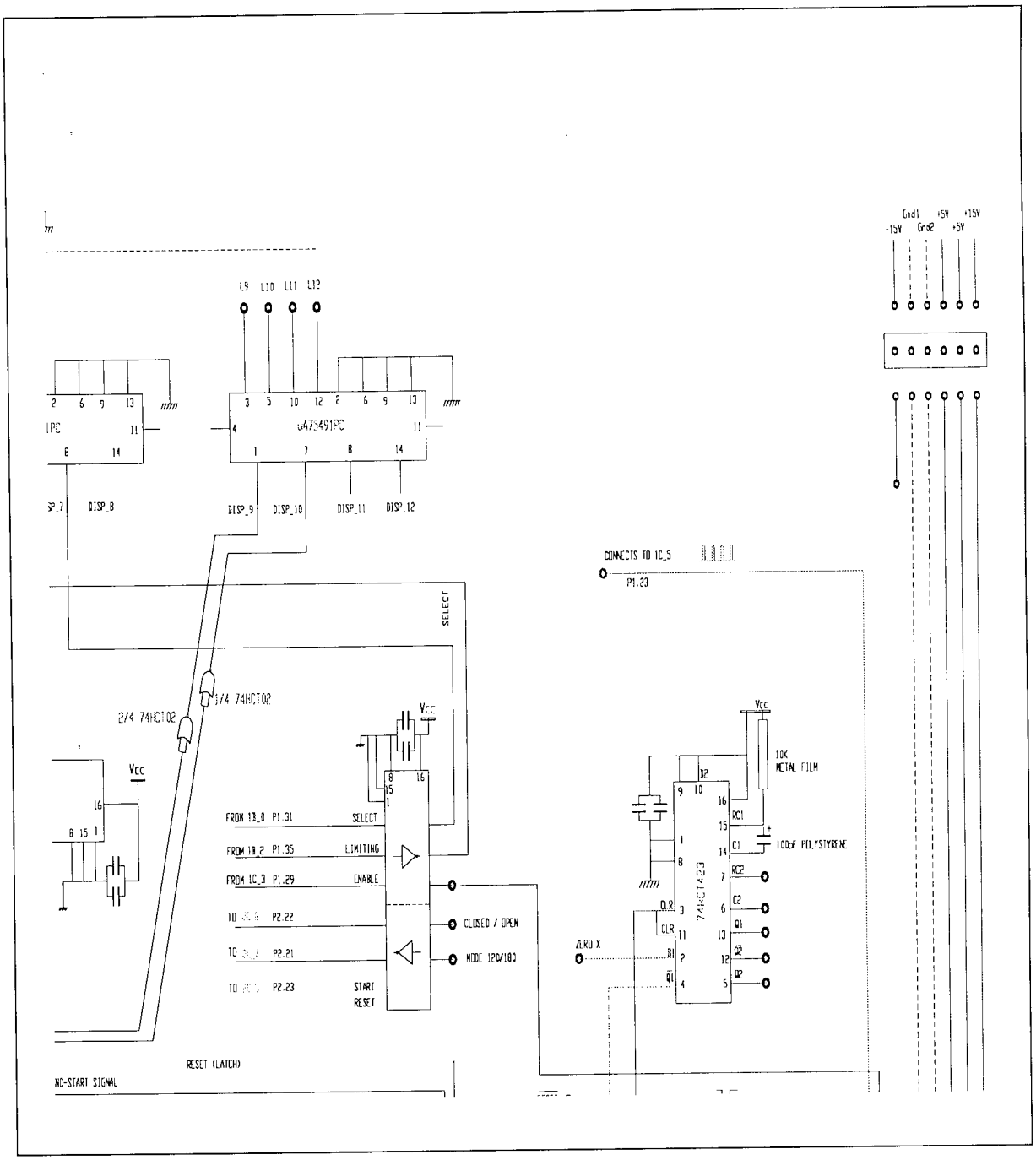

Fig C-3 - Switching synchronisation and buffering

The edge triggered monostable shown on the right generates a narrow pulse of about 100ns every positive going edge of zero cross. This forces the 12-bit synchronous counter to load and so eliminate potentially cumulative error. The buffers show the routing of signals between the computer, the display drivers and other devices on the board. Also shown on the right is the power supply to the high voltage side.

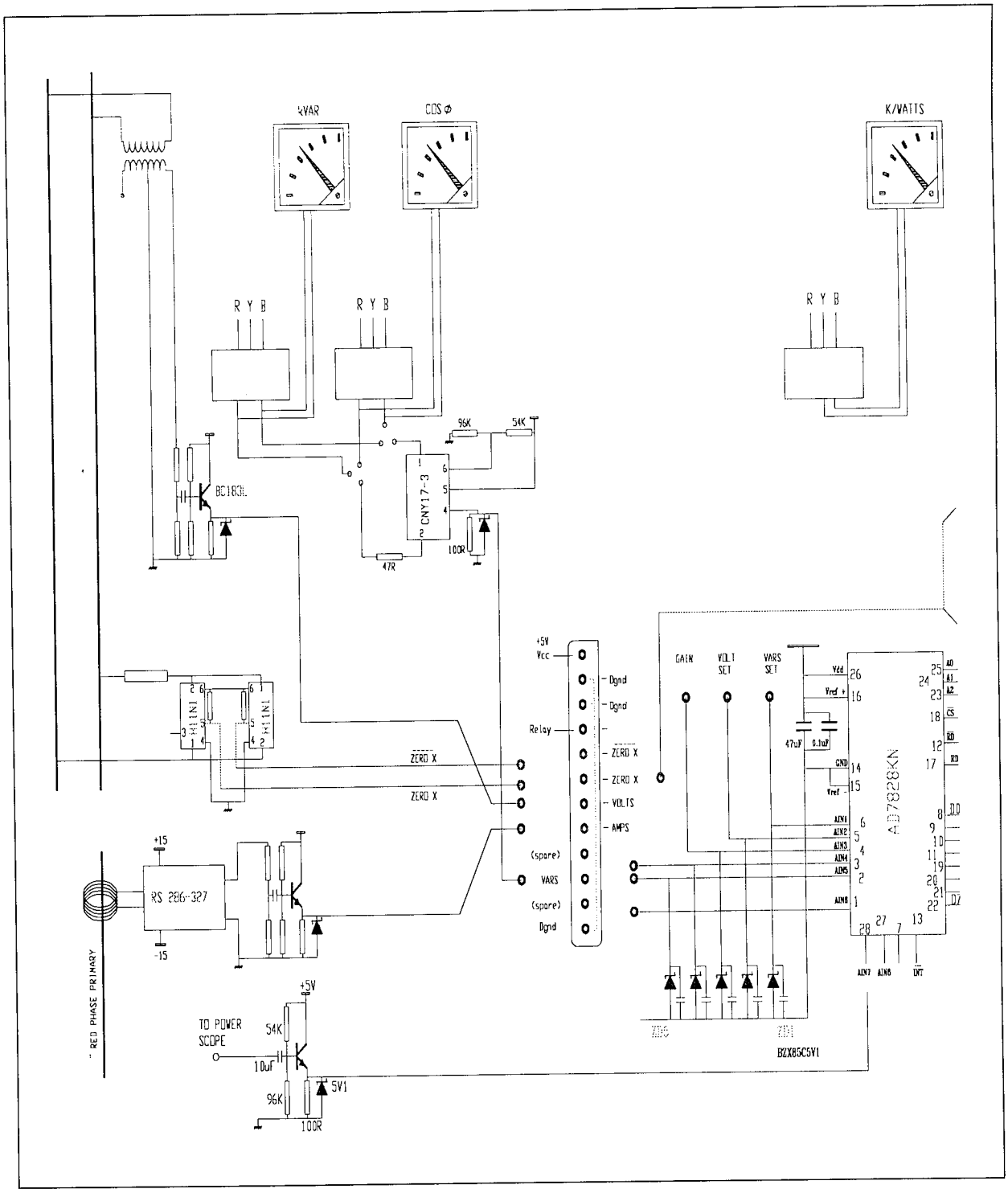

Fig C-4 - Signal acquisition and interfacing for conversion.

The centre-tapped transformer shown has a 240V primary winding and a ± 4.5V output. It provides the voltage waveform. The current waveform is based on a hall effect device and has a variable sensitivity. It was set to output the maximum +5V for a current of 15A.

The opto coupler for d.c. level translation has been described in chapter 5. The transistor level shifter at the bottom of **Fig C-4** connects to the output from a power scope was used to capture high voltage inverter and capacitor waveforms.

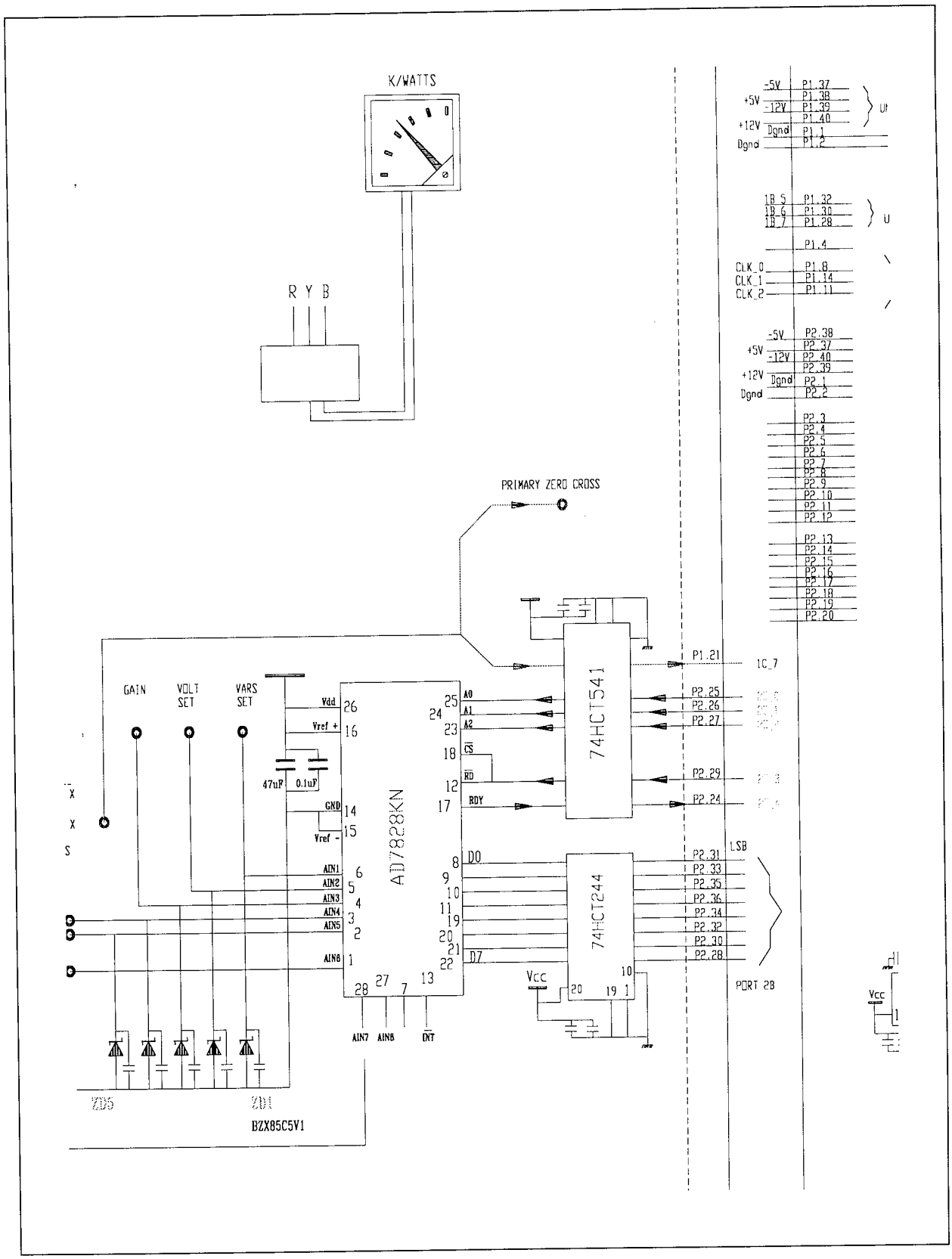

Fig C-5 - ADC device connections.

All zener diodes are 5.1V rated. Channels for waveform capture do not have the 10µF transient suppresser. Signals between ADC and PC are buffered and have no pull up resistors.

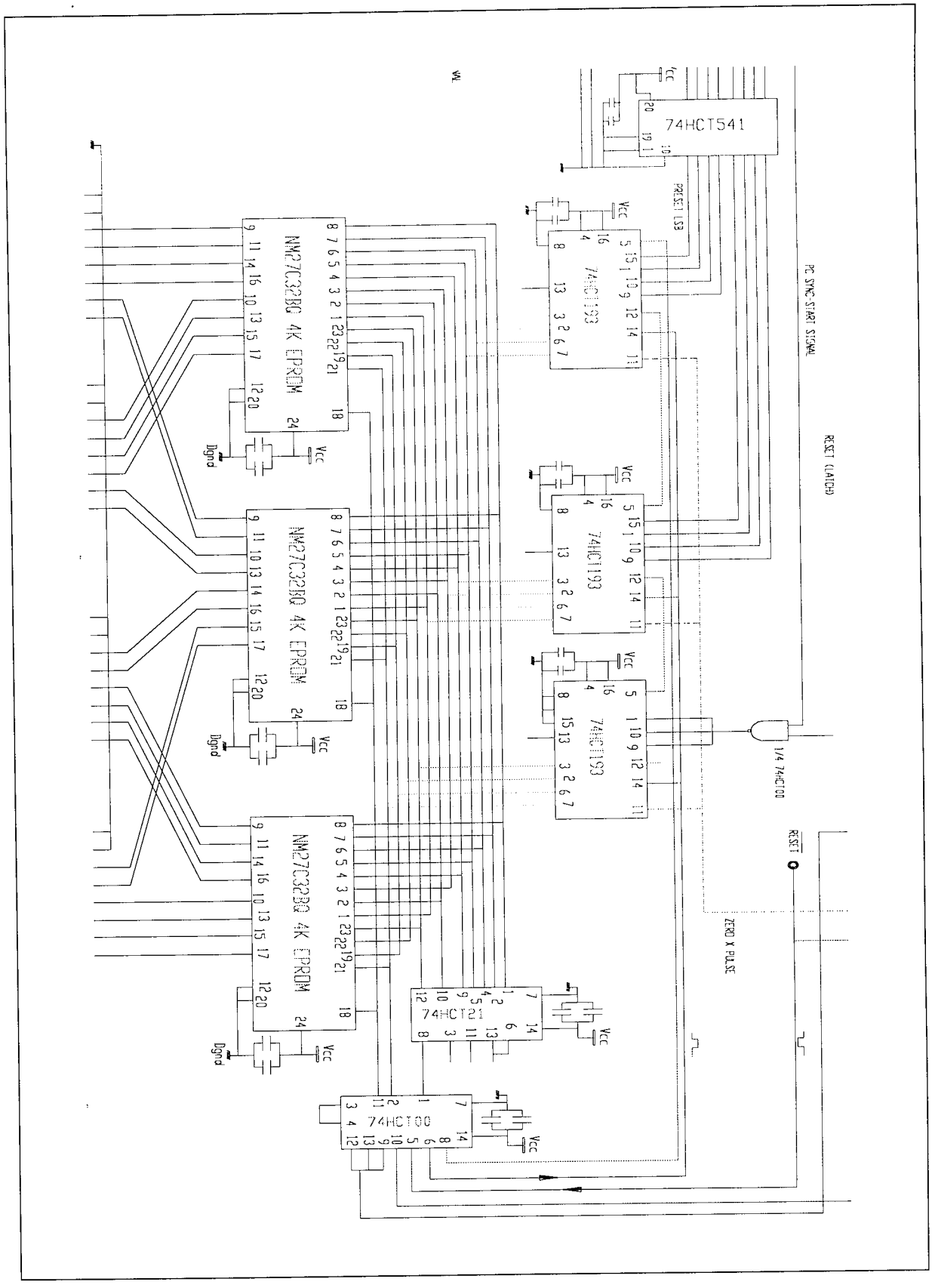

Fig C-6 - Pattern generator circuit.

The 74HCT541 at the top of the page carries the preset for the synchronous counter which is three 4 bit devices, type HC193, connected in series. The decoder made up of gate devices 74HCT21 and the 74HCT00 NAND is shown. Also shown are the EPROMs.

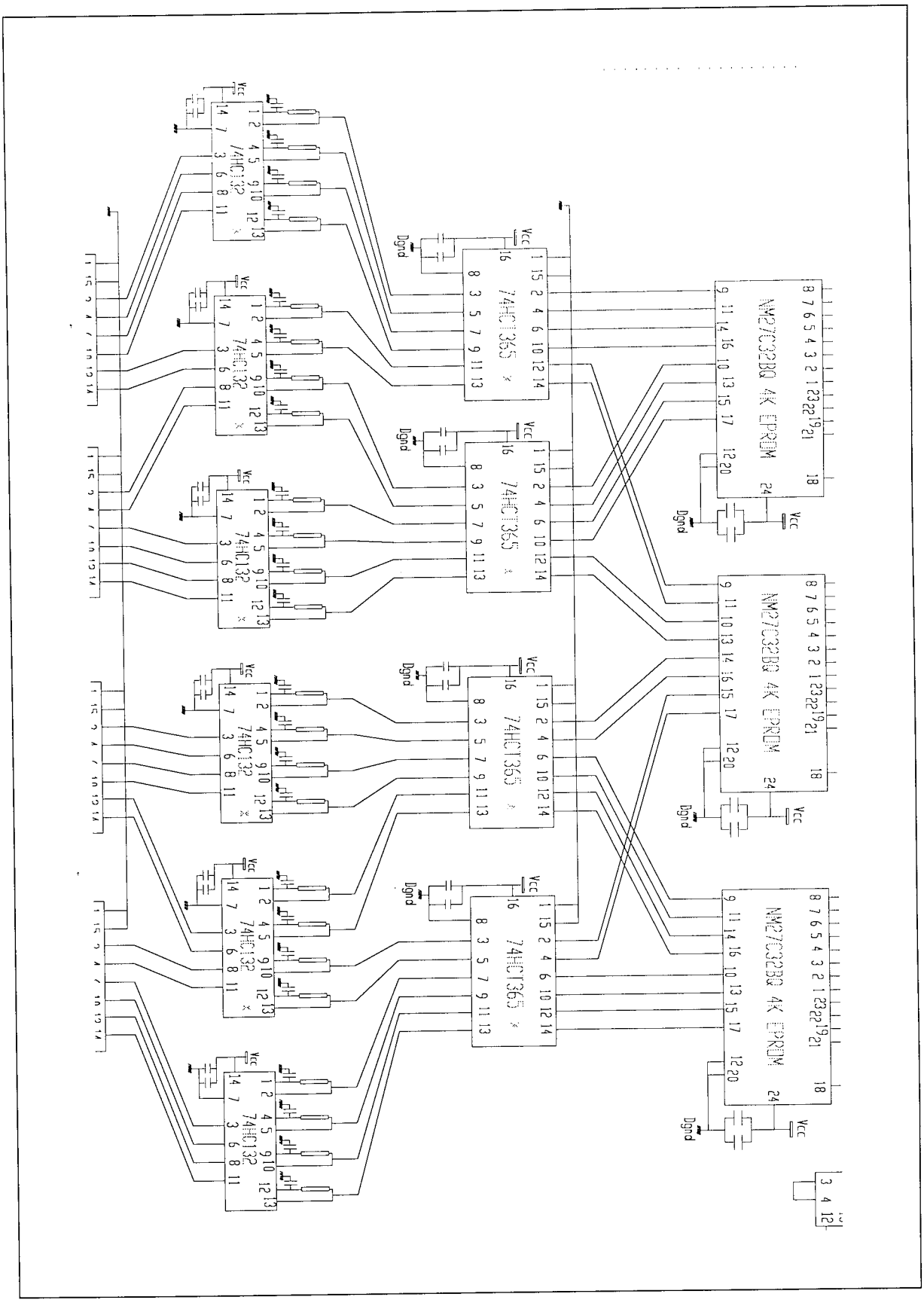

Fig C-7 - NAND schmitt switching interlock.

The triggers are type 74HC132 driven by buffers connected to the EPROM outputs. Timing components are 51kΩ and 33pF.

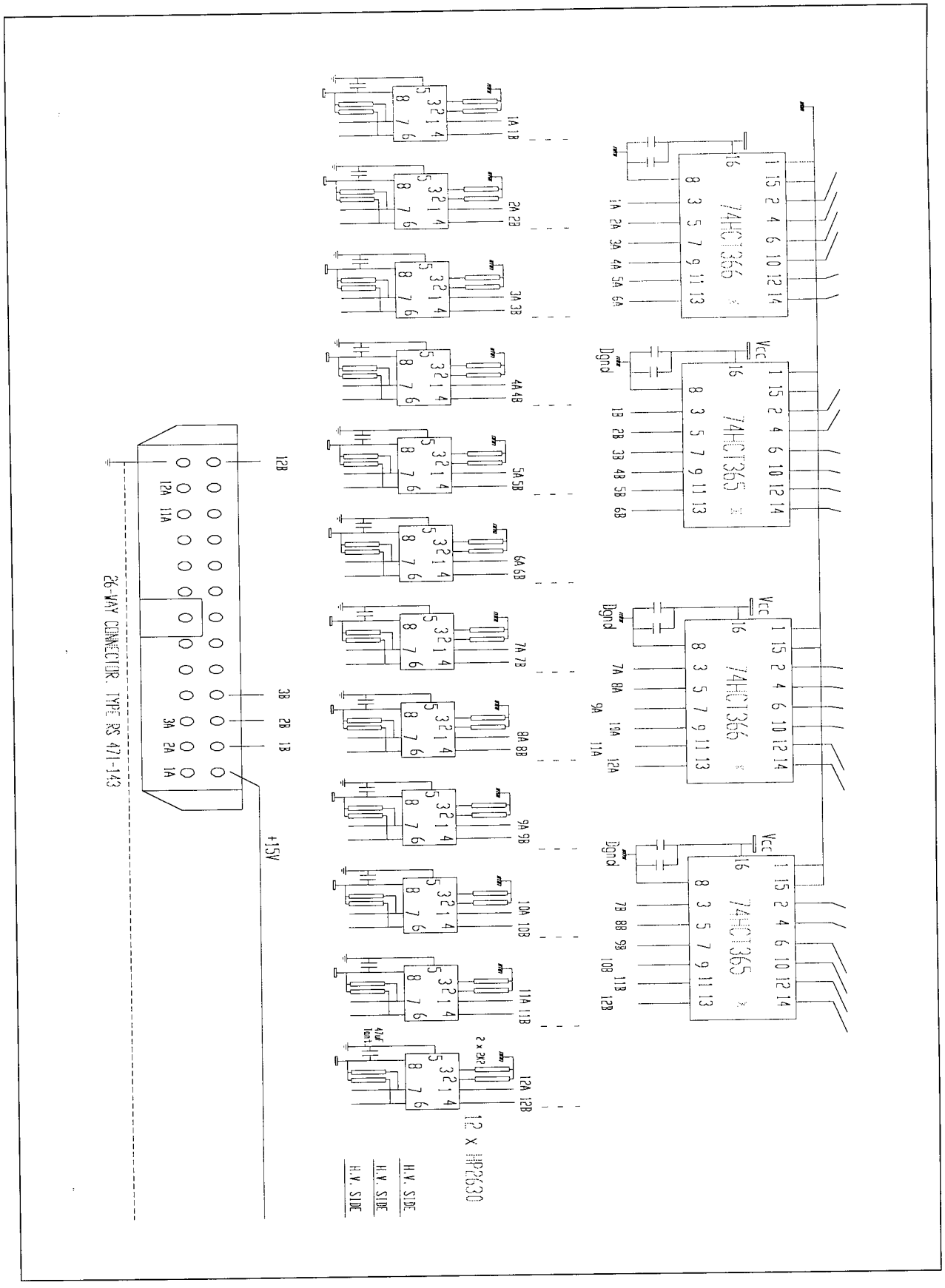

Fig C-8 - Opto isolation.

Opto input side resistors are 1k and pull up resistors are 2.2k. Capacitor between pins 5 and 8 is 47µF and provides local voltage support. Also shown are the output connector assignments.

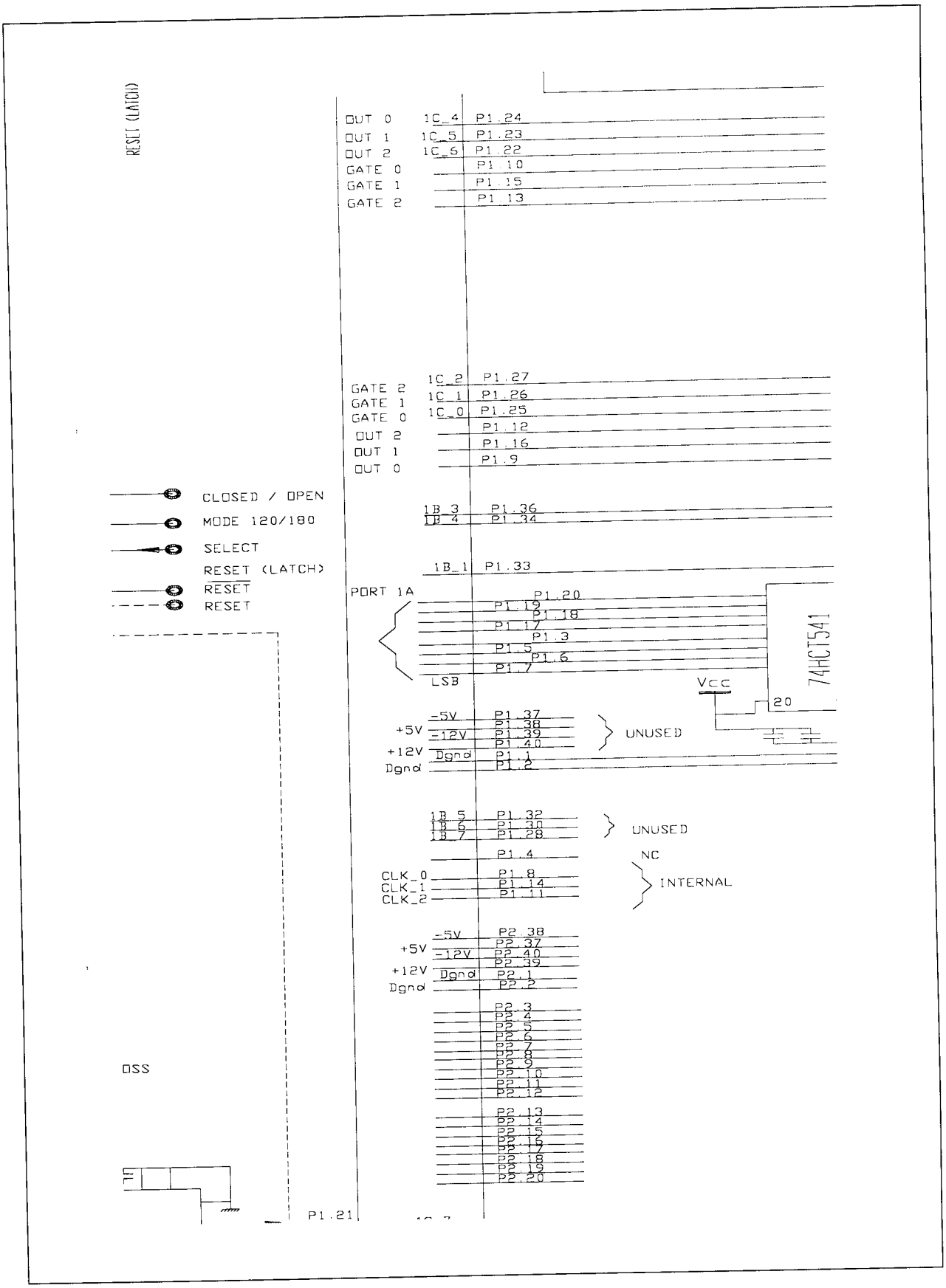

Fig C-9 - PC interface connections.

All outputs *from* the computer have 4.7k pull up resistors. Port assignment is described in chapter 7.

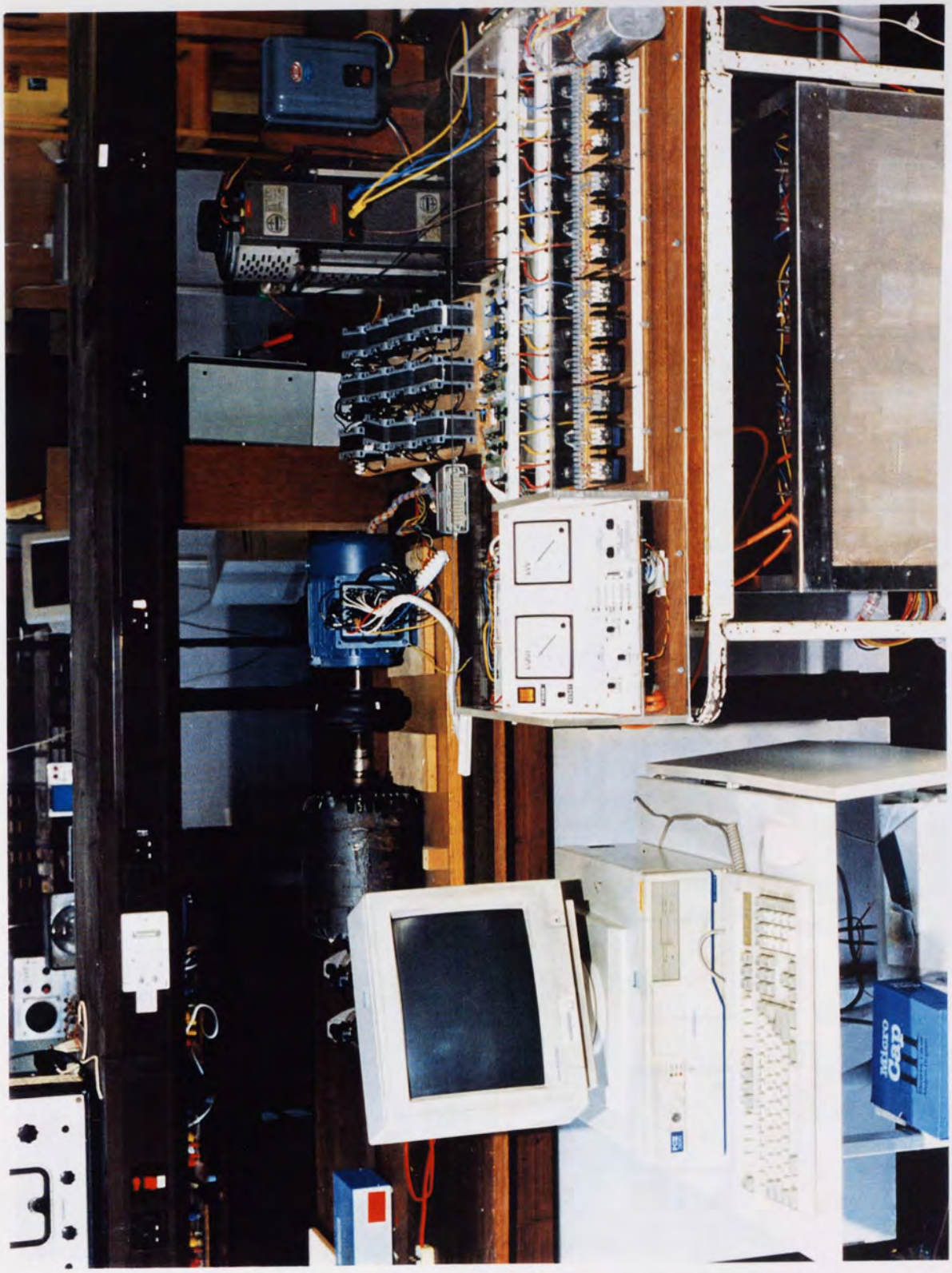

Fig C-10 - Model 24-pulse STATCON experimental apparatus.

Viewed in landscape, the computer shown connects to the control circuit by ribbon cable (not shown). The zigzag transformers are visible under the bridge. Behind the computer monitor is the d.c. machine coupled to the induction machine, to the right of which is the array of iron cored coupling reactors. The variac is visible immediately to the right of the reactors.

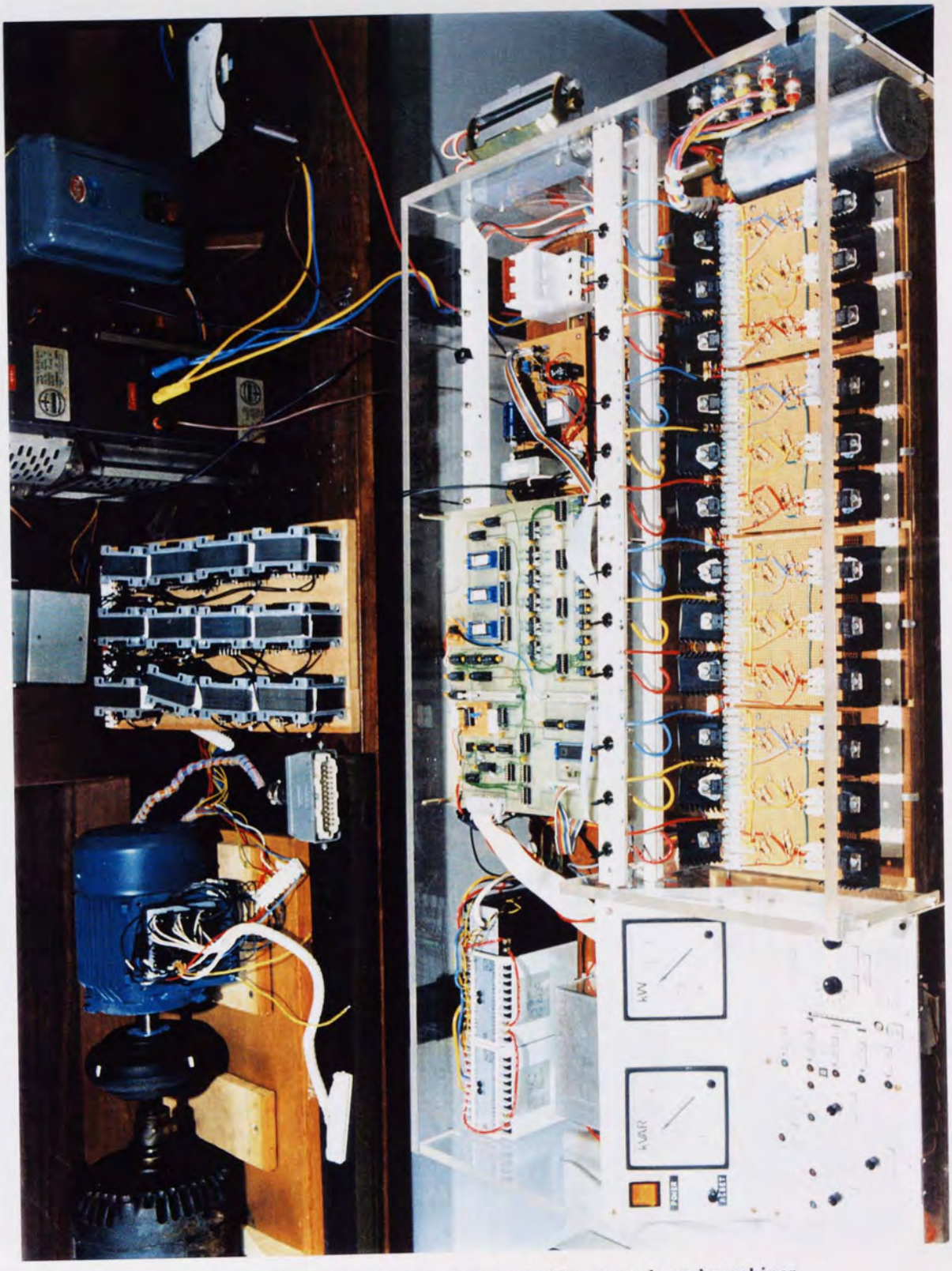

Fig C-11 - Close-up of experimental apparatus showing bridge, console and machines.

Viewed in landscape, the operating console is shown, bottom left. Behind it are the 3-phase transducers. The MOSFETs are shown in four panels of six in the foreground, and to the right is the storage capacitor. Above the bridge are the toggle switches and behind them the control electronics. In the background are the machines, coupling reactors and 3-phase supply units.

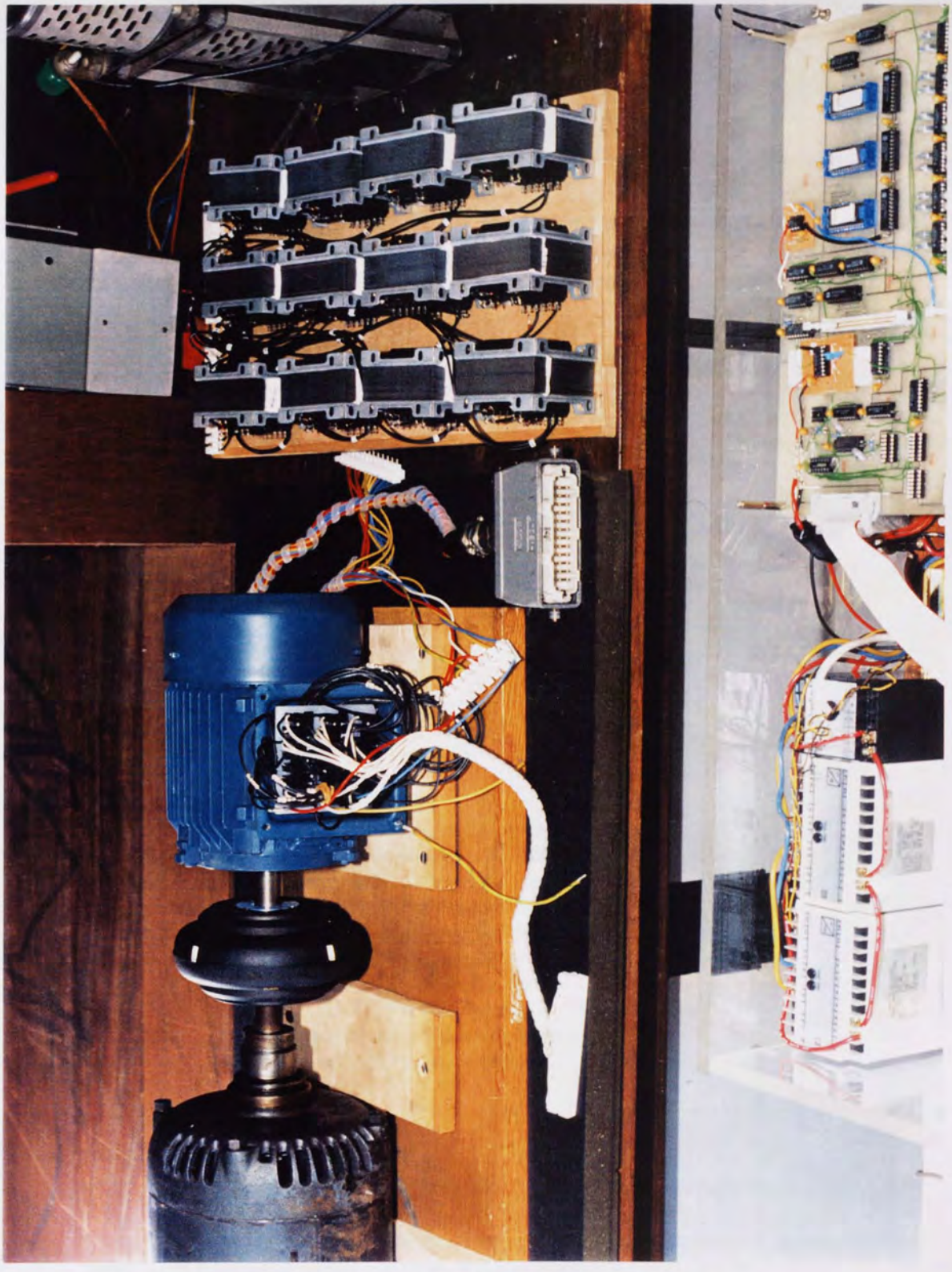

Fig C-12 - Close up on induction machine and coupling reactors.

Viewed in landscape, the three phase transducers for the kVAr, power factor and kW are shown in the bottom left hand corner. In the background, left to right, are the d.c. machine, induction machine and coupling reactors. The multiple phase connectors to the induction machine are visible. The larger connector couples the machine to the STATCON.

APPENDIX D

CONTROL SOFTWARE PROGRAM LISTING

The listing as shown here has been styled to improve legibility. The styling however, is limited to the use of tabs, bold, italicised and underlined text only. No text of any sort has been added however, and the frames around some of the major headings are present in the actual source code using the DOS extended ASCII character sets. All the commentary included is also part of the actual code. A copy of the program has been included with the thesis.

```
/*      TITLE STATCON.EXE   SI-8255 based Statcon controller
        ---------------------------------------------------

        Author -        Chris M. Chileshe
                        Electric Power Group
                        Department of Electrical Eng.
                        Aston University
                        Aston Triangle
                        Birmingham B4 7ET

        Revision number - 3

        ---------------------------------------------------
                        REVISION  NOTES
        ---------------------------------------------------

Differs from previous versions in that
                1) it expects non-inverted zero cross
                2) samples the actual current & voltage ADC channels
                3) reads in all 8 channels of the ADC
                4) it does not display instantaneous values of a.c. sigs.
                5) it is a Turbo C++ program with no inline assembler
                6) it features optional Keyboard control
                7) it features a real time spectrum analyser
                8) it is a .CPP file using the COMPLEX.H include file
                9) port 1B has a different pin assignment
               10) keyboard control is disabled

        ---------------------------------------------------
                        PROGRAM  NOTES
        ---------------------------------------------------
This program forms the software core of a controller for a 24-pulse STATCON or ASVC.

The program is subroutine based to assist in the time sharing and  allocation of system resources
between the control and display functions. It is developed in a Turbo C++ environment, but does  not
use C++ OOP constructs. It does use some C++ features however, such as complex number libraries
e.t.c.      . To all intents and purposes though, it is essentially a standard C program.
Some features, especially screen handling functions, are not standard ANSI C. They are specific
to the DOS environment on IBM PC type machines, and unique to Turbo C/C++. Portability of source
code may require expansion of the relevant libraries.

In the form below, the program will run on 286 or higher processors. The effectiveness of the control
in terms of speed and response times however, is dependent on the speed of the processor.
```

CONTROL EXECUTIVE

The program behaves as an intelligent PLL, open and closed loop controller. It computes the supply fundamental frequency from the zero crossing signal using a 3MHz 16-bit timer. This choice of frequency is such that:

1) It is high enough to minimise the timing error
2) It is low enough to preclude overflow handling routines for supply frequencies down to about 46Hz.

Also, there are no procedures for handling the fraction part of the quotient resulting from dividing the fundamental period by the number of EPROM active states (2400). Thus, the choice of EPROM states s influenced by this. The Hardware is responsible for forced synchronisation of the control circuitry to eliminate cummulative error.

The zero crossing signal is assumed a square wave of as close to 50% duty cycle as possible. A narrow pulse would lead to error. The program uses the signal to determine when to start switching, and when is a safe instant to change the delay angle.

The main interface between the host processor and the external electronics that forms the dedicated STATCON is an ISA expansion slot type card featuring 3 16-bit timers (8253) and 6 8-bit digital I/O points.

PORT ASSIGNMENTS

PORT 1B pin assignments

bit 0 - user select enable
bit 1 - Sync start
bit 2 - Control limiting indicator
bit 3 - Control output increasing
bit 4 - Control output decreasing
bits 5 - 7 - unused

PORT 1A is an 8-bit output port connected to the preset input on a 12-bit synchronous counter. Program the first phase in byte ph_one as (-angle x 360/phases) e.g. -22.5 works out as 150. Minimum preset is 50, and maximum is 205

PORT 1C is an input/output port assigned as follows

Outputs:
bit 0 - Timer 0 gate control - enable (1) to run Timer 0
bit 1 - Timer 1 gate control
bit 2 - Timer 2 gate control
bit 3 - All enable control for external cct. Active low (0)
Inputs:
bit 4 - Timer 0 output
bit 5 - Timer 1 output
bit 6 - Timer 2 output
bit 7 - Primary zero crossing detector (see note above)

PORT 2A - is an input port configured as follows

bit 0 - Data acknowledge - not used
bit 1 - Synchronous zero cross
bits 2-7 - unused

PORT 2B - ADC data bus link

PORT 2C is an input/output port configured as follows

Outputs:
bit 0 - ADC address line A0
bit 1 - ADC address line A1
bit 2 - ADC address line A2
bit 3 - ADC Select/Read enable - Active low (0)
Inputs:
bit 4 - ADC data conversion complete
bit 5 - Console start/Reset
bit 6 - Console Open loop/ Closed loop control selection
bit 7 - Console 180/120 switch mode control selection

ROUTINE is a control byte that stores bitwise information about the initialisation of the program subroutines and functions by numbering its bits to match the subroutines.
bit 0 - function **main**()
bit 1- function **show_adc**()
bit 2 - function **plot_graph**()
bit 3 - function **plot_psd**()
bit 4 - function **disp_all**()

```
*/

/*
   Preprocessor directives and initialisation
*/
#define   BASE          0x1b0
#define   port_1a       BASE+0
#define   port_1b       BASE+1
#define   port_1c       BASE+2
#define   port_1        BASE+3
#define   port_2a       BASE+4
#define   port_2b       BASE+5
#define   port_2c       BASE+6
#define   port_2        BASE+7
#define   timer_0       BASE+8
#define   timer_1       BASE+9
#define   timer_2       BASE+10
#define   timers        BASE+11

#define   SAMPLES       500
#define   eprom_words   2400
#define   M             128          // PSD entries - must be power of 2
#define   M2            (2*M)        // useful for spectral analysis
#define   BEEP          printf("\a")
#define   toggle(x)     x = !x
```

```
/*
   Library include files declarations
*/

#include <stdlib.h>
#include <conio.h>
#include <stdio.h>
#include <graphics.h>
#include <string.h>
#include <dos.h>
#include <math.h>
#include <ctype.h>
#include "analyser.h"
#include <complex.h>

/*
   Global variables declarations and initialisations
*/

float phase_1, cycles, PSD[M], PPSD[M];          // first phase in degrees ( e.g. 22.5),
                                                 // number of cycles to display and
                                                 // storage arrays for power spectral
                                                 // density plots.

int scrn_width, scrn_height, glbl_3, routine;

unsigned char i_samp[SAMPLES];                   //storage for current waveform samples
unsigned char i_prvs[SAMPLES];                   // previous samples for plot masking
unsigned char v_samp[SAMPLES];                   // storage for voltage waveform
unsigned char v_prvs[SAMPLES];                   // plot masking
unsigned char q_samp[SAMPLES];                   // storage for miscellaneous 3rd signal
unsigned char q_prvs[SAMPLES];                   // samples and plot masking

unsigned char alpha,                             // stores delay angle as counter preset
              xdelay,
              keyboard,
              ph_one,                            // integer equivalent of phase_1 above
              loop_type,
              ROUTINE;


unsigned int sample_time,                        // computed sampling interval
             eprom_clk,                          // preset for timer that runs synchronous counter
             period,                             // fundamantal period
             midpoint,                           // reads the bias point on analog channels

int gloop;
```

```
/*
 Global strings declarations and initialisations
*/

static char *msg[6] = {
" FOR INSTRUCTIONS, PRESS <ENTER> TO CONTINUE <ESC> TO QUIT",
" SET 3-PHASE SUPPLY VOLTAGE TO MINIMUM ",
" POWER UP CONTROL CIRCUIT ..",
" SWITCH ON 3-PHASE SUPPLY WHILE SET TO MINIMUM ",
" SET UP PREFERENCES AND SETPOINTS.. ",
" PUSH 'START' BUTTON ON CONSOLE WHEN READY"};

static char *channel[10] = {
"  1 2 3 4 5 6 7 8",
" ",
"1 - Var   Setpoint ",
"2 - Volts Setpoint ",
"3 - Control Gain   ",
"4 - Inst. volts",
"5 - Inst. current",
"6 - Vars measured",
"7 - ( spare )",
"8 - ( Spare )"};

static char *help[12] = {
" ===  HOT KEYS ===",
" ",
"H Help / Channels",
"P plots on/off",
"V volts spect",
"I current spect",
"A Aux channel spect",
"S Save waveforms",
" ",
"2-4 plot cycles",
};

unsigned char adc_lines[12] = { 255,15,0,32,200,230,180,123,23,210,11,5};

/*
 Function prototypes declared here - in order of appearance
*/

void      io_set(void);
int       ask_user(void);
void      legend(char opt);
void      get_fall(void);
void      get_rise(void);
int       graph_view(void);
void      set_screen(void);
void      graph_margin(int x, int y, int wide, int high, int style );
void      plot_grid(int x, int y, int wide, int high, int space);
void      get_adc(void);
void      show_adc(void);
char      trap_zero(void);
unsigned int      mains_period(void);
```

```
int      round_off(unsigned int number, unsigned int divisor);
void     sync_start();
void     run_t1();
void     show_limit(unsigned char state);
void     control_status(void);
unsigned int     check_reset(unsigned char request);
void     sampler(unsigned char store1[], unsigned char store2[], unsigned char store3[]);
void     freeze(void);
void     plot_graph(int col1, int col2, int col3);
void     plot_psd(float x_axis[], int col, char analyse);
void     spectral(unsigned char wave[],char analyse);
int      control(int var_set, int var_meas, int loop_type);
void     disp_all(int preset, unsigned int cycle, unsigned char update);
void     msglin(char *text, int col, unsigned char beep);
void     store_view(int *col, int *bkcol, struct viewporttype *xview, struct linesettingstype *xline);
void     rstore_view(int col, int bkcol, struct viewporttype xview, struct linesettingstype xline);

/*
   Function main - calling function  to the various subroutines
*/
int main()

{                                                    // start main - ROUTINE bit 0

 /* initialise */

  int init_ok, run_ok;                               // graphics mode succesful, reset statue
  int dummy;                                         // variable for programmer's use
  int loop;                                          // loop counter variable for PLL action
  int var_set, var_meas;                             // VAR or PF setpoint and measurement
  int user_go;                                       // monitors port for console 'GO' status
  int words = eprom_words;                           // number of active EPROM states ( 2400 )
  char any_key, g_plots, locked;                     // keyb'd activity, plots on/off, Phase lock on
  char analyse, user_in[4], help_opt;                // spectrum select, text input, toggle help screen
  char first run;                                    // used to signal for initial set ups e.t.c.
  unsigned int temp, eprom_temp;                     // frequently accessed general purpose variables
  unsigned char monitor, channel;                    // general purpose, channel to sample e.tc

/*
   Ask user for first phase and plot preferences
*/
 ROUTINE = 255;                                      // set all bits to true to signal first run
 init:

  first_run = ROUTINE;                               // first run true; initialise variables
  first run &= 1;                                    // first run is true if initial run
  eprom_temp =0;                                     // temp storage for PL looping

  // get user values for initial setup

  cycles = 3;                                        // default
  g_plots = 1;                                       // default
  locked =0;                                         // if zero, frequency measurement required
/*
   check for graphic system and switch to graphics
*/
  init_ok = graph_view();                            // auto- detects graphics system in use
```

```
 if (init_ok == 1) exit (1);                    // Abort run if error initialising graphics
 analyse = 4;                                   // initialise for PSD on voltage waveform

/*
   Set up user screen and prompt user for setup
                                                */
begin:                                          // re-looping program starts here

   io_set();                                    // initialise and set up hardware on interface
card
   set_screen();                                // set up graphics screen with borders e.t.c.
   dummy = ask_user();                          // dummy set to 1 if user presses ESC key
   ph_one = phase_1/1;                          // type conversion
   ph_one -= 25;                                // compensate for zero cross error
   alpha = ph_one;                              // initialise preset for zero compensation
   if (dummy) goto end_main;                    // quit program in ESC has been activated


//--------- loop here waiting for user to activate console 'GO' ----------

   outp(port_1a, ph_one);                       // output the initial preset to the counter
   user_go = 1;                                 // set variable for access by other routines
   while (user_go)                              // repeat while no reset condition is present
    {                       // start WHILE loop 1
   get_adc(0);                                  // initialise ADC hardware but do not display
results
   show_adc();                                  // display ADC values
   user_go =  inp(port_2c);                     // read port with ADC control and options
   user_go &= 32;                               // test for console START/RESET
   if (kbhit()) {                               // check keyboard status
                  any_key = getch();            // if input present, identify
                  if (any_key == 27){           // if ESC, exit program, else ignore
                                     closegraph();
                                     exit(1);
                                     }
                  }
    }                                           // end WHILE

 // time mains period

run_ok = 1;

while (run_ok)
{                                               // start WHILE

/* run_ok can be altered by the ESC key or console reset button */

 if (locked) goto skip_lock;                    // if PLL locked, skip next routine, otherwise ...
   temp = mains_period();                       // measure supply frequency - return zero on
error
   locked = 1;                                  // initialise test variable
   if (!temp)                                   // If error has occurred ..
     {
        check_reset(1);                         // check if console RESET active
        msglin(" !! BAD OR MISSING ZERO CROSSING SIGNAL !! ",12,1);
        goto end_main;                          // exit program
     }
   else
```

```
  period = temp;                                    // set mains period to most recent

skip_lock:                                          // jump to here if PLL action not required

 // compute eprom clock rate

  temp = round_off(period, words);                  // compute timing period for EPROM counter
  eprom_clk = temp;                                 // store result in appropriate global

 // compute sampling interval

  sample_time = cycles * round_off(period, (scrn_width-185)); // no of cycles

 // if first run , synchronise start

  if (first_run) sync_start();

 // Execute phase locked loop action

phase_lock:

  run_ok = !check_reset(0);                         // check if any reset conditions have occurred
  if (!run_ok) goto end_main;                       //   and exit if so

  monitor = 0;                                      // initialise number of times frequency checked
  temp = mains_period();                            // measure mains period
  temp = round_off(temp, eprom_words);              // compute required counter preset
  if (temp != eprom_clk && monitor < 3 )            // if preset different .repeat measurment thrice...
       {
        eprom_temp += temp;                         // store result
        monitor ++;                                 // increment monitor
        goto phase_lock;
       }
  if (temp != eprom_clk && monitor == 3)            // if different over three cycles
       {                                             // start IF
       eprom_clk = eprom_temp/3;                    // compute average of last three readings
       period = temp * eprom_words;                 // compute period
       eprom_temp = 0;                              // reset temprorary storage
       run_t1();                                    // change preset on timer that runs counter
       goto phase_lock;                             // re-check in case frequency changing still
       }                    // end IF

       // read var_set and var_meas

  get_adc(0);                                       // use argument 1 to use keyboard for set point
  show_adc();                                       // display all channels read

 // run control algorithm and change alpha if required

  monitor = 0;                                      // number of times control effected undisturbed
  var_set =(int) adc_lines[0];                      // read ADC set point only
  var_meas = (int) adc_lines[3];                    // read VAR measurement

  temp = control(var_set, var_meas, loop_type);     // run control algoritm to get new preset
  control_status();
  if (temp != alpha)                                // if new preset differs from previous
       {                                             // start IF
        msglin("Controlling..", 15,0);              // inform user that preset is being changed
```

```
        alpha = temp;                                   // store preset in appropriate global
        get_fall();                                     // choose a safe instant to change delay
        outp(port_1a,alpha);
        monitor ++;
       }
  else                                                  // end IF
       monitor = 0;

  disp_all(alpha,period,0);                             // display current delay angle and frequency

  if (monitor) goto phase_lock;


// check if change in var_set
// if change, execute control and continue
// until control stable

    monitor = adc_lines[0];                             // previous set point
    get_adc(0);                                         // get new ADC values, 1 if keyb'd option
    if ((monitor/2.0) != (adc_lines[0]/2.0))            // check for change in set point > LSB
        {                       // start IF
        msglin("Tracking changing set point ..",15,0);  // inform user of set point tracking
        goto phase_lock;                                // check frequency stability - more important
        }
                                                        // end IF

// ------------ check if keyboard activated ------------ //

if (kbhit())
    {
    any_key = getch();
    any_key = tolower(any_key);
    switch (any_key)
            {
            case 's': freeze();             break;      // write samples to disk
            case 'h': {                                 // toggle between help screen and screen
                      toggle(help_opt);                 // showing ADC channel assignments
                      legend(help_opt);     break;
                      }
            case 'p': toggle(g_plots);      break;      // enable/disable graph plotting
            case 'i': analyse = 5;          break;      // set spectrum analyser to current
            case 'v': analyse = 4;          break;      // set spectrum analyser to voltage
            case 'a': analyse = 8;          break;      // set analyser to misc. 3rd signal
            case '1': cycles = 1;           break;      // set number of plotted cycles to entry
            case '2': cycles = 2;       break;
            case '3': cycles = 3;       break;
            default:  fflush(stdin);                    // other keys - clear keyboard buffer

            }                                           // end switch
    }                               // end if (kbhit)

  // if control stable and plotting enabled, sample voltage waveform

  if (g_plots)                                          // if plots active proceed with next section
    {                                                   // start if
    msglin("Sampling..",15,0);                          // display message on screen
    sampler(v_samp, i_samp, q_samp);                    // sample all three assigned channels
    plot_graph(12, 10, 13);                             // display sampled data
```

```
        switch (analyse)                                    // select channel for spectral analysis
          {
          case 4: spectral(v_samp, analyse);        break;
          case 5: spectral(i_samp, analyse);        break;
          case 8: spectral(q_samp, analyse);        break;
          }
    }                                                       // end if(g_plots)

 // scan for reset

run_ok = !check_reset(0);

// re-loop at "time mains period"
ROUTINE &= 254;                                             // clear bit 0 to signal first run complete
}                                                           // end WHILE

   end_main:
   getch();
   closegraph();

/*      Ask user if Exit or Re-run required          */

        gotoxy(1,24);
        printf(" E to exit    R to Run ..");
        any_key = 0;
        while (any_key == 0)
        {
        any_key = getch();
        any_key = tolower(any_key);
        if (any_key != 'r' && any_key != 'e') any_key = 0;
        }

        if (any_key == 'r' ) goto init;

        // clrscr();

/*
        END PROGRAM                                 */

return 0;

}                                                           // end MAIN()


/* SUBROUTINES FOLLOW */
```

```
/*
```

Function io_set - initialises hardware on 8255 control card

```
*/
void io_set(void)
{
/* procedure sets up the 8255 I/O chips and 8253 Timer I.C. on the
  SI-8255 control card as per description above. routine bit 0 */

short int val;

        outp(port_1,136);                   // sets A & B to o/p, C to in/out
        outp(port_1a, 254);                 // high preset to switch off MOSFETS
        outp(port_1b,25);                    // select off (1), preset high (0)

        val = inp(port_1c);                 // limit off(0), o/p inc/dec off (11)
        val &= 240;                          // Dummy read
        outp(port_1c, val);                 // reset all outputs. Timer gates off
         //                                 // write to port 1c.
        outp(port_2, 154);                   // A & B inputs, C is i/o
        val = inp(port_2c);                  // Dummy read on port 2c
        val &= 240;                          // reset all ouputs
        outp(port_2c,val);
        val = inp(port_2b);                  // dummy read on port 2b
        val = inp(port_2a);                 // dummy read on port 2a

        outp(timers,56);                     // Timer 0 - s/w strobe  - binary
        outp(timers,118);                   // Timer 1 - square wave - binary
        outp(timers,182);                   // Timer 2 - square wave - binary
                                             //

        val = inp(port_1c);
        val |= 7;                            // activate timer gates
        outp(port_1c, val);                 // in readiness for preset values

        ROUTINE |= 1;                       // set bit 0 true to indicate this function
                                            // has initialised
return;
}

/*
```

Function graph_view - Detects and sets screen graphics mode

```
*/

// ROUTINE bit 2

int graph_view(void)
{
 int loop, maxx, maxy;
 int gdriver = DETECT, gmode, errorcode;

 initgraph(&gdriver, &gmode,"..\\bgi");                    // turbo C/C++ function

  if (errorcode != grOk) /* error initialising */
        { printf ("Error : %s\n", grapherrormsg(errorcode));
          printf ("Any key to return ..");
          getch();
          return 1;
        }
```

```
// if graphic initialisation successful, proceed

  maxx = getmaxx();
  maxy = getmaxy();

  /* now pass on values to globals scrn_width and scrn_height */

  scrn_width = maxx;
  scrn_height = maxy;

  return 0;
}

/*
```

Function set_screen - Sets up User Interface and grid */

```
void set_screen(void)
{
/* uses the global variables scrn_width and scrn_height to draw */

  int loop, maxx, maxy, lspace, oldcolor, oldbkcolor, bar_high;
  struct viewporttype viewinfo;
  struct linesettingstype lineinfo;
  char message[30],help_opt;

  maxx = scrn_width;
  maxy = scrn_height;

/*
```

Store view port settings for restoration later */

```
store_view(&oldcolor,&oldbkcolor,&viewinfo,&lineinfo);

  setcolor(5);
  setlinestyle(0,0,3);

// Draw thick lines top & bottom of screen

  for (loop = 0; loop < 16; loop += 4)
  {
  line (0, loop, maxx, loop); line (0, maxy-loop, maxx,maxy-loop);
  }
  line (0, maxy-loop, maxx,maxy-loop);
  loop += 4;
  line (0, maxy-loop, maxx,maxy-loop);

// Draw borders around graphs and ADC display areas

  setlinestyle(0,0,1);
  setcolor(7);
  gloop = loop;                                    // establish global loop for other subroutines
  bar_high = (gloop+255);
  graph_margin(0,loop-4, maxx, maxy-loop-25,2);
  setlinestyle(0,0,3);
  graph_margin(maxx-160,loop,160-3,maxy-loop-30,1);
  setcolor(1);
  setlinestyle(0,0,1);
```

```
// Set up grid

  plot_grid(5,20,maxx-168,maxy-50,10);

// Set up legend under ADC channel display screen

        setviewport (maxx - 155+1,10+bar_high, maxx-5-1, maxy-loop-12,1);
        clearviewport();
        rstore_view(oldcolor,oldbkcolor,viewinfo,lineinfo);
        help_opt = 1;
        legend(help_opt);

// Restore Viewport to original and return to calling function

    rstore_view(oldcolor,oldbkcolor,viewinfo,lineinfo);

bar_high += 0;                                    // suppress compiler warning messages
return;
}


/*
   Procedure legend - displays ADC channels or help screen.   */

void legend(char opt)

// set opt to 1 for help, 0 for ADC channels

{
  int loop, maxx, maxy, bar_high, lspace, oldcolor, oldbkcolor;
  struct viewporttype viewinfo;
  struct linesettingstype lineinfo;
  char message[30];

  maxx = scrn_width;
  maxy = scrn_height;

  bar_high = gloop + 255;

/*
   Store view port settings for restoration later   */

store_view(&oldcolor,&oldbkcolor,&viewinfo,&lineinfo);

// new viewport

  setviewport (maxx - 155+1,10+bar_high, maxx-5-1, maxy-gloop-12,1);
  clearviewport();

  for (loop = 0, lspace = 0; loop < 10; loop ++, lspace += 15)
        {
        strcpy(message,channel[loop]);
        if (opt) strcpy(message, help[loop]);

        if (loop == 0)
          setcolor(15);
```

```
        else
          setcolor(14);
        outtextxy(2,lspace,message);
        }

// restore original view settings and return to calling function

  rstore_view(oldcolor,oldbkcolor,viewinfo,lineinfo);

return;
}


/*
   Function graph_margin - draws a margin to specified dims.   */

void graph_margin(int x, int y, int wide, int high, int style )
{
int loop, int endx, endy, line_space, line_wide;
struct linesettingstype lineinfo;

//   Establish settings and scale all accordingly
*/
        getlinesettings(&lineinfo);
        line_wide = lineinfo.thickness;
        line_space = 2*line_wide;
        endx = x+wide-line_space;
        endy = y+high-line_space;
        rectangle(x,y,x+wide,y+high);
        if (style==2) rectangle(x+line_space,y+line_space,endx,endy);
return;
}


/*
   Function plot_grid - Draws a grid on screen for plotting   */

void plot_grid(int x, int y, int wide, int high, int space)
{
/* plots a grid in preset color and line style, grid space = space */

        int loop;

//   Do Horizontal plots, then vertical

for (loop=y;loop< y+high;loop += space) line (x,loop,x+wide,loop);
for (loop =x;loop < x+wide; loop += space) line (loop, y,loop,y+high);

return;
}
```

```
/*
   Function ask_user - Guides user thru start up sequence                    */

int ask_user(void)
{
        /* returns 1 if ESC activated during course of set up */

int loop,any_key;
unsigned int temp, temp2;
char update;

// Prompt user to input first phase in degrees

char new_text[6], query[60], next_char, lastx;

strcpy(query,"Angle, in degrees, of first phase.. (e.g. -22.5)..");
next_char = lastx =  strlen(query);
msglin(query,15,0);
strcpy(new_text,"");                                          // initialise character string
any_key = 0;
while (any_key != 13)                                         // while any_key
    {
        if (kbhit())
          {                                  // if kbhit()
           any_key = getch();
           if (any_key ==8 && lastx < next_char)              // handle backspace
             {                               // if any_key
                  next_char --;
                  new_text[next_char-lastx]=query[next_char]='\0';
                  msglin(query,15,0);
             }                               // end if any_key
            if (strrchr("0123456789.-+",any_key))             // numbers and signs only
                  {                               // if strrchr()
                  new_text[next_char-lastx]=query[next_char]=any_key;
                  next_char ++;
                  new_text[next_char-lastx]=query[next_char]='\0';
                  msglin(query,15,0);
                   }                              // end if strrchr()
          }                                  // end if kbhit
        }                                    // end while any_key
     if (!strcmp(new_text, "")) strcpy(new_text,"-22.5");
     sscanf(new_text, "%f",&phase_1);
     if ( phase_1 < 0 ) phase_1 = -phase_1;
     phase_1 = (phase_1 * 150.0)/22.5;
     strcpy(query,"First phase has been set to ");
     strcat(query, new_text);
     next_char = strlen(query);
     query[next_char] = 'o';
     query[next_char + 1]='\0';
     msglin(query,15,0);
     getch();

// Loop thru messages while updating screen

        for (loop =0; loop < 5; loop ++)
          {
           msglin(msg[loop],10,0);
```

```
        if (loop == 4 )                                    // set up preferences
                {
                temp2 = inp(port_1b);                      // read port
                temp2 &= 254;                              // set LSB ( select ) low
                outp(port_1b,temp2);                       // activate select
                }                                          // select enabled

        trapkey:
              any_key = 0;
              while (!kbhit())
              {
                if (loop > 2 )
                {
                get_adc();
                show_adc();
                if (loop == 4)
                {
                        alpha = control(adc_lines[0], 0,0);
                        disp_all(alpha, temp, 1);
                }
                }
              }                                    // end while
         any_key = getch();

         if (any_key == 27) return 1;
         if (any_key != 13) goto trapkey;
         if ((loop ==3) && (any_key == 13))
                {                                            // start IF
                  temp = mains_period();
                  if (temp == 0 )
                        {                                    // start IF
         msglin("!! BAD OR MISSING ZERO CROSSING SIGNAL !!",12,1);
         goto trapkey;
                        }                            // end IF
                }                                  // end IF

  }                                                  // end for

                if (loop > 4 )
                 {
                 temp2 = inp(port_1b);
                 temp2 |= 1;
                 outp(port_1b, temp2);              // select disabled
                 }
disp_all(alpha, temp, 1);
msglin(msg[loop],10,0);
midpoint = adc_lines[6];
return 0;
}                                                  /* end function ask_user() */
```

```
/*
   Function get_adc - Reads all 8 ADC channels to memory                    */

void get_adc(void)

{
  /* reads adc channels and store results in appropriate adc_var.
     Procedure reads all 8 channels on an 8 channel multiplexed ADC */

char val, channel;

    for (channel = 8; channel > 0; channel --)
          {                                                    // start for
          val = inp(port_2c);
          val |= 8;
          outp(port_2c,val);                                   // deselect ADC required by h/w
          val &= 248;                                          // clear previous address
          val |= (channel - 1);                                // set up new channel address
          outp(port_2c, val);                                  // write to port
          val &= 247;                                          // prepare to enable ADC
          outp(port_2c, val);
          val = 1;                                             // preset variable for while loop

          while (val) {                                        // start while
                   val = inp(port_2c);
                   val &= 16;
                   }                                           // end while

          adc_lines[channel-1] = inp(port_2b);
          }
                                                               // end for
return;
}


/*
   Function show_adc - Displays ADC values as bar chart on screen           */

void show_adc(void)
{                                                              // ROUTINE bit 1
  int loop, plot, bar_high, maxx, maxy, oldcolor, oldbkcolor;
  char first_run;
  struct viewporttype viewinfo;
  struct linesettingstype lineinfo;

  maxx    = scrn_width;
  maxy    = scrn_height;
  plot    = 18;
  maxy += 0;
  bar_high = (gloop+255);

 /*
   Store view port settings for restoration later                           */

 store_view(&oldcolor,&oldbkcolor,&viewinfo,&lineinfo);

 //    Create view port and plot bar graphs
```

```
setviewport(maxx-155+1,gloop+1,maxx-5-1,bar_high,1);
first_run = ROUTINE;
first_run &= 2;                                    // check if bit 1 set to signal first run
if (first_run) {
                setfillstyle(10,14);
                bar(5,bar_high-255,10,bar_high);
                }
setlinestyle(3,0,1);  setfillstyle(1,6);  setcolor(7);

for (loop = 0; loop < 8; loop ++, plot += 16)
   { .
        setfillstyle(0,6);
        bar(plot,bar_high-255,plot+5,bar_high-adc_lines[loop]);
        setfillstyle(1,6);
        bar(plot,bar_high-adc_lines[loop], plot+5,bar_high);
   }
```

// Restore original view port settings and return to calling function

```
        rstore_view(oldcolor,oldbkcolor,viewinfo, lineinfo);
ROUTINE &= 253;                                    // clear bit 1 to signal first run complete
return;
}
```

```
/*
```

Function get_fall - Traps falling edge of zero cross

```
*/
void get_fall(void)
{
unsigned char val;

   val = 0;
   while (!val) {
          val = inp(port_1c);  val &= 128;
          }
   while (val){
          val = inp(port_1c);   val &= 128;
          }
return;
}                                                  // end get_fall()

/*
```

Function get_rise - Traps rising edge of zero crossing signal

```
*/
void get_rise(void)
{
unsigned char val;

   val = 1;
   while (val){
          val = inp(port_1c);  val &= 128;
          }
   while (!val){
          val = inp(port_1c);  vall &= 128;
          }
return;
```

```
}                                                   // end get_rise()

/*
```

Function trap_zero - Captures transitions on zero crossing signall

```
*/
char trap_zero(void)
{
/* returns 0 if frequency O.K. */

unsigned char watch, val, pval, bad_time;

        val = inp(port_1c);
        val &= 128;
        pval = val;
        watch = 0;

        while (val == pval && !watch)
                {
                val = inp(port_1c);
                watch = val;                    // routine returns 1 if error
                watch &= 64;
                val &= 128;
                }
return watch;
}

/*
```

Function mains_period - measures input signal frequency

```
*/
unsigned int mains_period(void)
{
/* returns 0 if frequency lower than permissible of about 45Hz */

int cycle;
unsigned char transit, val1, val2;

// start by configuring timer 2 to set high on time out

        cycle = 0;                                  // to be modified by procedure
        outp(timers, 56);                           // s/w strobe - binary
        outp(timers, 176);                          // set high on terminal count
        outp(timer_2, 255);
        outp(timer_2, 255);                         // start watch dog timer

transit = trap_zero();                              // check that zero cross o.k.
                                                    // use transition as start
if (transit) goto mains_exit;

        outp(timer_0, 255);
        outp(timer_0, 255);
        outp(timer_2, 255);
        outp(timer_2, 255);

transit = trap_zero();                              // capture mid transition

if (transit) goto mains_exit;
```

```
transit = trap_zero();                          // capture last transition

if (transit) goto mains_exit;

        val1 = inp(timer_0);                    // read timer value
        val2 = inp(timer_0);                    // read timer value
        _AL = val1;                             // uses register pseudo variables to
        _AH = val2;                             // conveniently manipulate 16-bit value
        _AX = ~_AX;
        cycle = _AX;

mains_exit:

        outp(timers, 182);
        outp(timers, 56);                       // restore timers

return cycle;
}


/*
   Function round_off - returns rounded quotient   */

int round_off(unsigned int number, unsigned int divisor)
{
/* executes integer divison and rounds off rather than truncate */

int quotient, fraction;

        quotient = number / divisor;
        fraction = 10 * (number % divisor);
        fraction = fraction / divisor;
        if (fraction >= 5 ) quotient ++;

return quotient;
}


/*
   Procedure Sync_start - synchronises firing of power devices   */

void sync_start()
{
unsigned char val1, val2;

          get_rise();
          _AX = eprom_clk;                      // use register pseudo variables to
          val1 = _AL;                           // conveneiently split 16 bit preset into
          val2 = _AH;                           // low (AL) and high (AH) bytes
          outp(timer_1, val1);
          outp(timer_1, val2);                  // start EPROM clock
          val1 = inp(port_1b);
          val1 |= 2;
          outp(port_1b,val1);                   // activate sync_start
return;
```

```
}
```

/*

Proc Control - executes open or closed control algorithm

*/

```
int control(int var_set, int var_meas, int loop_type)
{
/*      The argument loop_type specifies which of open or closed loop control has been
        requested by the user. Control is assumed linear at all times.

        Open loop assumes a straight line relationship of the form y = mx +c where y = preset,
        m = scaling constant 100/255, x the control variable var_set in the range 0-255, and c the
        ordinate = initial preset - 50

        Closed loop computes error = var_set - var_meas and calculates the incremental value of
        the preset that will cause the error  to reset to 0, i.e. var_meas = var_set.
        The control is ATC ( air to close ) i.e. if error large, reduce preset

        Algorithm: New Preset = Current preset + (100/254)(var_set - var_meas)
*/

int preset, temp, limit_high, limit_low;

limit_high = ph_one + 50;
limit_low  = ph_one - 50;
preset = alpha;                                  // start with preset = present alpha

// Open loop control

        if (loop_type == 0)                      // open loop
        {                                        // start if (loop_type...)
         temp = (100*var_set);
         temp = round_off(temp,254);
         preset = temp + ph_one - 50;
        }                                        // end if (loop_type...)

// Closed loop control

        if ( loop_type == 1)                     // closed loop
        {                                        // start if (loop_type ...)
         temp = 100 * abs(var_set - var_meas);
         temp = round_off(temp,254);             // Valid only for unsigned ints
         if (var_set > var_meas) preset = alpha + temp;
         if (var_set < var_meas) preset = alpha - temp;
         if (var_set == var_meas) preset = alpha;
        }                                        // end if (loop_type ...)

// Check for control limiting values of the delay angle

        if ((preset > limit_low) && (preset < limit_high)) show_limit(0);

        if (preset <= limit_low)
          {
           show_limit(1);
           preset = limit_low;                   // clamp preset to minimim allowed
          }
```

```
        if ( preset >= limit_high)
          {
           show_limit(1);
           preset = limit_high;      // clamp preset to maximum allowed
           }

return preset;
}                                                    // End function control()


/*
   Function Run_t1 - changes eprom clock rate if frequency changes
                                                                    */

void run_t1()
{
unsigned char val1, val2;

        _AX = eprom_clk;                             // use register variable for 16-bit manipulation
        val1 = _AL;                                  // extract low byte
        val2 = _AH;                                  // extract high byte
        outp(timer_1, val1);                         // write low byte
        outp(timer_1, val2);                         // write high byte
return;
}


/*
   Proc Show_limit - activates or deactivates LIMIT inidicator
                                                                    */

void show_limit(unsigned char state)
{
int status, mask;

status = inp(port_1b);                               // read current status of port

   if (state == 0)                                   // state is 1 to switch on limiting indicator
   {
    mask = 251;                                      // set appropriate mask
    status = status & mask;                          // set up output value
   }
   if (state == 1)
   {
    mask = 4;
    status = status | mask;
   }

outp(port_1b,status);                                // write outcome of processing to port

return;
}                                                    // End fucntion show_limit()
```

```
/*
```
Proc control_status - updates LED display for INC/DEC ctrl
```
*/

void control_status()
{

static short int prev_alpha = alpha;
int set_point;
unsigned char led_status, val1, val2;

        set_point = adc_lines[5];                   // read current set point value
        led_status = inp(port_1b);                  // input current led status

        if (set_point == alpha) led_status |= 24;   // switch off both indicators if output static

// compute required value for output increasing when set-point greater than present value

        if (set_point > alpha)
          {
          led_status &= 231;                        // clear previous status
          led_status |= 16;                         // set up new status
          }

// compute required value for output decreasing when set-point less than present value

        if (set_point < alpha)
          {
          led_status &= 231;                        // clear previous status
          led_status |= 8;                          // set up led status
          }
  outp(port_1b, led_status);                        // update leds
  return;
 }                                                  // End function control_status()


/*
```
Function check_reset - checks for console reset status
```
*/

unsigned int check_reset(unsigned char request)

{
/* the argument request determines whether or not reset action should be executed on
   establishing reset conditions */

unsigned int reset_status;
unsigned char temp, val1, monitor;

     monitor = reset_status = 0;
     while (monitor < 3 )                           // check reset more than once to ensure
     {                                              // signal is not transient or noise
     temp = inportb(port_2c);                       // input port_2c status
     temp &= 32;                                    // mask value to check reset bit
     temp |= request;                               // or with request to determine action
     if (temp)  { monitor ++; reset_status=1; }     // if reset required, double check
```

```
    if (!temp) { monitor = 3; reset_status = 0; }          // if no reset required, exit
    }

    if (reset_status)                                      // proceed with reset if valid
          {                                                // start IF

// Switch off Power devices and pause all control

          val1 = inp(port_1c);
          val1 &= 248;
          outp(port_1c, val1);                             // stop timers. Gates off

          outp(port_1a, 254);                              // push EPROMS to off states

          val1 = inp(port_1b);                             // sync_start disabled
          val1 &= 253;
          outp(port_1b, val1);

// Inform user of isolation and await restart

          msglin("CONSOLE RESET! SYSTEM ISOLATED!. . . Press Any key",15,1);

            reset_status = 1;                              // return value
           }                                               // end IF
return reset_status;
}
```

```
/*
******* DATA ACQUISITION (SAMPLERS) ROUTINES **********  */

/*
Function sampler - samples specified ADC channel  */

void sampler( unsigned char store1[], unsigned char store2[], unsigned char store3[] )
{
unsigned char val, select;
static char channel[3];
unsigned int hi_byte, lo_byte;
int loop;

channel[0] = 4;                          // ADC channels to sample
channel[1] = 5;                          // for volts (4), current (5)
channel[2] = 8;                          // and miscellaneous signal (8)

        _AX = sample_time;               // use register pseudovariables
        lo_byte = _AL;                   // to extract 8-bit bytes from
        hi_byte = _AH;                   // 16-bit value

        channel[0] --;                   // channell address is channel number - 1
        channel[1] --;
        channel[2] --;

get_rise();                              // synchronise with rising edge of zero cross
        outp(timer_2,lo_byte);
        outp(timer_2,hi_byte);           // sampling timer begins to run

for (loop = 0; loop < SAMPLES; loop++)   // start FOR loop for number of samples
   {
   for (select = 0; select < 3; select ++)   // start nested FOR loop for channels
         {
          val = inp(port_2c);
          val &= 248;                    // clear old address
      val |= channel[select];
          outp(port_2c, val);            // set up address

          val = inp(port_2c);
          val &= 247;                    // mask all but CS line on ADC
          outp(port_2c, val);            // activate ADC

          val = 1;
          while (val) {                  // start while (val)
                val = inp(port_2c);      // read ADC conversion status
                val &= 16;               // check if ADC conversion complete
                    }                    // end while (val)

          switch (select)                // select appropriate sample storage
                   {                     // start switch()
                    case 0: store1[loop] = inp(port_2b); break;
                    case 1: store2[loop] = inp(port_2b); break;
```

```
                case 2: store3[loop] = inp(port_2b); break;
                }                                                   // end switch()

        val = inp(port_2c);
        val |= 8;
        outp(port_2c, val);                                         // deactivate ADC

        }                                                           // end nested FOR loop


        val = 0;
        while (!val)
                {                                                   // start while (!val)
                 val =inp(port_1c);
                 val &= 64;
                }                                                   // end while (!val)

        while (val)
                {                                                   // start while (val)
                 val = inp(port_1c);
                 val &= 64;
                }                                                   // end while (val)
      }                                                             // end main FOR (loop)
return;
}                                                                   // End fucntion sampler()


/*
        Function freeze - writes samples to disk                    */

void freeze()
{

// creates auto-named file and writes samples from memory as ASCII text
// File names are of the form SAMP_1.DAT, SAMP_2.DAT e.t.c.

static char file_num = 0;
int loop;
FILE *fp1;
char ch_1[16],ch_2[10], file_1[14],tag[10];

file_num ++;                                                        // increment file name number
itoa(file_num,tag,10);                                              // convert file number to string
strcpy(file_1,"Samp_");                                             // set up general filename
strcat(file_1,tag);                                                 // concantenate file number
strcat(file_1,".dat");                                              // add a file extension

if ((fp1 = fopen(file_1,"wb+")) == NULL)                            // check for error initialising file
  { msglin("Error creating data file!!",12,1);
    goto file_done;                                                 // Abort sample writing
  }

loop = 0;

for (loop =0; loop < SAMPLES; loop ++)                              // start FOR loop for number of samples
  {
   strcpy(ch_1," ");                                                // clear string
```

```
   itoa(v_samp[loop],ch_2,10);                  // convert voltage sample to ASCII text
   strcat(ch_1,ch_2);                           // prefix with white space
   strcat(ch_1," ");                            // append another white space
   itoa(i_samp[loop],ch_2,10);                  // convert current sample to ASCII
   strcat(ch_1,ch_2);                           // concantenate with voltage sample
   strcat(ch_1, " ");                           // append white space
   itoa(q_samp[loop],ch_2,10);                  // convert third channel to ASCII
   strcat(ch_1,ch_2);                           // concantenate with first two samples
   ch_2[0] = '\n';                              // terminate with new line and
   ch_2[1] = '\r';                              // carriage return combination for DOS format
   ch_2[2] = '\0';                              // convert array to legal string
   strcat(ch_1,ch_2);
   fputs(ch_1,fp1);                             // write string with the three samples
  }

 if (fclose(fp1) != 0)
   msglin("Error closing data file!!",12,1);

file_done:                                      // label for GOTO instructions

return;
}                                               // End function freeze()


/*
 Function plot_graph - plots all sampled data to screen
*/
// ROUTINE bit 2
void plot_graph(int col1, int col2, int col3)

{
unsigned int loop, midy;
unsigned int plot_val1, plot_val2, plot_val3, plot_val4, plot_val5, plot_val6;
int maxx, maxy, x, y, xend, yend;
int oldcolor, oldbkcolor, bkcol;
char first_plot;

struct viewporttype viewinfo;
struct linesettingstype lineinfo;

double scaler = 0.75;

/*
   Store view port settings for restoration later   */

store_view(&oldcolor,&oldbkcolor,&viewinfo,&lineinfo);

// Create view port and establish req'd dimensions

maxx = scrn_width;
maxy = scrn_height;

x = 15; y = maxy/6; xend = maxx - 185; yend =  maxy/2 + 5;

setviewport(x, y, xend, yend, 1);

midy=(yend-y)/2;
first_plot = ROUTINE;
```

```
first_plot &= 4;                                        // test bit 2
if (first_plot)
        {
        clearviewport();
        x -= 2; y -= 2; xend +=2; yend += 2;
        setviewport(x, y, xend,yend,1);
        rectangle(0,0, xend - x, yend - y);
        x += 2; y+= 2; xend -= 2; yend -= 2;
        setviewport(x, y, xend, yend, 1);
        setcolor(12);outtextxy(3,01,"Voltage");
        setcolor(10);outtextxy(3,10,"Current");
        setcolor(oldcolor);
        }
```

// Plot pixels corresponding to sampled data

```
bkcol = getbkcolor();                                   // used to erase previous sample
for (loop = 0;loop < xend-2; loop +=2)
   {

   setcolor(bkcol);

   plot_val1 = midy+128-(scaler*v_prvs[loop]);
   plot_val2 = midy+128-(scaler*v_prvs[loop+2]);
   plot_val3 = midy+128-(scaler*i_prvs[loop]);
   plot_val4 = midy+128-(scaler*i_prvs[loop+2]);
   plot_val5 = midy+128-(scaler*q_prvs[loop]);
   plot_val6 = midy+128-(scaler*q_prvs[loop+2]);


   line(loop,plot_val1,loop+1,plot_val2);
   line(loop,plot_val3,loop+1,plot_val4);
   line(loop,plot_val5,loop+1,plot_val6);

   plot_val1 = midy+128-(scaler*v_samp[loop]);
   plot_val2 = midy+128-(scaler*v_samp[loop+2]);
   plot_val3 = midy+128-(scaler*i_samp[loop]);
   plot_val4 = midy+128-(scaler*i_samp[loop+2]);
   plot_val5 = midy+128-(scaler*q_samp[loop]);
   plot_val6 = midy+128-(scaler*q_samp[loop+2]);

   setcolor(col1);  line(loop, plot_val1,loop+1,plot_val2);
   setcolor(col2);  line(loop, plot_val3,loop+1,plot_val4);
   setcolor(col3);  line(loop, plot_val5,loop+1,plot_val6);

   v_prvs[loop] = v_samp[loop];                         // store current sample to use for erasing
   i_prvs[loop] = i_samp[loop];                         // when next plot done
   q_prvs[loop] = q_samp[loop];
   }
```

// Restore view port settings and return to caller

```
        rstore_view(oldcolor, oldbkcolor, viewinfo, lineinfo);

ROUTINE &= 251;                                         // clear bit 2 to signal first run complete
return;
}
/*
```

Function spectral - calculates PSD and writes data to files */

```
void spectral(unsigned char wave[], char analyse)
{

/* the input array contains real values of the sampled waveform as 8 bit unsigned integers.
   This subroutine runs the FFT on the data and produces PSD of the transformed data. This is
    then passed on to the plotting routine in array PSD[]
*/

int i,j,k,loop, isign;
char all_zero;
float *data, Pyy[M], freq[M], samp_f, peak, scaler;
complex fft[M];

data = vector(1,M2);

samp_f = (float)(3000*1000.0/sample_time);                    // clock at 3MHz

// for (loop=1;loop<SAMPLES;loop++) wave[loop] -= 147;    // remove DC offset

        all_zero = 1;
        for (i=1;i<M2; i+=2)
           {
            if (wave[i] != 0 && sample_time !=0) all_zero = 0;
            data[i] = (float)(wave[i]);
            data[i+1]=0.0;
            }
isign = 1;

if (all_zero)  msglin(" Sampled waveform all zeroes ",15,0);

if (!all_zero)
  {
        fourier(data,M, isign);                               // defined in analyser.h header file
        peak = 0;
        j=1;
                for (i=1;i<M2;i+=2, j++) fft[j] = complex(data[i], data[i+1]);
                for (i=1;i<M; i++)
                {
                        Pyy[i]=real(fft[i]*conj(fft[i]));
                        if ((Pyy[i] > peak) && (i>2)) peak = Pyy[i];// store highest
                        freq[i]=(samp_f/M2)*(i-1);              // peak
                }

        scaler = peak/(256.0);

        for (i=1;i<M; i++) PSD[i]=Pyy[i]/scaler;              // PSD is global
        PSD[1]=0;                                             // supress DC spectral component
        plot_psd(freq,7,analyse);                             // call plotting routine
   }

        free_vector(data,1,M);                                // free memory
return;
}

/*
```

Function plot_psd - plots power spectral density chart */

```
/*
  plots power spectral denisty in global array PSD against frequency
  values in array x_axis, color col. ROUTINE bit 3
*/
void plot_psd(float x_axis[], int col, char analyse)
{
unsigned int loop, bplot, bar_high, band;
int maxx, maxy, x, y, xend, yend;
int oldcolor, oldbkcolor, bkcol;
char title[20];
static char prvs_title[20] = " ";
char first_plot;

struct viewporttype viewinfo;
struct linesettingstype lineinfo;

double scaler = 1;

/*
  Store view port settings for restoration later */

store_view(&oldcolor,&oldbkcolor,&viewinfo,&lineinfo);

// Create view port and establish req'd dimensions

maxx = scrn_width;
maxy = scrn_height;

x = 15; y = maxy/2+20; xend = maxx - 185; yend =  maxy-maxy/10;

scaler += 0;
bar_high=yend-y-2;
setviewport(x, y, xend, yend, 1);

first_plot = ROUTINE;
first_plot &= 8;                          // test bit 3 to check if initialisation required
x_axis[0] +=0;                            // supress compiler warning
if (first_plot)
        {
         clearviewport();
         x -= 2; y -= 2; xend +=2; yend += 2;
         setviewport(x, y, xend,yend,1);
         rectangle(0,0, xend - x, yend - y);
         x += 2; y+= 2; xend -= 2; yend -= 2;
         setviewport(x, y, xend, yend, 1);
         setfillstyle(10,14);
         bar(5,y+2,10,bar_high);
         setviewport(x,yend+4,xend,yend+15,1);     // for legend
         clearviewport();
         outtextxy(1,1,"   1 3  5 7 9  11 13  15 17 19  21 23 25 27 29");
         setviewport(x,y,xend,yend,1);
    }


// Plot pixels corresponding to sampled data
```

```
bkcol = getbkcolor();
bplot = x+2;
band=100;
col = 10;

if (analyse == 4) strcpy(title, "Voltage spectrum ");              // select appropriate title
if (analyse == 5) strcpy(title, "Current spectrum ");
if (analyse == 8) strcpy(title, "Harmonic spectrum");
setcolor(bkcol); outtextxy(3,01,prvs_title); strcpy(prvs_title,title);
setcolor(12); outtextxy(3,01, title);setcolor(oldcolor);

// Read samples from array and plot bar graphs

   for (loop = 1; loop <= M/2; loop ++, bplot += (1024/M))
    {
         setfillstyle(0,bkcol);
         bar(bplot,1,bplot+1,yend-y+2);
         if (x_axis[loop]>band)
           {
           col ++;
           if (col > 15) col =10;
           band += 100;
           }
         setfillstyle(1,col);
         bar(bplot,bar_high-PSD[loop], bplot+1,bar_high);
    }

// Restore view port settings and return to caller

         rstore_view(oldcolor, oldbkcolor, viewinfo, lineinfo);
ROUTINE &= 247;                                                    // clear bit 3 to signal first run complete
return;

}
```

```
/*
```
Function Disp_all - Displays operating parameters
```
*/

void disp_all(int preset, unsigned int cycle, unsigned char update)
{

/* ROUTINE bit 4. If update = 1, display open/closed 120/180 options, if 0 ignore
   if 2, display only options settings in addition to fequency and delay angle updates
*/

float frequency, delay_ang;
int maxx, maxy, high, wide, oldcolor, oldbkcolor, x, y, xend, yend, col1, col2, ppset;
struct viewporttype viewinfo;
struct linesettingstype lineinfo;
char fvalue[20], fdisp[50], adisp[50];
unsigned char mode, loop, port_val;
char first_disp;

maxx = scrn_width; maxy = scrn_height;

/*
```
Store view port settings for restoration later
```
*/

store_view(&oldcolor,&oldbkcolor,&viewinfo,&lineinfo);

// Create view port and establish req'd dimensions

   x = 15; y =     gloop+10; xend = maxx - 175; yend = maxy/7;
   setviewport(x,y,xend,yend,1);
   first_disp = ROUTINE;
   first_disp &= 16;                                          // test bit 4
   if (first_disp) {
         clearviewport();
         setcolor (1);
         setlinestyle(0,0,3);
         rectangle(0,0,xend-x, yend-y);
                  }

delay_ang = (float) ((15.00 * (preset - ph_one))/100.00);
frequency =(float) ((50.00 *cycle)/60000.00);
ppset = inp(port_1a);
setcolor(15);
gotoxy(4,3);
printf("Freqn = %3.2fHz",frequency);
gotoxy(4,4);
printf("Delay = %2.2f°  %d ",delay_ang, ppset);

if (update) {
                  mode = inportb(port_2c);
                  mode &= 128;
                  if (mode)          { col1 = 15; col2 = 8; }
                  else               { col1 = 8; col2 = 15; }

                    setcolor(col1);
                    outtextxy(5*xend/12, 10,"_ Mode - 180");
                    setcolor(col2);
                    outtextxy(5*xend/12, 25,"_ Mode - 120");
```

```
                loop = inportb(port_2c);
                loop &= 64;
                if (loop == 0)      {col1 = 15; col2 = 8; }
                else                { col1 = 8; col2 = 15; }

                  setcolor(col1);
                  outtextxy(2*xend/3,10,"_ Loop - OPEN");
                  setcolor(col2);
                  outtextxy(2*xend/3,25,"_ Loop - CLOSED");
        }

// Restore view port settings and return to caller

        rstore_view(oldcolor, oldbkcolor, viewinfo, lineinfo);
ROUTINE &= 239;                                    // Clear bit 4 to signal first run complete
return;
}


/*
 Function Msglin - Displays graphics mode text in bottom screen
                                                                  */

void msglin(char *text, int col, unsigned char beep)
{
char message [80];
int locx, locy, x, y, xend, yend, wide, high, oldcolor, oldbkcolor;
struct viewporttype viewinfo;
struct linesettingstype lineinfo;

/*
   Store view port settings for restoration later   */

store_view(&oldcolor,&oldbkcolor,&viewinfo,&lineinfo);

// set up view port

        wide = (int)(0.75*scrn_width);
        high = (int)(scrn_height/27);
        x    = (int)(scrn_width/8);
        y    = scrn_height - (int)(scrn_height/25);

        setviewport(x,y,x+wide,y+high,1);
        clearviewport(); setcolor(col);
        graph_margin(x,y,x+wide,y+high,1);
        strcpy(message,text);
        locx = (int)((wide-textwidth(message))/2);      // centre message in
        locy = (int)(0.3*high);                         // frame wide
        outtextxy(locx,locy, message);
        if (beep) BEEP;

// Restore view port settings and return to caller

        rstore_view(oldcolor,oldbkcolor,viewinfo,lineinfo);

return;
}
```

```
/*
```
Function Store_view - Preserves current viewport settings
```
*/

void store_view(int *col, int *bkcol, struct viewporttype *xview, struct linesettingstype *xline)
{
*col = getcolor();
*bkcol = getbkcolor();
getviewsettings(*&xview);
getlinesettings(*&xline);
return;
}

/*
```
Function Rstore_view Restores previous viewport settings
```
*/

void rstore_view(int col, int bkcol, struct viewporttype xview, struct linesettingstype xline)
{
setcolor(col);
setbkcolor(bkcol);
setviewport(xview.top, xview.left,xview.bottom,xview.right,xview.clip);
setlinestyle(xline.linestyle,xline.upattern,xline.thickness);
return;
}
```